Bayerisches Landesamt für Umwelt

GeoMol – Assessing subsurface potentials of the Alpine Foreland Basins for sustainable planning and use of natural resources

Project Report

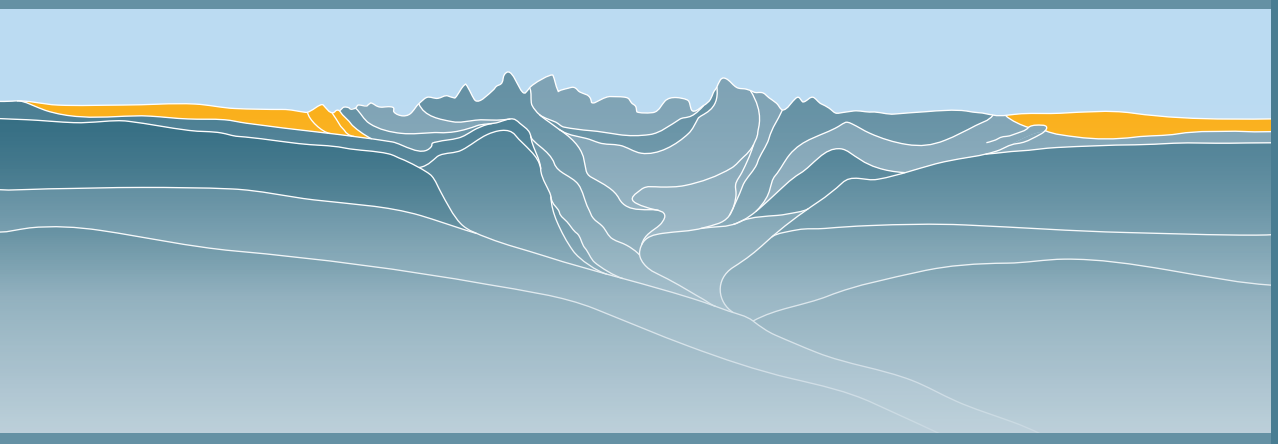

GeoMol

Assessing subsurface potentials of the Alpine Foreland Basins for sustainable planning and use of natural resources

Alpine SPACE
EUROPEAN TERRITORIAL COOPERATION
THIS PROJECT IS CO-FUNDED BY THE EUROPEAN REGIONAL DEVELOPMENT FUND
investing in your future

Bayerisches Landesamt für Umwelt

GeoMol – Assessing subsurface potentials of the Alpine Foreland Basins for sustainable planning and use of natural resources

Project Report

The GeoMol Team (2015)

GeoMol
Assessing subsurface potentials of the Alpine Foreland Basins for sustainable planning and use of natural resources

Alpine SPACE
THIS PROJECT IS CO-FUNDED BY THE EUROPEAN REGIONAL DEVELOPMENT FUND
EUROPEAN TERRITORIAL COOPERATION
investing in your future

Imprint

GeoMol – Assessing subsurface potentials of the Alpine Foreland Basins for sustainable planning and use of natural resources. Project Report

Publisher:
Bayerisches Landesamt für Umwelt (LfU)
Bavarian Environment Agency
Bürgermeister-Ulrich-Straße 160
86179 Augsburg
phone: 0821 9071-0
fax: 0821 9071-5556
e-mail: poststelle@lfu.bayern.de
website: www.lfu.bayern.de

Authors: The GeoMol Team (2015)
Gerold W. Diepolder[1] (editor in chief), Robin Allenbach[2], Roland Baumberger[2], Magdalena Bottig[3], Agnès Brenot[4], Anna Katharina Brüstle[3], Alessandro Cagnoni[5], Laure Capar[4], Renaud Couëffé[4], Chiara d'Ambrogi[6], Chrystel Dezayes[4], Mirjam Dürst Stucki[2], Charlotte Fehn[7], Fernando Ferri[6], Sunsearé Gabalda[4], Paul Gabriel[8], Jan Gietzel[8], Gregor Götzl[3], Katja Koren[9], Pascal Kuhn[2], Eva Kurmann-Matzenauer[2], Andrej Lapanje[9], Simon Lopez[4], Francesco Emanuele Maesano[6], Stéphane Marc[4], Salomè Michael[2], Fabio Carlo Molinari[10], Edgar Nitsch[7], Robert Pamer[1], Sebastian Pfleiderer[3], Andrea Piccin[5], Maria Ponzio[2], Dušan Rajver[9], Lance Reynolds[2], Igor Rižnar[9], Nina Rman[9], Isabel Rupf[7], Uta Schulz[1], Stephan Sieblitz[1], Helmut Schaeben[8], Dejan Šram[9], Giulio Torri[10], Gunther Wirsing[7], Heiko Zumsprekel[7].
[1]LfU, [2]swisstopo, [3]GBA, [4]BRGM, [5]RLB, [6]ISPRA, [7]LGRB, [8]TU BAF, [9]GeoZS, [10]RER-SGSS

With contributions of:
Pierfrancesco Burrato (Istituto Nazionale di Geofisica e Vulcanologia – INGV), Giancarlo Scardia (Istituto di Geologia Ambientale e Geoingegneria – CNR IGAG), Susanne Caspar & Kai Zosseder (TU Munich)

Editorial assistance:
Steve Mathers, British Geological Survey (BGS)

Technical editing:
LfU Referat 13, Sabine Schmidbauer

Picture Credits:
Unless indicated otherwise: GeoMol Team

Printing:
Schmid Druck + Medien GmbH & Co.KG, 86687 Kaisheim
Printed on 100 % recycled paper

Website:
http://www.geomol.eu

First edition (revised):
August 2015

Recommended citing:
GeoMol Team (2015): GeoMol – Assessing subsurface potentials of the Alpine Foreland Basins for sustainable planning and use of natural resources – Project Report, 188 pp. (Augsburg, LfU)

The GeoMol project is cofunded by the Alpine Space Programme as part of the European Territorial Cooperation 2007–2013.

The GeoMol Consortium:

Lead Partner

Bayerisches Landesamt für Umwelt

Bayerisches Landesamt für Umwelt (LfU) – Geologischer Dienst

Project Partners

Amt der Oberösterreichischen Landesregierung (LandOö)

Bureau de Recherches Géologiques et Minières (BRGM)

Schweizerisches Bundesamt für Energie (BfE)

Geološki zavod Slovenije (GeoZS)

Regione Lombardia (RLB) – Direzione Generale Territorio e Urbanistica

Geologische Bundesanstalt Österreich (GBA)

Istituto Superiore per la Protezione e la Ricerca Ambientale (ISPRA)

Regierungspräsidium Freiburg – Landesamt für Geologie, Rohstoffe und Bergbau Baden-Württemberg (LGRB)

Regionalverband Bodensee – Oberschwaben (RVBO)

Regione Emilia-Romagna – Servizio Geologico, Sismico e dei Suoli (RER-SGSS)

Schweizerisches Bundesamt für Landestopografie (swisstopo)

République et Canton de Genève – Département de l'environnement, des transports et de l'agriculture (DETA)

Technische Universität Bergakademie Freiberg (TU BAF)

The GeoMol Team:

Robin Allenbach[1], Nathalie Andenmatten[2], Jure Atanackov[12], Roland Baumberger[1], Magdalena Bottig[3], Agnès Brenot[4], Anna-Katharina Brüstle[3], Alessandro Cagnoni[5], Laure Capar[4], Nicolas Clerc[2], Renaud Couëffé[4], Gabriel Courrioux[4], Chiara d'Ambrogi[6], Chrystel Dezayes[4], Gerold W. Diepolder[7], Mirjam Dürst Stucki[1], Charlotte Fehn[8], Fernando Ferri[6], Sunsearé Gabalda[4], Paul Gabriel[9], Jan Gietzel[9], Gregor Götzl[3], Oliver Kempf[1], Guido Köberle[10], Christoph Kollmer[11], Pascal Kuhn[1], Eva Kurmann-Matzenauer[1], Andrej Lapanje[12], Simon Lopez[4], Francesco Emanuele Maesano[6], Stéphane Marc[4], Michel Meyer[2], Salomè Michael[1], Fabio Carlo Molinari[13], Gennaro Maria Monti[6], Edgar Nitsch[8], Nils Oesterling[1], Robert Pamer[7], Marco Pantaloni[6], Sebastian Pfleiderer[3], Andrea Piccin[5], Maria Ponzio[1], Clemens Porpaczy[3], Dušan Rajver[12], Damien Rambourg[4], Lance Reynolds[1], Nina Rman[12], Isabel Rupf[8], Uta Schulz[7], Gunter Siddiqi[14], Stephan Sieblitz[7], Helmut Schaeben[9], Matthias Selg[8], Yves Siméon[4], Günter Sokol[8], Dejan Šram[12], Gunther Wirsing[8], Heiko Zumsprekel[8].
[1]swisstopo, [2]DETA, [3]GBA, [4]BRGM, [5]RLB, [6]ISPRA, [7]LfU, [8]LGRB, [9]TU BAF, [10]RVBO, [11]LandOö, [12]GeoZS, [13]RER-SGSS, [14]BfE

Preface from the Alpine Convention Focal Point

Silvia Reppe

Focal Point
Alpine Convention
Germany

Federal Ministry for the Environment, Nature Conservation, Building and Nuclear Safety

The final report of this project states that geology does not respect political boundaries.

This statement can be applied to many features of the Alpine region – to rivers, biodiversity, mountain forests, glaciers, the clean mountain air, air pollutants and also to the transport routes that run right across the Alps.

Each project under the Alpine Space Programme addresses this fact by means of transboundary cooperation with as many partners as possible across the Alpine countries and thus makes a concrete contribution to transnational decision-making in line with national regulations.

In my opinion, this mirrors the core principle of the Alpine Convention, namely the joint contribution of all Alpine countries to protecting and sustainably developing the region using a comprehensive policy.

We have placed this comprehensive approach at the heart of the programme for the German presidency of the Alpine Convention for 2015–2016. Concrete joint projects of the Alpine countries, in particular those falling under the Alpine Space Programme, are, for Germany, a valuable means of demonstrating the practical implementation of the Alpine Convention and are important for awareness of the convention at local level. Therefore, our objective is to sustainably support the distribution and application of project results from the 2007–2013 funding period and to intensively use the possibilities of the INTERREG V B Alpine Space Programme 2014–2020 funding period for new projects.

The good results achieved by projects such as GeoMol have impressively highlighted what the Alpine countries can achieve together.

The conclusion I personally draw from this is that the Alpine Convention, contrary to the criticism often voiced, represents the solid foundations and well-functioning structures of this Alpine-wide cooperation.

Preface from EuroGeoSurveys

Koen Verbruggen

President
EuroGeoSurveys

The Geological Surveys of Europe

Among the most important challenges towards the further development of European society that the European Commission has prioritised are securing access to energy, water and natural resources, and the mitigation of natural hazards and climate change. In these domains the use of geological knowledge and spatial information on the subsurface is crucial to assist stakeholders from policy, research and industry in implementing sustainable solutions.

The long-term management of geological data and information systems is the core responsibility of any Geological Survey Organisation as the legal custodians of the subsurface, at national or regional levels. Since all GSOs a have a national rather than an overarching mandate, knowledge repositories and investigation activities are following separating political boundaries rather than connecting geological settings. Cross-border collaboration is not yet common unless stimulated by European funding or legislation.

Owing to EU cohesion policy, recently there are a number of cross-border projects geared towards interoperable, harmonised geoscientific information in multiple domains. However, most of them still focus on large scale two-dimensional map information or on specific issues. In contrast, sustainable management of deep subsurface potentials such as groundwater, mineral deposits, and the resources to boost green energy requires a holistic and three-dimensional assessment to tackle and anticipate possible conflicts in the use of the underground space as a finite spatial resource. Such integrated approaches to harmonise higher resolution multi-dimensional data and information, naturally, are not feasible immediately on a full European scale. They can be implemented successively only in geological structures of limited extension, featuring a common geological evolution and potential.

The Alpine Foreland Basins as evaluated in GeoMol are striking geological structures that feature a wide range of subsurface potentials which can substantially contribute to achieve Europe's ambitious targets in energy security and the reduction of greenhouse gas emissions. Shared by six countries these basins are particularly suitable for a transnational assessment to develop and establish methods and standards in order to serve cross-border planning and decision making in terms of the utilisation of subsurface potentials.

The increasing relevance of harmonised geological information for policy and the economy at transnational level has recently been recognised by the European Commission. GeoMol's transnational approach responds to that, providing consistent geological information based on harmonised baseline data and methodologies applicable also beyond the study area. GeoMol's web-based data infrastructure, developed for full interoperability among the partners and to allow the seamless visualisation of multi-dimensional geodata stored at different national repositories being subject to disparate legal requirements, is a valuable component for the future European geological data infrastructure.

Content

1 The GeoMol project – an introduction 9
1.1 Rationale 9
1.2 Objectives, requirements and solutions 10
1.3 Project organisation and visibility 13

2 Settings 15
2.1 The Project Area 15
2.2 Geological setting 17
2.2.1 Foreland basin evolution 17
2.2.2 Depositional evolution of the Alpine Foreland Basins 21
2.3 Geopotential setting – occurrence, issues, and approach 30
2.3.1 Geothermal potential 32
2.3.2 Storage potential 36
2.3.3 Geological risks 38

3 User requirements and legal constraints of data policy 41
3.1 User requirements 41
3.1.1 User groups and business sectors of the survey participants 41
3.1.2 Fields of activity of the survey respondents 42
3.1.3 Desired products, features and formats 43
3.2 Legislation and strategies for subsurface planning 45
3.3 Legal constraints of data policy 46
3.3.1 Availability of baseline date 46
3.3.2 Legal constraints on data publication and dissemination of products 49

4 Baseline data and data preparation 51
4.1 Seismic data 51
4.2 Borehole data 55
4.3 Published data and maps 56
4.4 Seismic signatures and the interpretation of horizons and structures 57
4.4.1 Fault interpretation 60
4.4.2 Velocity modelling 60

5 Three-dimensional geological modelling 63
5.1 Introduction 63
5.2 Technical implementation 64
5.3 3D modelling workflow 66
5.3.1 Input data sets & data preparation 66
5.3.2 Modelling of faults 67
5.3.3 Modelling of horizons 68
5.3.4 Consistency checks 69

6 Geopotential assessment – criteria, methods and products 73
6.1 Geothermal potential 73
6.2 Storage potential 75
6.3 Oil and gas potential 76
6.4 Further geopotentials 76

7 Temperature modelling 77
7.1 Introduction 77
7.2 Objectives 78
7.3 Data background 78
7.4 Overview on the applied workflow 81
7.4.1 Data processing 82
7.4.2 Temperature modelling 84
7.4.3 Model calibration and error estimation 86
7.5 Conclusion 86

8 Applications in Pilot Areas 89
8.1 Geneva-Savoy area (GSA) 89
8.1.1 Study area and geological setting 89
8.1.2 Geological model 91
8.1.3 Evaluation of geopotentials 93
8.1.4 Model application – geothermal potential of deep groundwater resources 94
8.2 Swiss Midlands area (SMA) 96
8.2.1 Study area and geological setting 98
8.2.2 Geological model 98
8.2.3 Evaluation of geopotentials 99
8.2.4 Model application – potential for geological storage of CO_2 100
8.3 Lake Constance–Allgäu area (LCA) 104
8.3.1 Study area and geological setting 104
8.3.2 Geological model 105
8.3.3 Evaluation of geopotentials 109
8.3.4 Model application – assessment of geothermal potential 112
8.4 Upper Austria–Upper Bavaria area (UA–UB) 114
8.4.1 Study area and geological setting 114
8.4.2 Geological model 115
8.4.3 Evaluation of geopotentials 118
8.4.4 Model application – temperature model and conceptual model of the hydrothermal system 120
8.4.5 Conceptual model of the hydrothermal system 122
8.5 Brescia-Mantova-Mirandola area (BMMA) 124
8.5.1 Study area and geological setting 126
8.5.2 Geological model 126
8.5.3 Evaluation of geopotentials 128
8.5.4 Model application – geothermal potential and seismogenic structures 129

9 Special studies 131
9.1 Assessment of seismogenic structures and active faults of the central Po Plain 131
9.1.1 Characterisation of faults 133
9.1.2 Active faults and seismogenic sources 134
9.1.3 Results 136
9.2 Assessment of the geothermal potential of medium-deep borehole heat exchangers in the Lake Constance–Allgäu area 138
9.2.1 Introduction and aim of the case study 138

9.2.2	Methods	139
9.2.3	Results	140
9.2.4	Development of the calculation module GEO-HAND^{POT}	142
9.2.5	Determination of geological and geothermal boundary conditions	143
9.2.6	Assessment of geothermal potential and visualisation of results	144
9.3	The 3D geological model and geopotentials of the Mura-Zala Basin	146
9.3.1	Introduction and objectives of this case study	146
9.3.2	3D geological framework model	146
9.3.3	Geopotential assessment	150
9.3.4	Summary of the geopotential assessment and the 3D model building	156
10	**Distribution of results**	**157**
10.1	The GeoMol Website	157
10.2	The GeoMol 3D-Explorer	158
10.2.1	The requisite behind the scenes – the GST 3D data base	159
10.2.2	The visualisation and query tool	161
10.3	The GeoMol MapViewer	165
10.4	The GeoMol SearchCatalogue	167
10.5	GeoMol's web map services	168
11	**Summary and outlook**	**170**
12	**Abbreviations, acronyms, trade names and units**	**172**
13	**References**	**174**

1 The GeoMol project – an introduction

1.1 Rationale

The subsurface, as a finite spatial resource, faces increasing competition from many different users. The utilisation of the subsurface potential of groundwater, mineral water, minerals, geothermal and other energy resources; and for underground storage of oil and gas reserves; and as underground repositories are important aspects for the security of supply and economic development of any nation. The realignment of energy policies is increasingly geared towards sustainability, coupled with the need to boost the exploitation of geothermal energy and the buffer storage of weather-dependent renewable energy, so, there will be further pressure on the subsurface. Now a principal challenge for spatial planning and licensing is the sustainable management of the subsurface, including consideration of the capacities required for increased renewable energy production and storage, and the continuing need for water supply, raw materials, and waste disposal.

Any exploration and development of the deep subsurface is recognised as an acknowledged high-risk investment. This applies in particular to geothermal energy generation in low-enthalpy systems, where tapping suitable temperatures commonly requires drilling to depths of more than 3 km. To mitigate the financial risks involved improved forecasting of the distribution of rock units and physical properties of the subsurface are essential. Furthermore, criteria for the exclusion of development in areas with potential geohazards have to be defined, and then these areas delineated.

In contrast to the well-established land-use planning at the surface, the planning and management of the subsurface is breaking new ground. The preparation of tools and methods for subsurface planning and utilisation inherently require a three-dimensional approach which will enable vertically defined licensing areas for multipurpose use to ensure resource efficiency. The geopotential assessment must, therefore, be based on a sound, unbiased and holistic three-dimensional evaluation of the geological structure utilising our advanced 3D modelling techniques.

Another challenge in modelling the deep subsurface tends to be the paucity of data and its uneven distribution at depth making it difficult to predict the geological structure. Fundamental data for modelling the deep subsurface is either scattered and clustered deep wells that have to be spatially linked and correlated using seismic section interpretations. The space in between these hard data in the model has to be populated by the geologists' expertise and understanding based on their conceptual model of the geological evolution and structure of the area.

To acquire, store, process and synthesise these data, and to make this data available to meet the economic and societal needs is the core responsibility of any Geological Survey Organisation (GSO), as the legal custodians of the subsurface. The inventories, archives and information systems maintained by these Geological Surveys coupled with the professional expertise of their staff are the prerequisites for mapping of the subsurface, the assessment of its potential, and the constraints due to the presence of geohazards.

The area of influence and impact of the development of many geopotential aspects often extends well beyond the actual licensed area, and geology does not respect political boundaries. Thus, the sustainable management and impact assessment of subsurface exploitation requires an integrated international approach whose extent must be guided by the geological structure rather than by political and administrative boundaries.

Shared by six countries, home to several million people and the location of a vast variety of key modern industries, the Alpine Foreland Basins – the Molasse Basin to the north and the Po Basin in the south (Figure 2.1-1) – are striking geological structures exhibiting a similar geological history and potential. These basins can contribute substantially to meet Europe's ambitious targets regarding low-carbon energy generation. Due to their geological evolution these sedimentary basins along the northern and southern fringes of the Alpine mountain range offer abundant deep geothermal potential, storage capacity to even out fluctuations in the generation of weather-dependent wind and solar energy, and space for underground storage of gas or carbon dioxide. The enhanced and sustainable use of these natural resources will add considerable value to the economy and will foster the technological and economic development. Especially the geothermal technologies using renewable energy resources to generate electricity or heat and producing very low levels of greenhouse gas emissions have an important role to play in achieving targets in energy security, economic development and the mitigation of climate change (IEA 2011).

The successful resolution of cross-border issues requires a comprehensive harmonisation of data, methodologies and software systems ensuring full interoperability among the project partners. It must also consider the disparate baseline data, historical settings and the diverse legal frameworks concerning data policy. The increasing relevance of geological information for policy and the economy at transnational level has recently been recognised by the European Commission, who called for the availability of harmonised data and information related to reserves and resources across the EU member states. GeoMol's transnational approach responds to that, providing consistent and seamless geological information based on harmonised baseline data and methodologies.

The objective and scope of this scientifically and technically ambitious project called for a high degree of organisation and coordination among all the parties involved. Even though experiences and developments of previous projects covering partial aspects or technical requirements could be captured and exploited, the partners had to meet many new challenges whilst breaking fresh ground. Knowledge and skills contributed by the project partners varied widely depending on their emphasis in scientific application, but this has been invaluable and mutually beneficial: Due to the cross-fertilising collaboration among the project participants and, as a consequence, the gain in knowledge and experience bringing the partners to a common, higher level, all parties involved will continue to benefit after the end of the project. The established expert network, including stakeholders beyond the territorial reach of GeoMol safeguards the continuing dialogue over the upcoming challenges of subsurface planning and its utilisation and facilitates an effective knowledge transfer in order to assess the geopotentials of other foreland basins. The tools and concepts developed for ensuring technical interoperability amongst the GeoMol partners are versatile modules immediately usable in the intended pan-European geological data infrastructure.

1.2 Objectives, requirements and solutions

The objective pursued in GeoMol is to provide trans-nationally harmonised, digital, up-to-date and further updatable knowledge and databases of the geology of the Alpine Foreland Basins at a regional scale, as the fundamental prerequisite for various applications in spatial planning and decision-making. Issues of the different options of subsurface use are the major focus addressed. A principal aim, because it is the basis for all subsequent steps, is to develop an unbiased and agreed transnational interpretation of the geology based upon a common and shared understanding. Subsurface spatial planning and management ensuring resource efficiency inherently requires the three-dimensional approach – outputs must be based on a three-dimensional evaluation of the geo-

logical structure utilising 3D modelling techniques. Further framework conditions guiding the control and implementation of the objectives accrue from the user requirements and the societal needs.

Society increasingly demands that earth and environmental resource issues are evaluated in terms of sustainability by an interdisciplinary approach from the scientific, engineering, planning, and regulatory bodies. Such cross-domain coordination requires interaction with a larger community of stakeholders beyond the geoscientific expertise. The recent technological advancements have supplied tools which allow a straightforward insight into the Earth's interior and to better comprehend subsurface geology. Modern 3D modelling and visualisation techniques enable an extended user community to explore and query the subsurface at arbitrary depths. However, unlike the established user community, such as resource focused primary industries and academia, many of today's potential users of geological models and visualisations do not have the capability to interpret basic geoscience data or evaluate the merits of alternative interpretations. They may be unable to distinguish between theories and facts – in brief: these users clearly desire "solutions, not data" and "information in understandable form" (TURNER & D'AGNESE 2009). The geo-information provided thus must be comprehensible for non-geoscientists. It also must be capable to be combined with information from other domains exploiting the achievements of modern information and communication technology. To provide users with the capability of searching, visualising, and querying information and data the key components, the knowledge portal and the underlying collaboration platform as the expert live system are required to function successfully within a web-based environment.

Preparing consistent and seamless geological information in a transnational approach demands that all processing steps are based on harmonised data and concerted methodologies which have to overcome proprietary nomenclatures and disparities resulting from historical reasons. The use of classified data and the different legal constraints with respect to data policy in the project's member states imposes particular requirements on the collaboration platform and the distribution of the results. A data infrastructure complying with both, the disparate data policy and the EU's request for harmonised geological information at transnational level (e. g. EU 2013, VAN DER KROGT et al. 2014), can be worked out in a distributed organised system only interconnected via a hub as part of the web-based environment.

However, at the outset of GeoMol no adequate tool or methodology was available to gather, merge, and distribute multi-dimensional geo-information of different sources constrained by diverse data policy, database systems and software solutions. The geological community still lacked the ability to exchange 3D geological data efficiently across the diverse systems (DIEPOLDER 2011) and to present them in an overall picture merged from different national repositories. Thus, a key objective of GeoMol was to build up a software-independent infrastructure for multi-dimensional geological data ensuring full interoperability among the partners in line with the data policy of the project's member states (and beyond) and responding to the need to provide cross-border harmonised information for a larger community of stakeholders. Core of GeoMol's IT developments is a hub interconnecting the remote live systems maintained and continuously updated at the legally mandated Geological Survey Organisations (GSOs). Via this hub open access 3D models (or spatially restricted portions thereof) can be merged, and visualised and queried exploiting the functionalities of the web portal (Chapter 10).

In contrast to web-based data management and analysis systems designed to serve the scientific community, a platform that employs "off-the-shelf" and consumer-oriented, hosted web-services (TURNER & D'AGNESE 2009) better reflects the needs of the non-geoscientific stakeholders. In order to deliver such tailor-made products serving the demands of planners and regulatory bodies GeoMol incorporated a variety of stakeholders from different areas of expertise in the design of its pro-

ducts and distribution channels. A stakeholder survey conducted in the GeoMol member states assisted in bringing the projects deliverables into line with the users' requirements (Chapter 3).

In summary, the project objective has to be considered two-layered: a scientific issue aimed at a trans-nationally harmonised basis for the assessment of the geopotential, and a technical solution for the collaborative environment and the dissemination of results serving different user communities. An expert system supplies various analytical tools for the assessment of the geopotential and the prioritisation of their use, based on four pillars:

- 3D geological models portraying the three-dimensional set-up of the principal litho-stratigraphic units and the fault network, down to the crystalline basement at a depth of up to six kilometres,
- lithological characteristics of the layered rocks suites as an estimate of the regional petrophysical parameters,
- temperature distribution models based on regional best-fit approaches,
- a metadata catalogue on the primary information used in 3D modelling.

These models are used in solving issues of the various use options of the deep subsurface, with a main emphasis on the assessment of the deep geothermal potential and the storage potential as related to the structural inventory (Chapter 6). The results can be also applied in a suitability assessment for the underground storage of wind and solar fuel, provided generally acknowledged rules and requirements with respect to geological properties are defined.

The spatial information GeoMol makes available is applicable also as a basic input in process modelling. Large advantages in providing specific and quantifiable answers have been demonstrated when 3D geological models have been linked to numerical models of physical processes, specifically groundwater flow models – applications usually performed by external experts. Such sharing of 3D geological models for external applications must be accompanied by metadata on the baseline data used and the rules that define the data flow, techniques, and standards of integration of the various inputs. The metadata information pool supplied via a web service (Chapter 10) as well as the workflows and best practice described in this report are basic requirements for the geoscience knowledge integration and for external users.

Three dimensional geological models are subject to iteration once new exploration data is made available and are therefore maintained as a live system at the legally mandated GSO. The web-based collaborative environment designed to serve the GSOs concerned and the scientific community allows the share of models and their merger with models from other sources. According to the target groups addressed, different web-based methods of dissemination are provided as described in detail in the chapter 10:

- a geo-data infrastructure for full interoperability of 3D geological information of the live systems among the GSOs and entitled experts,
- a map viewer in order to provide off-the-shelf map applications for planners, regulatory bodies and decision makers,
- a 3D browser-analyst for visualisation and query of open source 3D models to share the project's findings and to raise the awareness of the public.

This report represents an explanatory supplement to these technical implements as well as the scientific methods and results. It provides background information and an in-depth insight into the issues and challenges of addressing geopotentials at great depth and the solutions achieved.

1.3 Project organisation and visibility

The GeoMol project has been executed within the scope of the Priority 3 “Environment and Risk Prevention” of the European Territorial Cooperation Alpine Space Programme 2007–2013, running from September 2012 through till June 2015. The project established a partnership of 14 institutions from six member states of the Alpine Space Cooperation Area:

Figure 1.3-1: The consortium members of GeoMol’s partnership coming from Austria, France, Germany, Italy, Slovenia and Switzerland.

A total of 58 project collaborators contributed to the project implementation at least for certain phases and handling certain tasks. Dove-tailing the separate activities and adhering to the ambitious time schedule called for a high degree of organisation and coordination among all parties involved.

The governance of the overall project was the responsibility of the lead partner Bayerisches Landesamt für Umwelt – LfU, Geologischer Dienst (Bavarian Environment Agency, Geological Survey). Major parts of the administrative project management, including the support in reporting and grant monitoring were subcontracted to Bayerische Forschungsallianz – BayFOR (Bavarian Research Alliance).

The overall control of the project has been overseen by the GeoMol Steering Committee (GSC) constituted in compliance with the Partnership Agreement between the lead partner and the project partners. The GSC consisted of representatives of all project partners, thus incorporating all work package leaders as well, and met on a regular basis every six months chaired by the lead partner. Decision making processes of the GSC were based on Rules of Procedure agreed on at the inaugural meeting. All decisions of the GSC have been made by consensus. External experts of the Advisory Boards assisted the GSC in tackling the challenges specifically where GeoMol had to break fresh ground and in the design of its outputs.

The technical implementation of GeoMol was structured into five work packages each coordinated by one of the partner institutions depending on their specific expertise (Figure 1.3-2). A robust governance structure, numerous joint cross-thematic meetings of the working groups, a partnership meeting, continuous exchange via a web-based shared project platform and, most notably, a common understanding of the way to accomplish the project’s objectives ensured a smooth project execution. Knowledge and skills contributed by the project partners varied widely depending on their emphasis in scientific application, but this has been invaluable and mutually beneficial.

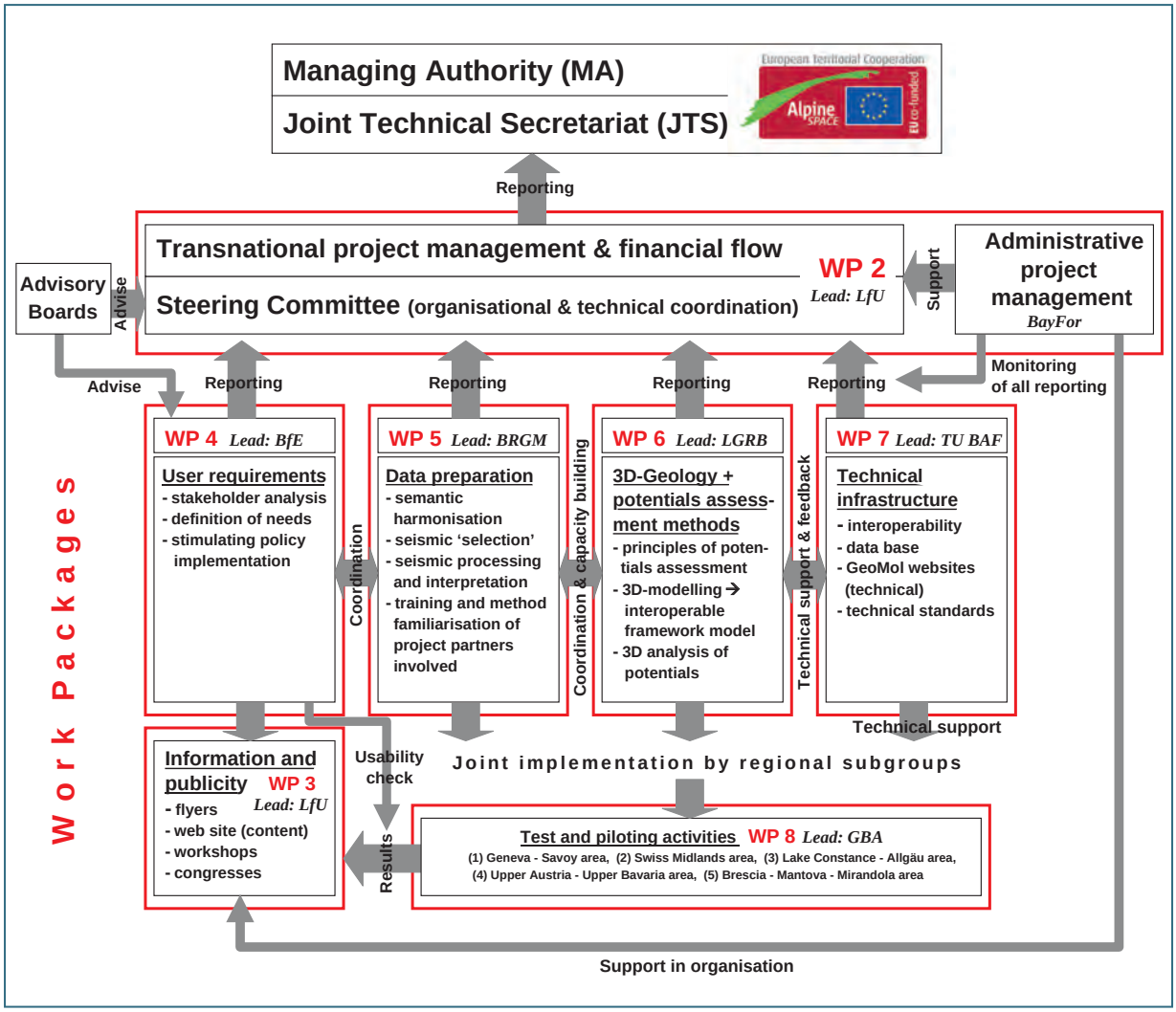

Figure 1.3-2: Organisation chart of the GeoMol project. Acronyms of the institutions in charge of work packages (WP) implementation as on page 3.

In line with the Programme regulations for appropriate information and publicity (I&P) GeoMol's website www.geomol.eu was launched at the very beginning of the project implementation for public perception and visibility. It is designed as the hub for all information dissemination to ensure that results achieved can be capitalised on by policy makers and stakeholders. Continually developed and enhanced throughout the project lifetime, it now holds available all contributions to GeoMol's major information events, the Kick-off Conference, the Brussel Information Day, and the Mid-term Conference, as well as the project's publications in scientific papers and in conference proceedings. Implemented incrementally since June 2014 it also features the central access point to GeoMol's geo data infrastructure, including the 3D-Explorer and web map service (WMS) for dissemination of the projects outcomes (Chapter 10).

Additionally, for a wider perception beyond the geoscientific community and serving the cross-sectoral stakeholder involvement native-language articles in laymen's terms (Diepolder & Kindermann 2013, Diepolder 2015) have been published in professional journals.

2 Settings

2.1 The Project Area

The GeoMol project area is located within the northern and southern Foreland Basins of the European Alps separated by the Alpine mountain range. The northern Foreland Basin, the Molasse Basin, roughly forms a northward convex arc extending over more than 1,000 km from Chambéry (France) in the southwest to Brno (Czech Republic) in the northeast, encompassing French, Swiss, German, Austrian and Czech territories. The southern Foreland Basin, the Po Basin, extends for about 500 km in northern Italy, from Turin to almost Trieste. It covers the plains between the southern fringes of the Alps and the northern rim of the Apennine Mountains and extends into the Adriatic Sea to the east.

The factual borders of the project's model areas are determined by both, the geological situation and the political respectively administrative constraints: The outlines of the Alpine Space Cooperation Area are tracing the borders of administrative units. The eligible area for implementing GeoMol's objectives and scope does not fully cover the Alpine Foreland Basins. Thus, the basin share of Lower Bavaria, the Czech Republic and Emilia-Romagna could not be considered within the project, even if a small sector of Emilia-Romagna Region is part of the Italian pilot area (Figure 2.1-1).

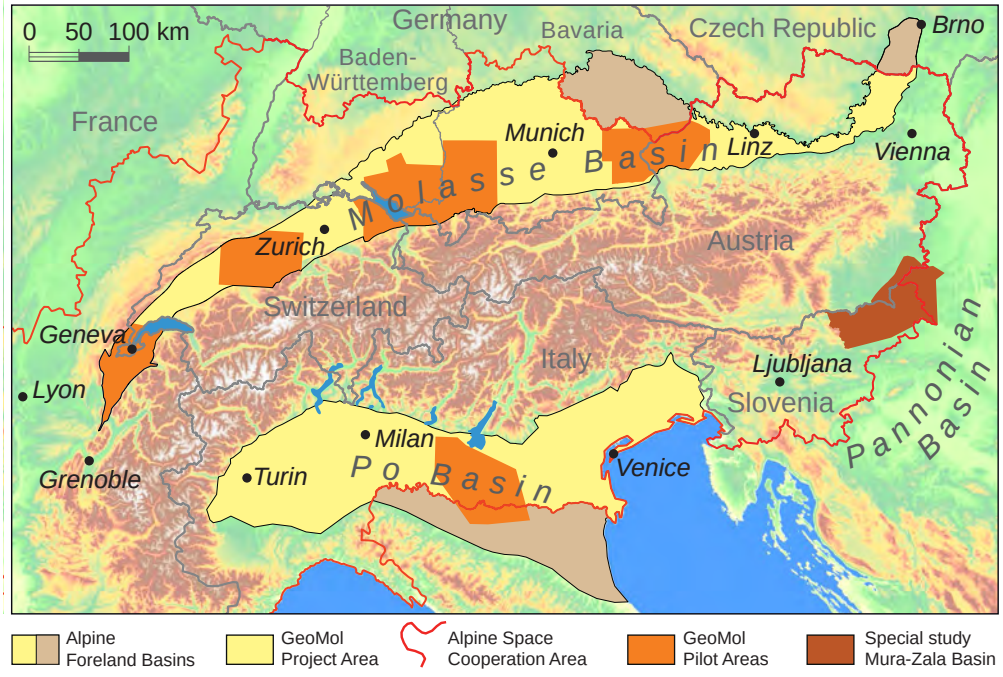

Figure 2.1-1: Outlines of GeoMol's project area and the five pilot areas as related to the Alpine Foreland Basins and the Alpine Space Cooperation Area, as well as the Special Study Area for testing GeoMol's approach beyond the Alpine Foreland Basins.

Apart from that, the model areas also disregard those parts of the Foreland Basins featuring a complex tectonic evolution (such as the Subalpine or Imbricated Molasse along the southern margin of the northern Foreland Basin) as the base data available in this area do not allow a sound three-dimensional assessment of the intricate geological set-up. Likewise, modelling the structural inventory of the Po Basin was restricted to a case study in a 5,700 km^2 large area, in order to harmonise the sedimentary and tectonic interpretation of the basin and assess seismogenic sources e. g. of the

May 2012 earthquake. Modelling and evaluating seismogenic structures had to break new ground and new approaches and methodologies had to be applied and validated – a task not viable in a larger area given the circumstances.

Framework model area

GeoMol's framework model is designed as a synoptic reference model to fit in all existing or future detailed models in their true spatial position. Its model area encompasses overall 55,000 km^2 covering the Foreland Molasse of the Rhône-Alpes region of France, the entire Swiss Molasse Basin, as well as the Molasse share of Baden-Württemberg and Bavaria (without Lower Bavaria) in Germany and of Upper and Lower Austria including small parts of Salzburg and Vorarlberg. The northern model border is defined by the southernmost outcrops of – from southwest to east – the Jura Mountains, the Swabian-Franconian Platform and the Bohemian Massif. The framework model's southern border coincides with the present-day Alpine orogenic front as defined by the northern limit of the Subalpine Molasse along the Alps' northern foothills. However, parts of the basically undeformed horizons of the Foreland Molasse overthrusted by thus underneath the Subalpine Molasse have been included into the framework model as well as the pilot area models.

Pilot areas

Five pilot areas have been defined for detailed 3D modelling and the assessment of geopotentials focused on current issues in the respective region and serving as use cases for the application and validation of methods in different geological settings. The specific objective and scope of the pilot areas and the peculiarities of their geological setting are addressed in chapter 8, featuring also more detailed maps of the areas and the model boundaries.

The **Geneva-Savoy Area** (GSA) encompasses the Canton of Geneva and its French environs down to Chambéry, comprising parts of the departments Ain, Haute-Savoie and Savoie. It thus includes the entire French share of the Molasse Basin as the south-western extension of the Swiss Molasse Basin. The GSA covers about 2,000 km^2 forming a NNE–SSW trending, approximately 100 km long, relatively narrow (max. 40 km wide) depression between the Subalpine frontal thrust and the eastern margins of the Jura Mountains folds (Chapter 8.1).

The **Swiss Midlands Area** (SMA) as part of "Espace Mittelland" covers an area of about 4,000 km^2 roughly in between the cities of Fribourg, Biel/Bienne, Olten and Luzern thus comprising larger territories of the Cantons Bern, Solothurn, Luzern and Aargau. The pilot area model spans the entire Plateau Molasse including the fringes of the Subalpine Molasse along its south-eastern margins (Chapter 8.2).

The **Lake Constance – Allgäu Area** (LCA) encompasses territories of three countries respectively four federal states including their share of the subsurface beneath Lake Constance: roughly the southern part of historical "Oberschwaben" in Baden-Württemberg and Bavaria, major parts of the Cantons of St. Gallen and Thurgau in Switzerland, and the very northwestern part of Vorarlberg in Austria. The model area covers a territory of about 8,850 km^2 comprising the deeper parts of the Foreland Molasse in the Western–Central Molasse transition zone and includes the peripheral Subalpine Molasse at the southern model boundary (Chapter 8.3).

The **Upper Austria – Upper Bavaria Area** (UA – UB) is equally distributed over both sides of the border embracing major parts of the Austrian and Bavarian "Innviertel" and a small share of Lower Bavaria in the north and Land Salzburg in the south. The model area overall comprises 4,730 km^2 including peripheral parts of the Foreland Molasse underneath the Subalpine Molasse (Chapter 8.4).

The **Brescia-Mantova-Mirandola Area** (BMMA) of the Po Basin, shared by Lombardia and Emilia-Romagna Regions, covers a realm of about 5,700 km^2 between the South Alpine piedmont in the north and the Apenninc orogenic front buried under central part of the Po Plain, one of the largest plains in Europe. Including the cities of Brescia and Mantova it is part of the most densely populated area of Italy, however threatened by various natural hazards (Section 2.3.3, Chapter 8.5).

2.2 Geological setting

2.2.1 Foreland basin evolution

Foreland basins result from large-scale downwarping of the Earth's crust due to tectonic forces; they are progressively infilled with sedimentary rocks some of which become disturbed by the ongoing tectonic processes. They develop along the margins of emerging orogenic mountain belts due to the enormous load produced by the crustal thickening that results from compressional tectonic forces. Foreland basins are filled with sediment that is eroded off the adjacent mountain belt, resulting in thick successions that thin away from the mountains. In the early stages of their evolution, when the rate of basin subsidence is greater than the sedimentation, deep-water and marine sediments tend to be deposited. Subsequently, as the basin becomes increasingly infilled and deposition is concentrated farther toward the foreland, the deposition of shallow marine and terrestrial sediments prevails. Typically, the latter are non-marine alluvial and fluvial sediments, commonly

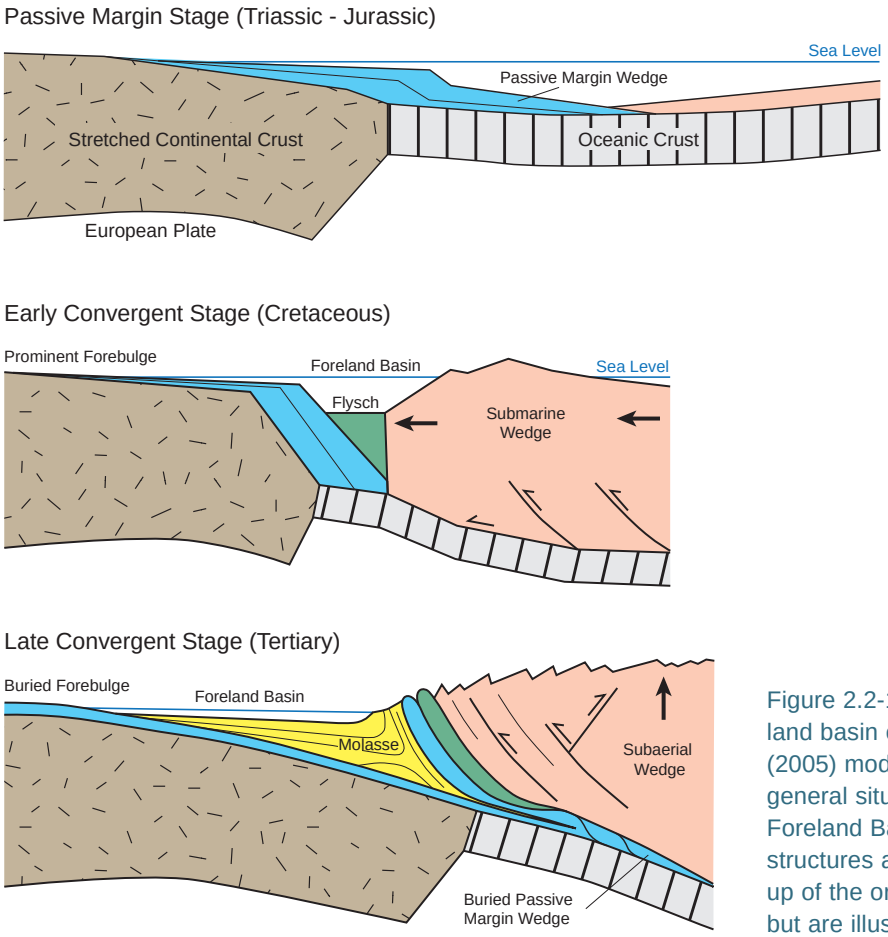

Figure 2.2-1: Schematic sketch of foreland basin evolution after ALLEN & ALLEN (2005) modified and adjusted to the general situation of the North Alpine Foreland Basin. For clarity the crustal structures and the complex internal set-up of the orogenic wedge are omitted, but are illustrated in figure 2.2-2.

known as *molasse*. Deformation and faulting of molasse deposits right in front of the orogenic belt and structural unconformities within the more distal sedimentary sequences prove that the compressional tectonic forces persisted during the sedimentation within the foreland basin.

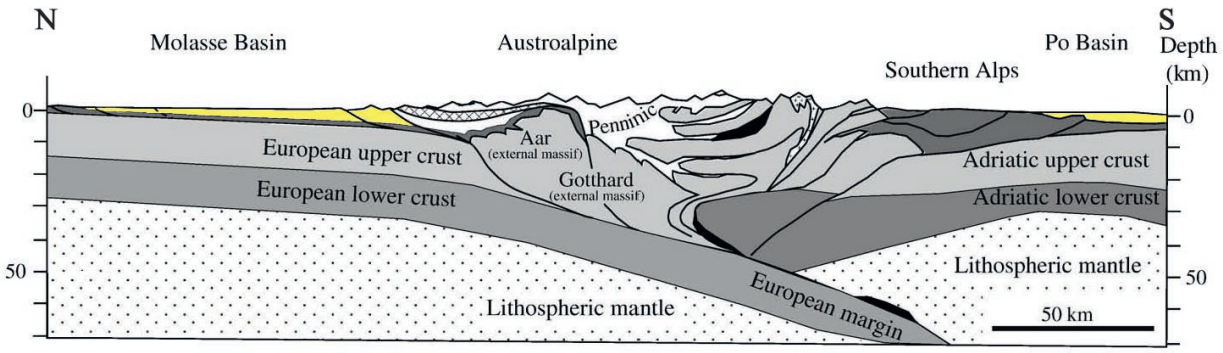

Figure 2.2-2: Schematic section across the Central Alps (from CHAMPAGNACA et al. 2009) demonstrating the structure and proportions of the Alpine orogeny and positons of the foreland basins.

2.2.1.1 The North Alpine Foreland Basin

The North Alpine Foreland Basin (NAFB), also known as the Molasse Basin, developed along the northern margins of the emerging European Alpine chain some 35 million years ago. As part of the Alpine-Himalayan orogenic belt the Alps have resulted from the collision of the African and Eurasian and associated smaller plates caught between them. The convergence of the African Plate from the south and the Eurasian plate from the north, caused the closure of the formerly extensive Tethys Ocean, and the progressive subduction of Tethyan oceanic crust culminating in a continent-continent collision between Africa and Europe. The enormous compressional stresses exerted scraped off wedges of sediment and continental crust from both the European and African Plate margins forming thick piles of northward-directed thrust nappes and resulting in pronounced crustal thickening. The mountain building processes culminated when the northward thrusting nappes emerged as a mountain range and the weight of the orogenic wedge made the adjacent European Plate bend downward, resulting in the formation of a deep elongated depression (the NAFB) north of the developing orogeny. In the Eocene (55 to 34 Ma ago) this foreland basin became deeper until it formed a small deep seaway, in which deep-water sediments including turbidites probably triggered by frequent seismicity are preserved. In addition to these *Flysch* sediments, shelf sediments on the southern margin of European plate, were incorporated into the frontal part of the orogenic wedge and deformed. Migrating northward the overthrusting load caused the gradual displacement of the NAFB farther north onto the downwarping foreland of the European plate. During this phase the NAFB became infilled with shallow marine and terrestrial sediments. Finally molasse sediments completed the infilling of the NAFB, creating a gently inclined depositional surface that was subsequently sculpted into an incised form by more recent erosion and glaciation.

The preserved NAFB forms a northward convex arc extending for more than 1,000 km from Chambéry (in France) in the southwest to Brno (in the Czech Republic) in the northeast: it encompasses parts of France, Switzerland, Germany, Austria and the Czech Republic (Figure 2.1-1). The basin has a maximum width of 130 km. Due to the last phase of tectonic uplift some 5 million years ago and the ongoing deposition of sediments washed down from the Alpine range the surface of the Alpine piedmont is now between 200 to 250 meters elevation at its eastern and western ends, but this rises to more than 1,000 m in the central areas adjacent to the mountain front. The southern

border of the NAFB was overridden by the frontal Alpine thrusts and so is buried beneath the Alpine nappes. In marked contrast the northern border of the NAFB is simply the erosional limit of the Tertiary basin sediments onlapping onto the older bedrock of the foreland.

The infill of the NAFB can be subdivided into two principal units, the Foreland Molasse and the Subalpine Molasse. The Foreland Molasse (or Plateau or Autochthonous Molasse), represents the majority of the infill of the Basin that is exposed today. It consists of gently southernly-dipping strata that thin out northwards where they onlap onto the older bedrock of the European Plate. In the south-western part of the NAFB the Molasse sediments of this outer rim are affected by the folding of the Jura Mountains (Figure 2.2-3 C) whereas the inner rim is incorporated into the Alpine thrusting. This relatively narrow zone, 10 and 30 km in width, along the Alpine foothills is characterised by steeply inclined strata, tight folds and overthrusts, constituting the Subalpine Molasse (also known as Folded, Imbricated, or Allochthonous Molasse).

The Subalpine Molasse terrane (as well as isolated small scale occurrences like the Jura Molasse or the Inner-Alpine Molasse, remnants disintegrated by uplift and erosion or small satellite basins) is not considered in the GeoMol project. Overthrusted parts of the Foreland Molasse underneath the Subalpine Molasse have been modelled as far as sufficient evidence was available.

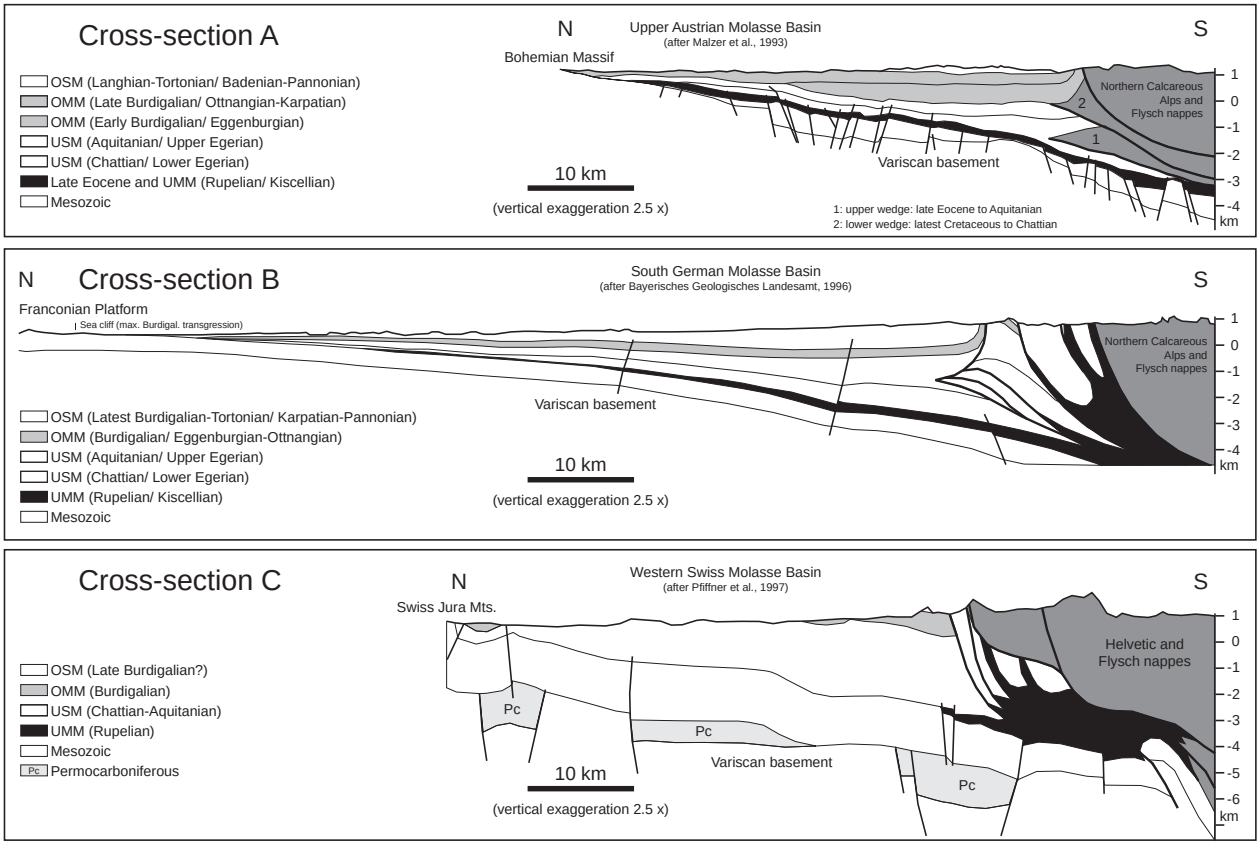

Figure 2.2-3: Generalised cross-sections of the NAFB portraying the different tectonic styles of the Alpine orogenic wedge front in Upper Austria (A), Central Bavaria (B) and Western Switzerland (C) (after MALZER et al. 1993, BAYGLA 1996 and PFIFFNER et al. 1997, from KUHLEMANN & KEMPF 2002).

2.2.1.2 The South Alpine Foreland Basin

The South Alpine Foreland Basin (SAFB) constitutes the Po Basin to the south of the Alps and in contrast to the NAFB, it is a retro-foreland basin, formed by compression between two concurrent orogenic thrust belts. These comprise the Alps to the north, and the Apennines to the south. The Apennine Mountains formed during the Alpine Orogeny from the northern part of the smaller Apulian Microplate – (also often referred to as the Adriatic Microplate) – which collided with the Eurasian Plate.

The Apulian (Adriatic) Microplate broke away from the African Plate in the Cretaceous. The Late Cretaceous to Cenozoic subduction of Tethyan oceanic crust and the subsequent continental collision between Africa and Europe partly deformed, rotated, overrode, and consumed the Apulian Plate, but a significant portion of it was preserved as a foreland region, that now lies beneath the Po Basin. By Oligocene times, when most of the Tethyan oceanic crust had been subducted, the Apulian Microplate was being compressed from several directions, and a change in the relative plate motion caused the southward thrusting present in the Southern Alps. Concurrently, during the Oligocene, thrust stacking of the marine platform carbonate deposits of the Apulian plate formed the proto-Apennines.

The widespread evaporites of Late Miocene (Messinian) age record the periodic isolation and desiccation of the Mediterranean Basin from the open marine circulation of the Atlantic Ocean. The Apennine Orogeny peaked in Pliocene time, with the deformed zone reaching its northeastern-most expression across much of Italy, although some deformation continued into the Pleistocene. Substantial proximal foreland basin subsidence resulted in the deposition of at least 6 km of Pliocene sediment, in the Po Basin, and finally the establishment of the modern Po River drainage system.

The present-day outcrop of the Po Basin infill extends for about 500 km from Turin in the west to around Trieste in the east with a maximum N–S width of 150 km. It includes parts of the Italian regions of Piedmont, Lombardy, Veneto and Emilia-Romagna. In the east the Basin continues under the Adriatic Sea; approximately two-thirds of the basin is onshore and one-third offshore. In summary the Po Basin is surrounded by the thrusted terranes of the Southern Alps to the west and north, the northern Apennine Mountains to the south, and the Dinaride Mountains along the eastern coast of the Adriatic. The offshore extent is not considered in this chapter.

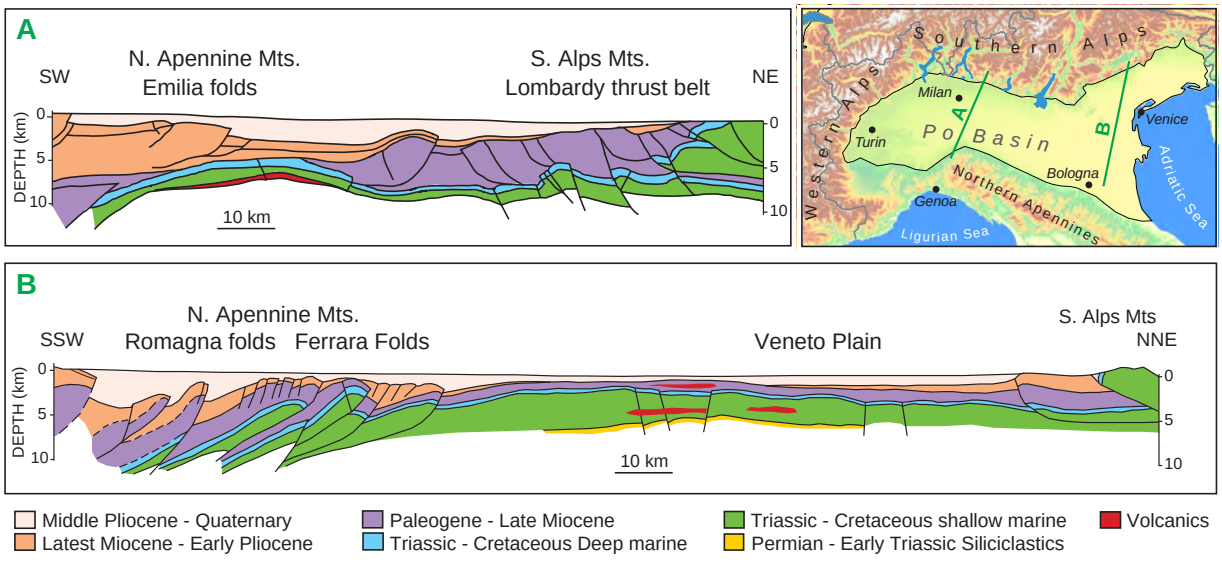

Figure 2.2-4: Generalised structural cross-sections of the Po Basin illustrating the tectonic style of the basin as a result of two concurrent orogenic thrusts (from LINDQUIST 1999, after ANELLI et al. 1996).

2.2.2 Depositional evolution of the Alpine Foreland Basins

More than 600 million years of Earth's history are documented in the geological record of the Alpine piedmont. The stratigraphic understanding of the Alpine Foreland Basins, has inevitably evolved from regional approaches and also reflects the complex basin evolution. The diverse stratigraphic classifications that exist arise from different schools of thought, differing local and regional terminology and variations in the degree of subdivision and refinement.

The following sections give a brief outline of the depositional history of the Alpine Foreland Basins as considered in the GeoMol project. The account is based on a range of publications, mainly resulting from hydrocarbon exploration between 1950 and 1990 and more recently, the investigation of the geothermal potential. However, specifically in the case of the NAFB the differing regional stratigraphic sequences have not been correlated and integrated into an overall understanding. Although the NAFB is considered among the best-investigated foreland basins worldwide (Kempf & Pross 2005), the regional studies of the NAFB still reflect national schemes and borders rather than integrating the Basin's evolution (Kuhlemann & Kempf 2002).

To try to overcome the lack of an overall synopsis, a three-dimensional approach based on a common understanding of the geological setting is required, and this has been one of the principal objectives of the GeoMol project (Chapter 1.2). The structure of the deep subsurface is illustrated by cross-sections directly derived from GeoMol's investigations including the production of harmonised trans-national 3D models.

2.2.2.1 Depositional history of the North Alpine Foreland Basin

The following summary of the depositional evolution of the NAFB is based on the work of Allan et al. 1991, Bachmann et al.1987, Bachmann & Müller 1991, 1992, BayGLA 1996, Doppler et al. 2005, Kempf & Pross 2005, Kuhlemann & Kempf 2002, Lemcke 1988, Pfiffner 2009, Sommaruga et al. 2013, Strunck & Matter 2002, Trümpy 1980 and Wagner 1998. These references are not quoted at specific points within the following text.

Within the NAFB as depicted in the GeoMol project's framework model, three principal units can be distinguished, each separated by a pronounced hiatus or unconformity. From oldest to youngest these are:

- the crystalline basement including clastic sediments of Permo-Carboniferous age accumulated in graben structures of the post-Variscan land surface,
- Triassic to Cretaceous shallow marine sediments up to 2.5 km thick, deposited as the first stage of the evolution of the foreland basin comprising passive margin shelf deposits of the European Plate – shown in blue in figure 2.2-1,
- Late Eocene to Late Miocene shallow marine and terrestrial deposits up to 5 km thick, representing the foreland basin infill, these are the *Molasse* sediments in the strict sense – depicted in yellow in figure 2.2-1.

The oldest basement rocks beneath the Molasse Basin are gneisses and associated Variscan granitic plutonic rocks that are proved in several deep boreholes, these are petrographically similar to the rock suites exposed in the Bohemian Massif, the Black Forest, the Vosges and the Massif Central. The top surface of the crystalline basement dips gently towards the Alpine range with a deepest record of its top surface at more than 5.6 km in the Sulzberg 1 well (see Figure 2.2-9 A). Late Carboniferous to Permian clastic sediments are restricted to a system of graben structures and sag basins sediment traps so they were preserved during the subsequent post-Variscan peneplanation.

Depending on the depth of the graben structures the preserved deposits, including fluvial sandstones, intercalated conglomerates, silt- and mud-stones, and sporadic coal seams, can reach a thickness of more than 1 km. The crystalline basement and these Permo-Carboniferous graben sediments are separated from the Mesozoic sedimentary sequence by a major post-Variscan erosional unconformity.

The Mesozoic sediments flooring the NAFB are Triassic to Late Cretaceous in age. These gradually encroach onto the basement from NW to SE. Continental to shallow-marine sediments were deposited in a rim-basin environment near the passive southern margin of the European Plate. This so-called Germanic Basin, was initially separated from the Tethys Ocean by the Bohemian Massif and Vindelician Swell, but the basin gradually extended to the SE, and the Vindelician Swell was inundated in the Upper Jurassic, thus establishing connectivity with the Tethys Ocean.

The Lower Triassic red-beds of the Buntsandstein are limited to the Swiss and Savoy (French) parts of the Molasse Basin floor whereas the subcrop of the overlying evaporates and carbonates of the Middle Triassic (Muschelkalk) stretch considerably further beyond the Lake Constance area. During the Upper Triassic (Keuper) the sediments progressively extended over the central (Bavarian) part of the NAFB, with mudstones prevailing in an alternating sequence with sandstones and marls, and with evaporites in the middle parts. Fluvial sand deposits dominate the marginal areas eventually encroaching to deposit red-beds throughout the basin during the Upper Keuper.

The Lower Jurassic (Lias) and the Middle Jurassic (Dogger) predominantly consist of shallow-marine shales with minor limestones and sandstones. All these formations become increasingly sandy towards their margins and demonstrate further transgression towards SE. Up to 600 m of carbonates of the Upper Jurassic (Malm) subsequently cover the entire realm from Savoy to Upper Austria. Limestones, marls and dolomites developed in a tropical shallow shelf sea including reefs, lagoons and shallow basins. At the base of the Cretaceous a marine regression resulted in emergence of large parts of this carbonate platform of the European shelf – this resulted in deep weathering and karstification of these rocks during the Early Cretaceous. Deposition, however, continued in the Tethys Ocean and the proximal shelf, depositing sedimentary sequences that were subsequently displaced and incorporated into the Alpine thrusts. Regional scale marine transgressions of Middle and Late Cretaceous age deposited coastal and shallow marine sediments in major parts of the NAFB. A pronounced unconformity marks the boundary with the overlying Molasse part of the basin infill.

The depositional history of the Molasse infill begins with deep-marine Flysch sediments of Palaeocene to Early Oligocene age, shown displaced by the thrusting (green in figure 2.2-1). Subsequently, in the Oligocene and Miocene, shallow-marine and terrestrial sediments were deposited, consisting mainly of material eroded from the emerging Alps to the south, and to a much lesser degree, from the uplifted parts of the northern foreland such as the Bohemian Massif. Therefore this clastic basin infill forms an asymmetric wedge of sediment, increasing in thickness from north to south. In detail the complex interaction of sediment supply, basin subsidence and sea-level fluctuations engendered shifts between marine, brackish and continental depositional environments.

The traditional subdivision of the Molasse sediments is based on lithological criteria because lithostratigraphy is easily traceable and thus allows correlation over wide areas. However, the boundaries of the lithostratigraphic sequences are known to be diachronous: with different lithological units deposited co-evally in different parts of the Basin (Figure 2.2-5). In addition the changing directions of the axial sediment transport as shown in figure 2.2-6, and the enormous quantity of sediment supplied by the gravel fans from the rising Alps caused a pronounced south to north migration of depositional environment during the infill of the Basin.

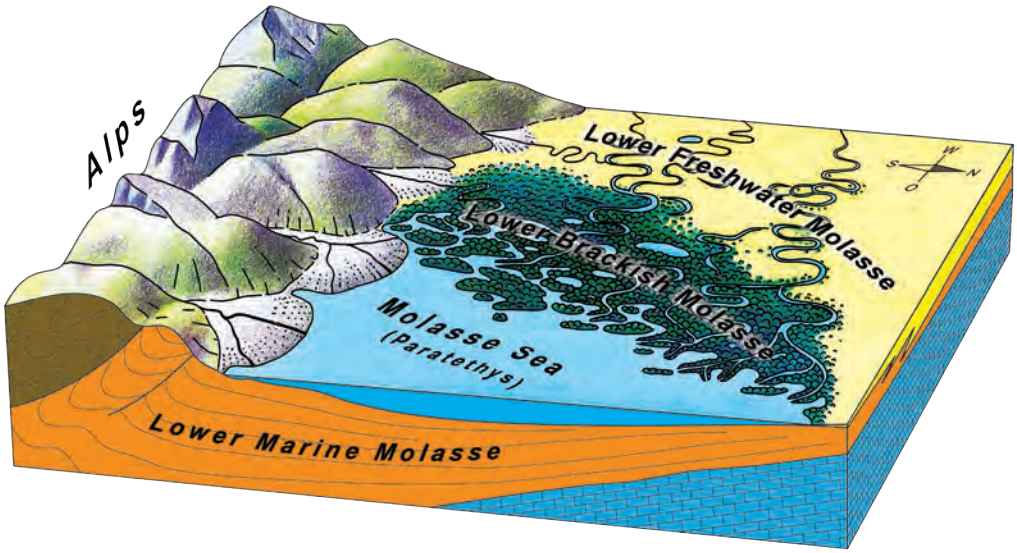

Figure 2.2-5: Depositional environment in the central part of the Molasse Basin during Egerium, approximately 27–21 Ma ago (from BAYGLA 2004) exemplifying the complex, diachronous facies changes during replenishment of the Alpine foreland basins. See paleogeographic maps in figures 2.2-7 for illustration of the changes of the depositional environment in space and time.

Two sedimentary megacycles can be recognised in the basin, both beginning with a marine transgression and ending with regression evidenced by the deposition of terrestrial fluvial and lacustrine sediments. The sedimentary sequence of the basin infill is traditionally divided into four lithostratigraphic units reflecting the evolving palaeo-environmental conditions: these are the Lower Marine Molasse (UMM), Lower Freshwater Molasse (USM), Upper Marine Molasse (OMM), and Upper Freshwater Molasse (OSM). As the changes in depositional environment did not affect the entire basin equally and simultaneously a Western Molasse and an Eastern Molasse can be distinguished with interdigitation occurring in the central (Bavarian) part of the Basin as shown in figures 2.2-5 and 2.2-6. The deposits of the Lower Brackish Molasse (UBM) and Upper Brackish Molasse (OBM) are considered to represent the transition zone between the Western and Eastern Molasse.

The Western Molasse consists of two megacycles separated by a pronounced hiatus in the transition zone, whereas in the Eastern Molasse only one megacycle is developed as marine conditions continued through to the end of the second marine period in the Western Molasse. These deposits were superseded by brackish, and subsequently fluviatile and lacustrine terrestrial deposits, of the OSM across the entire basin. The deposits of the second megacycle can be traced throughout the basin, but exhibit significant regional variations in thickness.

Characteristic of the entire Central Foreland Molasse and the adjacent parts, are antithetic and synthetic faults parallel to the long axis of the basin forming lineaments several tens of kilometers long and featuring displacements of several tens of meters, rarely as much as 100–200 m. The fault planes are usually curved with concave and convex segments. The concave segments of the overall prevailing antithetic normal faults provide the structural traps for most of the oil and gas fields that have been found in both, the Tertiary basin fill and its Mesozoic bedrocks (Figure 2.2-3 B)

In the central part of the Western Foreland Molasse, the Swiss Plateau Molasse, is characterised by predominantly flat bedding gently dipping towards the Subalpine Molasse (Figure 2.2-3 C), single open anticlines are recognisable. Further to the southwest, broad NE–SW oriented anticlines and N–S to WNW–ESE trending tear faults are common. The Sub-Jura Zone along the southern rim of

the Jura Mountains is characterised by various narrow anticlines, which also affect the underlying Mesozoic strata. Deformation zones and detachment horizons are to be found mainly in the Tertiary sequence (central and eastern part), whereas the western Mesozoic and Tertiary cover is detached by a décollement horizon.

In the south-western continuation, the French part of the Molasse Basin, wedged between the Jura Mountains and the Alpine orogeny strong compression formed N–S to NE–SW trending ramp anticlines partitioning the Molasse Basin fill into several sub-basins. The axes of these Mesozoic anticlines are displaced by several NW–SE transverse faults that acted as transfer faults during thrust tectonics.

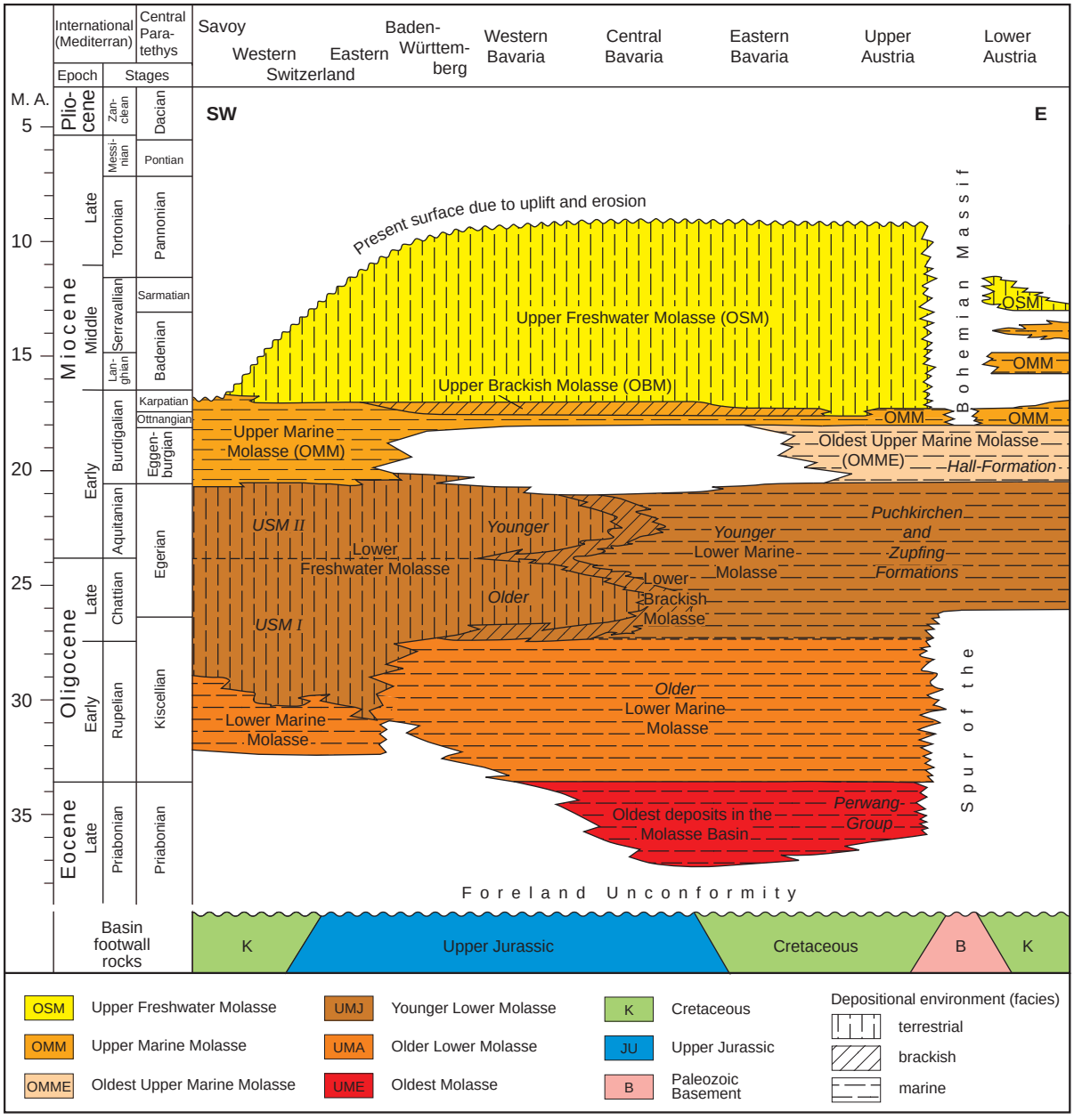

Figure 2.2-6: Lithostratigraphic units of the Molasse as distinguished in GeoMol's framework model, plotted versus the chronostratigraphic subdivision of the Molasse Basin fill. Some regional terms are listed in *italics* for comparison. The summarising SW–E sketch profile runs along a fictive axis in the Foreland Molasse. Certain variations may be due to the fact that the chronostratigraphic datings have been carried out also in proximal and distal parts of the basin. Heterochroneity in the UMM–USM transition in the Western Molasse e. g. is attributed to strong radial sediment supply by alluvial fans.

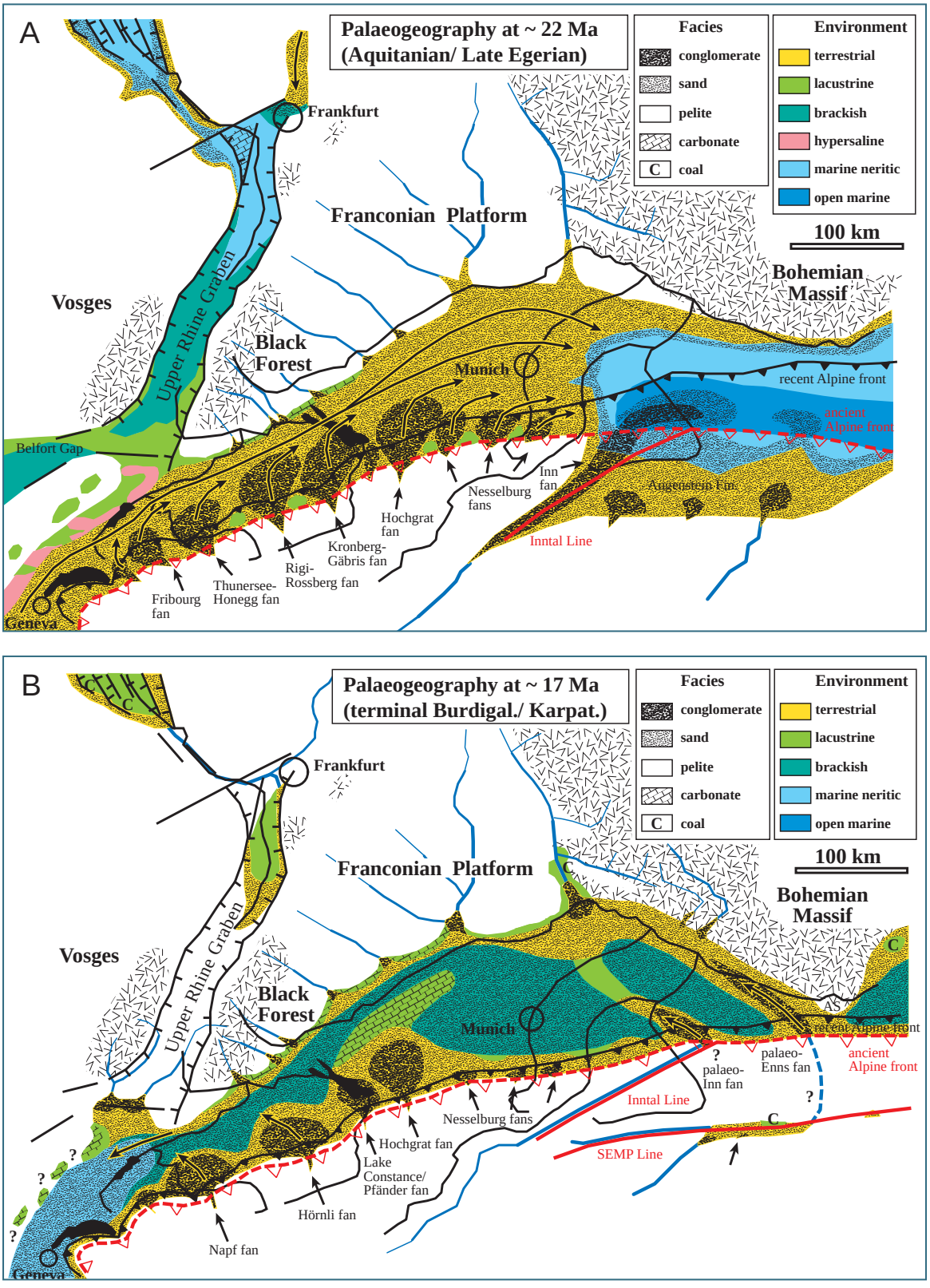

Figure 2.2-7: Sketch maps of depositional environment distribution in the Northern Alpine Foreland Basin and connected depressions during Late Egerian, approximately 22 Ma ago (A) and during Karpatian, approximately 17 Ma ago (B) (from KUHLEMANN & KEMPF 2008, slightly modified). The strong radial sediment supply through large gravel fans out of the rising Alpine front caused pronounced disparities in the marine–terrestrial transition specifically in the western Molasse Basin.

The easternmost section of the Molasse Basin is wedged between the Bohemian Massive to the north and Alpine thrust sheets to the south. Sedimentary evolution was strongly influenced by the spur of the Bohemian Massive dividing the basin into two parts up to the early Neogene. Pre-Tertiary NNW–SSE striking faults and Oligocene faults parallel to the long axis of the basin in W–E direction are predominant. To the far east faults are more strongly NW–SE oriented due to the basins position closer to the Carpathian mountain range. Alpine thrusting over large parts of the NAFB sediments resulted in a subalpine autochthonous part and an allochthonous so-called imbricated Molasse stack.

2.2.2.2 Depositional history of the South Alpine Foreland Basin

The Po Basin in northern Italy represents the retro-foreland basin of the Alpine orogeny and the (pro-)foreland basin for the Apennine orogeny. It consists of a faulted basement made up of Permo-Triassic sedimentary and volcanic sequences resting on the crystalline basement of the Variscan orogeny. The basement is overlain by a complex sedimentary sequence (Figure 2.2-8) dating from Late Triassic to Holocene. The oldest mapped units are Carnian evaporites overlain by a stack of Late Triassic to Early Jurassic platform carbonates, followed by a Middle Jurassic to Early Cretaceous succession of well stratified carbonates. These units are dissected by normal faults related to the Mesozoic extensional tectonics (Scardia et al. 2014) (Figure 2.2-9 D). The Carnian evaporites represent a regional detachment horizon (L1 in Figure 2.2-8) for the Alpine and Apennine thrusts.

Further up, an Early Cretaceous to Late Miocene stratified sequence of marls occurs, replaced by the clastic succession of the Gonfolite Group at the northern fringe of the basin. In this stratigraphic succession a major unconformity is related to the Alpine compressive tectonic phases (Livio et al. 2009). The marly deposits of Oligocene to Miocene age often act as a detachment level for thrusting (L2 in Figure 2.2-8, see also SW part of cross section D in Figure 2.2-9). In their upper parts they feature evaporitic episodes and coarse grained deltaic units, both at the fringes of the Alpine and Apennines orogenes. The intra-Zanclean unconformity (PL in Figure 2.2-8) leads over into the marine clay dominated deposits of Pliocene age which contain fine-grained sandy turbidites, while the intra-Gelasian unconformity is corresponding to the Apennines tectonic phases (Ghielmi et al. 2013).

The Quaternary succession is well developed, representing an up to 2,400 m thick basin fill of debris eroded off the adjacent Alpine and Apennines mountain belts and deposited by the Po river and its tributaries. This clastic sequence is subdivided into seven units (Figure 2.2-8) with lower limit surfaces defined by their respective age (Ma) and by the correspondent climatic stages (Marine Isotope Stage, MIS), when applicable. The lower four units mainly consist of marine sand deposits, while the upper four units are built up of sand and gravel units representing transitional and continental environments. Most of the surfaces confining these units correspond to unconformities, well developed especially at the Apennines margin and therefore very useful to constrain the tectonic evolution of the buried structures (mainly fold and thrust systems), within both, Alpine and Apennines domains.

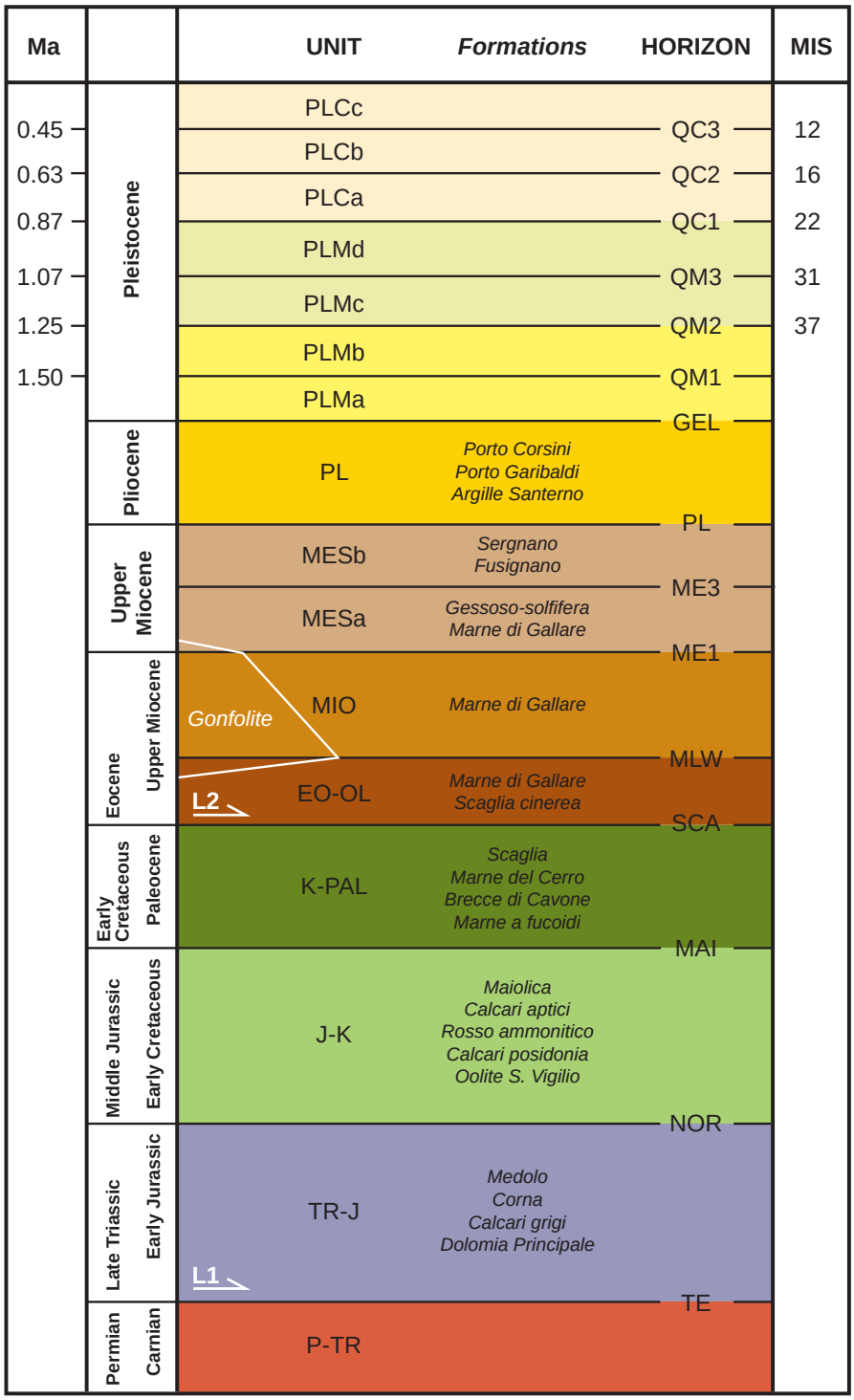

Figure 2.2-8: Stratigraphic scheme of the central part of the Po Basin as considered in the respective pilot area. The colours refer to the units as distinguished in the 3D geological model (cf. D in Figure 2.2-9). Only main formations are listed. MIS (Marine Isotope Stage) refers to climatic stages used for subdivision of the Pleistocene sediment sequence.

Figure 2.2-9 (following pages):
Cross-sections derived from GeoMol's 3D geological models as examples for the stratigraphic and structural makeup of the Alpine Basins: (A) in the Western–Central Molasse transition zone, (B) in the Greater Munich area as the focal area of geothermal utilisation, (C) in Lower Austria as the easternmost part of the NAFB, and (D) in the Brescia-Mantova-Mirandola area of the Po Basin. Note the contrasting stratigraphic subdivisions of the NAFB and Po Basin due to their disparate geological evolution.
Further cross-sections are part of the pilot area descriptions in chapter 8.

Cross-section A

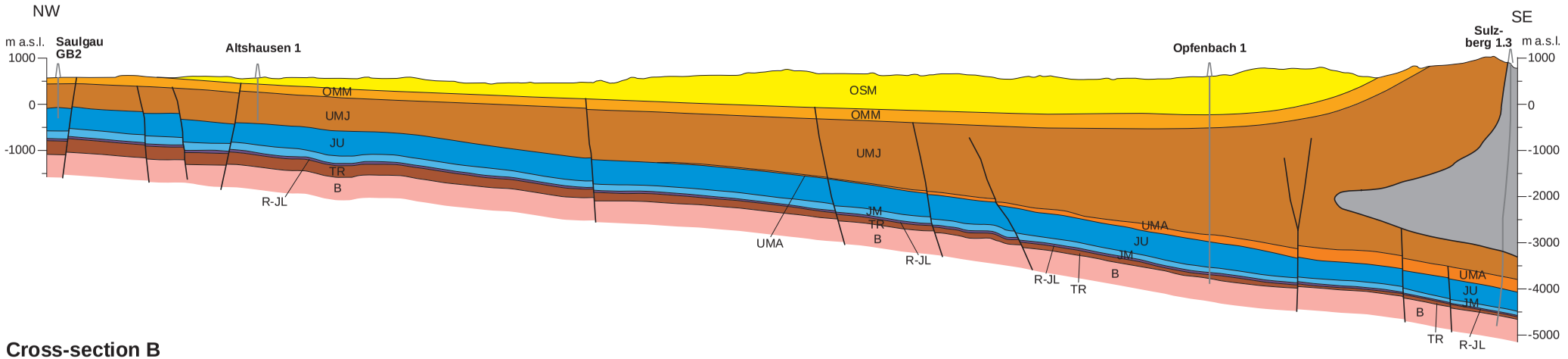

Cross-section B

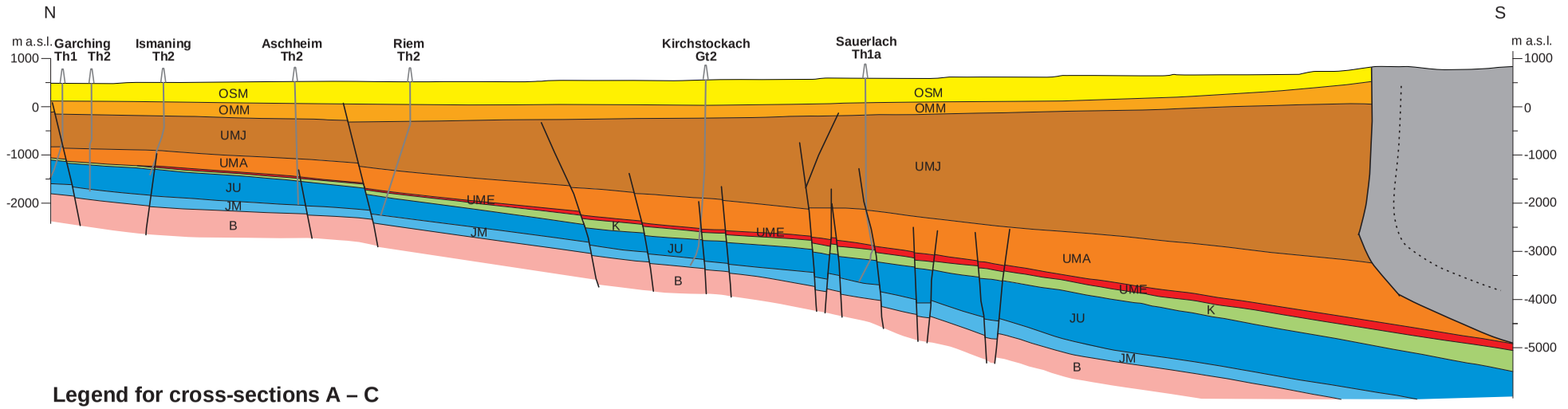

Legend for cross-sections A – C

OSM	Upper Freshwater Molasse	UMA	Older Lower Molasse	JM	Middle Jurassic		Subalpine Molasse and Alpine units not modelled in GeoMol
OMM	Upper Marine Molasse	UME	Oldest Molasse	R-JL	Rhaetian – Lower Jurassic		Borehole partly projected
OMME	Oldest Upper Marine Molasse	K	Cretaceous	TR	Triassic		Fault
UMJ	Younger Lower Molasse	JU	Upper Jurassic	B	Basement		

0 5 10 km

Vertical scale 2x exaggerated

Cross-section C

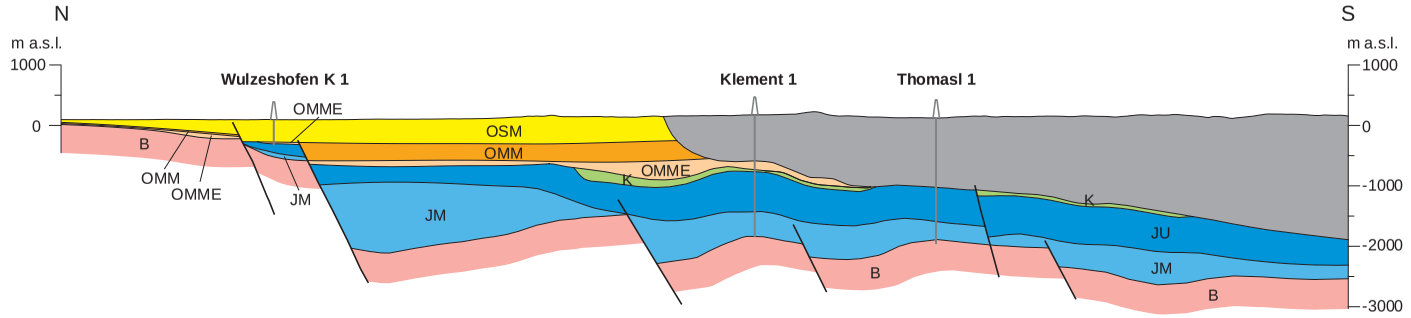

Cross-section D

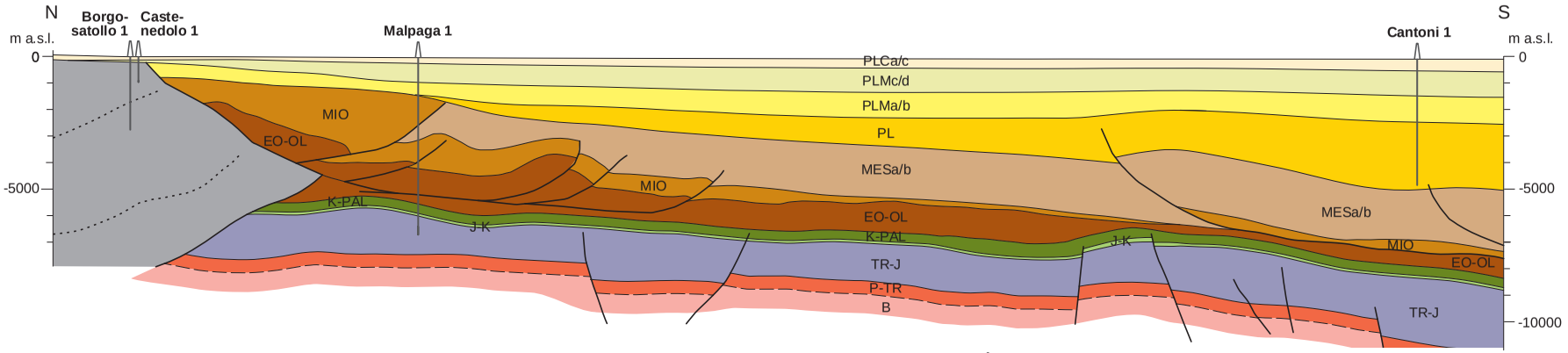

PLCa/c	Pleistocene continental units	MESa/b	Upper Miocene	J-K	Middle Jurassic – Early Cretaceous		Borehole projected
PLMc/d	Pleistocene marine upper units	MIO	Lower – Upper Miocene	TR-J	Late Triassic – Early Jurassic		Fault
PLMa/b	Pleistocene marine lower units	EO-OL	Eocene – Oligocene	P-TR	Permian – Carnian		
PL	Pliocene	K-PAL	Early Cretaceous – Paleocene	B	Basement		

0 5 10 km

Vertical scale 2x exaggerated

2.3 Geopotential setting – occurrence, issues, and approach

The term “geopotential” is used to generally refer to the Earth’s natural resources with regard to their capability for human use and valorisation. From the holistic point of view geopotentials consist of the natural environment with all the resources provided by nature: the favourable, utilisable ones as well as the unfavourable, harmful ones (e. g. MANHENKE 1999). Unfavourable geopotentials are also referred to as geological risks which can significantly constrain or entirely exclude the utilisation of the favourable geopotentials. Furthermore, as a result of the use of natural resources over the centuries, especially in primary industries and for building and dumping, man-made geopotentials have been created which in turn can represent an utilisable geopotential e. g. for urban mining.

Natural (geo-genetic) potentials		**Man-made geopotential**
Utilisable geopotential	**Unfavourable geopotential**	
Earth’s surface	Volcanism	Dumps and landfill
Soil	*Earthquakes (seismicity)*	Cavities
Building ground	Mass movement and landslides	Accumulation of substances
Groundwater	Swamp formation	
Geothermal energy	Salinisation	
Mineral resources	Sand drift	
Oil and gas	Flooding	
Storage formations		
incl. *karst as a reservoir*	Karstification (sink-holes)	

Table 2.3-1: Classification of geopotentials (from MANHENKE 1999, modified). The geopotentials considered in GeoMol are shown in italics.

In GeoMol only the natural geopotentials of the deep subsurface – as shown in italics in table 2.3-1 – are assessed and portrayed whereas groundwater preliminarily is considered in respect of its geothermal capability only. According to current knowledge mineral resources in an economically viable distribution are not expected in the project area. Likewise, after decades of investigation resulting in more than 250 discoveries the Alpine Foreland Basins are considered mature in terms of oil and gas exploration by the end of the 20th century. Most oil and gas fields are regarded as economically depleted, new large discoveries including unconventional targets are unlikely. Oil and gas potentials are portrayed only contextually with other conceivably competing geopotentials and to balance against possible geogenic risks. Depleted oil and gas deposits, however, feature a considerable potential for the underground storage of fluids. Hydrocarbon deposits are thus primarily addressed concerning their after-use within the scope of the storage potential.

Geological risks can substantially constrain or entirely exclude the use of geopotentials. Thus, any assessment of geopotentials also has to face up to the presence of geological risks, regardless whether naturally initiated or inducible by human impact. The only significant geohazard originating from the deep subsurface of the Alpine Foreland Basins is the potential threat of seismic activities. Major seismic events or perceivable earthquakes in the Alpine Foreland Basins are confined to the southwestern part of the Molasse Basin and to the Po Basin (Section 2.3-3).

Within the scope of the project the geopotential of deep geothermal energy and for underground storage of gas are evaluated. One principal objective of the Po Basin pilot area is the characterisation of buried active faults and seismogenic structures as the root of seismicity in the Po Plain. For each of these geopotentials as regarded in GeoMol the set-up and structural inventory of the subsurface is a crucial factor. Fundamentals for geopotential assessment are thus the 3D geological models as well as the spatial distribution of the temperatures at depths, based on data sets and methodologies as described in the chapters 6 and 7.

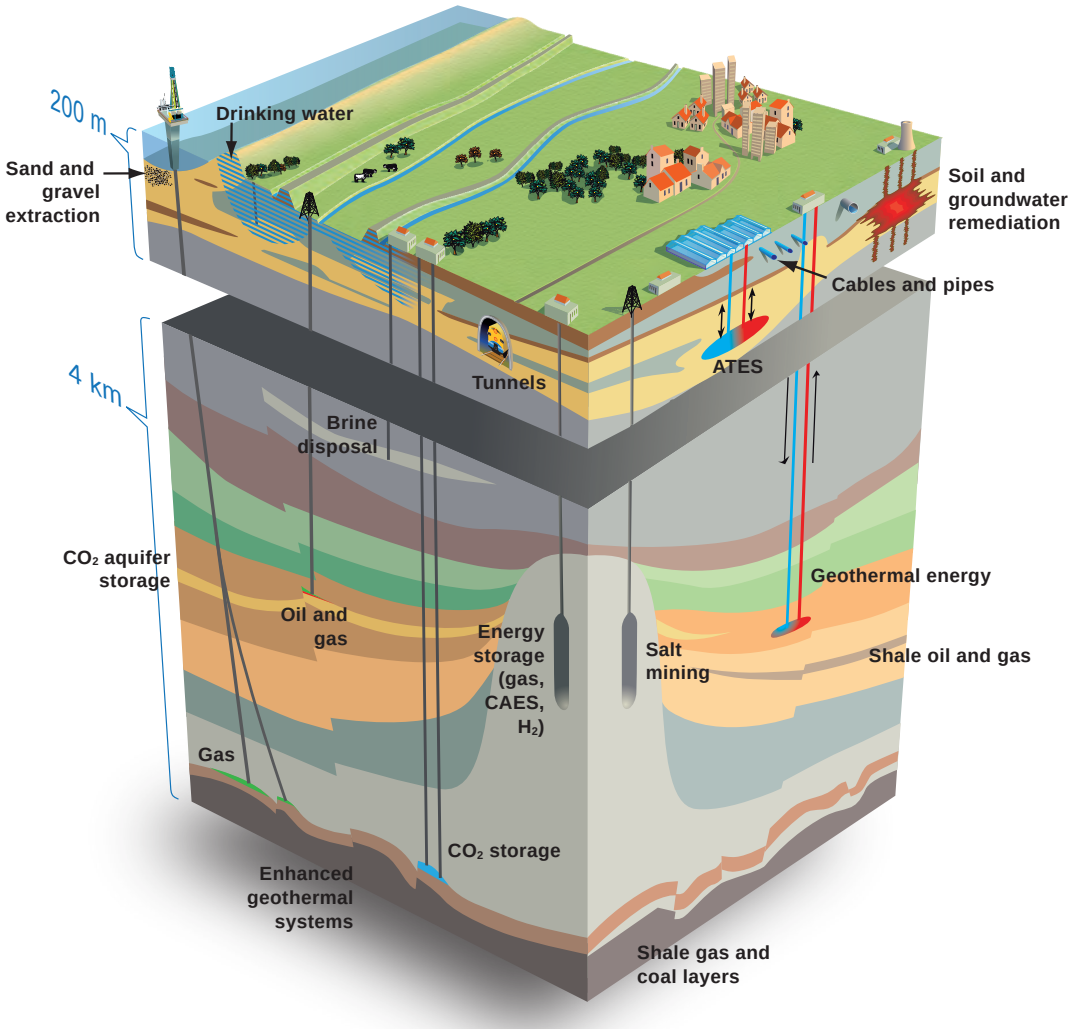

Figure 2.3-1: Synoptic view of geopotential utilisations (courtesy of TNO – Geological Survey of the Netherlands), ATES: Aquifer Thermal Energy Storage, CAES: Compressed Air Energy Storage

Major limitation on the significance and scope of the methods developed arise from the data availability. Most parameters essential for the detailed evaluation of geopotentials are classified data from primary industries only partially available in the project (Chapter 3.3). The geopotential assessment as implemented in GeoMol thus can be regarded as best practice under the given circumstances, considering the following properties of the subsurface:

- Lithological characteristics of the layered suites units on a regional scale
- Structural set-up of the major tectonic features, comparable to 1 : 100,000 scale
- Temperature distribution based on regional best fit approaches.

The methods as outlined in chapter 6 and 7 have been applied in the different geological settings of five pilot areas (Chapter 8) with a different focus on subsurface utilisations or on use restrictions due to geological risks.

The use of geothermal energy and the underground storage of e. g. wind and solar fuels are undoubtedly an enormous eco-political benefit and apply technologies which are well advanced, but are still an acknowledged high risk investment. GeoMol provides the fundamental information for mitigating these risks as far as potentially arising from geological issues and on a larger scale.

Further parameters for assessing e. g. the thermal potential, such as the volume flow rates of the fluids circulating in the subsurface, are not addressed. Also concrete in situ structures, local hydraulics and other parameters that require site specific investigations are not considered in GeoMol.

As the distribution density and quality of data available does not allow a differentiated evaluation of the various options of use in the deep subsurface the information given by GeoMol corresponds to a screening of the overall suitability, i. e. the assessment of the theoretical geopotential, of the units described (Chapter 6). Consequently, the information provided does not delineate realms of compelling evidence for one specific use or at least a particular capability.

2.3.1 Geothermal potential

Geothermal energy refers to the thermal energy generated and stored in the subsurface. The geothermal energy of the Earth's crust originates from the original formation of the planet (about 30 %) and from the radioactive decay of minerals in the Earth’s interior (about 70 %). For the Earth’s core, representing more than 15 % of the Earth’s volume, temperatures between 4,800 and 7,700 °C are assumed, and about 98 % of the Earth’s interior is hotter than 1,000 °C. The difference in temperature between the Earth’s core and its surface, the so-called geothermal gradient, drives a continuous conduction of heat from the core to the surface and an advective heat transfer by fluids or melts.

The geothermal energy in the Earth’s crust is stored in rocks and in vapour or fluids, such as water or brines. These geothermal resources can be used for the generation of electricity and for providing heat (and cooling). The geothermal potential describes the capability of the subsurface to make available this thermal energy. Geothermal technologies use these renewable energy resources to generate electricity and/or heating and cooling while producing very low levels of greenhouse gas emissions. They thus have an important role to play in realising targets in energy security, economic development and mitigating climate change (IEA 2011).

Generally, subsurface temperature within the Earth's crust increase with depth averages 30 to 40 °C per kilometre. In places of anomalies, such as volcanic areas, subsurface temperatures can reach several hundred degrees at depths of two or three kilometres forming high enthalpy geothermal resources. In the areas covered by GeoMol no high enthalpy systems exist. Thermal water of 100 °C or more, thus, occurs only at great depths, but might reach shallower levels when tapped by deep reaching faults.

With respect to temperature distribution in the subsurface three principal modes of use can be distinguished – shallow, medium and deep geothermal systems:

In the shallow subsurface (50 to 400 m), rocks and groundwater systems have a constant, year-round temperature of about 10 to 25 °C. Exploited by ground source or ground water coupled heat pumps using closed loops or wells for space heating solutions, this technology currently provides about 50 % of total geothermal heat worldwide (IEA 2011). The efficiency of shallow geothermal installations depends mainly on highly localised geological conditions beyond the scope of GeoMol.

At medium depths (from approximately 400 m to 3,000 m), the subsurface temperatures range between 25 and 100 °C. Water that circulates in aquifers or along faults and fractures can be pumped and directly used in thermal installations, e. g. for district heating, if water temperatures exceed 60 °C, or for heating greenhouses and balneology-wellness.

In addition to (open) hydrothermal systems, geothermal energy at medium depth can be also extracted by means of closed loop ground source heat pumps, as medium-deep borehole heat exchanger (MBHE) systems (Figure 2.3-2). This technology exploits underground temperatures at depths between 400 m and about 3,000 m. There is no exact limit for deep geothermal systems, which by definition directly utilise geothermal energy without additional enhancement of temperature (PK TIEFE GEOTHERMIE 2007), that means, they provide temperatures of more than 60 °C. Compared to the hydrothermal system, MBHE technology has little exploration risk concerning the choice of location.

At deeper levels (roughly 3 to 6 km), temperatures can reach almost 200 °C. Commonly exploited by tapping hydrothermal resources of deep-seated hot groundwater occurrences and piped to surface via deep wells, the heat is extracted by a binary cycle heat exchanger, and the cooled water is re-injected into the geothermal aquifer in a closed loop (geothermal doublet). The yield of heat extracted can be used for district heating or, if the water's temperature is well above 100 °C, for the economically viable generation of electrical power.

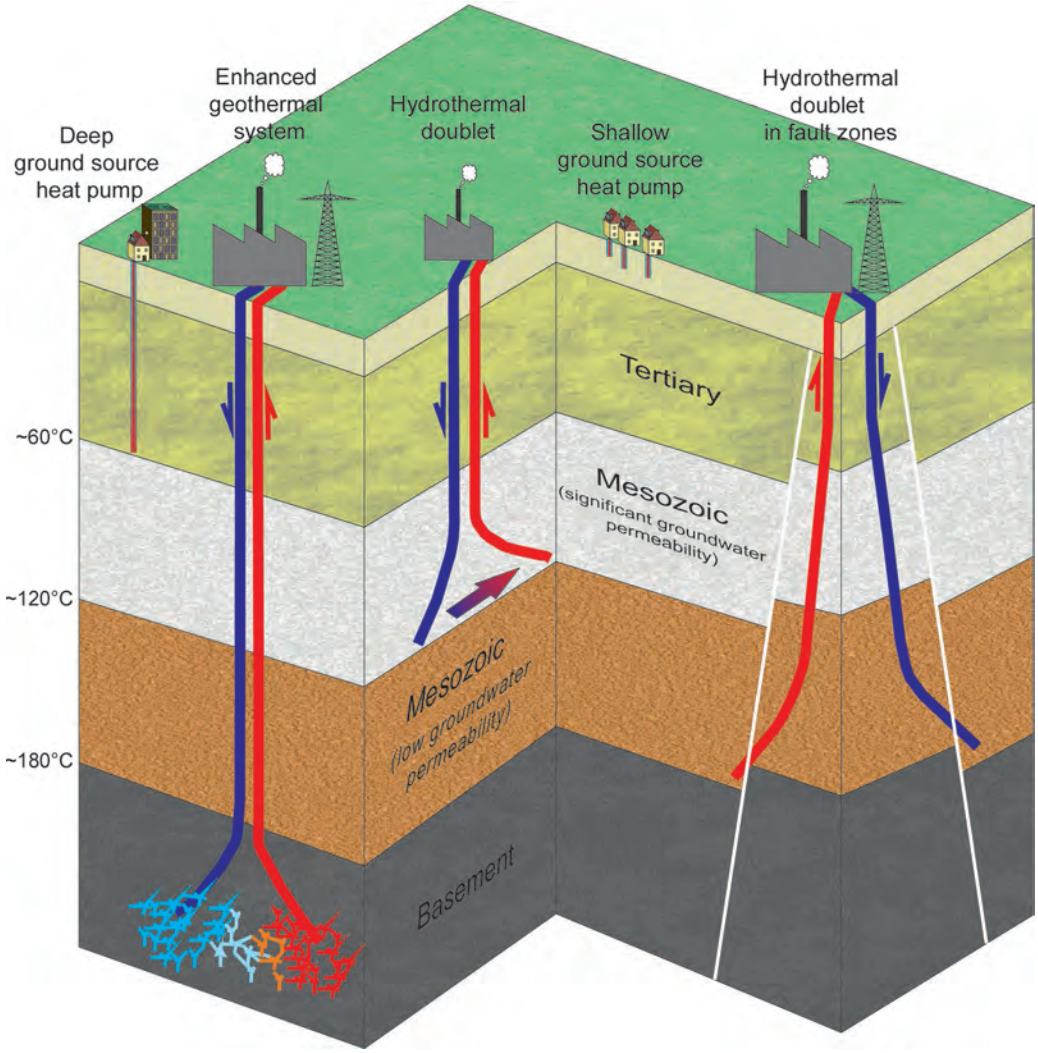

Figure 2.3-2: Principles of geothermal energy generation (from GEORG PROJEKTTEAM 2013, modified). The shallow geothermal potential is not considered in GeoMol.

At the same high subsurface temperatures but insufficient water or steam Enhanced or Engineered Geothermal Systems (EGS) are applied, geared towards to "stimulate" the rock mass by increasing its permeability. EGS is centred on creating large subsurface heat exchange areas allowing the water pumped down in a borehole to circulate and extract the heat stored in the country rock. Using one or several wells the heated water is produced to surface for energy generation similar to hydrothermal systems. The EGS technology has not been applied in the Alpine Foreland Basins yet.

Among the deep geopotentials of the Alpine Foreland Basins geothermal energy is by far the most important and most widely deployed. Even though foreland basins are considered hypothermal (cooler than normal) with low geothermal gradient and heat flow (Allen & Allen 2005) the Alpine Foreland Basins, particularly the NAFB, feature the highest geothermal potential in Central Europe: Due to highly productive aquifers at great depths an average geothermal gradient of about 3 °C/100 m in the NAFB – but varying considerably on a regional scale – and even less in the Po Basin allows for viable geothermal installations.

Early indications of thermal water aquifer systems in the NAFB and its bedrocks emerged since the hydrocarbon exploration campaigns starting in the 1930s. Encountering thermal water at a depth of about 1,000 m the Füssing (Lower Bavaria) oil exploration drilling in 1938 first furnished evidence (Nathan 1949).

In the Po Plain, naturally ascending (via transtensive faults) thermal waters of Sirmione (Lake Garda district) are known and used since the early 1900s for therapy and balneology, while thermal waters encountered at a depth of about 5,000 m by the oil exploration well Rodigo 1, north of Mantova, are used since 1975 for greenhouse heating and balneology.

Solely exploited for balneological use until the 1990s, geothermal energy has become increasingly important for energy generation over the last decade. Due to especially favourable conditions with respect to geology and the high exploitation of the utilisation potentials for district heating in densely build-up areas, the Greater Munich area at present features 15 deep geothermal installations for district heating or combined heat and power generation in operation or running-in tests (Figure 2.3-3), totalling a 150 MWt heat exchanger capacity. Beyond the present focus on the eastern Bavarian Molasse Basin further installations for hydrothermal energy generation are in operation, under development or in an advanced planning stage all over the Alpine Foreland Basins with major projects in Upper Austria, Geneva in Switzerland, Lake Garda district and Ferrara in Italy.

Geothermal exploration and development is an acknowledged high-risk investment. This applies in particular to the low enthalpy system of the Alpine Foreland Basins, where tapping suitable temperatures in the hydrothermal aquifer system requires drilling depths of more than 3,000 m. Varying hydraulic characteristics of the geothermal reservoir further increase the development risk as the actual local performance of hydrogeothermal installations strongly depends on the natural flow conditions in the deep aquifer system and the specific discharge. Spatial information on the physical rock properties is crucial for the dimensioning of the installation. This must include the characterisation of the fault network which defines the preferential flow path of the thermal water and the possible compartmentalisation of the aquifer.

The spatial interpretation of the fault network is a principal feature of GeoMol's 3D geological models. By providing structured volumes as the basic input for numerical hydraulic modelling, they not only assist the evaluation of the hydrogeothermal potential but also deep groundwater issues in general that have been rated a major field of interest in the stakeholder survey (Chapter 3.1).

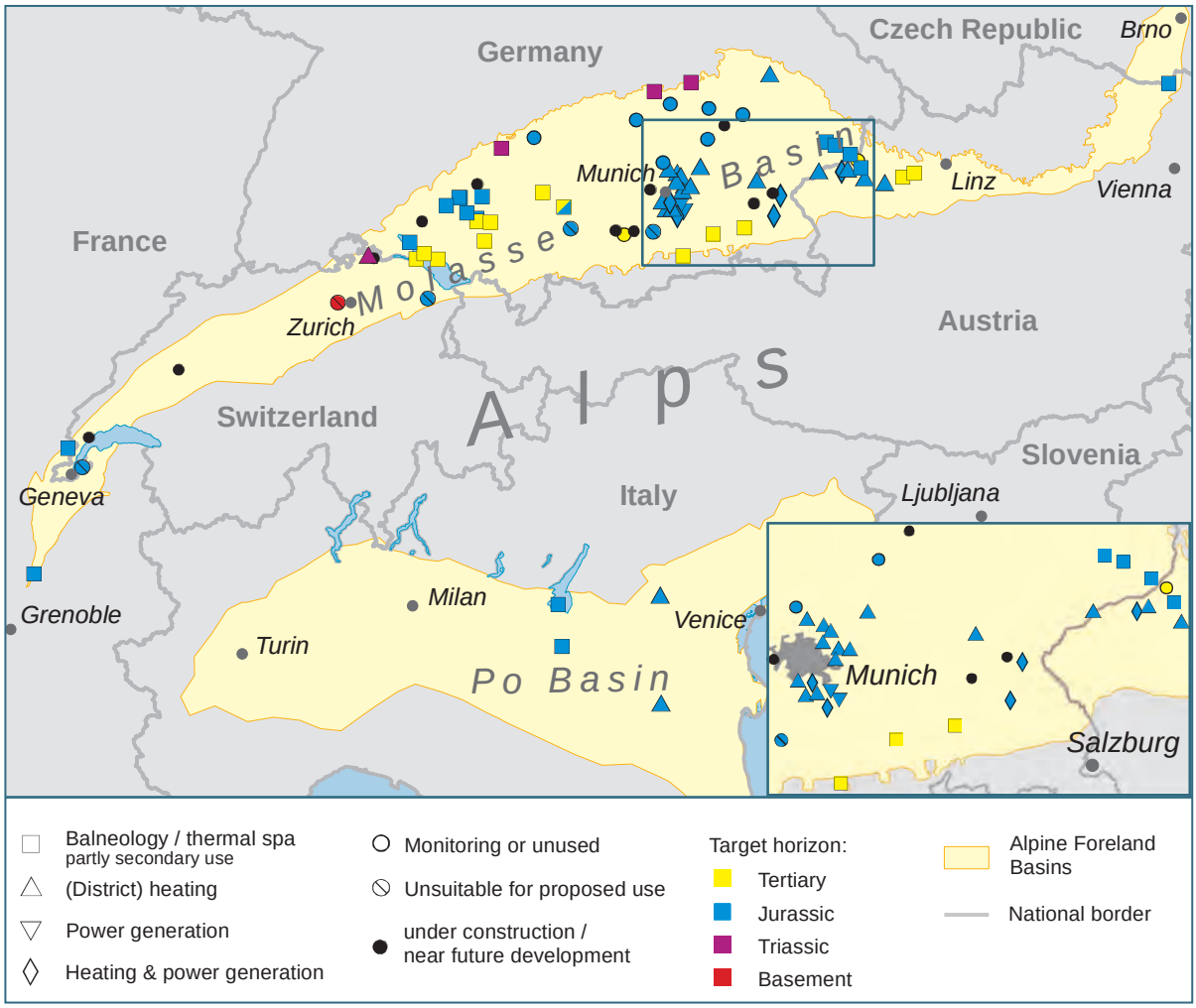

Figure 2.3-3: Geothermal installations within the Alpine Foreland Basins and their current use. Near future developments refer to projects with an approved operations plan.

The efficacy of geothermal installations also is greatly influenced by the temperature encountered at depth. Recently, the overestimation of temperatures required the substantial downsizing of a geothermal project and led to a significant financial loss. The need for a revised temperature model providing improved forecast accuracies has been evident from other temperature deviations as well. Thus, an effort has been made to compile an improved spatial temperature model, based on the comparison of the different methodologies for temperature modelling, the comprehensive review of all base data available and the validation of the different correction methods (Chapter 7). However, this improved temperature model requires a statistically adequate distribution and resolution of the base data. It could not be applied in all pilot areas.

2.3.2 Storage potential

Apart from use of geothermal energy for power and heat production the deep subsurface can be used for storage of fluids or gas such as methane, natural gas, compressed air or for the disposal of CO_2. The volume for large liquid or gas storage is most economically provided by suitable bedrock structures. Two principal types of underground storage potentials can be exploited: rock formations featuring an inherent high porosity (porosity storage reservoir) or solution-mined caverns in thick salt formations, especially salt domes (cavern storage). The efficacy of the seal of salt caverns is proven by the salt's physical properties and the cap rock. High porosity rock formations, e.g. limestone or sandstone, however, are suitable for underground storage only when covered by an impermeable barrier rock in structural traps. Depleted oil and gas reservoirs are the most commonly used underground storage sites because seal integrity is unquestioned and conversion from production to storage duty can take advantage of existing wells and gathering systems (Figure 2.3-4 B). Furthermore the volumetric heat capacity of rock suites can be used for direct Underground Thermal Energy Storage (UTES) particularly in dense rocks (e. g. Midttømme et al. 2008).

Target horizons for cavern storage do not exist in the Alpine Foreland Basins. At present, underground storage in high porosity rock formations is focused on safe-guarding the availability of gas by balancing the seasonal swings in demand and mitigating import disruptions. Overall 13 gas storage plants are in operation in depleted oil and gas deposits in the German and Austrian parts of the Molasse Basin, covering an important amount of the total installed working gas volume. Further sites are under development. The Po Basin hosts 9 gas storage sites in exploited hydrocarbon deposits, with three more under permission procedures.

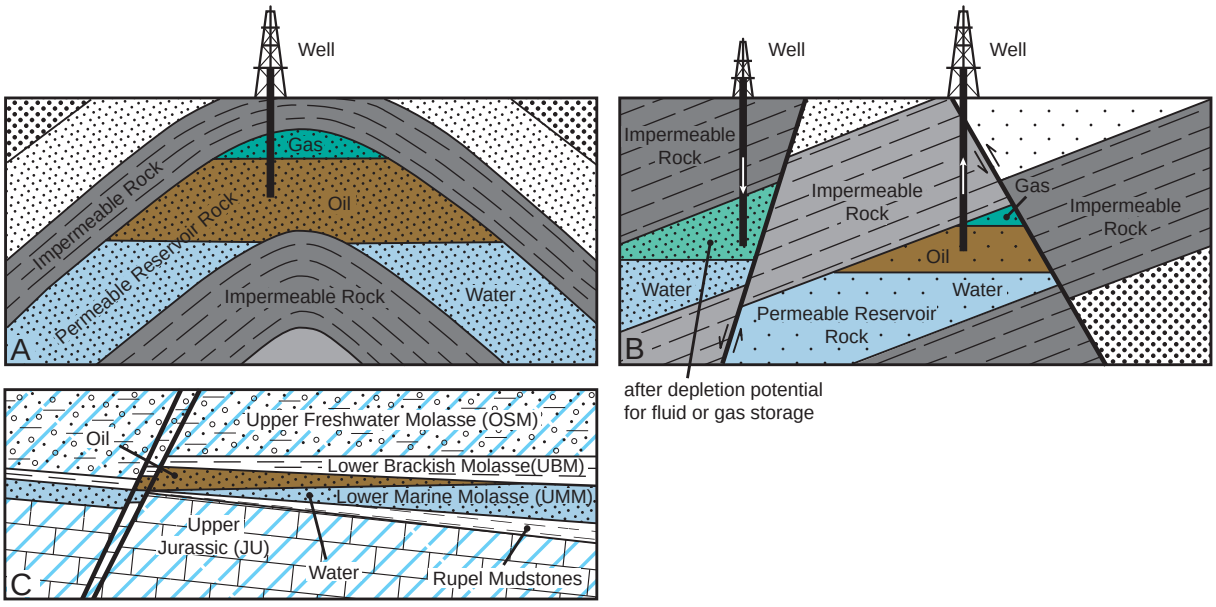

Figure 2.3-4: Schematic sketch of structural traps as occurring in the Alpine Foreland Basins, A: Anticlinal trap, B: Fault trap, giving rise to hydrocarbon deposits and (in B) their potential after-use for underground storage (from Nelson 2012, modified). Unlike in these schematic, vertically exaggerated cross-sections, the equivalent structures in the Alpine Foreland Basins are buried under a thick succession of younger undeformed sediments, thus, they cannot be detected and traced from surface exploration. C: Schematic cross-section portraying the principal setting of a hydrocarbon deposit bound to antithetic faults in the Arlesried oil field, western part of the Central Molasse (from Diepolder & Schulz 2011).

With the realignment of the energy policy increasingly geared towards sustainability additional subsurface space for the buffer storage of weather-dependent renewable energy fuels will be demanded and further use competition will arise (e. g. Crotogino et al. 2009). Moreover, a number of countries consider the geological storage of sequestered CO_2 in the context of Carbon Capture and Storage (CCS) an option for the effective reduction of greenhouse gas emissions.

Research in the field of underground geological storage of greenhouse gases and, to a lesser extent, of compressed air energy storage (CAES) and other solar and wind fuels is advanced and minimum requirements for the technical implementation are generally accepted. Key geological criteria for the selection of CO_2 storage sites include reservoir depth, thickness, porosity, permeability, seal integrity and – for storage in deep aquifers – salinity (IPCC 2005, Chadwick et al. 2008). Given the buoyant nature of gases, the proven efficacy of the topseal is an indispensable prerequisite for the long-term safety of storage sites. A general requirement for storing liquids and gas in the subsurface thus is the occurrence of sealing barrier rocks on top of the reservoir. Typical formations with appropriate sealing properties are clay, clay stone, marl and rock salt. The integrity of the seal is governed by the thickness of the barrier rocks and the presence (or absence) of faults intersecting the formation. A net thickness of the sealing formation of more than 20 m is considered secure (Chadwick et al. 2008).

Depths criteria are due to the reservoir pressure required to ensure the best capacity utilisation: For optimal storage saturation the injected CO_2 must be in a dense phase – liquid or supercritical. Thus the temperature and pressure conditions must exceed the critical point for CO_2 which, assuming an average geothermal gradient for deep basins of 2.5 °C/100 m, is achieved at a hydrostatic pressure corresponding to a depth of 800 m (IPCC 2007). At depths below 1.5 km, the density and specific volume become nearly constant. With respect to efficacy and economic viability the depth range between 1 and 2.5 km is considered most appropriate (Diamond et al. 2010). However, depths respectively pressure requirements are substance-specific and may be different for other fluids.

A first-step screening of suitable rock formations in the Molasse Basin has been implemented within the scope of studies for Baden-Württemberg (Fehn & Wirsing 2011) and Bavaria (Diepolder & Schulz 2011) as part of the project “Storage Catalogue of Germany” (Müller & Reinhold 2011) as well as for Switzerland (Diamond et al. 2010). An assessment study on possible usage conflicts of CCS and geothermal energy has been provided by Suchi et al. (2014). All these studies, however, have been carried out on a 2D basis and thus disregard the nature of the lateral sealing and the spill point as depending on the structural makeup. Especially in inclined rock suites like the sedimentary sequences of the NAFB effective structural traps are crucial to prevent the buoyant fluids from leaking up dip (cf. Diepolder & Schulz 2011). A three-dimensional revision thus can considerably downsize or fully eliminate certain target areas.

GeoMol’s 3D geological models provide comprehensive insight into structural inventory of the Alpine Foreland Basins as the key prerequisites to identify suitable structures for the long-term safety of reservoirs. They further feature information on the extension and thickness of potential reservoir rocks and adjacent barrier rocks.

Detailed evaluations and capacity planning as the basis for use prioritisation depend on porosity and permeability of the reservoir rocks. These parameters are part of classified data mainly from hydrocarbon industries which are only insufficiently available for a reasonable regionalisation. Consequently, the information provided by GeoMol does not delineate realms of particular capability for one specific use.

As discussed, pressure and hence minimum depth requirements for the reservoir rock are a substance-specific issue and may differ widely. GeoMol does not supply any storage potential assessments for particular depth ranges. Nevertheless, horizontal sections at any depth or sections along fault planes can be easily derived from the 3D models on demand.

To keep the outcomes general complies with GeoMol's overarching aim to provide harmonised and unbiased information and regards the diverging regulatory framework reflecting the political prioritisation in the member states of the GeoMol consortium. As a result of the public perception of underground storage in general and CCS in particular, mainly with regard to concerns about groundwater vulnerability and induced seismicity (e. g. Evans et al. 2012, Zoback & Gorelick 2012), the geological underground storage is under controversial public debate in many countries. Some governments already made use of the opt-out clause for a general prohibition of the underground geological CO_2 storage.

The three-dimensional compilation of the geological fundamentals can be regarded as the lowest common denominator for the assessment of storage structures, possible use competitions and risks of the geological underground storage. The theoretical geopotential for the geological storage of CO_2 is given for all model units of the GeoMol pilot areas (Chapter 8) and the Mura-Zala Basin (Chapter 9.3). A more detailed spatial assessment is provided for the Swiss Midlands area in chapter 8.2. Prioritisation of use, capacity planning and the verification of the environmental and economic viability require more detailed evaluations not provided by GeoMol.

The storage potential with respect to geological repositories is not considered in GeoMol. Depending on the country, even basic criteria for the site location procedure are not yet conclusively defined or under controversial political debate. However, the regional scale geological inventory as portrayed in GeoMol might assist the first step screening for site location once reliable criteria have been established.

2.3.3 Geological risks

Geological risks encompass all kind of natural hazards caused by geological conditions: Volcanic eruptions, earthquakes, tsunamis, mass movements (e. g. landslides), floods and sinkholes are a matter of common knowledge. Any utilisation of the subsurface has to face up with the presence of geological risks, regardless whether naturally initiated or inducible by human impact.

It is generally acknowledged that the seismic risk is the only major hazard as related to the subsurface of the Alpine Foreland Basins. Earthquakes usually evolve in the Earth's crust at depths of several kilometres and are related to rock stress and ruptures caused by tectonic processes such as apparent in recent orogenic belts like the Alps and Apennines. Even though hypocentres of stronger earthquakes are located at depths far beyond the reach of human impact, any major utilisation of subsurface potentials must consider the possible seismic risk.

In the northern Molasse Basin the seismic risk is comparably low, major earthquakes are few and far between, but featuring considerably more seismic events in the western part of the basin than in the Bavarian or Austrian parts. In general, most major seismic perceptions are long-distance effects of earthquakes induced by tectonic structures beyond the NAFB, such as the seismogenetic structures due to Alpine thrusting or the rifting of the Upper Rhine Graben. Destructions by earthquakes in historical times have been reported only occasionally for the south-western part of the basin, la-

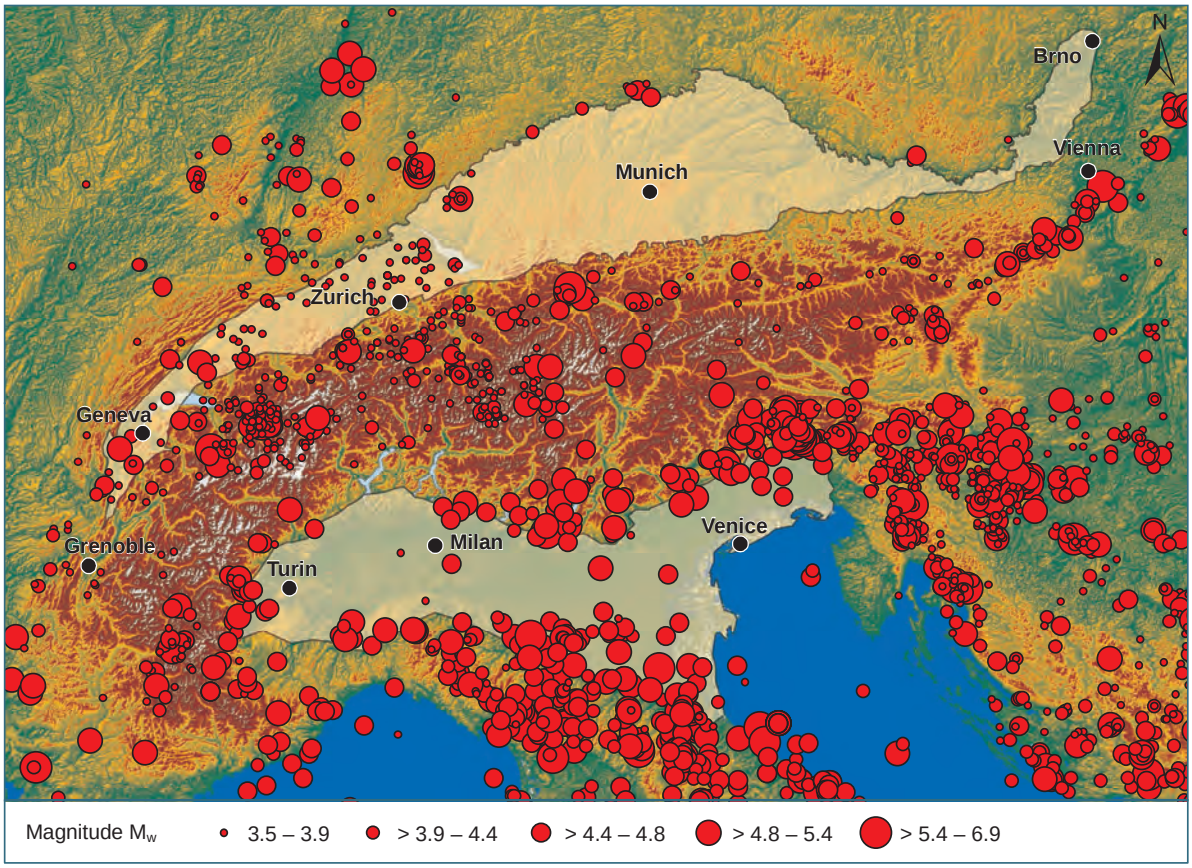

Figure 2.3-5: Locations of earthquakes > M_w 3.5 in the years 1900–2006 as related to the Alpine Foreland Basins (after GRÜNTHAL & WAHLSTRÖM 2012). See text for discussion.

tely near Annecy (Savoy) in July 1996 reaching a 5.3 magnitude (M_w). Wedged between the Alpine orogenic front and the Jura Mountains the ongoing Alpine thrusting has an enhanced effect.

On the contrary, the Po Basin, compressed between two opposite verging orogenic thrusts – the south-verging back-slip of the Southern Alps in the north and the north-verging Apenninic nappes in the basin's south – is characterised by a significant seismic risk, recently testified by the magnitude (M_w) 6.1 May 2012 seismic sequence in the Mirandola area.

The general framework of the historical (ROVIDA et al. 2011) and instrumental (PONDRELLI et al. 2011) seismicity shows that the greatest number of earthquakes which affected the Po Plain concentres south of the Po River. Prior to the May-June 2012 earthquakes, the most recent damaging earthquakes of the region occurred in 1971 and 1983 near Parma (M_w are 5.7 and 5.0 respectively), and in 1996 near Reggio Emilia (M_w 5.1). On the contrary, earthquakes are less numerous and do not follow any particular alignment north of the Po River, showing an apparently random epicentre distribution. Despite the difficulties in the interpretation of earthquake distribution patterns, the northern part of the Po Plain was the origin of the Veronese earthquake (1177, M_w 6.7), the most destructive earthquake in the area in historical times, and of other important events included between the mountain front and the more external (southernmost) buried Alpine thrust front (Basso Bresciano earthquake of the 1222, M_w 5.8; Soncino earthquake, 1802, M_w 5.7), or linked to the NE–SW Giudicarie fault system (Salò earthquakes, 1901, M_w 5.7). This seismic release pattern

is different from that observed east of the Schio–Vicenza Line, in the eastern portion of the Southern Alps, where it is mainly concentrated along the mountain thrust fronts and is associated with the important seismicity recorded both in historical and instrumental catalogues in the Friuli and Slovenia regions.

As evident from the 2012 Po Plain earthquake sand liquefaction caused by the seismic shock waves may strongly amplify the seismic impact. An assessment of seismic risks, thus, must also consider the distribution of unconsolidated sediments at shallow level alterable by seismic impact.

Sustainability of geopotential development requires a sound assessment of the geological structures which may generate a seismic hazard or enhance its impact – at least in those areas where a seismic risk is proved or assumed. A special study (Chapter 9.1) provides a three-dimensional characterisation of seismogenic structures in the most imperilled area. An evaluation of unconsolidated top layers which might enhance the earthquakes' effect is outlined (ISPRA 2015). The models prepared feature information on the structural set-up of the subsurface thus providing an important foundation of decision-making for the secure deployment of green energy generation and underground geological storage ensuring sustainability and consensual societal perception.

The 3D reconstruction of fault geometries is the fundamental constraint to any type of restoration and slip rates evaluation (Maesano et al. 2015a) and for the further steps in the construction of a seismic hazard scenario (Chapter 9.1).

3 User requirements and legal constraints of data policy

In terms of sustainability society increasingly demands that geological, environmental and resource issues are evaluated by a wider community of stakeholders than just the geoscience community. However, many of these potential users of the geoscience information do not have the training and knowledge to evaluate this data. So, they require the interpretations and information to be translated into a more understandable form for non-specialists. In contrast to data management and analysis systems designed to serve the general scientific community, consumer-oriented "off-the-shelf" products better reflect the needs of these non-geoscientific stakeholders (TURNER & D'AGNESE 2009). In order to deliver such tailor-made products to users such as planners and regulators GeoMol involved a wide variety of stakeholders in the design of its products. In addition, as a broader approach aimed at bringing the projects deliverables into line with the users' requirements, a stakeholder survey was conducted in the GeoMol partner states (Chapter 3.1).

However, the preparation of GeoMol's products could not be guided solely by the user needs. Their form and substance was also constrained by the diverse legal requirements of the partner states (Chapter 3.3). These affect both the availability of baseline data and the constructed models, with the need to balance the competing demands of data protection and freedom of information.

3.1 User requirements

To identify the requirements of users of subsurface information and potential clients with respect to GeoMol's products a stakeholder survey was conducted in spring 2013 at an early stage of the project. A questionnaire was designed to gauge the need for specific types of subsurface information and formats for delivery. This was undertaken independently from considerations of the actual feasibility of implementation and delivery within the GeoMol project. About 200 copies of the questionnaire were distributed in the various national languages of the partner states to stakeholders and clients for subsurface planning and resource information. The responses were regarded as confidential and are only to be used for the purpose stated. In all 78 completed questionnaires were received.

The evaluation of the feedback did not reveal any significant differences between the GeoMol partner states. So, the following analysis and summary does not consider between country variations, this is also because the products – based to GeoMol's objective to provide harmonised information – are intended to be uniform and applicable across the partner states.

3.1.1 User groups and business sectors of the survey participants

In order to adapt GeoMol's outputs to the user needs one objective of the survey was the classification of the participants into distinct user groups and business sectors. The participants were asked to classify themselves in terms of 8 pre-defined user groups and 14 business sectors, where appropriate, multiple answers were permitted (Figure 3.1-1). Even though the participants were selected because of their perceived interest in the study, we nevertheless selected as broad a spectrum of respondents as possible.

The largest three business sectors together comprising 48 % of the respondents are "project development", "governing authority" and "supply of services". In addition, "surveillance / regulatory functions", "research", "industry" and "communication / mediation" account for another 37 %. Six nomi-

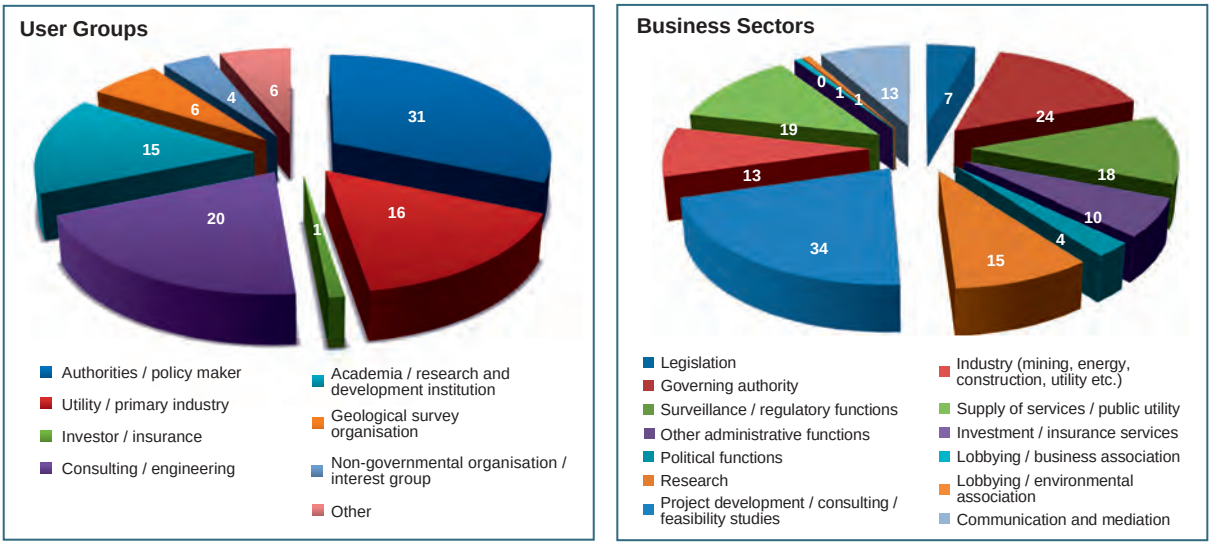

Figure 3.1-1: Pie charts showing the distribution of the respondents into user groups (left, n = 99) and business sectors (right, n = 159), for both multiple answers were permitted. Users groups quoted as others are water board (3), technology partner (2) and supplier of infrastructure (1) – business sectors quoted as others include trade associations, telecommunications, and the thermal and mineral water industry.

nations were made for “other affiliation”: these included trade associations, telecommunications, and the thermal and mineral water industry. There was only one response each for “lobbying / environmental association” and “lobbying / business association”, and none for “investment / insurance services”.

Concerning the educational background with respect to geoscience knowledge 60 % of the respondents regarded themselves as geoscientists, 28 % as non-geoscientists, 12 % left this question unanswered. Compared with the user groups and business sectors this obvious preponderance implies that geoscientists are appointed to cope with subsurface issues in non-geoscience sectors and so perhaps reduces the strength of the case for readily understandable interpretations for non-geoscience stakeholders.

3.1.2 Fields of activity of the survey respondents

The interests, and or, activities of the participants were further explored by two sets of polar questions, one referring to the relevant employment sectors and the other concerning their involvement (or otherwise) in specific subsurface resource issues (geopotentials). Each respondent was asked to indicate whether they were active or not (active) for nine fields and six subsurface resource types (geopotentials).

GeoMol’s objectives and scope meet the fields of activities and interest of the respondents to a high degree, and the products are not intended to be a principal tool for legislation and research issues. The geopotentials ranking coincides with the relevance of the regional level of detail provided by GeoMol. CO_2 storage and geological repositories are under active political debate and/or are lacking commonly accepted criteria for their evaluation. Site location assistance requires more detailed information than GeoMol can provide. However the GeoMol outputs can act as a useful framework within which to commence such more detailed site-level studies.

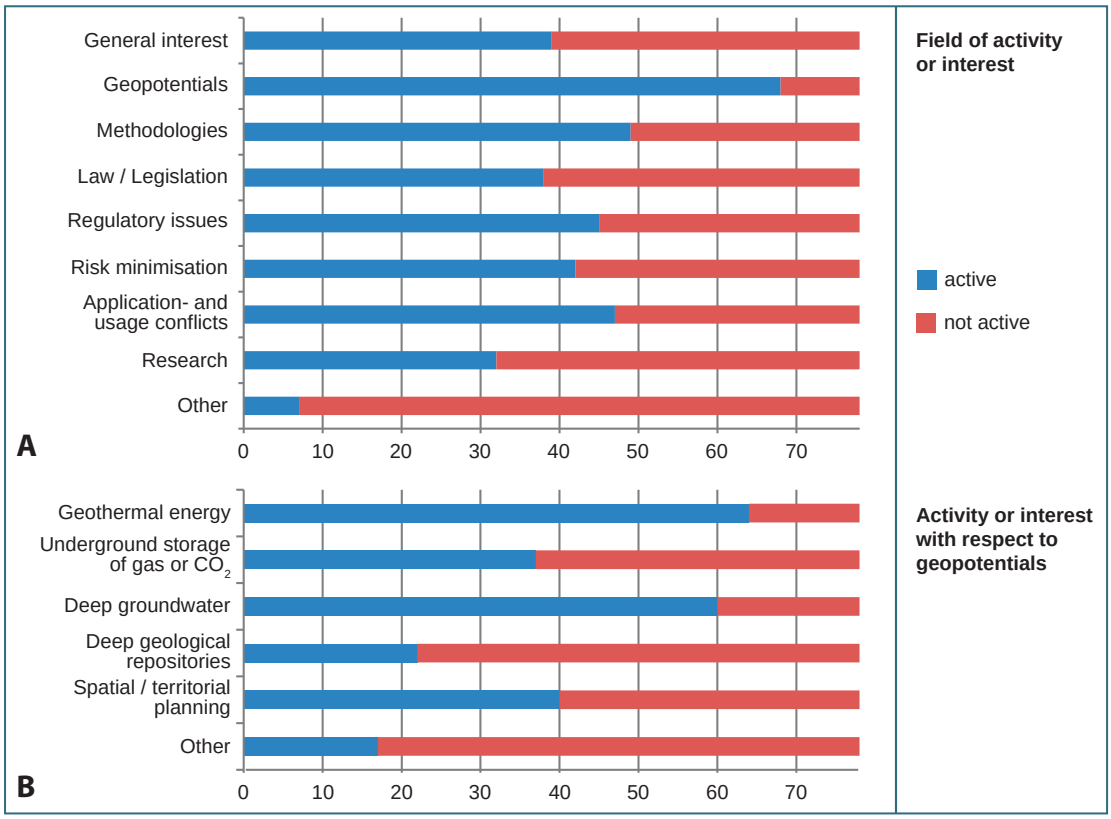

Figure 3.1-2: Cumulative bar chart (n = 78 per topic) showing the main activities or interests of the respondents with respect to their field of work (A) and their emphasis concerning geopotentials (B). “Others” refer to petrophysics, chemistry of deep waters, transmissivity of deep aquifers, spatial energy planning, thermal water, and underground infrastructure in the upper chart – to hydrocarbon exploration and production (oil, gas, unconventional gas), mining of mineral resources including coal, natural hazards, geosites / education, ground water / potable water treatment and management, mineral water and thermal water resources, as well as heat storage in the lower chart.

3.1.3 Desired products, features and formats

The principal objective of the stakeholder survey was to determine the requirements of potential users of subsurface information in order to deliver tailor-made products from the GeoMol project. Therefore a key part of the survey were questions on the product types, features and formats desired, this was carried out without regard to whether these could be effectively generated within the actual GeoMol project programme.

Using polar questions, seven types of common geoscience information output were rated as desirable or not (desirable) by the participants.

The chart in figure 3.1-3 shows no true preference for a certain product type, however, analogue maps do seem to be somewhat dated and out of favour. On the other hand, none of the digital products meet with overwhelming approval. A possible explanation might be that not all respondents are fully aware of the benefits of certain newer or more technologically advanced products. So, it also seems likely that technical hurdles may still be a major obstacle in the consequent use of digital products.

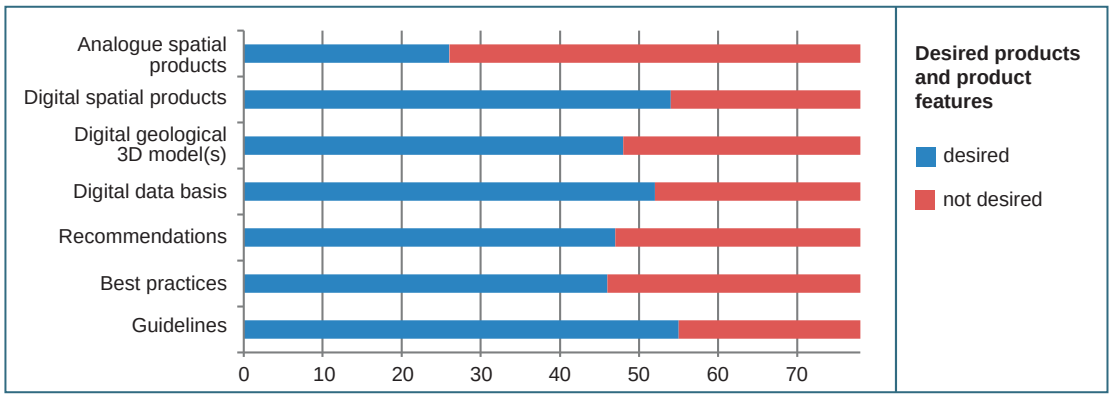

Figure 3.1-3: Cumulative bar chart indicating the non-preference for a certain product category (n = 78 per topic). See text for discussion.

The geoscientists who represent a major part of the respondents apparently prefer digital datasets which allow for easy combination in GIS with other information, distinct evaluations and alternative interpretations. Non-geoscientists favour off-the-shelf solutions (not data), supplemented by clear recommendations and guidelines. However this relation is blurred because also some geoscientist involved in licensing procedures prefer “frozen state” analogue maps because such immutable maps are indispensable in for the legal permits.

The further specification of the products desired revealed a clear preference for “digital vector maps and sections” which 80 % of the respondents consider useful, arguably because the GIS software needed for editing is widespread. “Editable extracts of 3D models” has been rated as desirable by 53 %, but this refers to existing 3D models that require the 3D modelling software in order to be exploited. This implies that although the merits of 3D models are undoubted only few institutions have the capacity to employ 3D modelling software. They prefer horizontal and vertical sections derived from 3D models which can processed by means of 2D workflows and GIS tools that are well established also in smaller institutions and administrative bodies.

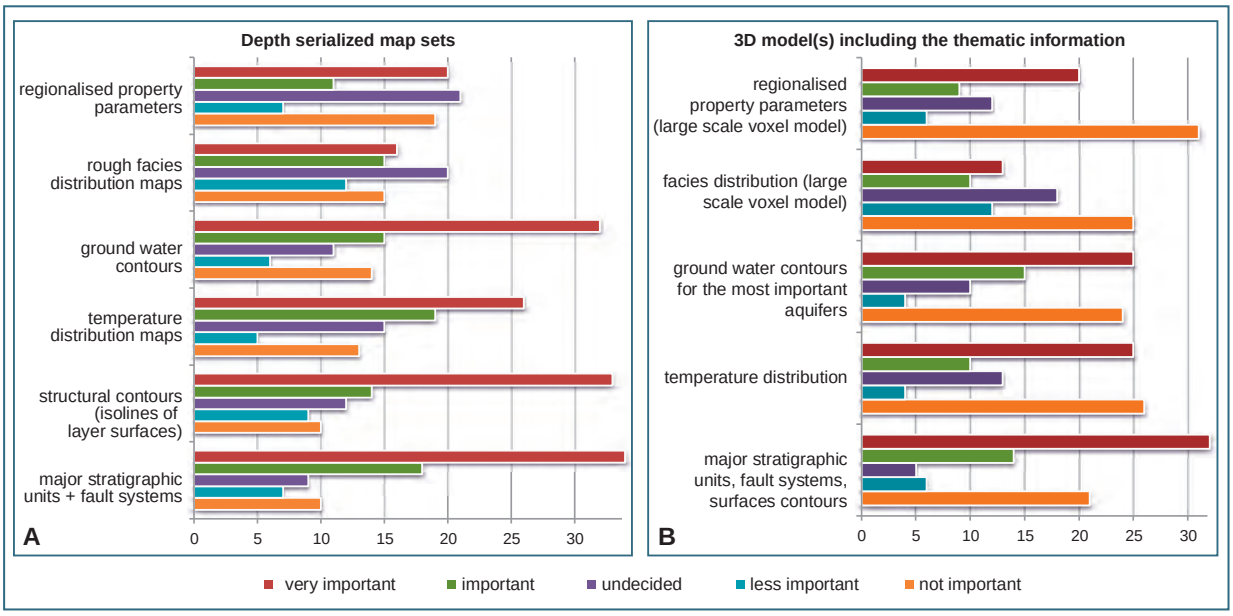

Figure 3.1-4: Bar chart showing the importance of features and products in the 2D domain (A) and 3D domain (B) as rated by the respondents (n = 78 per topic). See text for discussion.

For assessing the desirable content of the GeoMol products a five point *Likert* scale was used to query the “importance for daily work” ranging from very important through to not important (Figure 3.1-4).

The distribution pattern of figure 3.1-4 reveals a clear preference for “major stratigraphic units + fault systems”, and “structural contours” (both portrayed in 3D volumes), “ground water contours” and “temperature distribution maps”. “Facies distribution” and “regionalised property parameters” seem to be of less importance to the respondents. The obvious preferences of topics to be addressed in Geomol’s products correlate with the principal fields of activities or interest as summarised in figure 3.1-2. However, there seems to be a contradiction between the topics categorised as of lower importance in figure 3.1-4 and the prevalence of “geothermal energy” and “deep groundwater” in fields of activity or interest (Figure 3.1-2). This discrepancy implies that not all respondents may be fully aware of the relevance of “rock properties” and “facies distribution” which control rock behaviour e. g. with respect to permeability and thus the hydrogeothermal viability.

3.2 Legislation and strategies for subsurface planning

A further topic of the questionnaire was a personal, subjective, view regarding the legislation and strategies with respect to subsurface planning and the deficiencies encountered in everyday practice. This issue was addressed by means of polar questions with either nine of four possible responses depending on the question type. The responses are very varied with 33 to 48 % left unanswered. However, disregarding the nil returns, the remaining responses suggest that the main reasons for the wide range of opinions seem to be diverse planning procedures resulting from the highly fragmented administrative units and responsibilities (e. g. cantons in Switzerland, states, regions or counties in Germany depending on the issue) and the lack of overarching trans-national or EU regulations or implementing provisions. Spatial planning of the subsurface is breaking fresh ground. Unlike the scientific / technical requirements determined by a knowledge-based common understanding of the natural surface assets, practical subsurface planning is facing a paucity of established criteria and strategies to cope with the three-dimensional nature of the considered area.

The rather clear response bias concerning three questions underpin this assessment, even though there are considerable between country differences:

- only 16 % of the respondents indicate that there are national regulations or strategies on prioritising the geopotential resources,
- 76 % of the respondents indicate that new legislative requirements are needed to fill the gaps in present planning or licensing procedures to enable development of the subsurface potential,
- 81 % of the respondents would like trans-national strategies or guidelines (as would the EU).

Although here we are not interpreting a true, statistically proven survey the analysis of the responses on “legislation and strategies” allows a general conclusion to be made:

The large-scale impact of many subsurface activities clearly contrasts with the highly fragmented distribution of the spatial planning authorities and the differing regulations and criteria applied. To avoid conflicts and comply with the standards of sustainability a clear policy and applicable guidelines for a wider – preferably trans-national – field of application is now imperative.

3.3 Legal constraints of data policy

Responding to user needs, as summarised in chapter 3.1 was one of the guiding principles for the design and the preparation of GeoMol's outputs. In addition, distribution of GeoMol's spatial information is constrained in two respects by legal restrictions. Firstly, much of the baseline data used in GeoMol studies are classified as confidential or commercial in confidence, and the disparity in policy on data availability in the partner states, strongly impedes the cross-border harmonisation of the subsurface information. This caused uncertainties and omissions that could have been avoided if a matching data policy existed. Secondly, the dissemination of information involving confidential data is subject to different statutory provisions in the partner states but it generally has to balance the conflict between the data protection and freedom of information policies.

Because many data sets used in 3D modelling – as the foundation for all GeoMol products – contain confidential data, access restrictions require that all model building and further product preparation may only be implemented by the legally mandated regional or national GSO. For a trans-national project, geared towards providing harmonised information, this imposes particular requirements on the content and modes of dissemination in order to comply with both, national data policies and the EU's requirement for seamless trans-national information.

3.3.1 Availability of baseline date

Geological data at great depth as used in GeoMol, apart from a few research drillings all come from high investment exploration and production (E&P) activities, mainly for oil and gas, of late increasingly for deep geothermal. Seismic, borehole and rock property data are thus subject to business interests and mostly are classified as company secret. The following sections summarise the disparity in policy on data availability of classified data by giving an overview of the statutory provisions for all GeoMol partner states – with an emphasis on seismic data as the pivotal input for structural 3D geological modelling and thus geopotential assessment.

Austria: The law on geological resources (Lagerstättengesetz) regularises the obligation to report geological findings to the mining authority and the GBA as the legally mandated GSO, but does not specify the data types. Due to the lack of clear data definition, the obligation for data provision is met generally for borehole data, but, since the mid-1980s when digital data became the state of the art, not for seismic data. Data of modern seismic surveys as stored and maintained at the E&P companies are made available to the GBA on request, but only as a gesture of goodwill. Especially concerning data essential for time-depth conversion (cf. Section 4.4.2) and thus for the integration of seismic data into other, published information, a very restrictive disclosure policy is pursued by the E&P companies. Likewise, the publication of metadata as a qualitative indication of the uncertainty of the model is subject to substantial restrictions (Section 3.3.2).

In **France** the mining law (Code Minier) allows for the open access to most exploration data, regarding onshore hydrocarbon exploration wells immediately after finalisation of the drilling operations, for geothermal wells, offshore exploration wells and seismic raw data after a protection of confidence latency period of ten years. Well data of hydrocarbon production in operation are confidential.

The national *Bureau Exploration-Production des Hydrocarbures* (BEPH) is the central archive for all relevant data and the compulsory delivery point for all non-French E&P companies. After BEPH in 2006 has delegated the management of seismic and well data to the national GSO

BRGM, all seismic data held by BEPH and at French E&P companies was successively transferred to BRGM's *Guichet H* ("Counter for Hydrocarbon Data"), since 2008 also including all deep hydrocarbon wells. BRGM, thus, has unrestricted access to all seismic raw data and borehole information. These data are retrievable also via the web portal http://www.beph.net/.

In **Germany** the federal law on geological resources (Lagerstättengesetz) enacts the reporting obligation for all geological findings towards the authorised GSO in order to support their mandate to gather, store and evaluate information on the subsurface. This statutory duty for data provision covers borehole data was well as seismic surveys, however, the regulations are general in nature and are lacking clear implementation rules. For many decades the information reporting commitment in hydrocarbon exploration, was stipulated in a bulletin distributed by the mining authority of Lower Saxony, this was later extended to include digital data. These implementation rules have been widely enforced in other states of Germany and extended to other sectors, e. g. geothermal projects.

Accordingly, the data of E&P campaigns are stored at the companies and in the archives of the state authorities in charge. The State Geological Surveys are allowed to use these data within their core task of geoscientific surveying provided the outputs only show generalised information. Seismic data of the members of the Trade Association Oil and Gas (Wirtschaftsverband Erdöl- und Erdgasgewinnung – WEG) can be employed when older than 5 years and when at least 50 % of the 2D-lines respectively 3D-areas are located outside current concession areas. The use of data not complying with this accord or data from non-WEG companies have to be requested individually at the data owners.

In **Italy** the law on permits and concessions regarding hydrocarbon exploration and production (Attuazione della Direttiva 94/22 CEE relativa alle condizioni di rilascio e di esercizio delle autorizzazioni alla prospezione, ricerca e coltivazione di idrocarburi) obliges the E&P companies to provide entire set of well logs and the most representative seismic sections when the permit expires. This borehole and seismic information is published in raster format on the webpage of the Ministry of Economic Development http://unmig.sviluppoeconomico.gov.it/videpi. The entire set of seismic sections in an evaluable form, also for existing permits, can be solicited at the E&P company in charge for consultation. It may be exploited and published only with their case-by-case agreement.

In **Slovenia** there is no law which regulates the disclosure of findings of geophysical investigations. According to the mineral law geophysical methods are part of the mineral resources screening as a pre-investigation open to anybody and free of any obligation. Reporting obligations only exist for the holder of exploration (prospecting) permits and of mining permits (exploitation). However, neither type of permit states seismic or geophysical investigations. In practice, seismic data are considered company property of the E&P enterprise giving them the sole discretion to whom and how they provide the data. Thus, also public archive acts do not apply and effectively no seismic sections are available for the GSO.

Concerning borehole data the mining law requires a mining exploration permit for all boreholes deeper than 300 m. Borehole data from exploration campaigns is stored at Geological Survey of Slovenia, GeoZS, performing the mining related public service for the mining authorities. All water wells of more than 30 m depth and of water wells drilled in the water protection zones require a ground water exploration permit from the Slovenian Environmental Agency (ARSO) according to the Water Law (Zakon o vodah). It is foreseen that the metadata of these water wells will

be open disclosure via the Internet in the future, as part of the Environmental Atlas of Slovenia (http://gis.arso.gov.si/atlasokolja/profile.aspx?id=Atlas_Okolja_AXL@Arso). Boreholes of less than 300 m depth and not drilled for water purposes are not regulated.

As **Switzerland** comprises 26 cantons and subsurface regulation is under their sovereignty, up to 26 different regulations may apply – there is no federal regulation for the provision, storage and retrieval of underground data. The laws applied concerning data ownership and disclosure of subsurface data are found in the civil code (paragraphs on ownership), the copyright law and the intellectual property rights, the latter solely for processed and interpreted data. In only very few cantons regulations exist that require the contractors (E&P companies) or their clients to provide the data to the relevant cantonal authority. Access is usually restricted and closely tied to projects with limited duration. In all cantons without an explicit regulation the data is the property of the contractor and the National Archives Act only applies if public bodies are the contracting authorities. Only for those projects, which receive federal co-funding, authorities have enforced the data owners to supply the data to swisstopo as the national GSO in recent years.

Data on rock characteristics, e.g. porosity and permeability parameters which control the reservoirs' volumes and thus the economic viability of the deposit, are among the best kept secrets of the E&P industries. These physico-chemical parameters of the subsurface, when covered by the statutory provisions as above, are available only in terms of global average values from few publications.

Accordingly, in France property data and borehole logs are available for the national GSO via the *Guichet H* ("Counter for Hydrocarbon Data").

In Germany these data are archived at the legally mandated GSO and, according to an agreement between the E&P board on data exchange and the *KW-Verbund* ("hydrocarbon network"), at the *Kohlenwasserstoff-Fachinformationssystem* ("hydrocarbon database") maintained at the Geological Survey of Lower Saxony (LBEG). Access and data retrieval is granted to the entitled members of the *KW-Verbund* based on a general confidentiality agreement. The hydrocarbon database includes also data from geothermal projects.

Even though these property data are available in some countries for the use of geoscientific surveying and for outputs as generalised information, their data density is viable for a regional scale geopotential assessment – as required in GeoMol – only in rare cases. Consequently, the information provided corresponds to an assessment of the theoretical geopotential.

Temperature data constituting the foundation of temperature modelling (Chapter 7) are more commonly available from the technical borehole records covered by the statutory provisions as above. However, the quality of the records varies widely and only few are suitable for temperature correction methods as required for a regionalised, depth-dependent temperature prognosis (Casper & Zosseder 2015, see also Chapter 7).

3.3.2 Legal constraints on data publication and dissemination of products

The dissemination of information based on confidential data is subject to legal restrictions in order to comply with data privacy, so that the underpinning hard data cannot be observed or derived from the resulting outputs. A 3D geological model is a virtual representation of the form of the subsurface. It is created from datasets such as borehole records, surface geological maps and geophysical data (most notably seismic) by the interpolation between these interpreted data points. As a rule, this interpretation and spatial interpolation brings about sufficient blurring of the data, and trends within it, that the underpinning data cannot be derived. However, as the accuracy of the geological model is dependent on the density and distribution of the data used, a plot of the distribution of the baseline data is often supplied to give a qualitative indication of the uncertainty across the model area. Provision of such metadata may still be subject to substantial restrictions placed on the data by the owners (cf. Figure 4.1-1).

The combination of zoom features and advanced query tools generally allow for a detailed inspection and analysis of 3D geological models and thereby some back-engineering, hence “de-anonymisation”, of the baseline data may be possible. Generalisation of the topographic information is an additional means of blurring the actual location of the data used. All spatial products of the GeoMol project, including 3D geological models and derived 2D map outputs, are being provided in digital form via web services. Thus, they can be arbitrarily combined with any other digital georeferenced spatial data that itself can provide high resolution positional information.

Furthermore, subsurface data is considered as information related to the Environment. Thus the regulations that ensure freedom of access to information (FOI) to all Environmental data held by public authorities (EU 1990), apply here. This means that GeoMol has had to make provision for improved access to its information for public awareness, but taking into account the restrictions regarding ”commercial and industrial confidentiality, including intellectual property” (IPR) and “the confidentiality of personal data and/or files” (cf. EU 1990, 2000). A more comprehensive discussion of the statutory issues of the GeoMol products arising from inconsistencies of these diverse legal restrictions, examined within the German regulatory framework, is presented by Diepolder (2015).

As a result, taking account of both the users’ needs, as described in chapter 3.1, and the balance of legal requirements between data privacy and freedom of information, the following modes of dissemination have been deployed by the GeoMol project:

- The original 3D geological models containing all baseline data are kept confidential and are maintained at the respective legally mandated GSOs. These can be iterated with any relevant new scientific findings or interpretations, improved data holdings and modelling software. These comprise the project’s internal **Live System** and form the basis for all the detailed and site-specific disclosure of information. Access and data retrieval is only granted on request to those institutions entitled to such data, and this is subject to a confidentiality agreement. This confidentiality agreement applies also to those parts of the live system’s 3D models which may be made available to research institutions and external experts for further processing and upgrade – like model parameterisation or numerical modelling, and their feedback for the incremental improvement of these models.

- The web application **MapViewer** for web-based visualisation and interactive analysis of 2D thematic maps is provided to meet the user needs (Chapter 3.1). These off-the-shelf maps are derived from the 3D Live System from May 2015 onwards. The MapViewer enables the user to

select, query, analyse and print the 2D thematic maps from the GeoMol Project areas via a web map service (see Chapter 10.3) and is complemented by appropriate metadata information. The maximum permitted scale for visualisation of these maps is 1 : 80,000, this is deemed sufficiently general (low resolution) to prevent the derivation of any specific underpinning confidential data.

- the **3D-Explorer,** a 3D browser-analyst for the web-based visualisation of open source 3D models featuring query tools to generate synthetic boreholes and vertical and horizontal cross-sections (see Chapter 10.2). Two different, role-based access modes are provided: a password-protected access to the more detailed 3D models of the GeoMol pilot areas and a public domain portal to the framework model to raise the awareness of the public to the subsurface conditions. Both access modes are subject to the users' acceptance of the *terms of use* stating the limitations of the data especially with respect to the resolution of its use.

A comprehensive description of the different tools and methods for the distribution of the GeoMol project results, through an interconnected collaborative environment serving the respective GSOs, is given in chapter 10.

4 Baseline data and data preparation

A major challenge in 3D modelling at great depths is the availability of data with an adequate distribution and resolution to address issues properly. Even though several 3D geological models on or comprising parts of the Molasse Basin have been built over the last years (e. g. Rupf & Nitsch 2008, Pamer & Diepolder 2010, Sommaruga et al. 2012), the merger of existing 3D geological models by just filling the gaps in between is not feasible: they are made for different purposes and address distinct issues, and are based on different baseline data originating from multiple sources and various dates of origin. Thus, providing coherent 3D geological information imperatively requires harmonisation from the very beginning of the model building workflow starting with the selection and preparation of the input data applying consistent methods and common parameters.

Principal baseline data for GeoMol's 3D geological models are seismic data, scattered and clustered deep boreholes and a variety of geological maps and contour line drawings that are available in all partner states. However, the disparate legal framework of national data policies (cf. Chapter 3.3) specifically concerning the provision of industrial data had a strong influence on the availability of this fundamental information and prevented the share of data among the GeoMol partners. All classified data had to be retained at legally mandated GSO and harmonisation procedures were performed discretely, but using jointly defined rules and parameters. Data availability, thus, is described separately for each country respectively the GSO in charge showing marked differences in the GeoMol partner states (Figure 4.4-1). This implies that all partners make use of their existing data infrastructure. Only derived products (models, interpretations) and metadata is shared via the GST infrastructure (Chapter 10).

4.1 Seismic data

By far the largest data pool for 3D modelling input is the network of 2D seismic sections. A variety of seismic surveys, including raw or reprocessed older 2D lines from hydrocarbon exploration exist in all countries. New 2D lines and 3D surveys are available only in areas of recent focus on geothermal exploration. Overall more than 28,000 km seismic lines have been compiled, reprocessed and harmonised as the basis for structural 3D modelling, to interconnect legacy 3D geological models in their true spatial relation and to integrate cross-sections of earlier syntheses implicating the concepts and tacit knowledge of decades of geological expertise. Where available, the base data of recent syntheses have been re-processed in compliance with GeoMol's best effort workflows to achieve trans-border consistent results. The reprocessing of the seismic sections using comparable parameters ensures a better comparison and correlation of seismic facies across the Alpine Foreland basins.

Various issues had to be addressed for the harmonisation of the seismic data: Two types of seismic data had to be combined, raw and processed. Acquired since the early 1950's the processed data show heterogeneous quality and processing parameters. Thus, it is imperative to harmonise the data prior to further analysis applying consistent parameters and methods in reprocessing to avoid misfits at crossing points between seismic lines and artefacts at the country borders. A principal challenge was to harmonise all lines at the same seismic reference level, static replacement, amplitudes and step of signal processing from France to Austria, in an area spanning more than 1,000 km in length (Capar et al. 2013). However, the vertical difference of more than 700 m between the surfaces of the different parts of the Molasse Basin, impeded the use of one uniform datum plane. Instead several, somewhat levelled values have been used to settle differences between certain segments (Table 4.4-1 at the end of Chapter 4).

The selection of seismic data was based on a number of criteria applied in all sub-territories:

- availability of raw data or reprocessed data,
- quality of data and acquisition parameters,
- location within the study area to optimise the coverage and to achieve a consistent spatial distribution,
- proximity of wells to guide the geological interpretation,
- preference of profiles with complete metadata and processing data description.

In **France** about 780 km of seismic lines, acquired between 1957 and 1990 by different companies could be used – 215 km reprocessed prior to GeoMol, 565 km reprocessed within the project. For the Swiss part of the **Geneva-Savoy** pilot area 23 migrated seismic lines acquired between 1973 and 2010, totalling about 200 km in length, could be integrated.

In **Switzerland**, the seismic interpretations of the Seismic Atlas of the Swiss Molasse Basin (Sommaruga et al. 2012) were used. 263 already reprocessed seismic sections were selected from 1957 to 1994 acquisition campaigns.

While in **Baden-Württemberg** only seismic interpretations can still be retrieved from surveys of the 1950s to mid-1970s, large-scale plots of seismic data are widely available from seismic surveys carried out since the mid-1970s. Out of the seismic data available at the LGRB archive, 135 plots from surveys carried out between 1975 and 1991 have been selected for a digital reprocessing in time domain.

In **Bavaria** all seismic data acquired in the state's territory is archived at the LfU, however, only data of the last two decades are available digitally, older seismic sections are on hand as paper plots. Within the GeoMol project 467 seismic lines have been digitised, reprocessed and migrated into the time domain. Overall 8,777 km of seismic lines are now available in digital SEG-Y format which corresponds to 44 % of the total length of 2D seismic data in Bavaria.

In **Austria** 65 seismic lines with raw seismic data were made available by the Austrian companies OMV and RAG. They were originally acquired during the years 1963 to 2002. The seismic data was reprocessed by the Institute for Water, Energy and Sustainability (Joanneum Research). Of the 65 seismic sections, 16 sections were newly reprocessed while post-stack processing was carried out for 38 sections. The remaining 11 sections originated from a 3D seismic project and did not require any additional processing.

For **Italy** 759 seismic lines with a total length of 11,900 km were available for modelling the Po Basin pilot area and the wrap-around. Most of the seismic data was acquired in the 1952 to1991 period and further reprocessed by ENI SpA within the scope of their exploration and production projects. In addition, published seismic interpretations (Pieri & Groppi 1981, Ravaglia et al. 2006, Fantoni & Franciosi 2010, Ghielmi et al. 2010, 2013) have been used for model building.

All seismic data available only as paper plots, like the data of Baden-Württemberg and Bavaria, and the older seismic sections in France, had to be digitised prior to the reprocessing sequence. This procedure of digitalisation included preparation of the paper plots (removing notes and markers, etc.) as well as scanning and image enhancements (mainly filtering).

The reprocessing procedure, finally resulting in SEG-Y format, required the vectorisation of the all data prior to the processing steps including top/bottom mute (to eliminate the insignificant top and

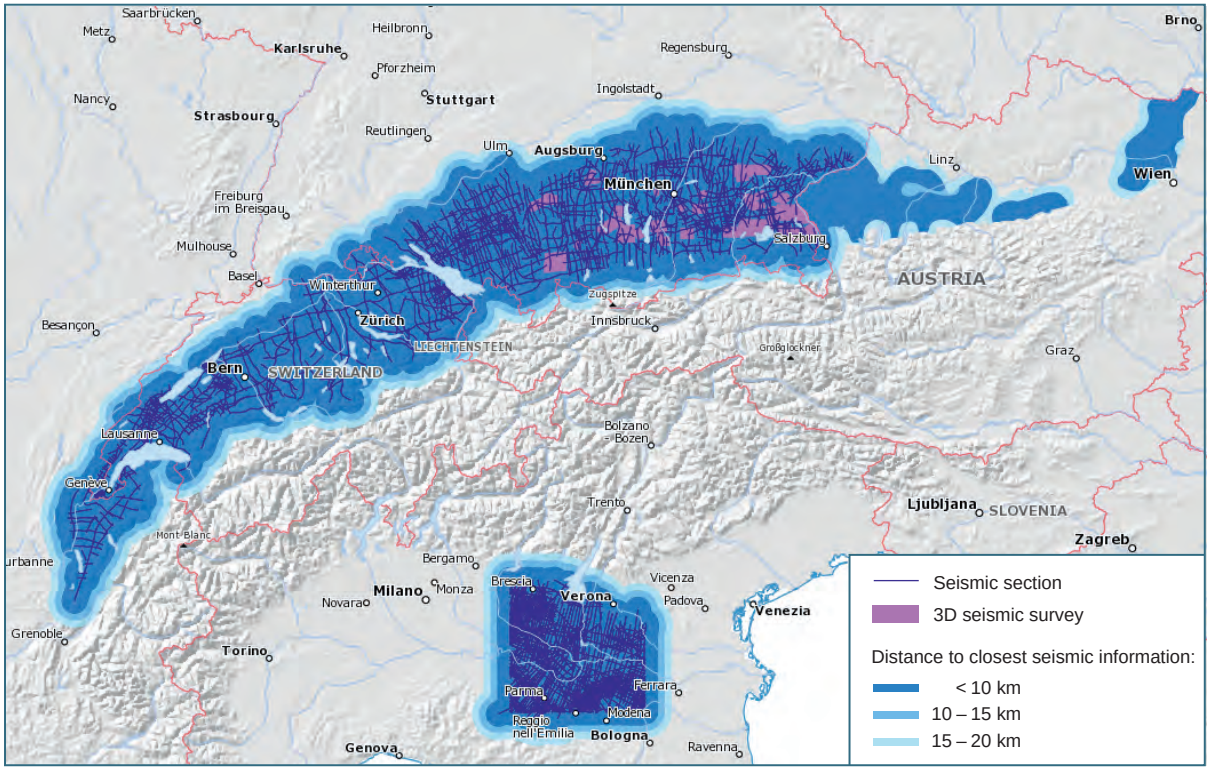

Figure 4.1-1: Density and distribution of seismic baseline data (clip of a screenshot from the GeoMol MapViewer http://maps.geomol.eu). Because the MapViewer allows to zoom in up to the 1:80,000 scale, on the Austrian territory discrete seismic lines may not be displayed for data privacy reasons.

bottom part of a seismogram), deconvolution and amplitude scaling. Subsequently, an optional mistie-analysis was carried out, geared towards correcting unavoidable mismatches on crossing seismic lines, followed by a migration procedure that corrects the images for real geometries of faults and dipping horizons. This step is especially valuable in areas of a complex structural inventory (see Figure 4.1-2). As the scanned data available for the GeoMol project basically are lacking

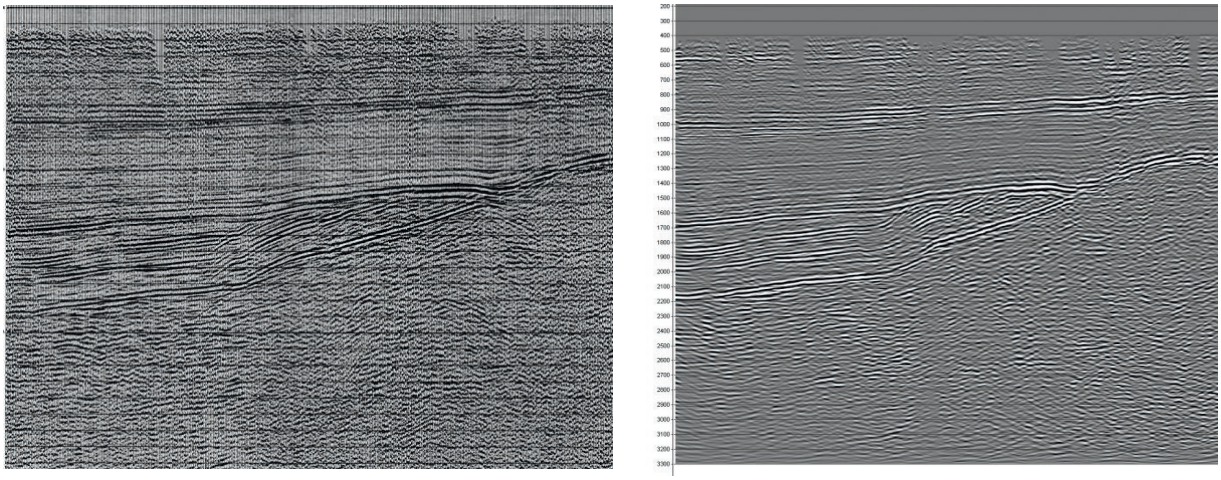

Figure 4.1-2: Example of a reprocessed 2D seismic line, left: scanned from paper plot, not migrated, right: after post-stack reprocessing including migration. Continuous horizons become clearer, fault geometries are better traceable and distinctive artefacts around discontinuities (diffraction hyperbolas) are minimised.

information on frequency and amplitude, advanced seismic analysis using seismic attributes could not be applied.

Two general procedures have been applied for preparation of the seismic profiles depending on the base data, both using comparable parameters for the entire study area. The main processing steps applied when starting from raw data can be summarised as follows:

- Geometry updating and trace editing: manual and automatic trace editing to eliminate spikes, random noise and artefacts.
- Amplitude recovery: spherical divergence correction to compensate the energy decay with depth; energy level of traces set to a constant value while using the whole trace to compute the root mean square amplitude.
- Deconvolution: improvement of temporal resolution by wavelet compression; conversion to minimum phase equivalent for vibroseis; polarity reversal if necessary.
- Application of several filtering processes.
- Primary static computation.
- Noise attenuation.
- Several iterations of velocity analysis and residual static computation.
- Post-stack or pre-stack time migration: depending of the quality of the data and the coverage.
- Post processing after migration: to facilitate interpretation of horizons, coherency enhancement, band pass filter and automatic gain control can be applied.

The main processing steps applied when starting from processed data, commonly paper plots, can be summarised as follows:

- Scanning and image enhancement: distorsion (horizontal alignment), noise filtering, contrast enhancement, conversion into black/white.
- Vectorisation: semi-automatically with interpolation in between traces of variable quality; equalizing of amplitudes, anti-alias-filtering (appropriate to the sweep frequency) and top and bottom muting for noise removal.
- Filtering.
- Scaling of amplitude (root mean square over 3000 ms).
- Export as minimum phase in SEG-Y format (to fill in the traces).
- Zero phase transformation for mistie-analysis.
- Mistie-analysis.
- Post-stack time migration.
- Zero phase transformation.
- Application of mistie-correction.
- Correction for seismic base level.

The geo-referenced SEG-Y sections resulting from these reprocessing procedures have been the basis for picking reflectors and the interpretation of horizons and structures (Chapter 4.4) as the fundamental input for 3D model building (Chapter 5).

4.2 Borehole data

The evaluation and interpretation of seismic information is the most appropriate practice to address the structural inventory in a spatial approach. However, the seismic information does not allow for an unambiguous assignment of the detected reflectors to distinct units of litho-stratigraphic successions. The only unequivocal interpretation of the subsurface geology comes from borehole evidence. Thus, borehole data are crucial to correlate the seismic interpretations (after being converted into depth-domain) with the stratigraphic sequence. Furthermore, borehole information is used to interpolate the boundaries of layers with no significant seismic signature by depth constraints (see Chapter 4.4 for details).

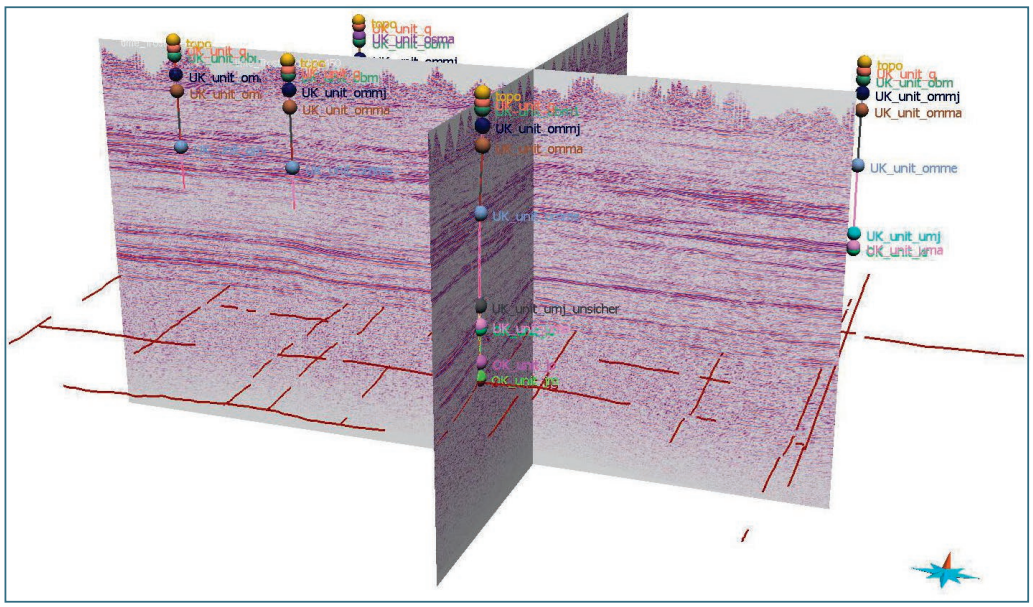

Figure 4.2-1: Calibration of interconnected seismic sections (SEG-Y) using borehole markers re-converted into time-domain. The red lines mark traces of the base of the Upper Jurassic (Malm) geothermal aquifer as picked from seismic sections (from DIEPOLDER et al. 2015).

As the legal custodians of the subsurface the GSOs have available a vast amount of borehole data acquired over more than a century, stored and maintained in their archives and data bases. They furthermore have access to classified data in accordance with the respective statutory regulations in the territory of their responsibility (see Chapter 3.3). However, the area coverage of borehole data is unevenly and information density strongly decreases with depth, being scarce and clustered in a few areas of exploration focus at depths relevant for deep geopotentials (Figure 4.2-3). Also the quality of the geological and geo-technical records may vary widely. Among others, they are subject to the type of drilling, the general advancements of drilling techniques and the changes of geo-scientific paradigms during the last decades.

Borehole information used for model building was chosen from the GSO's data bases and archives guided by the following criteria:

- The borehole must intersect at least one stratigraphic unit considered in model building,
- the data must feature a good quality and reliability of the geological records,
- a preferential selection of deep boreholes, even though if clustered in focal areas,
- a preferential selection in areas of (interfered) disturbed layering or faulting,
- a distribution as uniform as possible in undisturbed areas.

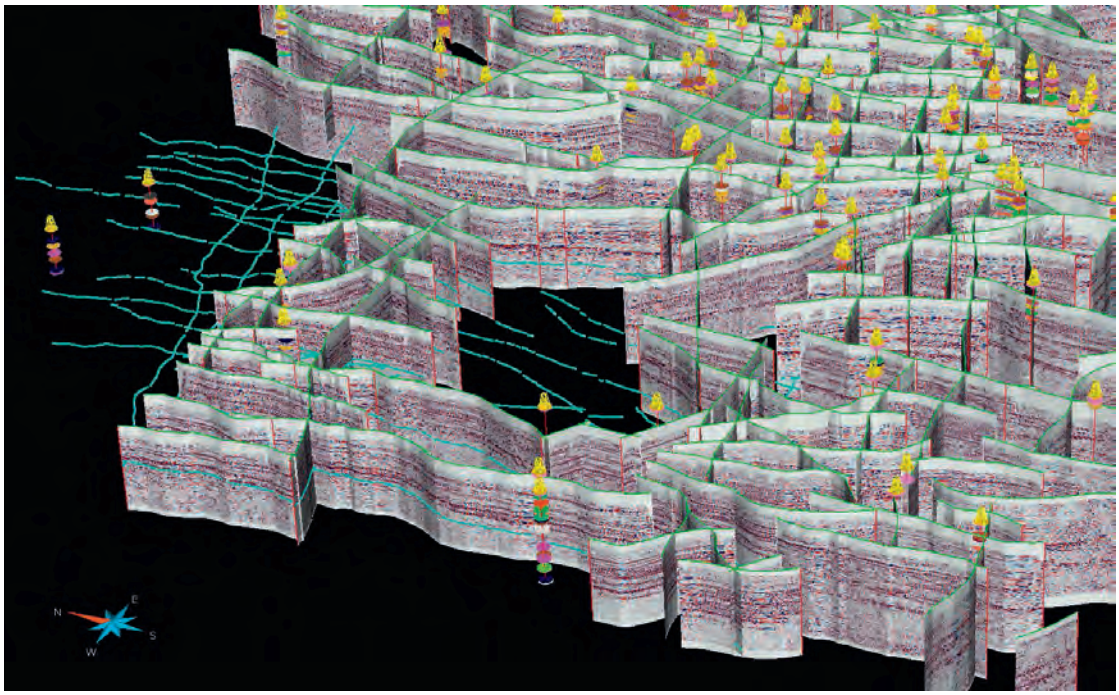

Figure 4.2-2: Screenshot of a scene with an exceptionally dense area coverage of the SEG-Y network and borehole information. The borehole information is used to derive regionalised depth constraints for areas with no significant seismic signature or without stratigraphic control and to overall calibrate the scene (from DIEPOLDER 2015).

Table 4.4-1 at the end of chapter 4 lists the number of boreholes considered in model building of certain areas. Figure 4.2-3 gives an example of the spatial distribution of the borehole information. Full information on the borehole data used and its spatial distribution in the GeoMol project areas is available at http:\\maps.geomol.eu.

4.3 Published data and maps

To further constrain the 3D modelling and to validate concepts, various published geological cross sections, structural maps and data from previous projects have been exploited (see Table 4.4-1).

3D models are strongly determined by layer thickness variations as well as the depositional history. This kind of information – on a regional scale – is a core expertise of the GSOs and consequently many published synopses are available. Structural information such as contour maps represents the records of conceptual models integrating the implicit knowledge of generations of geologists. However, they usually refer to specific horizons only and are compiled in the 2D space which, due to the lack of appropriate methods and techniques, does not allow to fully consider the coherence with the contours of other layers and structural features to gain a truly spatial view. These structural syntheses are thus only partly applicable in 3D modelling, but are a valuable contribution to the validation process of the 3D models.

Principal synopses covering larger areas that have been considered in the GeoMol project are listed in table 4.4-1. Cross-sections used for model building and validation are referred to in the respective sections.

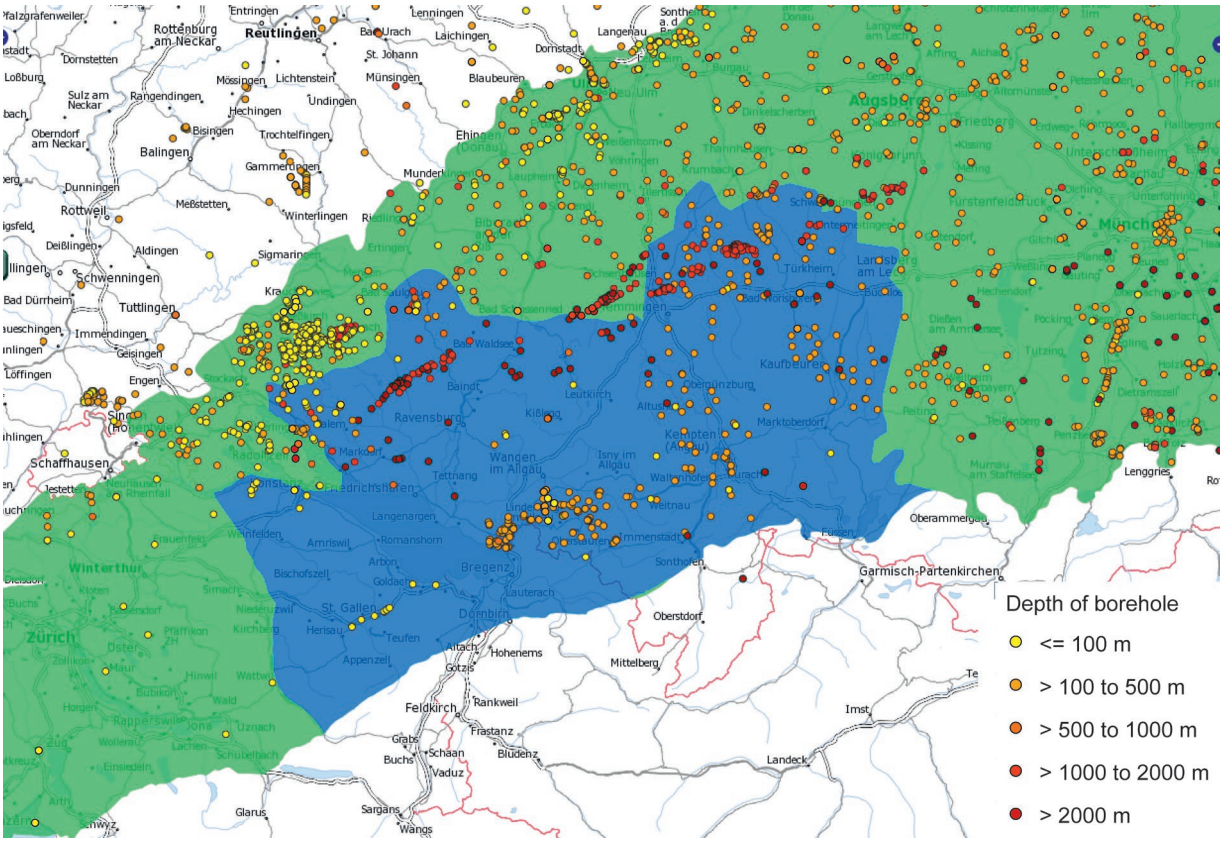

Figure 4.2-3: Well location map of the central part of the framework model (green) including the Lake Constance – Allgäu pilot area (blue) as an example of the uneven distribution of borehole information (clip of a screenshot from the GeoMol MapViewer http://maps.geomol.eu).

4.4 Seismic signatures and the interpretation of horizons and structures

To improve the accuracy and reach of correlating the lithological set-up and its seismic signature, several synthetic seismograms based on drillhole measurements have been generated and parallelised with the stratigraphy of the borehole evidence where data was available (Figure 4.4-1). Synthetic seismograms aim to compare recorded seismic with calculated seismic based upon measured physical properties (density and seismic velocity) at wells with robust stratigraphic information. This gives an accurate indication about the stratigraphic position of individual reflections and allows for fine tuning of the velocity model. However, this analysis was not possible in all parts of the pilot areas due to lack of representative data.

An effort has been made to record in detail all units deemed distinctly identifiable as well as their range of variation, to eventually provide a catalogue of characteristic seismic signatures for all model units of the entire NAFB. This has been the basis for a common understanding of the seismic response to interpret and to correlate with the modelling units (Figure 5.1-1). Due to the heterogeneous nature of the seismic data ensemble and the lack of metadata on the original processing, the uncertainty of the interpretation itself can be as high as one full wavelength in time domain (corresponding to approximately 50 m). Further uncertainties of the interpretations in depth domain arise from possible variations of the seismic velocities, including the static correction used for harmonising to a common reference level.

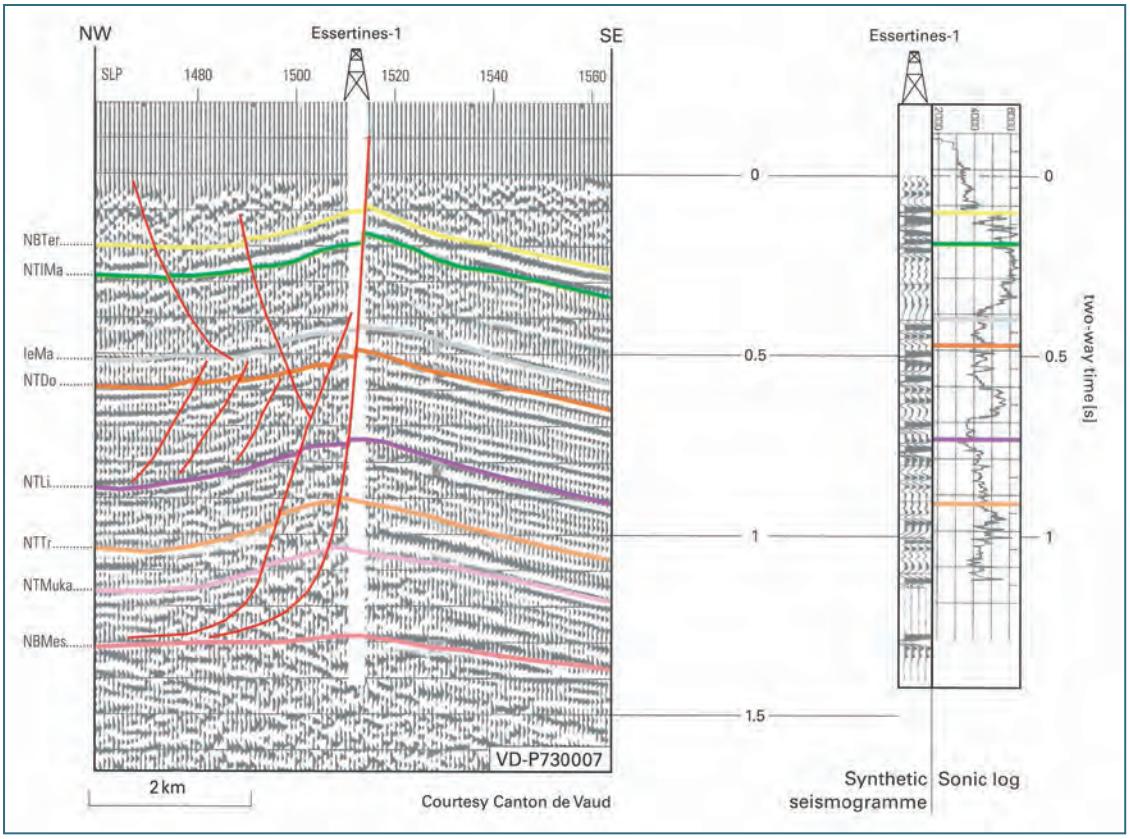

Figure 4.4-1: Example of a seismic profile calibrated with borehole data in time domain (after SOMMARUGA et al. 2012). The seismic section is compared to a synthetic seismic profile (Essertines-1 well) and a sonic log showing instantaneous rock velocities between 2000 m/s and 6000 m/s.

Regarding the stratigraphic units defined in the project, up to seven principal reflectors could be identified in the NAFB: Base OMM, Base Tertiary, Top Upper Jurassic, Top Middle Jurassic, Top Lower Jurassic, Top Triassic, and Top Basement. Visibility of seismic reflectors depends on changes of the petrographic composition and the quality of seismic profiles. Therefore it is not possible to trace every reflector through the whole basin (see Figure 5.1-1). In the Italian pilot area 17 horizons were interpreted, but not all of them were included in the final 3D model.

The Cenozoic sediments (between Base Quaternary and Base Tertiary) generally show considerable variations of thickness and composition. To constrain the geological interpretation of seismic data, four types of information can be used: well data, synthetic seismograms, outcrops from the geological maps, and geometrical relationships between seismic reflectors.

With respect to the stratigraphic units, most seismic sections can be partitioned into three main units from top to bottom with the following characteristics of amplitude, frequency, and configuration for the seismic reflectors:

- Tertiary and Quaternary (Cenozoic) sediments feature reflectors of general weak to medium amplitudes, low frequencies, low continuities with subparallel to hummocky configuration. In this monotonous section reflectors cannot be traced over long distances. In many sections the Quaternary and the uppermost Tertiary units are not recorded because the seismic survey was designed to image deeper reflectors.

- The reflectors of Mesozoic sedimentary rocks generally show high amplitudes, medium frequencies, high continuities with parallel configuration. Dip-parallel zones of subdued reflections can occur within these packages of strong reflectors.

- The crystalline basement rocks exhibit a general noisy to reflection-free or monotonous appearance. In this segment, mainly artefacts of seismic processing and multiples occur and might be misinterpreted as sedimentary rocks.

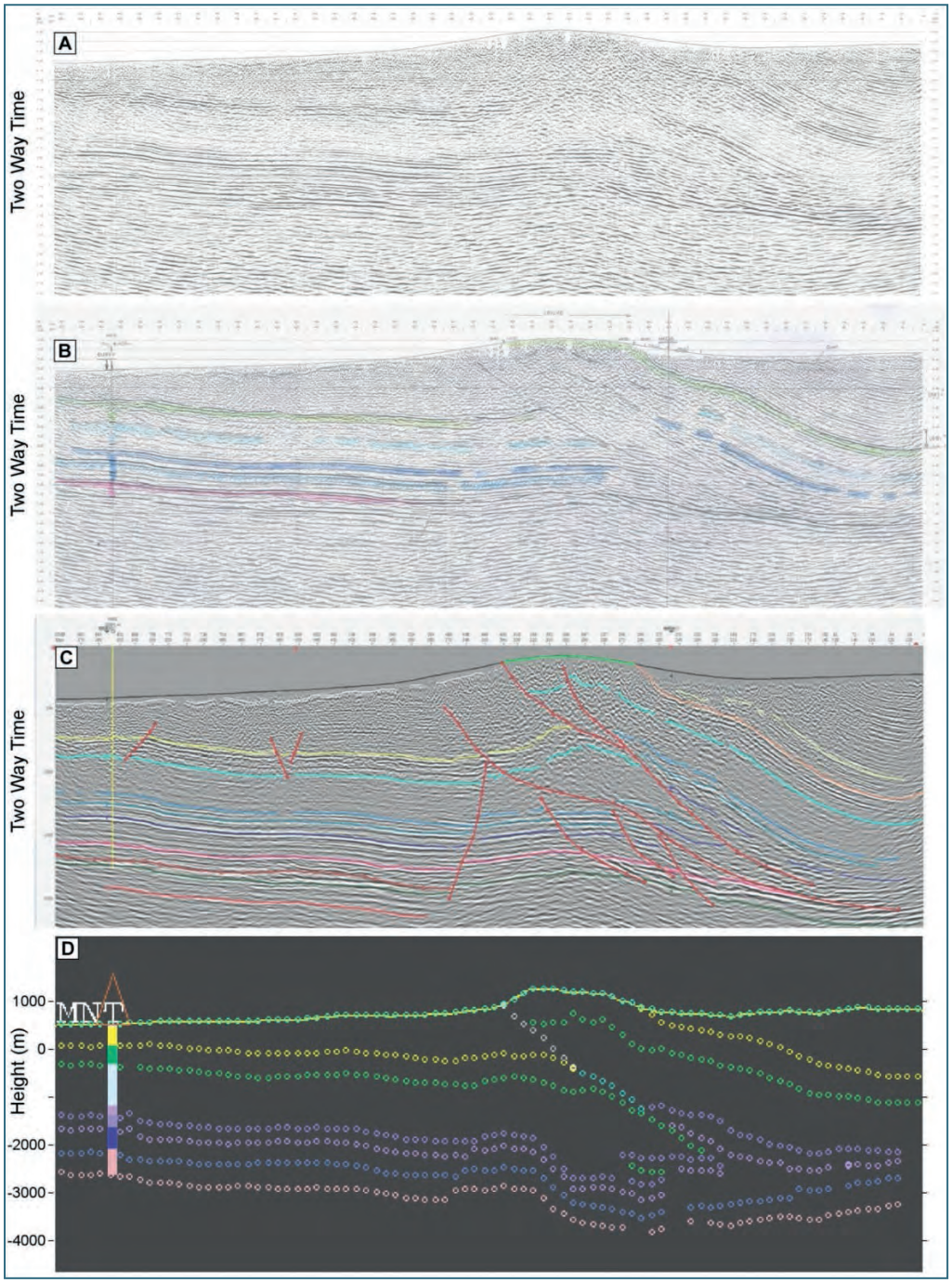

Figure 4.4-2: Example of the geological interpretation of seismic data from the 88SVO07 seismic line in Geneva-Savoy pilot area. A: blank seismic image, B: manual picking and on-paper interpretation, C: digital interpretation in the SeisVision software, D: depth-converted section integrated into GeoModeler software used at BRGM.

The horizons in the Italian Po basin can be divided into two types, basal unconformities and top horizons. The basal unconformities are marked by onlap of reflectors on the underlying seismic facies, however the discrimination of the hierarchy of some unconformities can be difficult in places. The top horizons are marked by a major impedance contrast of reflectors which corresponds to the main formation tops in the well markers.

4.4.1 Fault interpretation

Most of the geopotentials of the Alpine foreland basins are bound to structural features such as fault traps, or are controlled by the fault network, which determines the rock mass permeability and is crucial for hydrothermal utilisations (Chapter 2.3). Furthermore, the assessment of the seismic risk is based upon the localisation of seismogenic structures and active faults (cf. Chapter 9.1). The identification and evaluation of the spatial arrangement of the fault network thus is a principal topic of the GeoMol project. The evaluation and interpretation of seismic information is the most appropriate practice to address this issue.

Although fault displacements are mostly rather low, the occurrence and dip directions of faults are detectable where prominent reflectors of the Mesozoic are interrupted, disturbed or blurred, specifically when the fault intersects the seismic profile at a wide angle. Fault traces are much more ambiguous in the Tertiary sedimentary succession. Fault sticks picked within the Mesozoic layers sometimes can be extrapolated by the occurrence of narrow, more transparent zones within the Tertiary units or by the interruption or sagging of Tertiary reflectors in extension of the fault sticks. The upper termination of a fault is generally difficult to determine within the Tertiary succession, if not further constrained by well markers or the results of surface exploration such as geological or structural maps.

Important background information for the detection of fault sticks in single seismic profiles and especially for the spatial correlation of fault sticks has been derived from several comprehensive structural maps, as the harmonised version of the French geological maps 1 : 50,000, compiled 1 : 50,000 maps from the oil and gas exploration in Baden-Württemberg (LBEG 2007), surface fault traces of the Geological Atlas of Switzerland 1:25,000 (SWISSTOPO 2012) and the Geological Map 1 : 500,000 of Switzerland (SWISSTOPO 2005) as well as the Geothermal Atlas of Bavaria (BAYSTMIVT 2010).

4.4.2 Velocity modelling

Since the data from seismic reflection surveys usually displays geological sections in time domain, the data has to be converted into depth domain (time-depth conversion) with the help of a velocity model.

In all pilot areas except for Upper Austria – Upper Bavaria a common datum plane could be used (Table 4.4-1) allowing for the joint alignment of interpretations in time domain. Velocity models for time-depth conversion were built separately by each partner but in accordance with the models of adjacent areas. In contrast, because of the significant difference in base levels and thus the datum planes, within the pilot area Upper Austria – Upper Bavaria also the seismic interpretation had to be done separately and trans-border match of the two models was implemented in depth domain only.

Velocities can be estimated from general velocity trends, borehole seismics (VSP) and/or stacking velocities resulting from seismic processing and converted to interval velocities using the formula of DIX (1955) and optionally corrected using synthetic seismograms. GeoMol's velocity models were calculated assuming a near homogeneous distribution within stratigraphic layers. Due to data restrictions several regional velocity models for time-depth conversation were developed taking into account the regional differences in rock composition and parameters as well as methods adopted according to the territorial scope. Generally, the estimation of a velocity model is probably the part with the highest data uncertainty within the workflow of 3D modelling and consequently there is a wide range of methods and algorithms suitable for different settings and data structures to choose from.

If modelled in time-domain, refinement of layer surfaces was partially done by borehole data reconverted into time-domain (Figure 4.2-1) either by a velocity model in depth domain and/or check-shot data available for many hydrocarbon exploration drillings. Time-depth conversion was implemented at the latest possible stage of modelling in order to facilitate subsequent model refinement by additional seismic sections when needed.

France: Due to the scarcity of time-depth data interpreted seismic lines were individually converted from time into depth domain by using generalised mean interval velocities calculated from few wells.

Switzerland: Velocity grids were generated from interval velocities at well locations and additional constraint points. Time-depth conversion was performed with a stacked interval velocity method.

Baden-Württemberg: Two-way-traveltimes (TWT) from check-shot measurements at boreholes and the time-depth correspondence of the interpretations to the existing framework model of Baden-Württemberg were used for parameterisation of a regular 3D volume grid. Time increments of TWT were interpolated by the inverse-distance method to ensure a continuous increase of TWT with increasing depths. Afterwards time increments were summed up to calculate average velocities.

Bavaria: Interval velocities from checkshot measurements at boreholes and stacking velocities (converted to interval velocities) were used to geo-statistically parameterise a structurally distorted 3D-volume grid with interval and average velocities using the kriging with external drift method. Faults and structural trends are taken into account by a two-step trend evaluation process. Cross-check with depth data added further velocity constraints that were re-introduced into the velocity modelling workflow.

Austria: Interval velocities from check shot measurements at boreholes and stacking velocities (converted to interval velocities) for 7 stratigraphic layers, corrected using synthetic seismograms were used. Due to the small overall number of velocity data or sonic logs, the velocity model was geo-statistically calculated assuming a near homogeneous distribution within stratigraphic layers by using a minimum curvature function.

Italy: Velocity gradients and the velocities (v_0) at the top of each interval of a 4 layer model were each geo-statistically interpolated in 2D from sonic logs measured in boreholes and stacking velocities in the proximity of wells with interval velocity data. Thus, the initial velocity for each reference horizon and the gradient of velocity variation with depth is obtained. Interpolation was done by using the spline with barriers method, taking into account the main geological discontinuities represented by the main faults.

Table 4.4-1: Benchmarks and parameters of data preparation and 3D model building in the different areas of the Alpine Foreland Basins

	Austria	Bavaria	Baden-Württemberg	Switzerland (w/o GE)	France and Geneva	Italy
Institution in charge	GBA LCA: Univ. Innsbruck	LfU	LGRB	swisstopo LCA: Univ. Basel	France: BRGM GE: Univ. Geneva	ISPRA
3D modelling software (® / ™)	GoCAD LCA: Move	SKUA	GoCAD	Move LCA: GoCAD	GeoModeller	Move
Seismic interpretation software (® / ™)	SeisSpace/ProMAX R5000, Petrel	SKUA	GoCAD	GGX SeisVision LCA: Kingdom Suite	GGX SeisVision	SeisWorks (provided in ENI data room)
Coordinate system	WGS1984 UTM33N LCA: CH1903+ / LV95	Transverse Mercator DHDN3 Gauss-Krüger Zone 4	Transverse Mercator DHDN3 Gauss-Krüger Zone 3	CH1903+ / LV95	Lambert 93	WGS1984 UTM32N
Seismic data input	95 seismic lines of overall 1,502 km	467 seismic lines, totalling ~ 8,700 km; 2600 km^2 3D seismic projects	135 seismic lines, overall 2373 km	263 interpreted seismic profiles, overall 4357 km	54 seismic lines, overall 780 km; GE: 23 migrated seismic lines, Σ ~ 165 km	759 seismic lines totalling 11,900 km
Datum planes	E: 150 m, W: 300 m LCA: 500 m	500 m	500 m	500 m	200 m	40 m
Reprocessing	pre- and post-stack	digitised, post-stack	digitised, post stack	pre- and post-stack	France: pre-stack GE: mostly post-stack	already reprocessed by provider ENI
Borehole data input	707 boreholes 608 > 500 m depth	2360 boreholes 817 > 500 m depth	1014 boreholes 221 > 500 m depth	~ 50,000 top bedrock 43 > 500 m depth	531 boreholes 24 > 500 m depth	123 boreholes 108 > 500 m depth
2D syntheses on structural inventory considered	Structural map of the Molasse base 1 : 200,000 (KRÖLL et al. 2001, 2006)	Geothermieatlas (BAYSTMWIVT 2010), Alpenvorlandstudie (LBEG 2007)	Alpenvorlandstudie (LBEG 2007)	Seismic Atlas of the Swiss Molasse Basin (SOMMARUGA et al. 2012)		Structural Model of Italy and Gravity Map (BIGI et al. 1990)
Legacy models integrated		Greater Munich Area (BAYLFU 2012), KLIP models (BAYLFU 2014), Top Basement (SATTLER & PAMER 2009), Top Upper Jurassic (BAYSTMWIVT 2010)	Landesmodell (RUPF & NITSCH 2008), ISONG2 Modell (RUPF & ARMBRUSTER 2008)	Seismic Atlas of the Swiss Molasse Basin (SOMMARUGA et al. 2012)		
Domain started with	depth LCA: time	time	Framework: depth LCA: time	time	depth	time
Type of model	surface	volume	surface	surface	surface	surface

5 Three-dimensional geological modelling

5.1 Introduction

The preparation of tools and methods for subsurface planning inherently requires a three-dimensional approach which will enable the prioritisation of utilisations with regard to resource efficiency. Any geopotential assessment must, therefore, be based on sound, three-dimensional planning tools availing advanced 3D modelling techniques. A principal task of GeoMol, thus, was 3D geological modelling.

A geological model is a virtual representation of the geology in three dimensions. Geological models provide information on geological unit surface elevations and thicknesses and can be queried to generate synthetic boreholes and cross-sections, vertically as well as horizontally. Geological models are created by geologists' expert knowledge using geological data such as borehole records or geophysical surveys (or 2D synopses derived thereof) and are combined with field observations and digital terrain models. These data are interpreted and the conceptual geological understanding is captured via geological cross sections, geological maps and/or point interpretations that describe a layer surface. The 3D geological model is created by interpolation between all interpreted points. The accuracy of the geological model is dependent on the data density, the prevailing understanding of the geology at the time of modelling and the geological complexity. The metadata representation as in figures 4.1-1 and 4.2-3 provides evidence of the baseline data considered in model building. The spatial distribution of this information is an indication of uncertainty.

Within the scope of GeoMol a 3D geological framework model of the Northern Molasse Basin as a whole, and more detailed of five pilot areas have been built (cf. Chapter 2.1 and 8). The framework model is designed as a synoptic reference model to fit in all existing or future detailed models

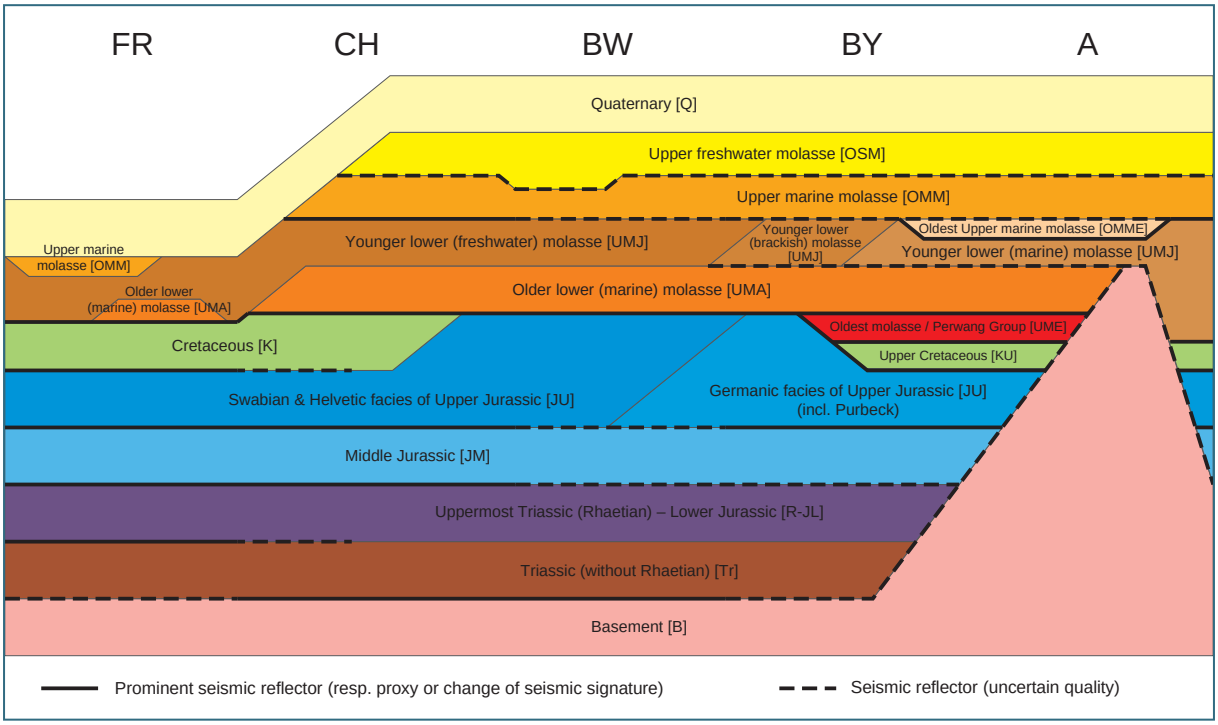

Figure 5.1-1: Lithological units as distinguished in GeoMol's framework model and seismic reflectors used for their delimitation. Due to lateral changes in rock composition and the disparate quality of the seismic surveys originating from multiple sources and various dates of origin the perceptibility and rigour of the seismic reflectors varies widely (Sketch not to scale – vertical axis does not represent thickness or time).

in their true spatial position. It encompasses overall 55,000 km^2 covering the Foreland Molasse of the NAFB within the Alpine Space Cooperation area (Figure 2.1-1). The framework model comprises the principal litho-stratigraphic units of the NAFB infill and the flooring sedimentary succession down to the top of the Palaeozoic basement, consisting of up to 12 modelled horizons in places where the stratigraphic sequence is developed completely (Figure 5.1-1).

Criteria for the selection of the horizons as modelled in the framework model have been:

- the lateral extension and seismic traceability throughout the basin,
- distinct vertical boundaries caused by compositional changes, forming a pronounced seismic reflector,
- the importance for geopotential assessments.

GeoMol's framework model is complemented by four more detailed 3D geological models of the pilot areas in the NAFB featuring additional horizons that are important for the evaluation of the geopotential. Further 3D geological models have been built in the Po Basin pilot area for the general geopotential assessment as performed in all pilot areas but also geared towards the localisation and assessment of seismogenic structures and active faults (Chapter 9.1) and in Slovenia's Mura-Zala Basin for testing GeoMol's approach also outside the Alpine Foreland Basins (Chapter 9.3). For detailed descriptions of the pilot area models see chapter 8 and the corresponding pilot area reports (Capar et al. 2015, GBA 2015, GeoMol Projektteam LCA 2015, ISPRA 2015, Šram et al. 2015).

All 3D modelling, both, for the framework model as well as in the pilot areas, placed special emphasis on the tectonic structures as principal characteristics defining subsurface potentials: Specifically in inclined sedimentary sequences many geopotentials are bound to structural features such as fault traps or anticline traps. Fault and fracture networks as the arrays of increased permeability have significant effects on the productivity and economic viability of hydrogeothermal developments – they can significantly impact drilling, resource operations and potential recovery. The structural inventory also controls the compartmentalisation of reservoir rocks for underground storage and the sealing characteristics of cap rocks and is thus crucial for storage security. On the other hand, seismogenic structures like buried orogenic fronts in the Po Basin are the source of geological hazards and any utilisation of subsurface potentials must consider their possible seismic risk.

5.2 Technical implementation

As many data sets used in 3D modelling are classified industrial data, access restrictions demand that all model building must be implemented at the legally mandated regional or national GSO (but may be subcontracted based on a non-disclosure agreement). For transnational 3D modelling this fragmentation of activities means a maximum of coordination and harmonisation of the 3D modelling process and requires regular cross-border consistency checks. However, all GSOs involved in model building had 3D software solutions ready prior to GeoMol (Table 4.4-1) and could fall back to modelling workflows established for this software in their proprietary IT environments and coordinate systems. The use of different software and disparities in data formats, however, have fundamental impact on the harmonisation of the models as direct comparison and consistency checks at intermediate stages are time-consuming and difficult or virtually impossible. As the lack of tools to exchange 3D geo data efficiently across the diverse systems has been evident (Diepolder 2011), a key issue of GeoMol was to provide an open infrastructure to store and exchange multi-dimensional geo data complying with both, the disparate data policy and need of harmonised geological in-

formation at transnational level. This geo data infrastructure (Chapter 10) was developed during the implementation of GeoMol and has not yet been available at the earlier work steps of 3D modelling.

Another constraint regarding the 3D modelling workflow applied arises from the kind of input data used. If seismic data sets are the principal input data 3D modelling ideally starts in time domain. If predominantly borehole data, cross-sections and/or contour maps are provided, model building reasonably is performed in depth domain throughout. Time-depth conversion and v. v. using velocity models enables to shift interim models between the domains and to integrate data of the other domain. The fundamental workflow for both domains is portrayed in figure 5.2-1.

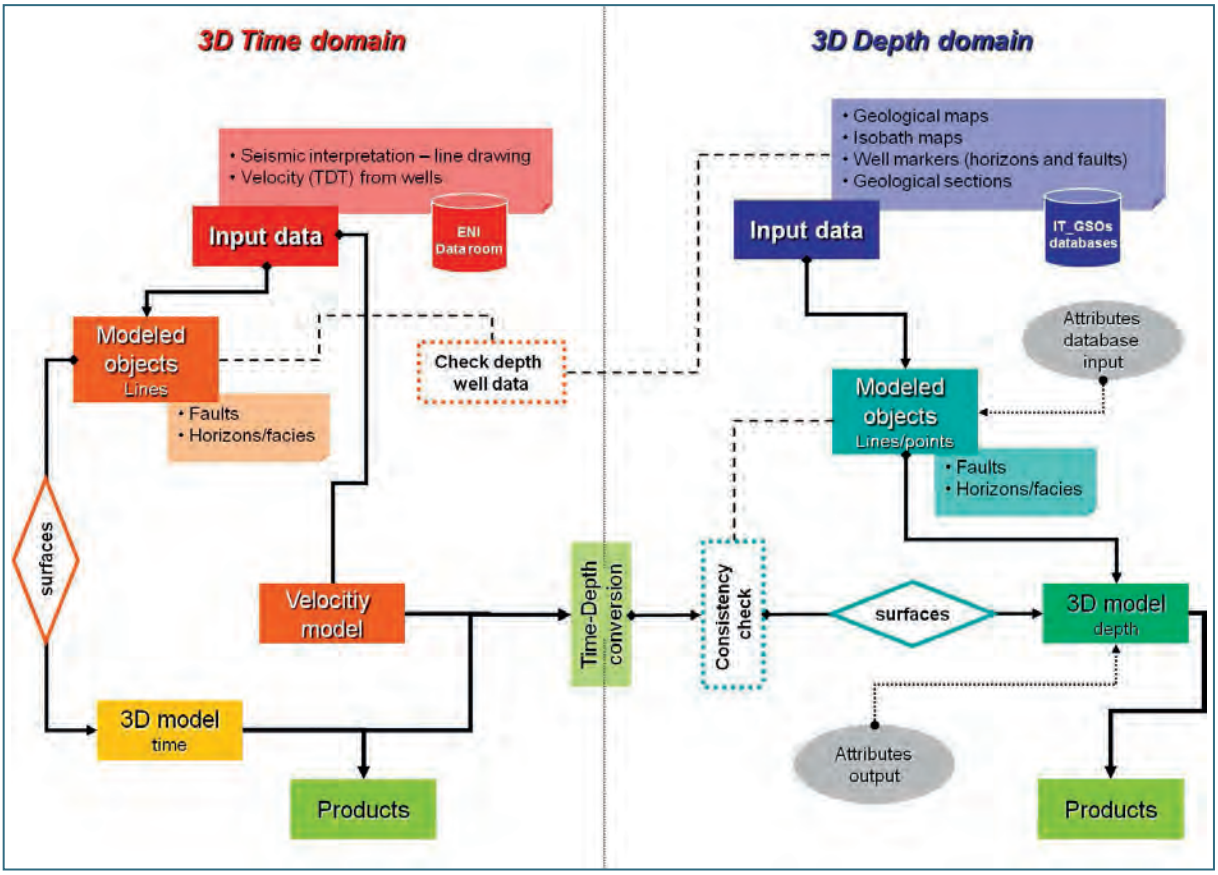

Figure 5.2-1: Schematic diagram of the two basic workflows applied in 3D modelling depending of the kind of data used for model input (from MAESANO et al. 2014). See text for discussion.

Irrespective of the domain of 3D modelling all partners had to model in the “local” coordinate system (Table 4.4-1) as all input data stored in the GSO’s data bases (as well as the information derived thereof) are based on these proprietary positional reference systems. For the exchange of input data sets (as far as possible with respect to legal constraints), intermediate and advanced modelling steps for consistency checks between adjacent areas of different partners coordinate transformations were necessary. As 3D modelling software packages provide no or only limited transformation functionalities, this work step had been performed separately after the export of the 3D objects using GIS software such as ArcGIS or, specifically designed for GoCAD objects, the tools of KoordTrans (KARICH 2010). With the advanced implementation of GeoMol’s geo data infrastructure the functionalities of the GST database, featuring an on-the-fly coordinate transformation, could be applied for model exchange and consistency checks (cf. Chapter 10).

Due to the many cross dependencies between the framework model and the pilot area models of the NAFB two different approaches for integral model building were applied: Modelling in realms with only minor or no legacy models available normally started on the pilot areas level followed by the derivation of the framework model after cross-border consistency checks. If legacy models covering larger areas have been available at the beginning of the project (as in Baden-Württemberg and Switzerland), the modelling procedure started with the upgrade of surfaces and fault networks on the framework model scale by integrating additional input data sets, followed by model refinement according to resolution required in the pilot areas. Both approaches, however, were guided by the agreements on lithological subdivision (Figure 5.1-1) and based on harmonised input data (Chapter 4) thus resulting in cross-border consistent models.

5.3 3D modelling workflow

5.3.1 Input data sets & data preparation

Table 4.4-1 gives an overview on the input data sets and modelling parameters used in the framework model and the pilot area models. Besides seismic and well data input information from geological and structural maps, cross-sections and legacy models play an important role for the model construction. The collection and preparation of input data sets, in particular the harmonisation of seismic data sets, is described in chapter 4.

The construction of occurrence polygons is prerequisite for the set-up of the geological model, because large parts of the Tertiary Molasse units and the Mesozoic rocks in parts of the project area are covered by younger rocks. Besides outcrops, well markers and seismic sections provide information about the subsurface distribution of these geological units.

Hence several horizons are not traceable in seismic sections other modelling techniques have been used. Knowledge about thickness distribution of the modelling units is important for the derivation of these horizons from previously constructed surfaces by addition or subtraction. Additionally, they help to keep realistic thicknesses in areas with little or no information from wells. Depending on the type and on the availability of pre-existing information different modelling techniques have been used for this task. The modelling based on well marker sets is the standard procedure, which has been applied for the majority of thickness distributions. If there is a pre-existing thickness map it can be used as a soft data set e. g. in a co-kriging approach. The modelling of subunits with percentages is a modelling technique to estimate the thickness of sub-units with the help of a given main unit. It ensures that the sub-unit does not exceed the thickness of the superordinate unit.

Lateral variations of petrographic composition within modelled units lead to different rock properties and have an important impact on the assessment of geopotentials. Besides outcrops wells serve as main data source for these changes of facies. They can be used to define several laterally varying facies and transition zones between them. Hence facies distributions correlate strongly with palaeogeographic elements it has to be ensured that both match each other. Additional information is provided by further data sets, mainly textual descriptions from literature.

5.3.2 Modelling of faults

The fault network has been set up mainly from seismic interpretation (see Figure 5.3-1). Complementary information is provided by geological cross sections, structural maps, legacy models and wells. Depending on the partner-specific workflow fault modelling has been carried out in time or in depth domain. A geologically reasonable correlation of fault sticks between different seismic profiles and cross-sections as well as the geological and structural maps is very important for the set-up of the 3D model.

The interpretation of tectonic structures followed some basic rules which have been previously used in the GeORG model of the Upper Rhine Graben (GeORG Projektteam 2013).

- plausible geometry of the fault plane in terms of dip, vertical offset and free from twist-effects
- geometric and genetic reasonable relation to adjacent tectonic elements
- consistency with geological and structural maps
- consistency with well markers correlations

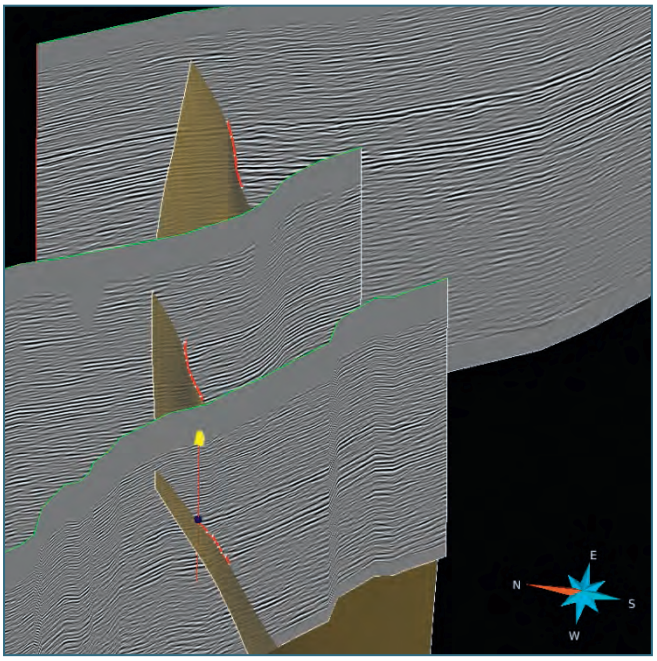

Figure 5.3-1: Fault modelling based the correlation of on fault sticks picked on seismic sections (red lines) and well markers.

In some cases complex fault pattern had to be simplified for 3D geological modelling. Small, subparallel faults were amalgamated into single objects and dip angles were harmonised for fault sticks of the same tectonic segment. Vertices of fault traces in digital geological and structural maps used have been reduced prior to 3D modelling.

Hence the resolution of the upper hundred meters of the seismic profiles is reduced, the upper boundaries of the faults are often not detectable. In such cases, per definition, faults cease beneath certain horizons, e. g. beneath the Base Quaternary or the Base Upper Marine Molasse. However the position of the upper boundary of faults has been investigated more in detail in the Italian pilot area to constrain, as better as possible, the age of activity of faults (Chapter 9.1).

5.3.3 Modelling of horizons

Depending on the availability of input data sets and the interaction between seismic interpretation and geological 3D modelling, different methods have been applied to fit horizons into the 3D model. In some cases (e. g. Austria, France) horizons have been modelled completely in depth domain based on time-to-depth converted seismic picks and further input data sets naturally rendered in depth domain, like borehole information, geological and structural maps and cross-sections. From the beginning, the geological 3D model is implemented in the target domain. Calibration of the output of seismic interpretation with further input data sets like well markers and structural maps are possible without restrictions. However, errors in seismic interpretation like erroneously picked horizons are observable in an advanced stage of modelling only – an ensuing correction of the seismic interpretation is possible only elaborately or may be completely impossible.

Where seismic reflection data sets – method-related acquired and rendered in time domain – have been the principal input data 3D modelling started in time domain. Besides the fault patterns all reliably detectable horizons in the seismic sections have been modelled. In this case, seismic interpretation and geological 3D modelling highly interact with each other and lead in an iterative interaction to more consistent results (see Figure 5.3-3). After time-depth conversion further structural elements can be integrated into the existing scaffold based on borehole information, structural maps and thickness distributions. However, the position of the horizons in time domain has to be verified and adjusted frequently after time-depth conversion, because the integration of intermediate horizons often leads to unrealistic thicknesses or horizon crossings.

This workflow starting in time domain (Figures 5.2-1 (left) and 5.3-2) has been used for most framework model components as well as for most of the pilot area models.

	Acquisition and harmonisation of input data (Chapter 4)	
	Velocity modelling and depth-time conversion of wells	
Time domain	Seismic interpretation of faults and horizons	
	3D modelling of faults	
	3D modelling of selected horizons	
	Velocity modelling and time-depth conversion of model	
Depth domain	Addition of data in depth domain and modelling of intermediate horizons	
	Parameterisation of the model	
	Derivation of products	

Figure 5.3-2: Basic workflow as commonly used in model building starting with seismic data as principal input.

A special case is the Baden-Württemberg part of the framework model. It is based on two pre-existing 3D geological models (Rupf & Armbruster 2008, Rupf & Nitsch 2008), which have been extended and upgraded with further horizons and faults from additional input data sets. The modelling has been implemented entirely in depth domain.

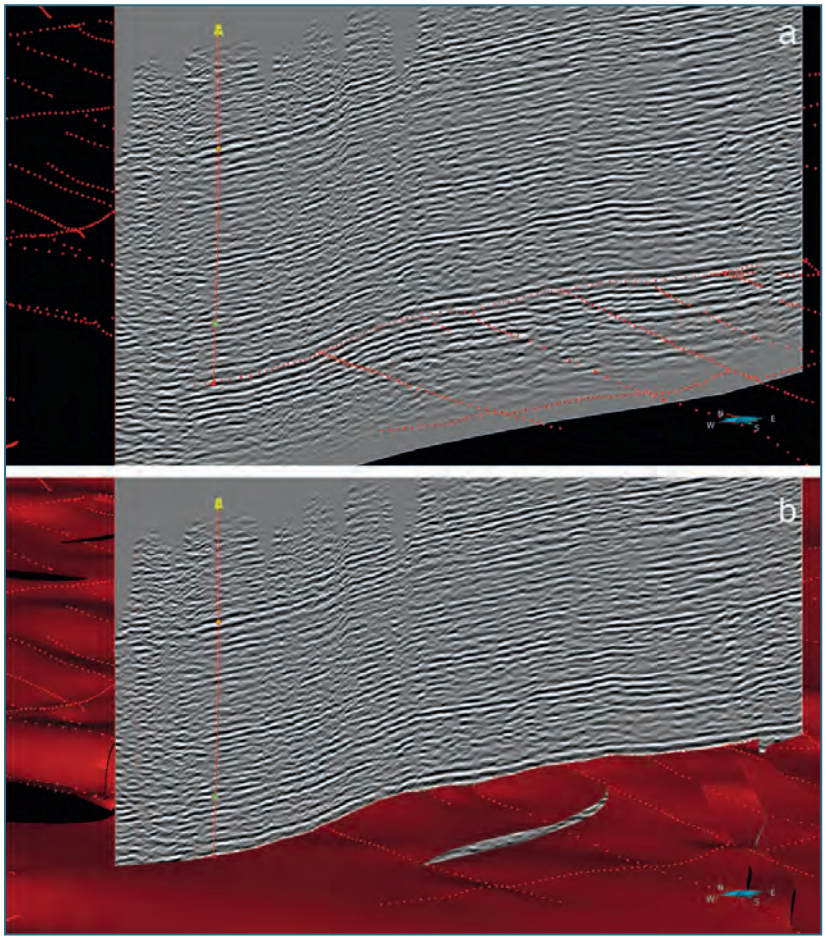

Figure 5.3-3: Horizon modelling in time domain based on horizon traces picked from seismic sections and well markers; a) shows the input data sets (seismic picks, well information) and b) the modelled horizon (red).

5.3.4 Consistency checks

Internal consistency checks of the framework model were carried out after finishing the modelling of faults and horizons. They comprise the check for horizon crossings with the ground level, an inspection for horizon crossings and a test for well marker fit. Furthermore, the “Structure and Stratigraphy” workflow of the SKUA-software ensures proper modelling of eroded horizons and consistent modelling of fault throws. Because the modelling system calculates the full pile of horizons at once, no horizon crossings can occur. However, a proper and thorough check of all data together with all its dependencies as well as a complete check of borehole interpretation is the prerequisite to obtain a robust model.

In cases where the framework model is directly derived from pilot area models, consistency checks between both are not necessary. In Baden-Württemberg and Switzerland framework models and pilot area models are partly based on different input data sets. Hence, a complete consistence between both model types is not possible. Particularly independently constructed fault patterns exhibit differences. On the other hand, the position of horizons and the thicknesses of the geological units have been mutually adopted, so that horizons of both models match each other.

An important factor for the final model fit is a harmonised data base with a uniform classification of litho-stratigraphic horizons in wells, standardised technical parameters for seismic processing,

agreements on reflectors to be picked and cross-border correlation of fault systems. The following actions are prerequisite for the consistence of the models:

- Exchange of well data sets which are close to GeoMol-internal borders, common interpretation of petrographic descriptions and geophysical well measurements
- Agreement on the workflow of technical processing of seismic profiles as well as technical parameters (datum plane, replacement velocities) between partners
- Workshops for seismic interpretation, agreements on picking principles for seismic reflectors, common interpretation of cross-border seismic profiles
- Correlation of cross-border fault systems

Furthermore, the position of horizons and faults are directly dependent from seismic velocities. The exchange of checkshot measurements and velocity models is mandatory for a seamless fit of adjacent model parts.

Although the 3D model of the Brescia-Mantova-Mirandola pilot area (e. g. Figure 5.3-4) does not adjoin to any other model (Figures 2.1-1 and 4.1-1), the principle modelling steps have been the same as in the workflow for the distributed organised NAFB models. Thus, a comparable approach on both sides of the Alps has been established.

After transformation of the different sub-models into depth domain, an intense exchange of data sets between partners and the fine tuning of horizons and fault systems across the borders was implemented. In this context a comparison of input data sets, readjustments of model objects as well as recalculations of the velocity models resulted in a better fit of neighbouring model parts.

The following figures provide some examples of modelling results in different areas and their use in addressing various issues of deep subsurface geology.

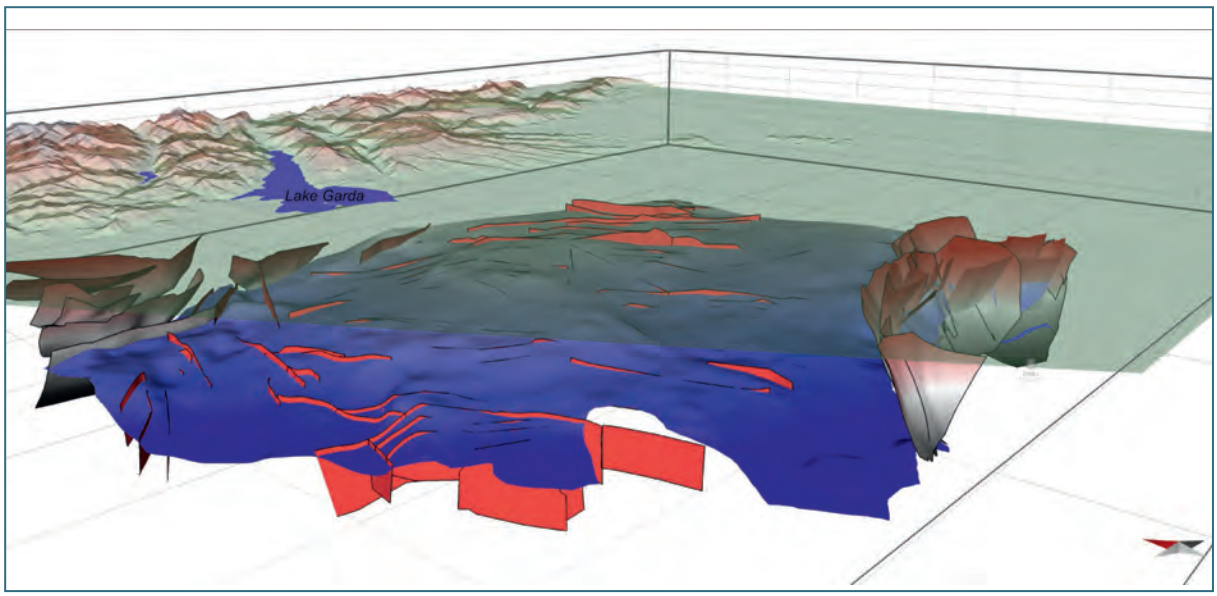

Figure 5.3-4: Depth level of the top of Late Triassic–Early Jurassic in the Po Basin pilot area; blue colours indicate depths of more than 8 km below sea level, light blue colours of about 2 km below sea level. The surface is intersected by several extensional faults (light red) that controlled the evolution of the basin. The brown-to-black surfaces are the main thrusts of the Alpine orogen, on the left, and the Apennines nappes, on the right.

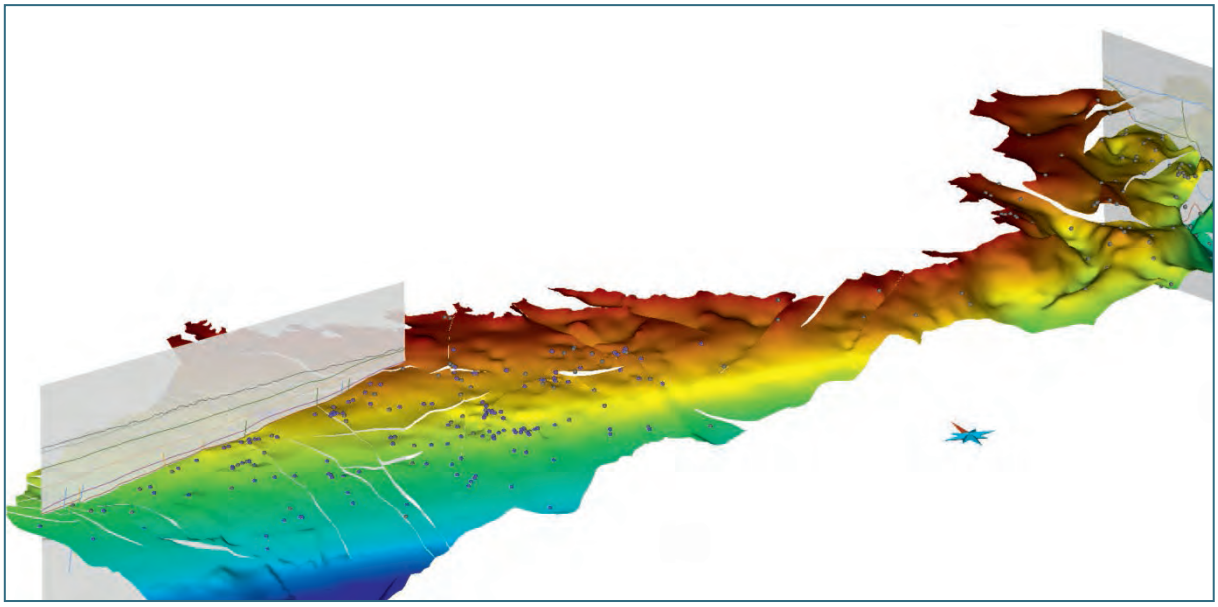

Figure 5.3-5: Depth level of the Base Tertiary in the Austrian part of the framework model modelled in depth domain. Brown colours indicate depths of about 200 m above sea level, dark blue colours of about 5,000 m below sea level. Two screens showing sketches of geological cross-sections derived from the full 3D model are superimposed. The white omissions in the model represent the offset of faults, the purple dots indicate the position of boreholes of varying depths.

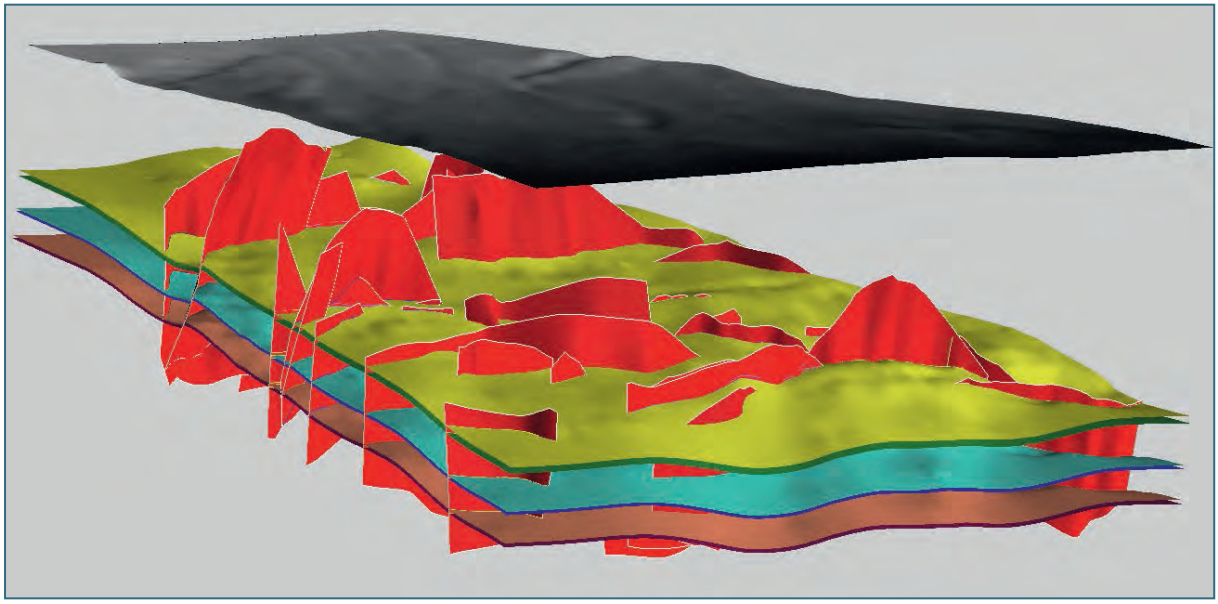

Figure 5.3-6: 2,000 km^2 clip of the framework model in eastern Bavaria, view from SW, as an example for the complex fault pattern reflecting the tectonic evolution of the basin (from DIEPOLDER et al. 2015). Depicted are six pre-Tertiary layer surfaces of the south dipping sedimentary sequence down to a depth of more than 5 km. For clarity the Tertiary units are omitted and the layers are shown in jazzy colours deviating from the accord as in figure 5.1-1.

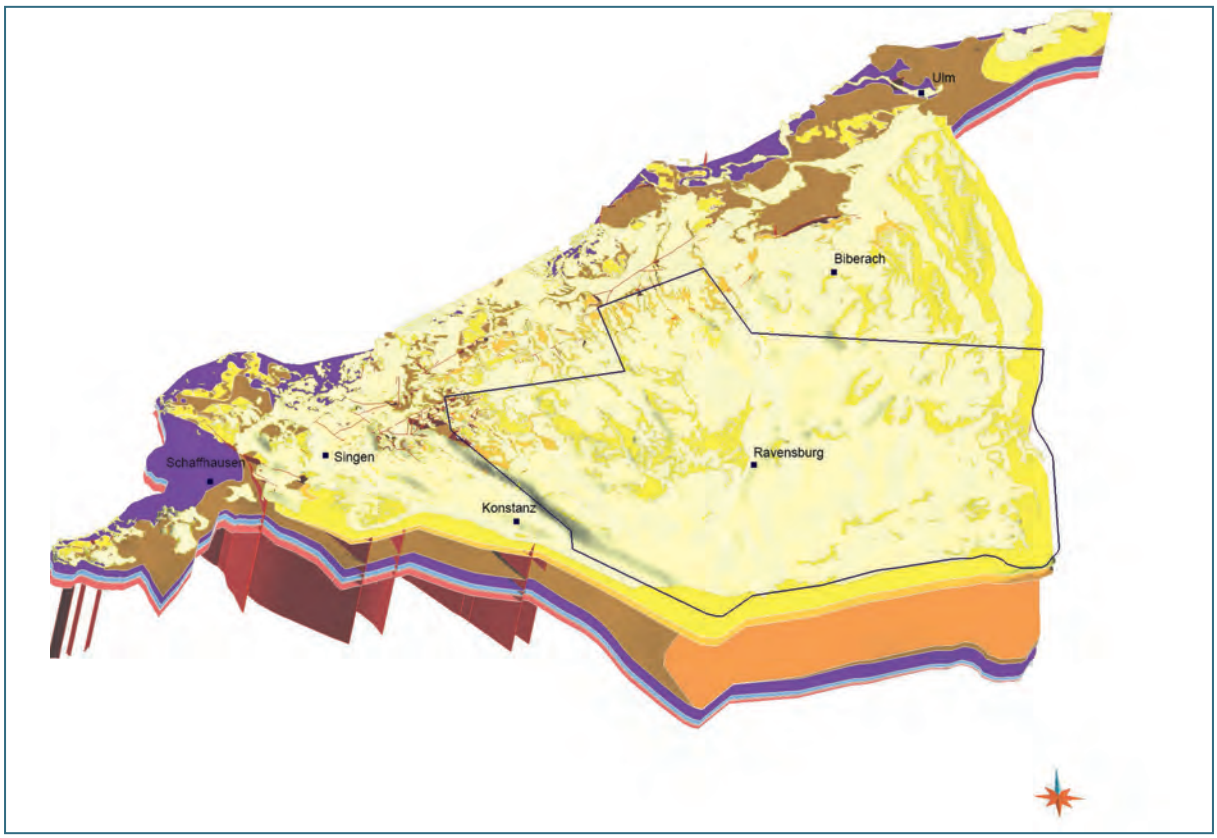

Figure 5.3-7: The framework model in Baden-Württemberg (view from SW) is based on two pre-existing models, which have been updated and merged using the GeoMol input data sets. Particularly in the southern part the fault pattern is simple.

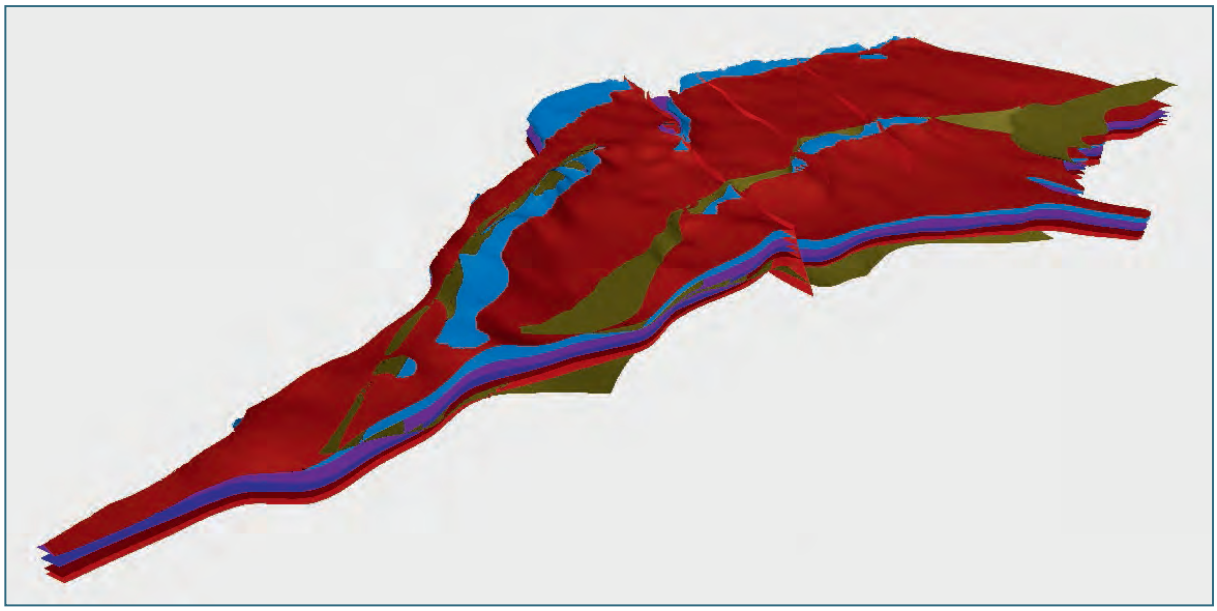

Figure 5.3-8: The 3D geological model of the Geneva-Savoy pilot area (GSA) view from SE. In GSA the framework model and pilot area model are identical. Due to the complex geological situation, only main tectonic structures have been modeled. In the central part, the Vuache fault can be recognised. The surfaces in the model show preliminary colours not yet adjusted to the accord in figure 5.1-1.

6 Geopotential assessment – criteria, methods and products

The general characterisation of the geopotentials germane to the deep subsurface of the Alpine Foreland Basins, their incurrence and relevance in terms of economic and environmental issues, has been given in chapter 2.3. This chapter describes shortly and in general terms the prerequisites required and methods applied for geopotential assessment in GeoMol. Further it portrays the products that have been derived, their possible applications and constraints of use. The implementation of geopotential assessment in the pilot areas is described in more detail in chapter 8. Results of these spatial applications, i.e. the geopotential map series produced, are available via GeoMol's MapViewer http://maps.geomol.eu.

The imperative prerequisite for the evaluation of any subsurface potential is the profound knowledge of the geological situation. This knowledge critically depends on the availability of information on the structure of the subsurface, ideally provided by 3D geological models, on the rock's texture and on the physico-chemical characteristics of the subsurface. This applies to both, the assessment of an individual geopotential as well as to the interaction of geopotentials in terms of interferences at multiple use. Due to possible interferences, utilisations may be mutually exclusive even if implemented at different depth levels of the subsurface or/and time-displaced.

Major limitation on the validity and scope of geopotential assessment ensue from availability of baseline data. In the deep subsurface, parameters on rock characteristics essential for the detailed evaluation of geopotentials are dispersed and clustered and do not allow for an appropriate regionalisation. Furthermore, many of them are classified data from E&P industries which are only partially available for the project (Chapter 3.3). The geopotential assessment as implemented in GeoMol, hence, can be considered as the best effort under the given circumstances taking into account the following characteristics of the subsurface:

- the positional relationship of the lithological units distinguished, including
- the set-up of the major tectonic features, both comparable to 1 : 100,000 scale,
- the bulk lithological properties of the distinguished units on a regional scale,
- and the spatial temperature distribution based on regional best fit approaches.

Consequently, the appraisal and synopsis of this information allows an assessment of the theoretical potential only (Figure 6.1-1). Accuracy and resolution of GeoMols results are appropriate to assist large-scale preliminary planning. GeoMol's products are not designed for site selection or evaluation. For the assessment of the technical potential or economic potential higher-resolution quantitative models and process models (based on small-scale investigations) remain indispensable.

6.1 Geothermal potential

The geothermal potential in the Alpine Foreland Basins basically refers to hydrothermal resources where heat is extracted from deep aquifer systems. The efficacy of hydrogeothermal installations strongly depends on the temperature encountered at depth and on the natural flow conditions of the geothermal reservoir. Principal issues that influence the potential yield of hydrothermal systems are the aquifers' permeability and the fault network which defines the preferential pathways of the thermal water and the possible compartmentalisation of the aquifer. Due to the paucity of data hydraulic properties and their spatial variation within modelled units as well as the hydraulic characteristics of the modelled faults could not be differentiated on the assessment of the geothermal potential. These aspects have to be considered in local-scale studies.

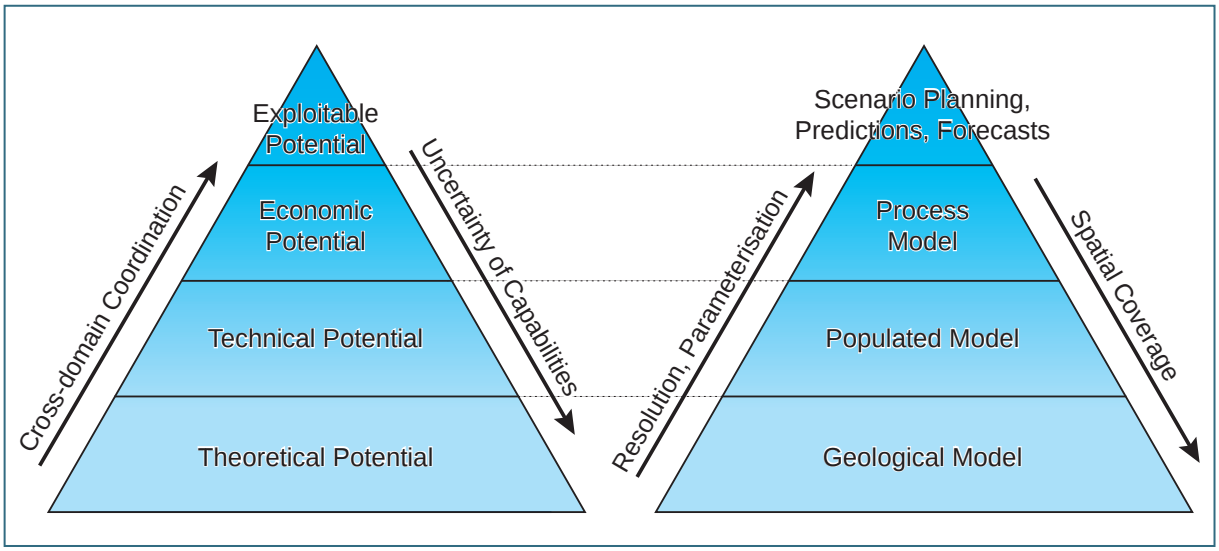

Figure 6.1-1: Schematic diagram showing the interrelationship between the levels of potential analysis (left) and the quantitative understanding of the subsurface by means of geo-models (right, modified from KESSLER et al. 2009). The potential levels in the left diagram roughly correspond to (bottom up) *Play*, *Lead*, *Prospect*, and *Recovery* of the oilfield terminology. The tabulations in chapters 8 and 9 show the theoretical potential, GeoMol's spatial representations like the geothermal potential distribution correspond to the basic level of the technical potential.

By combination of the information of the 3D geological model and the spatial temperature distribution calculated (cf. Chapter 7) the following geopotential issues have been addressed in the geopotential map series of the pilot areas and the Mura-Zala Basin:

- temperatures at the top of the most important productive aquifers,
- temperatures at 0.5 km, 1 km, 1.5 km, 2 km, 3 km and 4 km depths below surface,
- depths of the 60 °C, 100 °C and 120 °C or 150 °C isotherms,

each combinable with the distribution of the geological units and the transection traces of the principal faults at the respective depth levels.

The geothermal potential assessment also includes representations of temperature intervals of commonly accepted technical and economic boundary conditions for hydrogeothermal installations:

- 20 – 40 °C: balneologic use and/or direct use of heat by heat pumps,
- > 40 – 60 °C: balneologic use and/or direct use of heat by heat exchanger,
- > 60 – 100 °C: direct use of heat by heat exchanger,
- > 100 – 120 °C: use of absorption heat pumps and lower limit for power generation using Two-phase Expansion (*"Kalina-Cycle"*) techniques,
- > 120 – 150 °C: industrial heating, power generation (Organic Rankine Cycle (ORC), Two-phase Extension) and co-generation,
- > 150 °C: industrial heating and high potential for power generation.

This geopotential gradation is given in maps for the most important aquifers of the pilot areas (see examples in figures 8.1-3 (left) and 8.3-4) as well as a more general grading (20 – 60°C: *balneology*, 60 – 100 °C: *direct heating*, > 100 °C: *power generation*) in the tabular "compilation of theoretical geopotential" for all model units considered in the pilot areas. In these tables the latter grade also refers to petrothermal systems requiring temperatures well above 120 °C for geothermal power generation from stimulated rock suites with poor natural permeability.

6.2 Storage potential

The volume for large liquid or gas storage is most economically provided by suitable bedrock structures, either in porosity storage reservoirs (rock formations featuring an inherent high porosity) or in solution-mined caverns in thick salt formations (cf. Chapter 2.3). Target horizons for cavern storage do not exist in the Alpine Foreland Basins. High porosity rock formations, like limestones or sandstones, are widespread, however, given the buoyant nature of gases, they are suitable for underground storage only when covered by an impermeable barrier rock and sealed laterally e. g. by structural features. Depleted oil and gas reservoirs are the most commonly used underground storage sites because their seal integrity is unquestioned by sealing off oil and gas over millions of years.

A general requirement for storing liquids and gas in the subsurface is the occurrence of a porous reservoir rock superimposed by sealing barrier rocks, a so-called aquifer-seal pair, in a suitable geological setting ensuring lateral sealing. Typical formations with appropriate sealing properties are clay, clay stone or marl. The integrity of the seal is governed by the thickness of the barrier rocks (subject to the formation pressure in the infilled reservoir), the presence (resp. absence) of faults intersecting the formation, a favourable stress regime and the absence of active seismicity.

No stringent geological criteria exist for the underground storage of fluids and gases. Indications may be derived from the minimum requirements for geological storage of CO_2 following IPCC (2005) and Chadwick et al. (2008).

Commonly a porosity of > 10 % and a permeability of > 10 mD of the reservoir rock is deemed adequate for the efficient storage of low viscosity fluids at “normal” recharge-discharge rates (thus precluding Compressed Air Energy Storage (CAES) which requires a rapid alternate replenishment and discharge feasible only in cavern storage). A net thickness of sealing formation of 20 m or more is considered secure.

Depths respectively pressure criteria are substance-specific and may differ widely for different gases. For example, geological storage of CO_2 is economical only in very large volumes. Thus, for the optimal utilisation of the capacity, the injected CO_2 must be in a dense phase – liquid or supercritical. Therefore the temperature and pressure conditions must exceed the critical point for CO_2 which, assuming a regular geothermal gradient, is achieved at a formation pressure corresponding to a depth of 800 m. With respect to efficacy and economic viability the depth range between 1 and 2.5 km is considered most appropriate for the geological storage of CO_2.

Due to the substance-specific factors determining the storage potential of the subsurface, no synoptic spatial appraisal and representation thereof is given in GeoMol – except for the Swiss Midlands pilot area focussed on the CCS potential. The theoretical potential for natural gas storage in general and CO_2 storage in particular, based on the existence of aquifer-seal pairs, is summarised in tabular form for all model units considered in the pilot areas. By combination of the spatial information provided (e. g. depth of the aquifer-seal pair bearing unit, temperature distribution, fault network, etc.), areas featuring a potential corresponding to the substance-specific requirements for the gas under consideration can be delineated.

The three-dimensional compilation of the geological fundamentals can be regarded as the lowest common denominator for the further assessment of storage structures and their positional relationship to possible competing utilisations in the GeoMol pilot areas. The appraisal of the technical and economic potential like prioritisation of use and capacity planning require more detailed evaluations on top of GeoMol’s outputs.

6.3 Oil and gas potential

After decades of E&P activities the Alpine Foreland Basins are regarded mature in terms of hydrocarbon exploration. Most oil and gas fields are economically depleted, new significant discoveries are unlikely. The geological situation of (exploited) hydrocarbon deposits is well examined by the E&P industries as are the reserves for a possible enhanced recovery utilising advanced technologies. Investigations of new targets or proof of new concepts require specific routines for seismic processing and analysis not available at the GSOs and are thus beyond GeoMol's scope.

Within the scale and scope of GeoMol the oil and gas potential is considered primarily in the context of its after-use for gas storage. The theoretical potential for oil and gas production (as summarised in tabular form for all model units considered in the pilot areas) is based on the geological position of the (now mostly depleted) oil and gas fields. Spatial representations are confined to the overarching structural inventory – although in between the hydrocarbon fields – as mapped and modelled in the 3D geological models. In focal areas the faults are classified with respect to their inclination relative to the sedimentary layering (synthetic: same direction as the strata, antithetic: reverse dip in relation to strata), because, specifically in the NAFB, antithetic faults give rise to structural traps for oil and gas deposits (Figure 2.3-4 C) or may form the lateral seal for stockpiling natural gas. Furthermore, the lateral extent of the hydrocarbon deposits at the depth level of the water-oil contact surface (prior to production, as decisive for permission granting) is portrayed in focal areas.

6.4 Further geopotentials

Mainly carried out in the eastern parts of the Subalpine Molasse **coal production** has been a considerable economic factor in the NAFB till the 1960s. Due to dwindling competitiveness mining activities ceased in the 1970s in Germany and the 2000s in Austria. In the light of a low carbon economy, coal production cannot be referred to as a potential even though considerable coal reserves are left. The theoretical potential for coal production thus is only listed for the sake of completeness in the pilot areas with major former mining activities – also in terms of an option of CO_2 sequestration by injecting it into coal seams (IPCC 2005, PK NTU 2014).

Given the economic viability of the drilling and development depths the use of groundwater of the – by GeoMol measure shallow – subsurface for **drinking water** supply is widespread in the Alpine Foreland basins. Basically, aquifers must feature a high permeability, a low vulnerability, a low solute content and a temperature of < 20 °C for immediate use. The theoretical potential as summarised in tabular form for all model units of the pilot areas only considers the occurrence of high permeability layers with a reasonable thickness and the global solute content. Temperatures as a function of depth can be estimated through combination with the temperature model. At greater depth superposing layers provide an appropriate protection against pollutants, at shallow depth groundwater vulnerability depends on small scale situations beyond the scope of GeoMol.

Although a natural potential in the broad sense (cf. Table 2.3-1), **seismicity** has not been regarded in geopotential assessment. It has been considered for the localisation and assessment of seismogenic structures and active faults in the Po Basin pilot area, in terms of a geohazard and a possible constraint for geopotential utilisation (Chapter 9.1).

7 Temperature modelling

7.1 Introduction

In general, the following transport processes determine the geothermal conditions in the technically accessible part of the Earth's crust:

- heat conduction,
- forced convection (advection),
- free convection.

These heat transport processes cause a general increase of temperature with depth, the geothermal gradient, which is about 3 °C/100 m in the NAFB, and less in the Po Basin. The geothermal gradient may show a variance in the order of magnitude two due to local to regional scale effects.

A regional scale the geothermal regime is predominately influenced by heat conduction. Described by the Fourier Law of heat conduction the distribution of subsurface temperatures is determined by

- the mean surface temperature,
- the surface relief,
- the distribution of thermal rock parameters (thermal conductivity),
- the distribution of internal radiogenic heat sources (rock parameter radiogenic heat production rate) and heat-flux resulting from deeper parts of the Earth's crust.

Superposed to the large-scale conductive regime, local variations in the GeoMol project area refer to convective transport processes driven by the movement of groundwater. Convective transport is governed by external processes such as gravitation – in this case defined as "forced convection" or "advection" – or internal processes ("free convection"). Free convection is the consequence of a thermal uplift of heated groundwater due to the reduction of water density. This effect leads to the development of vertical convection cells.

In general, temperature models should be able to consider the above-mentioned thermal processes either in an explicit or implicit way. Explicit temperature models result from numerical 3D models, which consider all listed transport processes (conduction, advection as well as free convection) in the spatial resolution needed to solve the specific questions. Implicit temperature models result from the geo-statistical interpolation as well as extrapolation of measured subsurface temperatures. Of course, there are various approaches, which found on a combination of the above mentioned two main procedures.

All procedures associated to explicit and implicit temperature modelling follow a general workflow based on the subsequently listed main tasks:

- processing of input data (temperature measurements),
- model setup and model calculation,
- model calibration and estimation of error,
- post-processing and visualisation.

The following chapter gives a brief overview on the approaches and methods applied in GeoMol in order to produce temperature models. We intend to compare these methods and the lessons learned from it in order to give an overview to the reader how to execute temperature modelling in a 3D subsurface.

7.2 Objectives

Due to the paucity and the uneven distribution of temperature data available, leaving large voids, the elaboration of a supra-regional temperature model for the entire project area of GeoMol has been beyond of the project's scope. Temperature modelling was limited to specific pilot areas. The common technical as well as scientific challenge for most pilot areas consisted in the elaboration of trans-nationally harmonised temperature models based on national datasets. In this context, in three of the five investigated pilot areas trans-national datasets had to be compiled and harmonised. Two pilot areas do not have trans-boundary coverage and were therefore carried out by a single project partner. Most temperature models elaborated during GeoMol aimed to provide 2D map series for different depth levels. Only in the Upper Austria – Upper Bavaria (UA – UB) pilot area a pure conductive 3D temperature model has been explicitly calculated in order to identify convection cells of moving subsurface thermal water.

Table 7.2-1: Overview on area coverage of the temperature models

Pilot area	Involved countries[1]	Specific objectives	Comments
Lake Constance – Allgäu Area (LCA) w/o Swiss territories	**Baden-Württemberg**, Bavaria, Switzerland, Austria	2D temperature map-series for information systems (web map services)	Due to the lack of sufficient data no input from Switzerland possible
Geneva-Savoy Area (GSA)	**France**	2D temperature map-series for information systems (web map services)	
Upper Austria – Upper Bavaria (UA-UB)	**Austria**, Bavaria	2D temperature map-series for information systems (web map services) Conductive 3D model for hydrogeological interpretation	All map series refer to the conductive 3D model, which was calibrated by measured subsurface data
Brescia-Mantova-Mirandola Area (BMMA)	**Italy**	2D temperature map-series for information systems (web map services)	The existing geological 3D model (software Move) was used to project interpolated subsurface temperatures to geological layers.
Mura-Zala Basin	**Slovenia**	Application add elevated geothermal gradients and comparison of methods	

[1] The country / state in bold letters was responsible for the elaboration of the temperature model

7.3 Data background

Temperature models base on measured subsurface temperatures. The temperature models, elaborated in GeoMol refer to already existing data, which predominately have been measured in at hydrocarbon exploration wells by the E&P industry. The most important data sources (methods of temperature measurements) are:

BHT-data: Bottom-Hole Temperatures (BHT) are measured during geophysical borehole logging surveys, mostly using analogous maximum temperature thermometers. As the temperature is supposed to raise with increasing depth of the borehole, the measured maximum temperature is therefore allocated to the deepest point in the well. BHT data only reflect the drilling mud temperature directly after the drilling process, which is strongly influenced by the circulation of the mud and the resulting thermal imbalance between the drilling mud and the surrounding rocks. For shut-down times up to several months, BHT data need to be corrected for the influence of the circulating mud (for further details see subsequent chapter 7.4). The absolute accuracy of most devices is limited to ±1 °C.

DST-data: Drill Stem Test temperatures are measured during hydraulic borehole tests at hydrocarbon wells (e. g. open hole or casing tests). In general, DST data reflect true formation temperatures, as the device measures the temperature of inflowing formation fluids (water, oil or gas). The most important sources of errors associated to DST data are: (a) low permeable or dry reservoirs, at which only backflow of drilling mud into the tester occurs, (b) mixture of formation water and drilling mud and (c) adiabatic cooling due to expansion of inflowing gas. If the documentation of the hydraulic test is available all above mentioned sources of error may be identified. The absolute accuracy of most devices is limited to ±1 °C.

Cementation logs (disturbed logs): Continuous temperature logs are used to identify the head of the cementation in the annulus of the well. In most cases, the entire borehole section is also logged during the cementation logs. For that reason, cementation logs deliver continuous temperature logs, which are in most cases thermally disturbed due to the influence of the circulating drilling mud as well as to the heat released by hydration of the cement. In order to achieve non-influenced temperature logs a shut-down period at the well of at least one week has to be achieved. In practice, the shut-down time of cementation logs varies between 24 and 48 hours.

In addition, the following data sources may also be available:

Temperature logs (undisturbed logs): In general, continuous temperature logs after a shut-down time of at least one week only show minor to negligible influence of the circulating mud. Of course, the needed shut-down period is also depending of the maximum depth reached at the well and the drilling period, respectively. Temperature logs are used to identify inflow zones at geothermal wells or have been executed for scientific purposes.

Outflow temperatures at geothermal wells: In general, outflow temperatures in geothermal wells do not reflect the true formation temperature, as the water is cooling during the ascent in the well. Outflow temperatures can be corrected for the true formation temperature, if they are measured during pumping tests at different yields. In that case, correction procedures similar to BHT correction can be applied (see also the subsequent Chapter 7.4).

The different methods, which were available at the pilot areas, are listed in table 7.3-1.

Table 7.3-1: Overview on available data background in the different pilot areas.

Pilot / Study Area		**Number of wells**				**Number of individual datum points**				**Sum of quality coefficients**
Name	Area km²	Total	BHT	DST	Logs undist	Total	BHT uncorr	BHT corr	DST	
Lake Constance – Allgäu Area (LCA) w/o Swiss territories	7,260	**350**	131	65	154	**691**	0	178	513	**522.53**
Geneva-Savoy Area (GSA)	2,000	**14**	13	1	0	**43**	0	40	3	**16.1**
Upper Austria – Upper Bavaria Area (UA – UB)	4,730	**346**	330	10	6	**659**	75	571	13	**365.85**
Brescia-Mantova-Mirandola Area (BMMA)	5,700	**39**	36	3	0	**331**	134	194	3	**88.76**
Mura-Zala Basin	5,400	**275**	225	10	40	**339**	211	107	21	**121.69**

As indicated in Table 7.3-1, the data background strongly varies between the investigated pilot areas. In order to allow a quantitative comparison between the data background in the different pilot areas, an evaluation method proposed by CLAUSER et al. (2002, p. 111) has been applied. The so-called “quality coefficients” reflect a normalised rating of the expected range of error associated to above listed sources of subsurface temperatures. In that context, a thermally non-disturbed continuous temperature log, measured after a shut-down period of at least 3 weeks, obtains the highest quality coefficient 1, while a single BHT measurement without documentation of the well geometry and shut-down period is associated with a quality coefficient of 0.14. An example of evaluated input-data for the LCA pilot area following the approach of CLAUSER et al. (2002) is shown in figure 7.3-1.

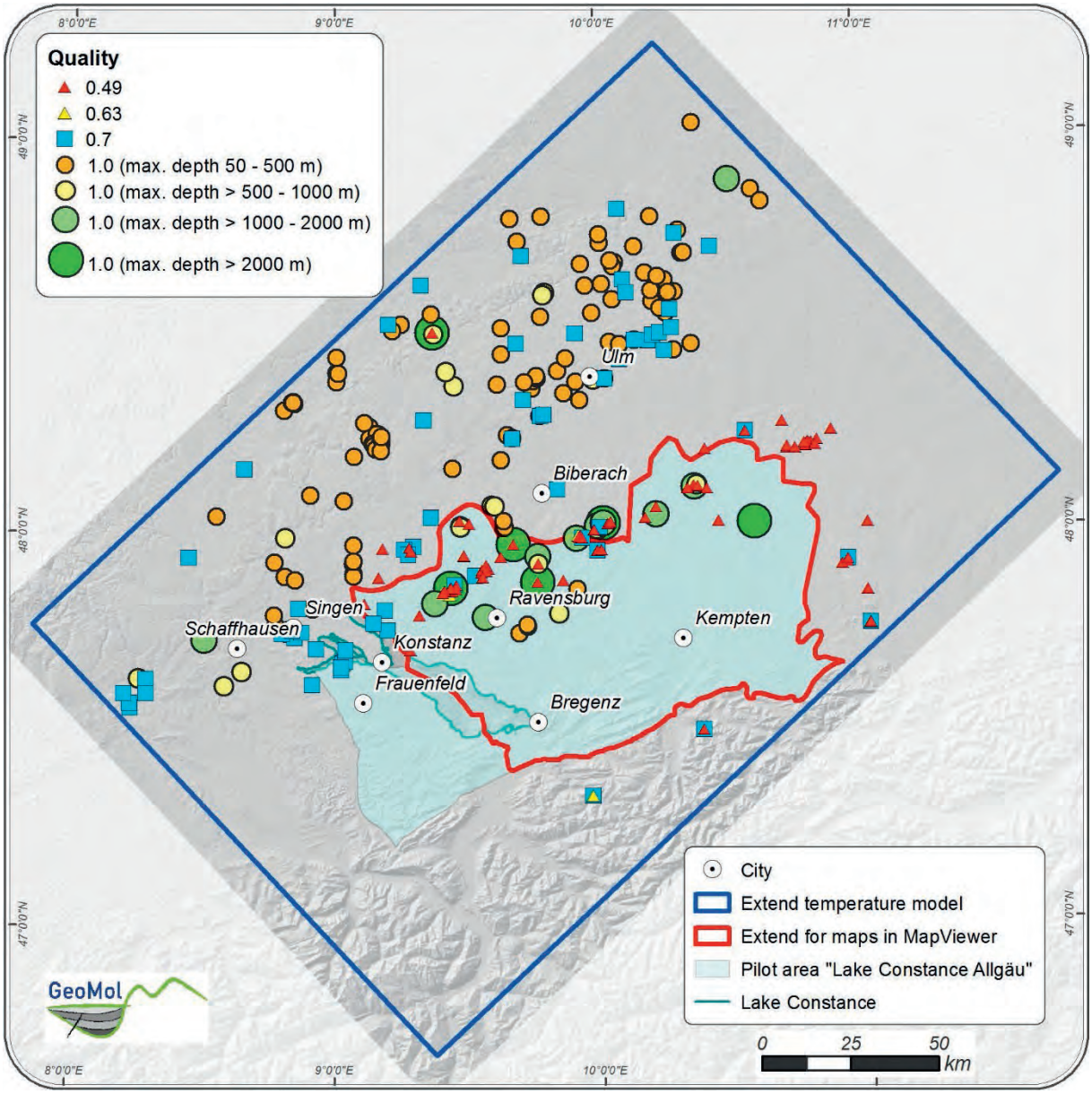

Figure 7.3-1: Overview on available temperature data at the LCA pilot area, which have been evaluated following CLAUSER et al. (2002). See text for discussion.

Table 7.3-1shows the summarised quality coefficients referring to CLAUSER et al. (2002) at the investigated pilot areas. Continuous temperature logs have been considered as a single measurement in order to avoid a clear overestimation of the data quality. As indicated in Table 7.3-1, the Lake Constance – Allgäu pilot area (LCA) and the Mura-Zala Basin show a sound data background, while the Geneva – Savoy (GSA) and Brescia-Mantova-Mirandola (BMMA) pilot areas are affected by both, a low number of temperature measurements as well as low quality data. In the Upper Austria – Upper Bavaria pilot area (UA – UB), the spatial density of input data strongly varies between Austria and Bavaria. More than 90 % of all available input data are located in Austria providing a profound data background. In contrast, in the Bavarian part of the pilot area only 37 single input data of predominately low quality were available. It has also to be pointed out, that only in the LCA pilot area and the Mura-Zala Basin a significant number of undisturbed temperature logs were available. All other pilot areas are dominated by BHT datasets.

7.4 Overview on the applied workflow

In general, the elaboration of subsurface temperature models requires the following general workflow:

Data processing includes the calculation of the true vertical as well as horizontal position of a single datum point at the subsurface as well as temperature correction. Temperature correction are only applied for BHT measurements as well as outflow temperatures at the wellhead in order to estimate the true formation temperature. All other available temperature sources are either estimated to reflect the true formation temperature (undisturbed temperature logs and DST measurements) or not able to be corrected (disturbed temperature logs). In a next step, the individual datum points may optionally be allocated to geological units in order to allow data filtering. This processing step has been applied for the UA – UB pilot area only. The final step of the data processing consists in a plausibility evaluation in order to eliminate temperature datum points affected by a large error.

Temperature modelling (2D, 3D) has been achieved by either data interpolation or / and forward modelling. Pure data interpolation or extrapolation is only recommendable in case of a sufficiently high density of datum points. In addition, there are general processing rules, which have to be considered for the extrapolation of temperature data in depth. For example, a maximum extrapolation distance of 20 % of the total drilling section is recommended (ČERMAK & HURTIG 1979). In contrast, numerical modelling requires more effort and a conceptional a-priori model, which will be translated into a temperature model. In many cases a combination of both approaches have been applied during GeoMol in order to achieve temperature models.

Model calibration and estimation of error: Temperature models, which rely on any kind of numerical or analytical modelling, need to be calibrated based on processed temperature data. For that purpose, residuals between modelled and observed temperature values are calculated and superposed to the a-priori model in order to minimise the prediction error at observation points. These residuals, which are often interpolated to a regular grid, also reflect the prediction error of the a-priori model. In contrast, error estimation of data interpolated to a regular grid is reflected by the statistical error of variance associated to the chosen interpolation method (e. g. Kriging).

In addition, error estimation also includes the varying spatial density of available input or calibration data as well as the quality of the data itself. Combining these two aspects may also lead to qualitative estimation of the expected plausibility and error of the elaborated temperature models.

Post-processing and visualisation: Post-processing covers the necessary processing steps in order to transform the calculated subsurface temperatures to maps and cross sections. In case of geo-statistical interpolation, the results are available in terms of raster datasets, which can be directly used for the creation of maps. In case of numerical models, the results have to be extracted from the code dependent internal grid and projected to the surface, which is shown in the output maps.

Table 7.4-1 summarises the different methods and approaches used at the individual pilot areas in order to achieve subsurface temperature models. Further descriptions of the methods applied are given in the following sections.

Table 7.4-1: Summary of methods applied and workflows for the elaboration of temperature models in GeoMol's pilot areas, respectively the national sub-areas.

Area	Involved country	Temperature correction	Temperature modelling	Model calibration, error estimation
Lake Constance – Allgäu Area (LCA) w/o Swiss territories	Baden-Württemberg	None, use of BHT data already corrected (KÜHNE 2006).	Analytical a-priori model based on regionalised geothermal gradients	Calibration based on residuals
	Bavaria	BHT: inverse and forward correction based on cylindrical heat source.		
	Austria	BHT: *Horner* plot		
Geneva-Savoy Area (GSA)	France	BHT: regionalisation methods (GABLE 1978)	Analytical a-priori model based on regionalised geothermal gradients	Calibration based on residuals
Upper Austria – Upper Bavaria Area (UA – UB)	Austria	BHT: inverse optimisation method, cylindrical heat source Outflow temperatures: *Horner* plot	Numerical a-priori model	Calibration and error estimation based on residuals
	Bavaria	BHT: inverse optimisation method, cylindrical heat source	Geo-statistical interpolation of geothermal gradients	
Brescia-Mantova-Mirandola Area (BMMA)	Italy	BHT: *Horner* plot, *Zschocke* method and regionalisation methods (PASQUALE et al. 2008)	Analytical a-priori model based on regionalised geothermal gradients (cf. MOLINARI et al. 2015)	Calibration based on residuals
Mura-Zala Basin	Slovenia	BHT: *Horner* plot, *Lachenbruch & Brewer* plot	Geo-statistical interpolation	None

7.4.1 Data processing

The general workflow of temperature data processing can be divided into:

- the correction of the relative position of the individual datum points,
- the correction of temperature values,
- quality and plausibility checks.

Correction of the relative position: In many pilot areas, the assessed temperature data were given in relative position with regard to the drilling depth. In a first step the true vertical depth (TVD) as well as the true horizontal position of the datum points have been calculated considering the dip as well as the azimuth of the drilling path.

Temperature correction procedures have only been applied on BHT datasets and on outflow temperatures (UA – UB). In all areas methods based on line heat source and cylindrical heat source approaches founding on pure conductive heat balancing were used. It has to be taken into account that methods based on more than two individual BHT values lead to the lowest ranges of errors. Especially single BHT correction methods using empiric nomograms may lead to significant errors. To quantify the accuracy and reliability of the different BHT correction methods applied in GeoMol, a calibration was conducted by comparing the extrapolated BHT-data with undisturbed temperatures taken from continuous logging (see also figure 7.4-1).

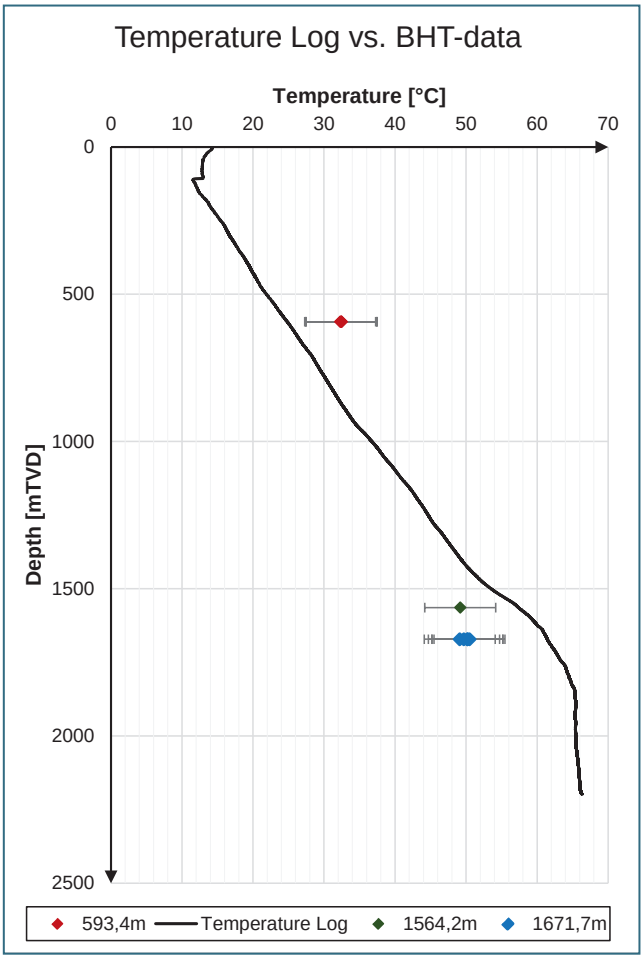

Figure 7.4-1: Comparison between BHT_{corr} data at different depths and an undisturbed temperature log in a well in the Bavarian part of the Molasse Basin. The error bar represents a fixed value of ±5 °C.

The investigation of five diverse BHT correction procedures results in a wide range of deviations by 0.2 K to 33.8 K. The forward modelling methods tend to be the most reliable approach combining the lowest range of deviation and the smallest mean value of 6.3 K (Casper & Zosseder 2015). In figure 7.4-2 the deviations out of the single BHT-correction method are plotted exemplarily against the true vertical depth (m TVD) representing overestimation of the equilibrium temperature in the shallow parts of a well (< 1000 m TVD) and underestimation deeper 1000 m TVD.

The methods applied are summarised in Table 7.4-2

Table 7.4-2: Overview on of the temperature correction methods applied in GeoMol

Input data	Name of method	Description of method
>2 BHT, outflow temperatures	*Horner* plot	Graphical method published based on HORNER (1951). This method assumes a logarithmic shaped thermal balancing after the end of drilling and circulation of drilling mud. In order to apply this method both before mentioned parameters have to be known.
	Lachenbruch & Brewer plot	Graphical method published based on LACHENBRUCH & BREWER (1959) based on *Horner* plot.
>2 BHT	Inverse optimisation based on cylindrical heat source.	Inverse optimisation method based on LEBLANC et al. (1981), adapted by *Goetzl* (ZEKIRI 2011). This correction method requires the shutdown periods of different individual BHT measurements, the geometry of the well (bit diameter). In addition, the initial mud temperature after the end of circulation has to be known or assumed. The true formation temperature as well as the thermal diffusivity of the drilling mud and the thermally disturbed rock mass is calculated based on a LSQ optimisation algorithm.
>1 BHT	Cylindrical heat source	Straight forward analytical method based on LEBLANC et al. (1981). This method needs estimation of assumptions of all parameters mentioned at the inverse optimisation method as well as assumptions considering the bulk thermal diffusivity of the drilling mud and the surrounding rock. The bulk thermal diffusivity can be regionalised based on lithological models of the subsurface.
1 BHT	*Zschocke* method	Analytical method based on a cylindrical heat source published by ZSCHOCKE (2005).
	Regionalisation methods	In case of single BHT values and no documentation of the shutdown period and/or the well diameter, different regionalised correction methods based on empiric observations have been used. For the Mura-Zala Basin a method published by PASQUALE et al. (2008) has been applied. For the GSA an empiric approach by GABLE (1978) has been used, which uses empirically gained nomograms for temperature correction with regard to the geological region and the depth of an individual datum point.

Based on the results of the calibration and the application of different methods in GeoMol the influence of the different temperature corrections on the temperature models are further investigated. The diverse methods lead to an uncertainty of at maximum 4 K to 8 K with a mean deviation of 1 K (CASPER & ZOSSEDER 2015).

Quality and plausibility checks: At most pilot areas the quality of the data source (type of temperature measurement) was assessed based on quality coefficients proposed by CLAUSER et al. (2002). At the LCA pilot area all data sources showing a quality coefficient of lower than 0.49 (less than 2 BHT values at a certain depth level) as well as all data from depths less than 50 m below surface have been sorted out. For the Bavarian part of the UA – UB pilot area all BHT values below 30 °C have been sorted out due to an expected strong masking effect by the circulating drilling mud (see Figure 7.4-2). At the Austrian part of the UA – UB pilot area all BHT data have been corrected. Low quality filtering has later been applied to data showing erratic geothermal gradients. Later on, a second stage low quality data filtering has been executed after the accomplishment of the a-priori numerical model, when all temperature values showing a deviation to the a-priori model of more than 20 °C have been filtered.

7.4.2 Temperature modelling

The temperature models achieved for the GeoMol pilot areas refer to the following approaches:

- analytical a-priori models based on regionalised geothermal gradients,
- numerical a-priori models based on pure conductive heat transport,
- geo-statistical interpolation of subsurface temperature values.

Analytical a-priori models: Based on the Fourier Law, analytical a-priori models combine the estimated surface temperature with regionalised geothermal gradients, while neglecting radiogenic heat production. This method has the advantage of taking convective heat transport into account, which is implicitly considered in the apparent regionalised geothermal gradients.

In a first step an elevation dependent mean annual surface temperature was calculated based on the following approaches:

For all surface temperature models a linear function between the surface elevation and the surface temperature has been applied, which was either derived from mean annual air temperatures or direct measurements of the soil temperature in shallow depths provided by meteorological stations. In the LCA pilot area the thermal influence of the Lake Constance has also been taken into account. The cooling effect of the lake on the surface temperature at the lake bottom and the surrounding littoral zone has been approximated by a reduced annual surface temperature. Based on a numerical test-model, the range of influence of the cooling effect has been estimated for a maximum depth of 4.2 km below the lake and a maximum lateral range of 1.7 km along the shore.

The regionalised geothermal gradients (°C/100 m) refer to conceptual as well as statistical models. All models consider the geological build-up as well as zones of expected convective heat transport. For the LCA, GSA and BMMA pilot areas generalised models of the estimated geothermal gradients have been applied. In the UA – UB pilot area the regionalised geothermal gradients were derived from geo-statistical interpolation of geothermal gradients calculated at individual wells for distinctive geological formations (e. g. Upper Jurassic formation or Cenozoic basin infill).

The calculation of subsurface temperatures at a certain depth level (z) has been implemented using the simplified *Fourier* Law:

$$T(z)=T_0 + \sum \nabla T_i \cdot \Delta z_i$$

Whereas T_0 is the mean annual surface temperature; ∇T is the geothermal gradient, valid for a certain depth interval Δz_i.

In addition, at the LCA pilot area a relief depending relative correction function has also been applied on the calculated subsurface temperatures in order to avoid tracing of the surface relief. The applied correction function was taken from the GeORG project (GeORG Projektteam 2013).

Numerical a-priori model: A numerical a-priori model has only be achieved for the UA – UB pilot area. It represents a pure conductive steady state model using the software FEFLOW. The boundary conditions of this model were given by a relief depending mean annual surface temperature and a basal heat-flow pattern at a depth of 7,000 m b. s. l., taken from Przybycin et al. (2014). Until now, there are hardly any datasets available for the thermal rock properties at the UA – UB pilot area. For that reason a start-up model of thermal conductivities, taken from literature data, has been elaborated, which has later on been optimised by parameter estimation routines. The pure conductive a-priori model does not implement heat transport by convection. For that reason, a model calibration by processed subsurface temperatures is inevitable.

Geo-statistical interpolation has been applied in the Mura-Zala Basin study (Chapter 9.3), where a sufficiently high density of good quality data have been available. In the UA – UB as well as the BMMA pilot areas, the calculated geothermal gradients have also been geo-statistically interpolated. The interpolation has mostly been executed based on the Co-Kriging method using the software pro-

ducts ESRI ArcGIS or Golden Software Surfer. In the UA – UB pilot area the regionalisation was also performed by the geo-statistical software SADA 5.0 (Steward et al. 2009) using indicator kriging for interpolation. This probabilistic approach is suitable for non-normally distributed input datasets. For further information see also Casper & Zosseder (2015).

7.4.3 Model calibration and error estimation

Except for the Mura-Zala Basin, all a-priori models have been calibrated by means of subsurface temperatures. In general, two different calibration workflows have been applied:

- Iterative adaption of the a-priori analytical model based on regionalised geothermal gradient.
- Superposition of calculated residuals on the a-priori model.

The latter approach has been applied on almost all pilot areas in order to fit the published maps on existing observation points. The residuals between the a-priori model and the observed surface temperatures have been interpolated to a regular grid for the different depth intervals shown at the project specific web map service. The achieved residual grid was afterwards superposed to the a-priori model. In the UA-UB pilot area, the calculated residuals between the numerical model and the observation points mainly reflect zones of heat transport by convection, under the restriction that the observation points represent equilibrium temperature without any further uncertainties or errors resulting from BHT correction for instance. For that reason, the residuals have also been used for hydrogeological interpretation. For the calculation of residuals with regard to certain surfaces (e. g. top Malm or certain depth intervals) a range of tolerance for the depth of an observation point of ± 200 m was used.

Error estimation as well as the evaluation of the quality of achieved maps refer to the density of available observation points as well as to the calculated residuals. In some pilot areas the evaluation of density of observation points also considers the quality coefficients leading to a qualitative evaluation of error. In addition the calculated and interpolated residuals are able to reflect the existing error in a more quantitative way.

7.5 Conclusion

The lessons learned during the elaboration of temperature models at GeoMol are discussed regarding the following aspects:

- data and workflow harmonisation
- data processing
- temperature modelling and model calibration

Data and workflow harmonisation: Except for the SMA and BMMA, all pilot areas are covering at least two different countries. For that reason, harmonisation of data and workflows has been a crucial issue. Considering the evaluation of the quality of different data sources the quality coefficients proposed by Clauser et al. (2002) have been applied for the pilot areas UA – UB and LCA. These coefficients are a good tool for a harmonised evaluation of the quality of input data and can also be used for the creation of data density maps. However, these quality coefficient do not reflect the quality of the method chosen for BHT correction. As the coefficients are normalised, they may also be used as weighting factors for geo-statistical data interpolation.

At GeoMol data processing was executed individually by all project partners involved at a certain pilot area. At the early stage of data processing the individual methods for data processing have been assessed by questionnaires. The assessment of applied methods show, that in most cases well established, internationally published methods have been applied. Only for datum points having less than two BHT values regionally differing empiric methods have been used for data correction. In most cases these methods are not transferable to other regions as they are only derived from regional datasets.

In contrast, the temperature models in the different pilot areas were elaborated by only one responsible project partner in order to avoid inhomogeneity related to different methods applied. Only in the UA-UB pilot area two different approaches (analytical and numerical a-priori model) have been applied for comparison purposes. To conclude, the elaboration of harmonised temperature models in the trans-national pilot areas based on harmonised input data was easy to be realised as these areas were affected by the same geological context.

Data processing: Error analyses on BHT correction methods at the Bavarian Molasse Basin (Casper & Zosseder 2015) revealed, that a minimum error of 1 °C to 3 °C has to be expected due to insufficient documentation of datasets (considering circulation and shut-down periods) and limitation of methods considering a pure conductive thermal balancing without post shut-down circulation of the drilling mud (instantaneous heat source assumption). In addition, BHT datasets at shallow depths (depth range of the 30 °C isotherm) should not be considered for BHT correction, as the drilling mud obtains a higher temperature than the surrounding rocks (see also Figure 7.4-2).

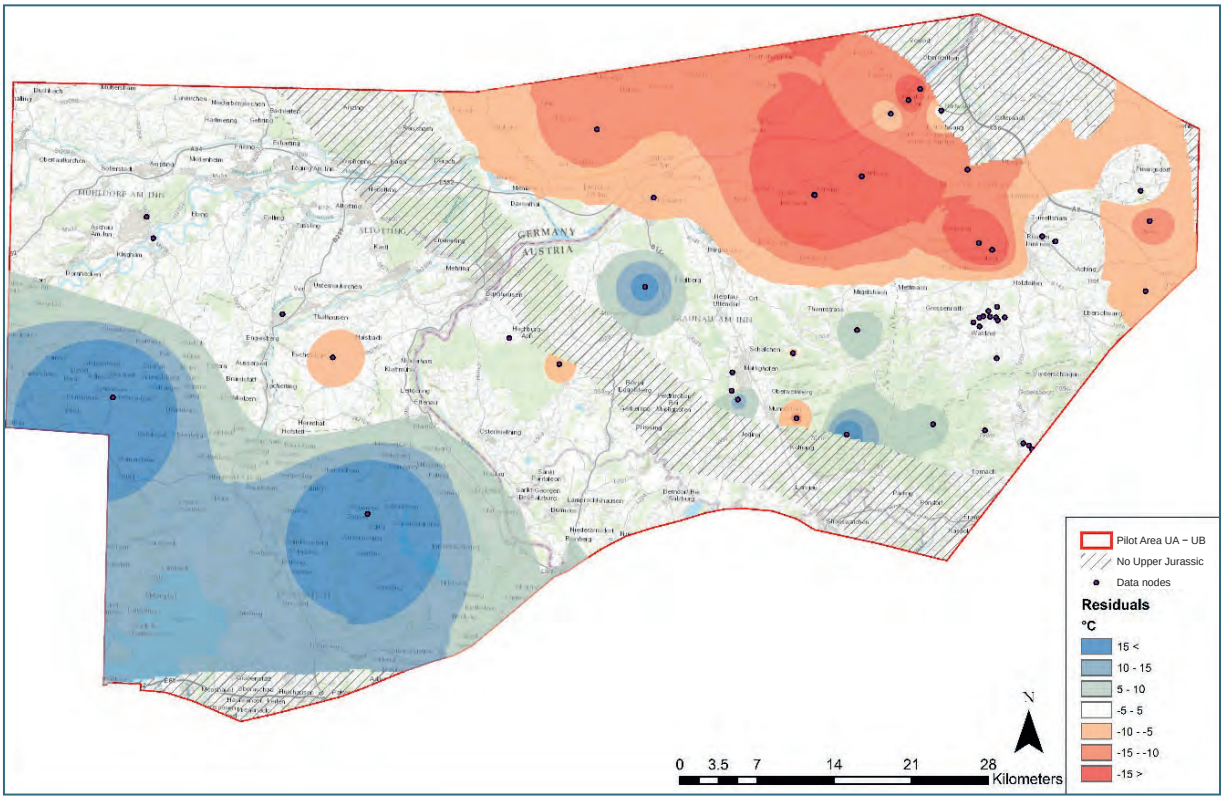

Figure 7.4-2: Interpolated residuals between the a-priori model in the UA – UB pilot area based on conductive 3D modelling and observed subsurface temperatures for the top of Upper Jurassic (surface Malm resp. Purbeck). Red colours indicate areas where the a-priori model underestimates the subsurface temperature due to influence of thermal water convection.

Temperature modelling and model calibration: Except for the UA – UB pilot area and the Mura-Zala Basin all achieved temperature models refer to an analytical a-priori model based on regionalised geothermal gradients at different levels of spatial resolution. This approach requires less calculation effort than the numeric a-priori models as well as less input data, as the thermal conductivity of the subsurface rocks is implicitly considered at the regionalised geothermal gradients. This method is also capable to approximate heat transport by convection by means of geothermal gradients. In case of geo-statistical interpolation of calculated geothermal gradients, this method is quite vulnerable to errors of the used input data. Furthermore, model calibration based on measured subsurface temperatures is not possible, as the datasets have already been used for the elaboration of the model.

Analytical as well as numerical a-priori models do not refer to measured subsurface data. For that reason, model calibration based on observation points is inevitable. In addition, the calculated residuals in most cases give valuable information about heat transport processes not included in the a-priori model (e. g. convective heat transport not included in a pure conductive heat transport model) and data errors. For the UA – UB pilot area the calculated residuals have also been used to identify erroneous observation points. In a second stage of quality control, all measured subsurface temperatures showing residuals of more than ± 20 °C have been once again checked for plausibility.

Based on the experiences gained from GeoMol, it is recommended to establish an a-priori temperature model, which is not directly derived from measured subsurface temperatures of varying data quality. A pure conductive numerical 3D model has, in addition, the advantage of allowing hydrogeological interpretation based on calculated residuals. If an a-priori model is not available for a certain region, it is recommended only to use high quality input data (e. g. quality coefficient referring to Clauser et al. (2002) of at least 0.7) for geo-statistical interpolation. Model calibration and quality checks can later be performed on low quality input data not considered for the interpolation. This approach is of course limited by the spatial density of available high quality input data.

8 Applications in Pilot Areas

The use cases of the five pilot areas focus on parts of the Alpine Foreland Basins in which subsurface use of varying objective and scope are currently planned, prepared or expanded or where conflicting use of resources looms ahead. The test areas were selected to cover a wide variety of situations with respect to the geological setting, planned subsurface uses and areal extents across national borders. Pilot activities exemplify the evaluation of subsurface potentials based on 3D models. Results will serve planning authorities, expedite the adoption of guidelines and best practice for spatial planning and resources management, and foster the incorporation into decision-making processes.

In the following sections many localities are quoted which can be shown in the enclosed large-scale maps only in a few cases. For localisation of these *places shown in italics* please refer to a higher zoom level of the GeoMol MapViewer http://maps.geomol.eu where all areal results of the pilot area uses cases are held available.

8.1 Geneva-Savoy area (GSA)

Pilot activities in the area of Geneva-Savoy aimed at modelling the subsurface geology and at assessing its geothermal potential. The area is currently the focus of transnational use of geothermal energy at medium and far depths. Parallel to the GeoMol project, the state of Geneva launched "GEothermie 2020", a geothermal prospection and exploration programme which started with the objective to improve the knowledge of the subsurface. The pilot activities in the Geneva-Savoy area were perfectly suited to fit into this programme by achieving a 3D geological model as well as a model of the temperature distribution at depth.

8.1.1 Study area and geological setting

The outer parts of the Western Alps form a classic foreland fold-thrust belt. In the Geneva-Savoy region this belt encompasses, from west to east, three different geological domains: the internal unit of the Jura Mountains, the Savoy-Geneva Tertiary Molasse Basin and the *Bornes* and *Bauges* massifs corresponding to external units of the subalpine chains.

The sediments in this area form a thin thrust wedge that was detached from its basement during Alpine collision stages (Mugnier & Ménard 1986, Guellec et al. 1990). The orogenic front accommodates, within the sedimentary cover of the Alpine foreland, a minor part of the shortening recorded in the crustal / lithospheric wedge of the Alps (Tardy et al. 1990). The Molasse Basin therefore constitutes the part of the foreland thrust system of the Alps that has been overlain by syntectonic Tertiary deposits.

The Savoy-Geneva Molasse Basin is the south-western prolongation of the Swiss Molasse Basin. It extends from the Geneva area to Chambéry area between, forming a narrow (max. 40 km in width) elongated (approx. 110 km in length) NNE–SSW depression between the subalpine frontal thrust and the eastern edge of Jura Mountains folds (Figure 8.1-1).

The Savoy-Geneva Molasse Basin features several N–S (Gros Foug) to NE–SW (Salève) Mesozoic structures which emerge from the Tertiary Molasse deposits. They correspond to ramp anticlines composed of Jurassic and Lower Cretaceous carbonate formations. The axes of these Mesozoic anticlines, particularly the Salève anticline, are displaced by several NW–SE transverse faults (e. g.

Vuache fault, *Cruseille* fault) which acted as transfer faults during thrust tectonics and influenced the distribution of Tertiary deposition.

The Tertiary infill of the Alpine Molasse Basin is subdivided into four different units which are to varying extents present also in the Savoy-Geneva basin. The oldest Tertiary unit encountered in the study area is the Lower Marine Molasse. These Rupelian shallow marine to brackish deposits are locally preserved east to the *Salève*, near the front of the subalpine ranges. They are tectonically implicated also in the *Bauges* and *Bornes* massifs (Figure 8.1-2). Above, the Lower Freshwater Molasse corresponds to Chattian to Aquitanian continental (fluvial to lacustrine) deposits which are present across the entire pilot area. The Upper Marine Molasse consists of Burdigalian to Langhian detrital marine deposits which are well exposed west of the Salève and south of the Vuache fault. The uppermost Molasse unit is the Upper Freshwater Molasse represented by Upper Miocene fluvial sediments which occur only in a few localities.

The Mesozoic sedimentary succession, known from outcrops in the *Salève* and the neighbouring Jura units, and from exploration wells, mainly consists of platform carbonates, Rhaetian to Barremian in age. These thick alternations of shallow marine bioclastic limestones and platform marls to mudstones superpose the top of Triassic sediments. The upper part of Triassic deposits, Keuper in age, is in part made of evaporites which constitute the basal decollement for the foreland thrust system. Beneath the Mesozoic series, local Permo-Carboniferous basins were observed in oil exploration wells drilled in the Savoy-Geneva Molasse Basin. Permo-Carboniferous sediments seem to be deposited within several narrow extensional basins within in the Palaeozoic (mostly Hercynian) crystalline basement.

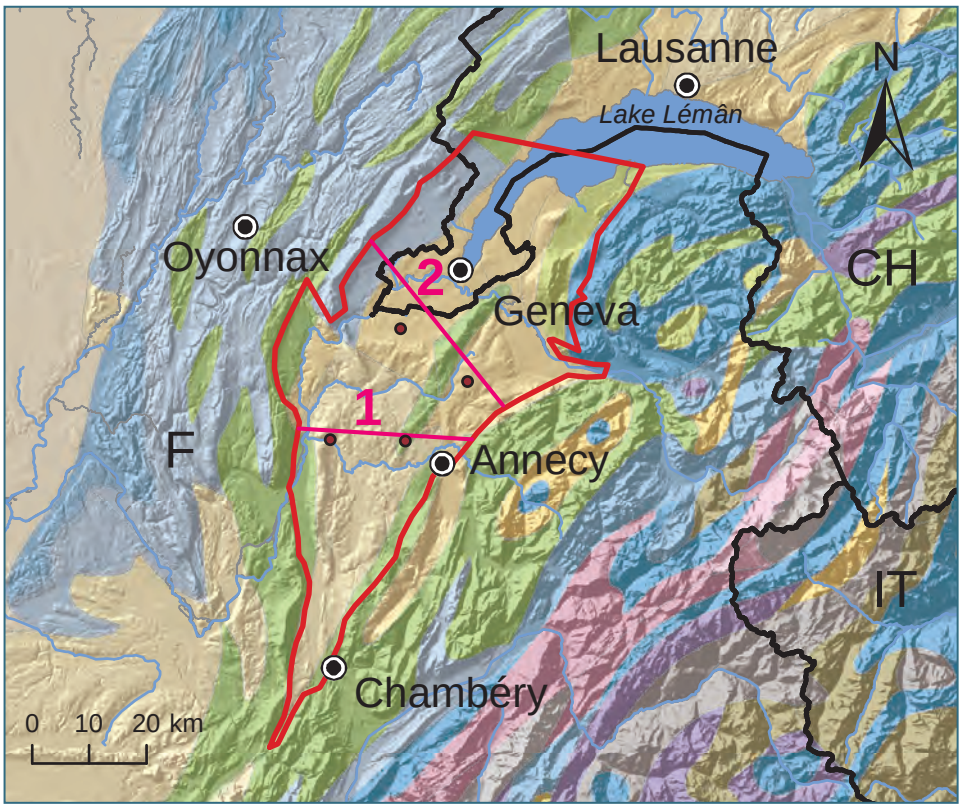

Figure 8.1-1: Extent of the Geneva-Savoy pilot area as well as the location of cross-sections and boreholes as portrayed in figure 8.1-2. Background map: The 1 : 5 Million International Geological Map of Europe and Adjacent Areas (IGME 5000), https://www.bgr.de/karten/IGME5000/igme5000.htm. Tertiary units like the Molasse Basin fill are shown beige-coloured.

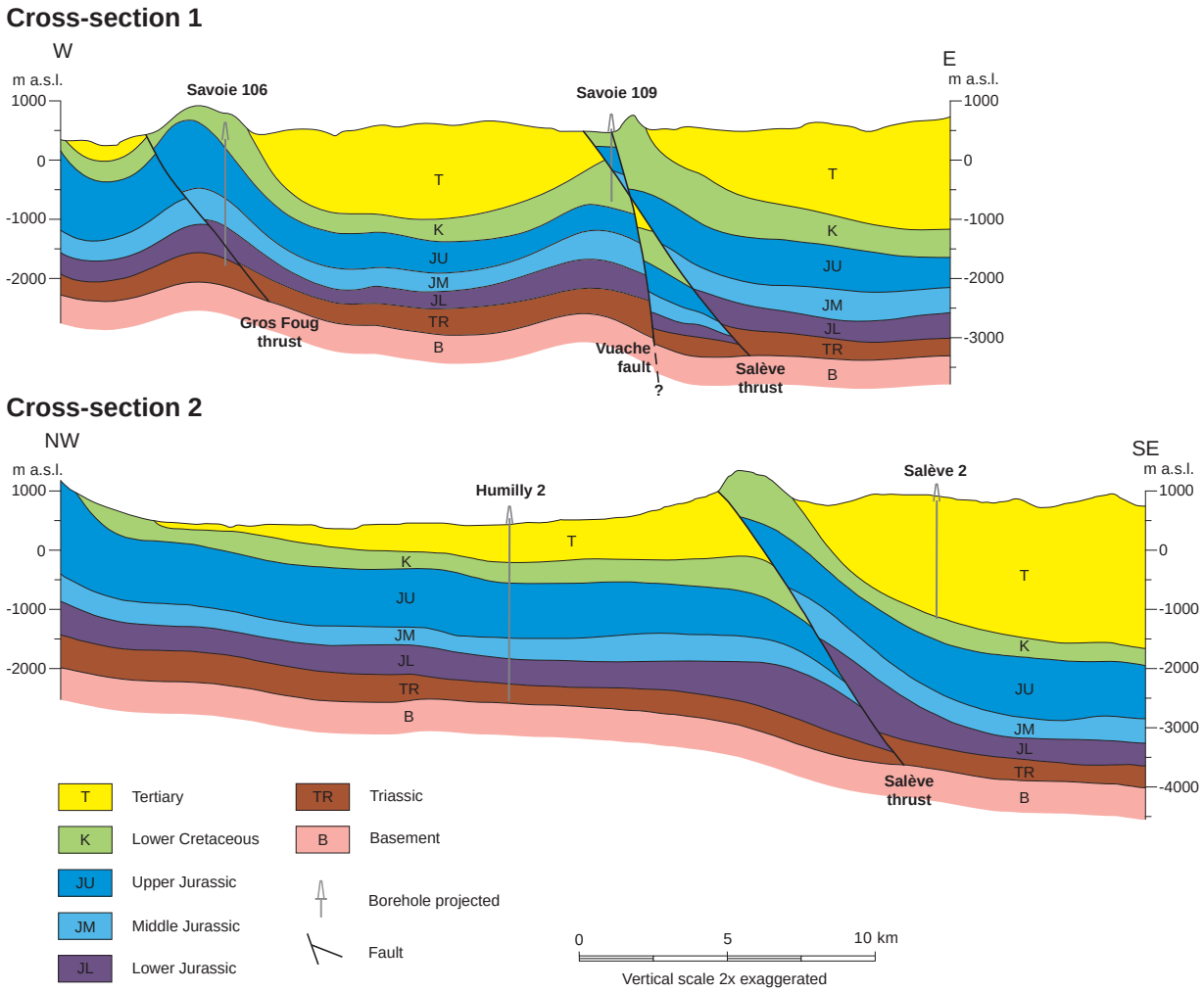

Figure 8.1-2: Cross-sections through the Geneva-Savoy pilot area as derived from the 3D geological model. Due to uncertain seismic signature the Tertiary Molasse Basin fill is not subdivided (see Section 8.1.2).

8.1.2 Geological model

The 3D geological model of the Geneva-Savoy area was constructed in collaboration between BRGM for France, Geneva University and “Canton de Vaud” for Switzerland. The software 3D GeoModeller was used for modelling. According to the available data and the aims of the project, the modelling was performed at a regional scale. The model is the result of interpolation of heterogeneous and discontinuous data (borehole logs, geological maps, seismic sections), which have been prepared and interpreted according to certain approximations and hypotheses (time / depth conversion, structural interpretations). This is the reason why the model must not be taken for strict reality but considered as an approximation of what can be expected at depth.

Modelling the Geneva-Savoy area included four steps:

- Seismic interpretation of horizons (time domain)
- Depth conversion of the seismic interpretation (depth domain)
- 3D modelling (depth domain)
- Quality control with borehole logs (depth domain)

Overall seven horizons were modelled. These are, from bottom to top:

- the "Top Basement" horizon which is the base of the Triassic series,
- the "Top Triassic" horizon which is the base of the Jurassic series,
- the "Top Lower Jurassic" horizon which is the base of the Middle Jurassic series,
- the "Top Middle Jurassic" horizon which is the base of the Upper Jurassic series,
- the "Top Upper Jurassic" horizon which is the base of Cretaceous formations,
- the "Base Tertiary" horizon which is the base of a series of Molasse formations. The Tertiary is modelled as one unit without internally resolving individual layers.
- the "Base Quaternary" horizon which is the base of a series of alluvial deposits of the Quaternary. The Quaternary is modelled using borehole data rather than seismic sections.

To model these horizons, their outcrop contours in the geological map were digitised and the position of horizons were marked in drilling and seismic profiles.

The boundaries of geological formations on the map were simplified using characteristic locations. The seismic data were correlated with borehole data during the digitisation of horizons. Due to uncertainties in the velocity model used for time- depth conversion, the position of seismic horizons had to be adjusted in some cases to be consistent with the borehole data. Taking into account the large size of the study area and the low data density, it was necessary to add additional constraints. Geological cross-sections were used to adjust the geometry of structures in some areas. In 3D GeoModeller, every digitised point is associated with one of the horizons to be modelled, allowing to restore the geometry in three dimensions for each of these horizons.

In the model, only the major structures are represented. The structural scheme is based on the structural information of the geological map and seismic interpretations.

The seismic picking overlap cannot be converted to depth; only horizons offsets indicate the position of these structures. In GeoModeller, each major shift is thus digitised and associated with recognised overlapping structures. Based on this information 3D GeoModeller restores the three-dimensional geometry of these tectonic structures.

Overlap detachment zones, as flat structures, cannot be represented because the software requires fault planes to have an apparent shift of horizons at either side of the fault. The result of the modelling of planes parallel to horizons is therefore not satisfactory. Only ramp structures could be digitised.

To construct a 3D model using discontinuous data (seismic profile, borehole logs), it is first necessary to prioritize the information between seismic data, drilling data and map display of tectonics structures. To progress from discrete information (point data) to continuous information (a horizon), it is then necessary to digitise the outcrop boundaries of units in the geological map and the seismic horizons converted to depth in order to produce a geologically realistic, three-dimensional surface by interpolation of these elements. In some cases this prioritisation requires to simplify the geometries and readjust seismic interpretations to avoid inconsistencies. Nevertheless, some inconsistencies can remain due to the fact that the velocity model for converting seismic data from time to depth is based solely on one deep borehole, the Humilly-2 well.

The Geneva-Savoy 3D model was cross checked and harmonised with the Swiss framework model in the vicinity of the *Bonmont-Yvoire* fault.

8.1.3 Evaluation of geopotentials

Petrophysical data are available for distinct lithostratigraphic intervals and reservoir units. For these units, it is possible to define mean values of the main petrophysical, hydrodynamic and thermal parameters (Table 8.1-1). If mean values for porosity or permeability did not exist, they were calculated using minimum and maximum values.

Table 8.1-1: Petrophysical, hydrodynamic and thermal data of the main reservoirs: a statistical overview on the basis of the database produced for the Geneva-Savoy area. The colours refer to the model units as in figure 8.1-2.

	Porosity (%)						
Reservoirs	Chattien	Urgonien	Portlandien	Séquanien	Rauracien	Bathonien	Bajocien
Number of data	9	15	19	8	32	14	15
Average	6.84	1.15	3.15	5.38	2.09	2.95	2.8
Standard	1.70	0.28	2.6	4.14	0.9	1.01	0.59
Min	4.3	0.6	0.5	0.55	0.7	1.3	1.8
Max	9.6	1.8	18	10.8	8.33	7.05	4
	Permeability (mD)						
Reservoirs	Chattien	Urgonien	Portlandien	Séquanien	Rauracien	Bathonien	Bajocien
Number of data	9	3	1	5	31	14	15
Average	13.1	0.9	0.07	0.46	0.15	1.62	0.049
Standard	15.4	0.6	0	0.55	0.13	2.66	0.051
Min	0.1	0.02	0.07	< 0.01	0.01	< 0.01	< 0.01
Max	50.75	1.8	0.07	1.83	1.4	19	0.395
	Salinity (g/l)						
Reservoirs	Chattien	Urgonien	Portlandien	Séquanien	Rauracien	Bathonien	Bajocien
Number of data	1	8	6	5	4	6	3
Average	0.8	0.78	18.37	3.81	0.27	21.08	4.29
Standard	0	0.53	18.13	5.68	0.30	14.58	2.97
Min	0.8	0.22	0.17	5.68	2.75	4.5	1.63
Max	0.8	2.71	49.50	18.00	3.13	40	8.75
	Flow rate (m^3/h)						
Reservoirs	Chattien	Urgonien	Portlandien	Séquanien	Rauracien	Bathonien	Bajocien
Number of data	1	19	15	13	5	7	1
Average	0.15	29.98	77.26	67.8	0.27	1.09	0.5
Standard	0	39.59	42.75	34.24	0.30	0.88	0
Min	0.15	0.08	1	0.69	0.005	0.04	0.5
Max	0.15	185	229.17	150	0.80	3.375	0.5
	Temperature (°C)						
Reservoirs	Chattien	Urgonien	Portlandien	Séquanien	Rauracien	Bathonien	Bajocien
Number of data	1	10	12	12	1	3	1
Average	55.57	47.36	61.35	62.93	101.66	111.27	65.81
Standard	0	23.60	14.03	10.86	0.00	0.00	0
Min	55.57	14.30	24.90	24.90	101.66	37.63	65.81
Max	55.57	92.73	74.82	72.20	101.66	111.27	65.81

Data on salinity and flow rates originate mainly from previous hydraulic borehole tests published in drilling reports. The most frequently used test is DST (Drill Stem Testing) which allows the determination of reservoir (oil and water) hydrodynamic features such as water static pressure, permeability or flow rate. In some cases, the flow rate was not directly given in the report and therefore calculated using the quantity of collected fluid and the duration of the test. In the absence of salinity measurements, fluid electric conductivity was used to deduce salinity.

During a drilling operation, the original temperature at depth is often disturbed. When mud circulation stops, the temperature progressively approaches the equilibrium temperature by thermal diffusion. In most boreholes, BHT (bottom hole temperature) measurements are taken during this return to equilibrium. Therefore, correction methods were applied to normalise data temperatures.

Based on these data and on the sequence of modelled units, geopotentials were assessed for the stratigraphic units of the Geneva-Savoy area (Table 8.1-2).

Table 8.1-2: Compilation of theoretical geopotential in the model units of the Geneva-Savoy Area.

Unit (Framework model reference)	drinking water	balneology	direct heating	power generation	oil and gas production	natural gas storage	CO_2 storage
Quaternary *(not included in 3D model)*							
Chattien (Molasse, undivided)							
Urgonien (K)							
Portlandien, Séquanien, Rauracien (JU)							
Bathonien, Bajocien (JM)							
Lower Jurassic (JL)							
Triassic (TR)							
Basement (B)							

unit contains layers with geopotential

unit possibly contains layers with geopotential

unit contains no geopotential

8.1.4 Model application – geothermal potential of deep groundwater resources

A 3D model of the subsurface temperature distribution was constructed using a vertical drift correction and estimating the temperature residual for the geological model of the entire pilot area (Figure 8.1-3). Based on this temperature model, serial maps were derived for the distribution of temperature at different depths (every 500 m from 500 m to 5,000 m below surface). Secondly, the poten-

tial for geothermal occupancy based on temperature was estimated at those depths. Finally, maps were derived showing the depths of various isotherms (40 °C, 60 °C, 100 °C, 120 °C, 150 °C) and the temperature at the top of the Upper Jurassic. All maps are made available via the GeoMol map-server (http://maps.geomol.eu). The results represent a large scale approach based on the present availability of baseline data. For more regional or local scales further studies are required.

The results indicate that temperatures in the Geneva-Savoy area range from 30 °C at a depth of about 500 m up to 160 °C at 5,000 m below surface. With increasing depth, the temperature distribution increasingly shows a regionally differentiated picture. For example, at 3,000 m below surface temperatures range between 87 °C and 112 °C, the geology shows a succession of basement rocks in the west to Upper Jurassic units in the east, and the geothermal potential indicates the viability of direct use of thermal heat (heat exchanger) in some areas while in other areas absorption heat pumps can be used (Figure 8.1-3).

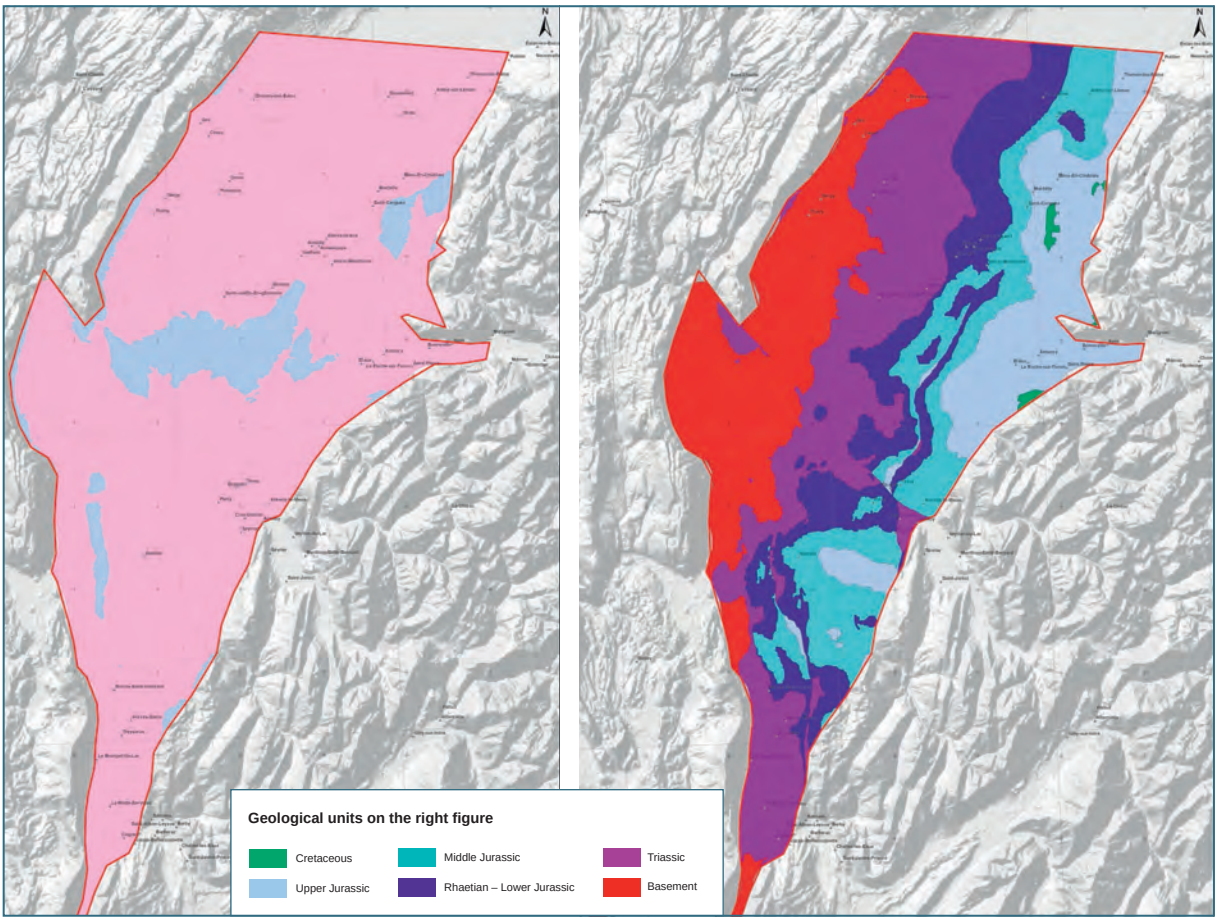

Figure 8.1-3: Left: Estimation of the geothermal potential based on the temperature distribution at 3,000 m below surface. Areas in blue are suitable for utilisations viable in the 80–100 °C interval (i. e. direct heating), the area in pink is suitable for uses requiring >100 °C (e. g. absorption heat pumps).
Right: The horizontal section shows the subcrop distribution of the geological units at the 3,000 m below surface level.

8.2 Swiss Midlands area (SMA)

The focus of the pilot activities in the Swiss Midlands area was on the compatibility of geological storage of CO_2. The study by DIAMOND et al. (2010) which estimated the CO_2 storage potential in Switzerland, formed an important input data set. In this study, regions with high storage potential were identified and the theoretical storage capacity was calculated.

The region in the Swiss Midlands was selected as a pilot area as it has, according to the above mentioned study, the highest potential for CO_2 storage in Switzerland. The initial aim was to visualise the 2D study "Potential for geological sequestration of CO_2 in Switzerland" of DIAMOND et al. (2010) in three dimensions. For this, the data and results of the 2D study were to be transformed into a detailed 3D fault and horizon model. As the data of the 2D study were processed and visualised, it became clear that not all of the results could be transformed into a 3D model. For this reason, only the potential aquifer-seal pairs identified in the 2D study were modelled, and not the quantified potential distribution itself. Nevertheless, the 3D model can now serve as the basis for future projects and future more detailed models.

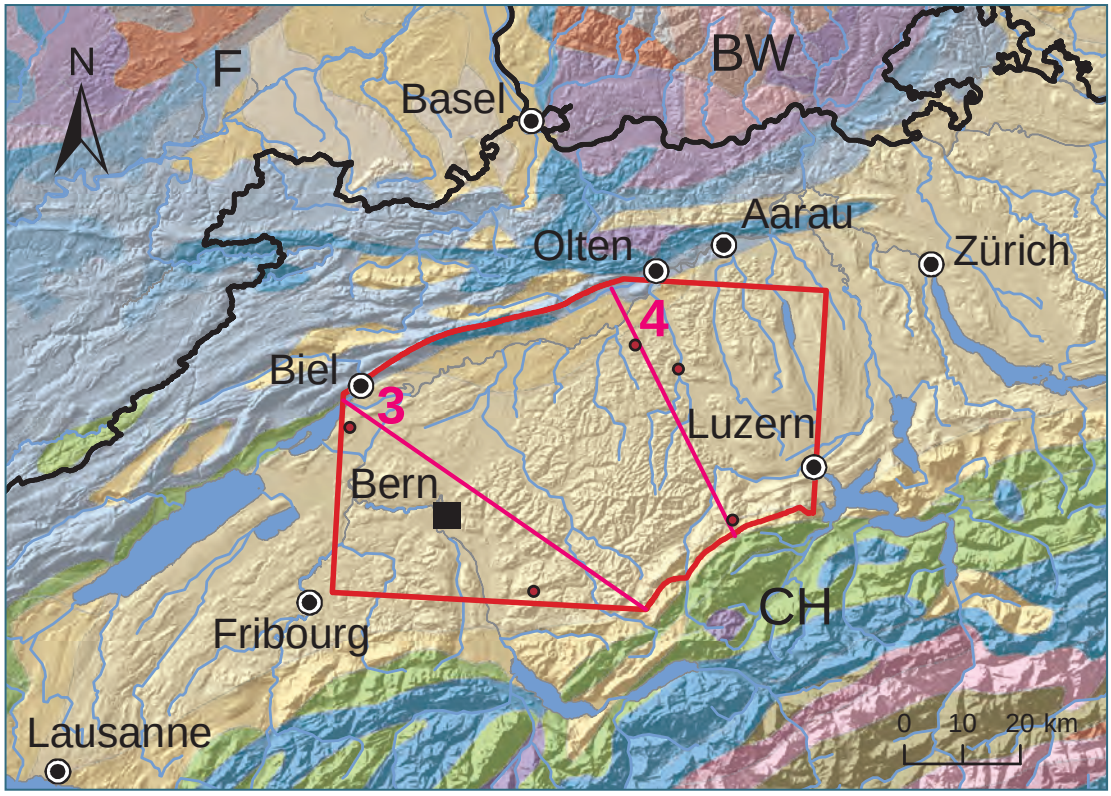

Figure 8.2-1: Extent of Swiss Midlands pilot area and location of cross-sections and boreholes as portrayed in figure 8.2-2. Background map: The 1 : 5 Million International Geological Map of Europe and Adjacent Areas (IGME 5000), https://www.bgr.de/karten/IGME5000/igme5000.htm. Tertiary units like the Molasse Basin fill and the Jura Molasse are shown beige-coloured. The blue colours refer to the Jurassic of the Jura Mountains and hinterlands in the NW and, in the SE, to the complexly folded and thrusted Jurassic of the Alpine nappes – intensely interlaced with Cretaceous (green) and minor Triassic (purple) units.

Figure 8.2-2 (following page): Cross-sections through the Swiss Midlands pilot area as derived from GeoMol's framework model. Due to uncertain seismic signatures and paucity of borehole evidence the Lower Freshwater Molasse (USM) and Lower Marine Molasse (UMM) could not be distinguished.

Cross-section 3

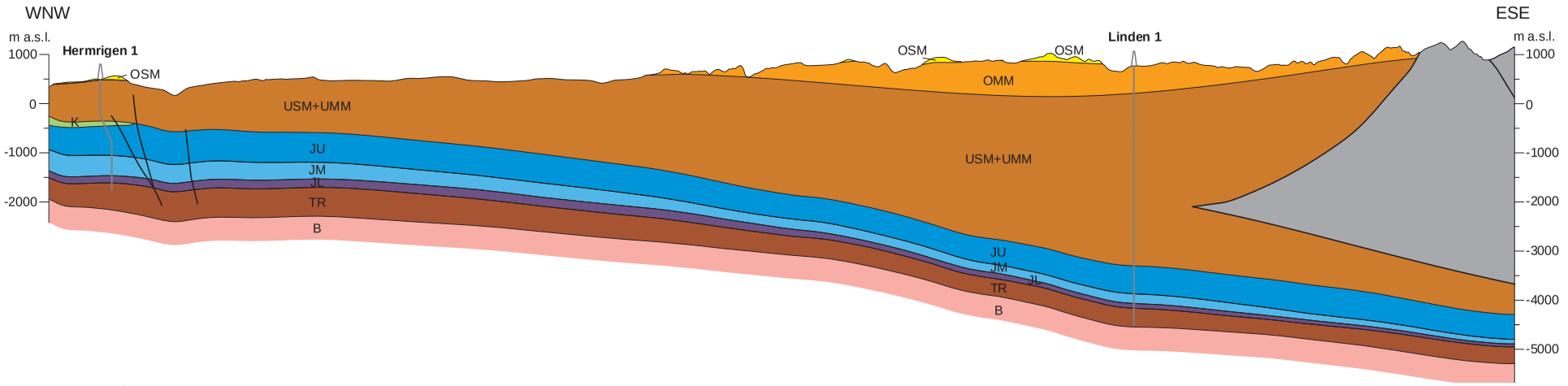

Cross-section 4

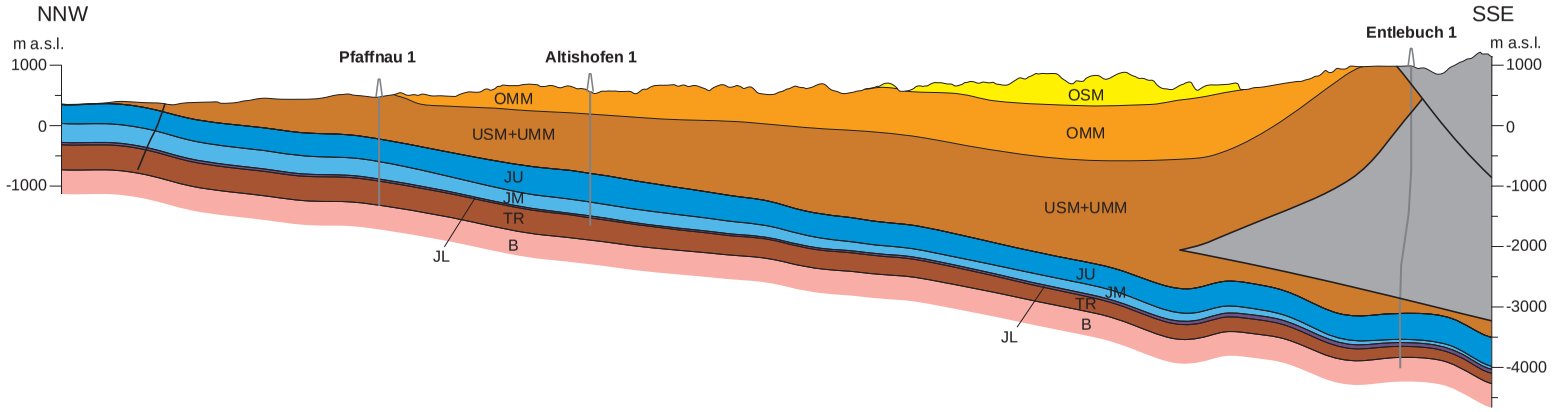

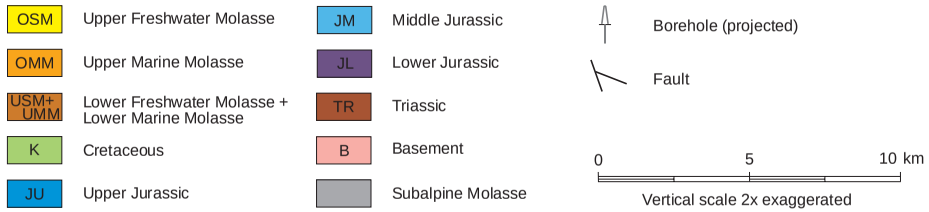

8.2.1 Study area and geological setting

The pilot area is situated in the area of Fribourg-Bern-Luzern-Olten and covers an area of about 4,000 km² (Figure 8.2-1). Geologically, it is situated in the Molasse Basin between the Jura Mountains and the Alps. At the surface, the geological units correspond in the north-western part to the Plateau Molasse and in the south-eastern part to the Subalpine Molasse.

8.2.2 Geological model

Data

The horizons of the Seismic Atlas of the Swiss Molasse Basin, which were used as input data for the GeoMol framework model (cf. Chapter 5), were also used for the 3D model of this pilot area. These horizons were previously generated from seismic sections (Sommaruga et al. 2012) and now adjusted so that the depths of the horizons, or the thicknesses of the units, correspond to the well data (well-tied). Not all of the horizons described in Diamond et al. (2010) were available in the data set of the Seismic Atlas of the Swiss Molasse Basin. Consequently, additional horizons needed to be modelled in the pilot area.

Initially, the concept for the construction of additional horizons was to use only well data, as these give the most detailed stratigraphic information. Furthermore, on the seismic sections it was not possible to meaningfully interpret the additional horizons, as the units above and below rarely have sufficient impedance contrasts. However, during the collection of data and the initial phase of this work, it was realised that the quantity of data in the modelling area and the adjoining buffer zones (Figure 8.2-1) was insufficient to model the required additional units. The units relevant for potential CO_2 sequestration were specific and, as it turned out, did not always appear in the wells' recorded stratigraphy information. In addition, more than one interpretation of the wells' stratigraphy existed in some cases. The reinterpretation and treatment of well data therefore resulted in a reduction of the number of wells considered.

Methods

Besides the common lithostratigraphic units of the GeoMol project, additional units were defined in order to visualise the geometry of barrier rocks (seals) and reservoir rocks (aquifers), as well as the CO_2 storage potential, in the pilot area. The modelling of these additional horizons was based on thickness interpolation. Table 8.2-1 summarises the modelled units in the Swiss Midlands pilot area and the modelling environment for their construction.

Several interpolation methods were tested in ArcGIS and Move aiming to minimise the error of interpolation, due not only to the method itself, but also to the small quantity of input data (well points). In an attempt to maintain the overall tectonic structure, the tested methods used the horizons of the Seismic Atlas of the Swiss Molasse Basin. However, the depth values of the horizons did not always correspond to the well data, especially at greater depths, as these surfaces had not previously been well-tied. This needed to be corrected before further modelling was carried out. The horizons of the Seismic Atlas of the Swiss Molasse Basin were therefore tied to deep well markers to form the framework model horizons.

Hereafter, the additional horizons for the pilot area were modelled using vertical thickness grids of the additional units. For this, the thickness of each unit was interpolated using the well data points. The thickness grids were then added to (or subtracted from) the existing framework model horizons to generate the additional horizon surfaces.

Properties of modelled units

Initially, porosity, permeability and salinity data of the modelled units were collected from the well data for parameterisation of the geological rock bodies. However, in the pilot area, as well as in the whole of Switzerland, there were not enough well data available to regionalise the rock properties. Due to this lack of data, it was not possible to parameterise the modelled units, nor to generate a voxel model of these parameters.

Table 8.2-1: Lithostratigraphic units modelled (except for *) in the Swiss Midlands pilot area, their construction methods and amount of well data considered.

Framework model unit	Unit	Construction method	No. of wells	Aquifer/ Seal
OSM	Upper Freshwater Molasse	Framework model horizon		
OMM	Upper Marine Molasse	Framework model horizon		
USM + UMM	Lower Freshwater Molasse + Lower Marine Molasse	Framework model horizon		Seal
K	Cretaceous	Framework model horizon		Aquifer
JU	Upper Malm	Framework model horizon		
	Lower Malm	Framework model horizon		Seal
JM	Dogger p.p.	Thickness distribution	11	Aquifer
	Opalinus-Ton	Thickness distribution	11	
JL	Lias	Framework model horizon		
TR	Upper Keuper	Thickness distribution	5	
	Gipskeuper	Thickness distribution	5	Seal
	Upper Muschelkalk	not modelled *		Aquifer
	Lower Muschelkalk + Anhydritgruppe	not modelled *		Seal
	Buntsandstein	not modelled *		Aquifer
B	Crystalline Basement, incl. Permo-Carboniferous Troughs	Framework model horizon		

*) The potential of these units was evaluated in Diamond et al. (2010), but due to insufficient data the units could not be modelled. They occur only in the northern part of the pilot area.

8.2.3 Evaluation of geopotentials

The geopotentials described below were assessed on a very basic level for each potential and remain theoretical without proof. It was not the objective to quantify these potentials. In general, if there is more than one geopotential per unit, this may cause usage conflicts, but these conflicts were not investigated any further. Table 8.2-2 summarises the described theoretical geopotentials.

Geothermal potential

The geothermal potential depends on the physically available thermal energy at depth, given by temperature and thermal rock properties. Feasibility of exploitation depends on the capabilities to extract energy at depth and transport it to the surface (Hirschberg et al. 2015). According to this, the aquifers in the fractured uppermost 500 m of the crystalline basement, in the Upper Muschelkalk, and in the Upper Marine Molasse are to be considered as geothermal resources in Switzerland. However, high uncertainties remain regarding key parameters such as temperature, permeability, and volumes. Therefore direct measurements are necessary to constrain models (Hirschberg et al. 2015).

Geothermal potential for electricity generation

To reach the target temperature range of 120 °C to 180 °C required for electricity generation, there is a need to drill to a depth range of about 4 to 5.5 km. At this depth, the natural geothermal resources are large and, for the most part, sustained by continuous replenishment although locally they would be depleted after approximately 30 years of operation (Hirschberg et al. 2015). Theoretically, geological units with geothermal potential for electricity generation are the crystalline basement, the Upper Muschelkalk and the Upper Malm (Baujard et al. 2007, Rybach 1992, Signorelli et al. 2004, Signorelli & Kohl 2006).

Geothermal potential for direct heating

In principle, high temperature geothermal heating systems with temperatures above 70 °C operate similarly to shallow heating systems. Such high temperatures, corresponding to well depths of about 2 to 3 km, would allow direct heating without the use of electrical heat pumps (Hirschberg et al. 2015). Theoretically, geological units with geothermal potential for direct heating are therefore the Upper Malm and the Upper Muschelkalk (Baujard et al. 2007, Rybach 1992, Signorelli et al. 2004, Signorelli & Kohl 2006).

Potential for hydrocarbon production

To date, only small and uneconomic gas accumulations have been discovered in the Swiss Molasse Basin. There are, however, sizeable structural traps within the Mesozoic sedimentary sequence, especially below the so-called Triangle Zone of the Subalpine Molasse (grey in Figure 8.2-2). In addition, hydrocarbon potential may exist in Jurassic reef bodies and in targets beneath Triassic salt deposits (Brink et al. 1992).

8.2.4 Model application – potential for geological storage of CO_2

Requirements

The geological requirements for suitable CO_2 storage sites are fundamental for assessing the potential for CO_2 sequestration. According to Diamond et al. (2010), a target site for CO_2 storage must consist of an aquifer-seal pair – a thick reservoir rock with sufficient permeability to permit rapid injection and sufficient porosity for high storage capacity, overlain by an extensive, low-permeability sealing rock suite. The formation water must be saline and slow-moving, and the site must be distant from its ultimate discharge zone. The aquifer must be at an appropriate depth to ensure that the injected CO_2 is in a dense phase, thereby optimising the storage capacity (see Section 2.3.2). Suitable CO_2 densities are reached at depths of 800 to 2,500 m below surface, depending mainly on the geothermal gradient of the basin (Bachu 2003, Chadwick et al. 2008). Simple rock structures are preferred, so as to limit the scope for unpredictable escape conduits for CO_2. Faults are not necessarily problematic, because many inactive faults are impermeable to fluids and even play an

Table 8.2-2: Compilation of theoretical geopotential in the Swiss Midlands area (not to be considered without the text).

Unit (Framework model reference)	drinking water	direct heating	power generation	oil and gas production	CO_2 storage
Upper Freshwater Molasse (OSM)					
Upper Marine Molasse (OMM)					
Lower Freshwater Molasse (USM) + Lower Marine Molasse (UMM)					
Cretaceous (K)					
Upper Malm (JU)					
Lower Malm (JU)					
Dogger p.p. (JM)					
Opalinus-Ton (JM)					
Lias (JL)					
Upper Keuper (TR)					
Gipskeuper (TR)					
Upper Muschelkalk (TR)					
Lower Muschelkalk + Anhydritgruppe (TR)					
Buntsandstein (TR)					
Crystalline Basement, incl. Permo Carboniferous Troughs (B)					

unit contains layers with geopotential
unit possibly contains layers with geopotential
unit contains no geopotential
not investigated

important role in forming structural traps (e.g. as is well known in the case of petroleum and natural gas reservoirs). However, active and permeable fault zones must be avoided to minimise the risk of leakage, same as seismic zones in general (DIAMOND et al. 2010).

Saline aquifers are widespread and voluminous, and the brines they contain are unsuitable for other uses, except in some cases for geothermal energy production. Saline aquifers are being targeted as they can trap CO_2 in several ways: as a fluid phase, as a dissolved component in the brine and eventually as stable carbonate minerals (DIAMOND et al. 2010).

The criteria required for the evaluation of the potential for geological storage of CO_2 therefore comprise

- the existence of an aquifer - cap rock pair within a depth range of 800–2,500 m
- an aquifer thickness exceeding 20 m at minimum, sealed by ≥ 20 m of cap rock
- an appropriate geothermal gradient (P-T-depth relationships)
- favourable hydrogeological conditions (zones of recharge vs. discharge of formation water)
- the presence of structural traps
- the absence of active seismicity
- a favourable stress regime
- sufficient knowledge of the subsurface
- sufficient knowledge of fault characteristics (density and dimensions)

Description

Within the sedimentary stack of the Molasse Basin and the Jura Mountains, Diamond et al. (2010) identified seven stratigraphic units which could potentially act as aquifer and barrier rocks for the geological storage of CO_2. Of these, four aquifer (a) and seal (s) pairs were evaluated within the Swiss Midlands pilot area. They comprise the Upper Malm + Lower Cretaceous (a) and Lower Freshwater Molasse (s), Muschelkalk (a) and Gipskeuper (s), Buntsandstein (a) and Anhydritgruppe (s), and finally, Hauptrogenstein (a) and Effingen-Member (s). A preliminary estimate of their storage capacity was calculated and mapped. Several criteria were considered in this calculation. As seismic active zones and complex geological structures were to be avoided, the Fribourg-Bern-Luzern-Olten region was identified as the most favourable area of high CO_2 storage potential (Figure 8.2-3).

The maps of CO_2 storage potential of individual sealed aquifers by Diamond et al. (2010) are visualised in the GeoMol map viewer. An assessment of the storage potential in 3D is not possible at the moment, due to the reasons stated above. Consideration of usage constraints and the assessment of the compatibility of underground gas storage with deep groundwater was planned but will not be accomplished due to the lack of reliable data. For the latter two assessments, it would need more studies on rock properties are required and a better knowledge of the subsurface structures, which could be gained only from further borehole evidence of the base of the sediments.

Current and future activities on CO_2 sequestration

The need for further investigations regarding the possibility of storing CO_2 in the Swiss subsurface remains. From a technical point of view, the study by Diamond et al. (2010) considered the available geological information about the Swiss subsurface. However, it is clear that this information is not sufficient for site location ensuring the safe and permanent storage of CO_2. More geological data are necessary, and the political, economic, legal and acceptance issues related to CCS in Switzerland have to be investigated. The results of the CARMA[1] project, as well as international experience indicate that in order to develop CCS technology in Switzerland to maturity, and to make it a viable commercial solution, it is first necessary to carry out a small scale pilot project, which includes a field test of geological storage (Mazzotti et al. 2013).

[1]CARMA (Carbon Management in Power Generation) is a Swiss research project that aims to explore the potential and feasibility of CCS systems deployment in Switzerland (Duration 2009–2012); http://www.carma.ethz.ch/

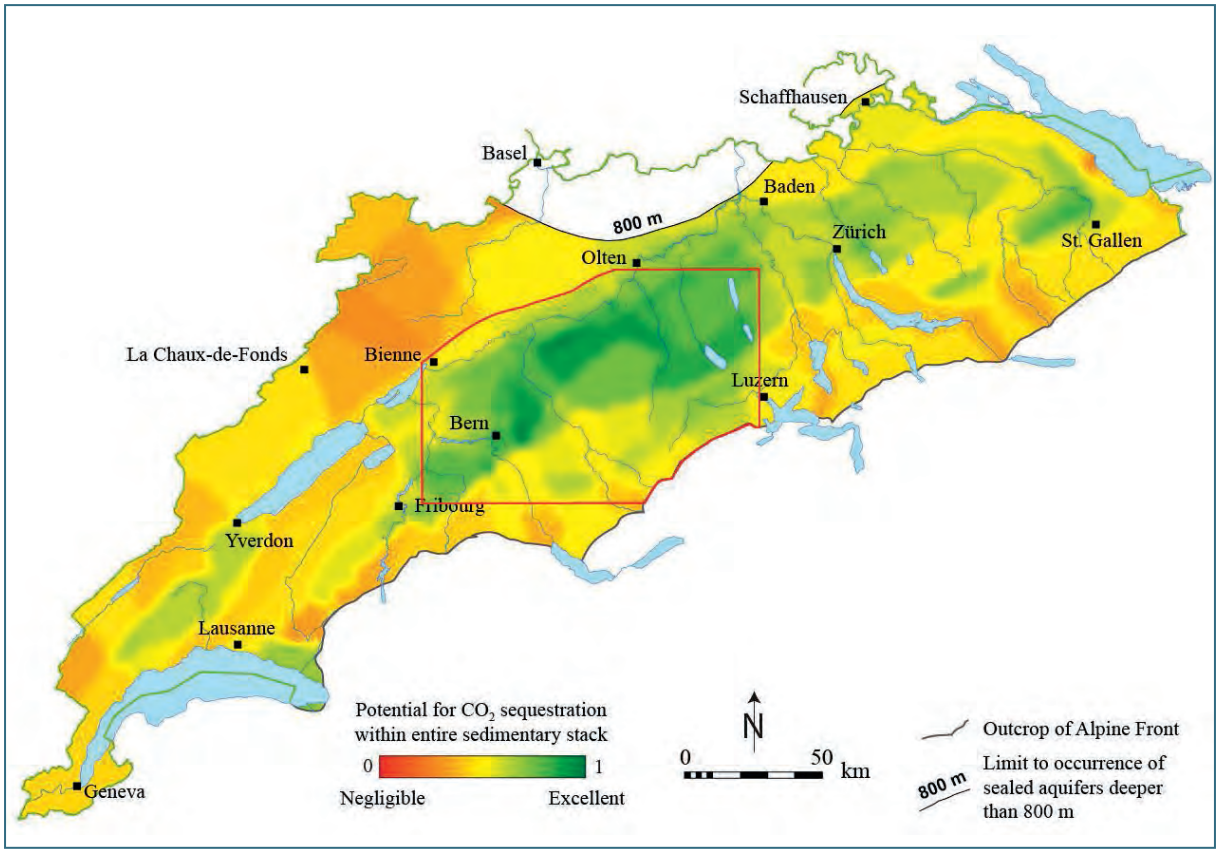

Figure 8.2-3: Potential for CO_2 sequestration in Switzerland within the entire Swiss Molasse Basin sedimentary stack (modified from DIAMOND et al. 2010). Boundaries of the Swiss Midlands pilot area are marked in red..

The Swiss Competence Center on Supply of Electricity (SCCER-SoE, http://www.sccer-soe.ch/), a national competence center considering these topics, has recently been established and includes various research and cooperation partners. According to its 10-years roadmap the SCCER-SoE will develop fundamental research and innovative solutions in the domains of deep geothermal energy, CO_2 storage and HydroPower (http://www.sccer-soe.ch/).

Furthermore, any future projects dealing with CO_2 storage should consider the international standards and methods for carbon capture and storage (CSS) from the International Energy Agency Greenhouse Gas Research and Development Programme (IEAGHG, http://ieaghg.org/). The role of this programme is to evaluate technologies that can reduce greenhouse gas emissions derived from the use of fossil fuels (http://ieaghg.org/).

8.3 Lake Constance – Allgäu area (LCA)

The Molasse Basin in southern Germany and Upper Austria, due to its highly productive aquifers at depth, is acknowledged the most important reservoir of geothermal energy for heat production in Central Europe (e. g. PASCHEN et al. 2003). For this reason, the focus of geopotential assessment in the Lake Constance – Allgäu area was on the geothermal potential. Presently, the deep groundwater in the LCA area is used for balneological purposes and for direct heating. So far, there is no utilisation of deep thermal water for power generation in the LCA area (Figure 2.3-3).

8.3.1 Study area and geological setting

The Lake Constance – Allgäu pilot area encompasses a territory of about 8,850 km², shared by three countries resp. four states: Switzerland (18 %), Baden-Württemberg (30 %), Bavaria (47 %) and Vorarlberg/Austria (5 %). It extends across from the hummocky terrains of the shallow marginal foreland molasse to the Alpine foothills of the Subalpine Molasse. Lake Constance, covering a surface area of 536 km² is the most striking geographic feature of the region.

The Lake Constance – Allgäu area represents the central part of the North Alpine Foreland Basin (Molasse Basin). The oldest geological units, the Palaeozoic basement, has been encountered by a few deep boreholes and can be traced in seismic sections between roughly 1 km depth at the NW margin of the pilot area and more than 6 km in the SE. It mainly consists of medium to high-grade metamorphic rocks, deformed during the Variscan orogeny, and subsequently intruded by plutonic rocks of predominantly granitic composition. Beneath the north-western part of Lake Constance, a Late Palaeozoic graben-like trough is known to contain more than 700 m of continental clastic rocks including some minor coal-bearing beds. The outline of this trough is poorly constrained and hardly distinguishable from the surrounding basement in seismic surveys.

The Palaeozoic rocks are superseded by a Mesozoic succession of Triassic and Jurassic sediments that show decreasing thicknesses towards SE. The Triassic succession, about 300 m to less than 50 m thick, begins with marginal marine sandstones and evaporites, followed by a marine limestone to dolomite succession of the Muschelkalk group, and ends with continental clastic rocks and minor evaporites of the Keuper group. The 80 to 300 m thick Lower and Middle Jurassic rocks are dominated by marine mudstones with intercalations of limestone and sandstone, followed by 300 to 550 m thick marine Upper Jurassic carbonates which represent the main target of geothermal interest. The thicknesses of the latter unit vary on a small scale due to some buried paleo-relief at the top, representing a hiatus from the latest Jurassic to the Eocene.

The Tertiary basin fill of the Molasse Basin features a significant thickness increase from 130 m near the NW margin of the pilot area to more than 3,500 m close to the Alpine Front. In the south, the Tertiary succession starts with Late Oligocene marine sandstones (Lower Marine Molasse, UMM), followed by more than 3,000 m of Late Oligocene to Early Miocene mud-dominated fluvial deposits (younger Lower Freshwater Molasse) (cf. Figure 2.2-6). These fluvial marls and sandstones drastically decrease in thickness towards the North, and lap on directly onto the eroded Jurassic rocks where the Lower Marine Molasse wedges out (Figures 2.2-1 and 2.2-3 B). 100 to 300 m thick Early Miocene marine sandstones and glauconitic mudstones (Upper Marine Molasse, OMM) overlay these non-marine deposits and are beautifully exposed alongside the northern parts of Lake Constance, capped in most parts by a contemporary pedocrete duricrust. Fluvial sands and marls (Upper Freshwater Molasse, OSM) of late Early to Late Miocene age complete the Tertiary basin fill succession. Originally covering the entire basin, Pleistocene erosion has disintegrated the OSM distribution especially at its northern margin.

Quaternary deposits of the Alpine foreland are highly variable in thickness and depositional environment, including glacial, melt-out, fluvial, and lacustrine deposits. Today remnants of Early Pleistocene fluvial sand and gravel are mainly found on hilltops, owing to intense erosion and reshaping of the landscape during the Middle to Late Pleistocene glacial periods. Ice streams out of the Alpine valleys covered most of the Lake Constance area. Deep subglacial erosive basins, elongated in shape following glacial meltwater flows, were subsequently filled or, as in case of Lake Constance partly filled, with melt-out clastic rocks and lacustrine mud up to more than 250 m thick. Apart from the overdeep Lake Constance basin these Quaternary deposits rarely exceed 75 m in thickness and mainly consist of gravels, sand, diamictites, till and intermingled deposits of glacial to fluvial origin.

The foreland basin evolution is commonly attributed to the downwarping of the lithosphere caused by the crustal thickening that results from the compressional tectonic forces (Section 2.2.1). Affected by these orogenic processes continuing during the infill of the basin, the sedimentary sequences of the foreland basins feature a complex network of fault pattern (see e. g. Figure 5.3-6). As the tectonic forces and thus faulting decreased at the later stages of the molasse deposition most of the tectonic structures are buried under younger undeformed sediments and thus they can be determined only in seismic sections or by parallelisation of borehole evidence. Normal faults with a vertical offset of a few tens of meters and an azimuth angle (strike) more or less perpendicular to the direction of the compressional forces (i. e. (sub-) parallel or at low angles to the Alpine Front) prevail. The amount of strike-slip (horizontal offset) along these steeply dipping faults is poorly constrained. Thrusts, folds and monoclines are confined to the Subalpine Molasse close to the Alpine Front, referred to also as Folded Molasse. The boundary of the Folded Molasse within the LCA area is built up by a roof-thrust and a floor-thrust forming the so-called *triangle zone* (grey in Figure 8.3-2, see also Figures 2.2-9 A and 8.2-2). The complex internal structures and marginal faults of these wedge-shaped thrusts have not been modelled in GeoMol.

The central part of the Molasse Basin (specifically in the LCA area N to NE of Lake Constance) is characterised by a system of extensional faults with a basin parallel strike: As a result of the rapid but uneven, sustained subsidence of the basin floor, subparallel systems of synthetic faults (dip synthetically / same direction as the layering of the deposits) and antithetic faults (antithetic / reversed dip) formed. The antithetic faults are among the preferential targets of the E&P industries as they give rise to structural traps for oil and gas deposits (Figure 2.3-4 C) or their after-use for stockpiling hydrocarbons.

8.3.2 Geological model

In line with the statutory provision for the use of classified data (Chapter 3.3) 3D geological modelling of the Lake Constance - Allgäu pilot area was carried out at the GSOs in charge for their area of responsibility or (in parts) was subcontracted to domestic institutions (cf. Table 4.4-1) using confidentiality agreements. Afterwards, the interpolated, thus anonymised information was cross-border harmonised employing the coordinate transformation described in chapter 10, and subsequently the geopotential assessment was implemented.

The vast majority of input data for geological modelling originated from drillings and 2D seismic surveys acquired during oil and gas exploration activities. The spatial distribution of well data clearly reflects the areas of interest of the E&P industry and the outlines of former oil fields (see Figure 4.2-3). Especially in the southern part of the LCA, very little deep well data is available. The deepest wells considered are Tettnang 1 (measured depth 3,253 m), Opfenbach 1 (measured depth

4,510 m) and Sulzberg 1.3 (borehole length 5,645 m / TVT 4,764 m) (see Figures 8.3-2 and 2.2-9 A). In addition to borehole data from E&P campaigns, data and records from deep wells of recent geothermal exploration activities (*Bad Waldsee* and *Saulgau* in Baden-Württemberg, *Bad Wörishofen* and *Mauerstetten* in Bavaria, and *St. Gallen* GT-1 in Switzerland) was considered. Besides the investigation by drillings, the pilot area has been intensively explored by 2D seismic surveys.

Preparation and processing of the input data is described in chapter 4. Table 8.3-1 summarises the number of wells and seismic sections underpinning the geological modelling of the LCA. In addition, syntheses of subsurface data such as geological and structural maps (BayStMWIVT 2010, LBEG 2007, Rupf & Nitsch 2008, Sommaruga et al. 2012) were used as additional background information during seismic interpretation and 3D modelling.

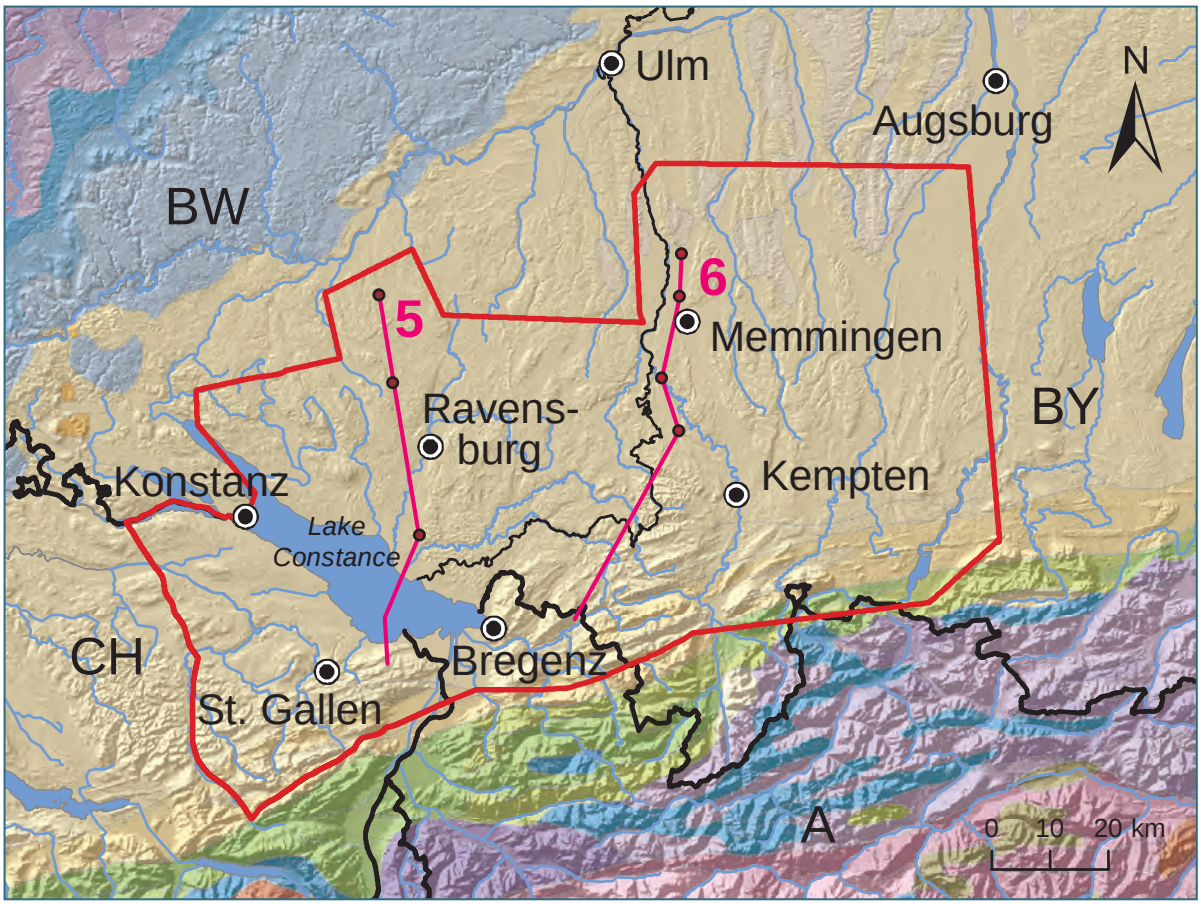

Figure 8.3-1: Extent of the Lake Constance – Allgäu pilot area as well as the location of cross-sections and boreholes in figure 8.3-2. Background map: The 1 : 5 Million International Geological Map of Europe and Adjacent Areas (IGME 5000), https://www.bgr.de/karten/IGME5000/igme5000.htm. The outcropping Tertiary units of the Molasse Basin fill are shown in beige colours. The blue colours refer to the Jurassic sequence of the Swabian Platform in NW, and, in the south, to the complexly folded and thrusted Jurassic, intensely interlaced with Cretaceous (green) and Triassic (purple) units representing the Alpine nappes.

Figure 8.3-2 (following page): Cross-sections through the Lake Constance – Allgäu pilot area as derived from GeoMol's framework model. Additional horizons (layer surfaces) have been modelled for certain subareas in the pilot area where appropriate baseline data have been available (Table 8.3-2).

Cross-section 5

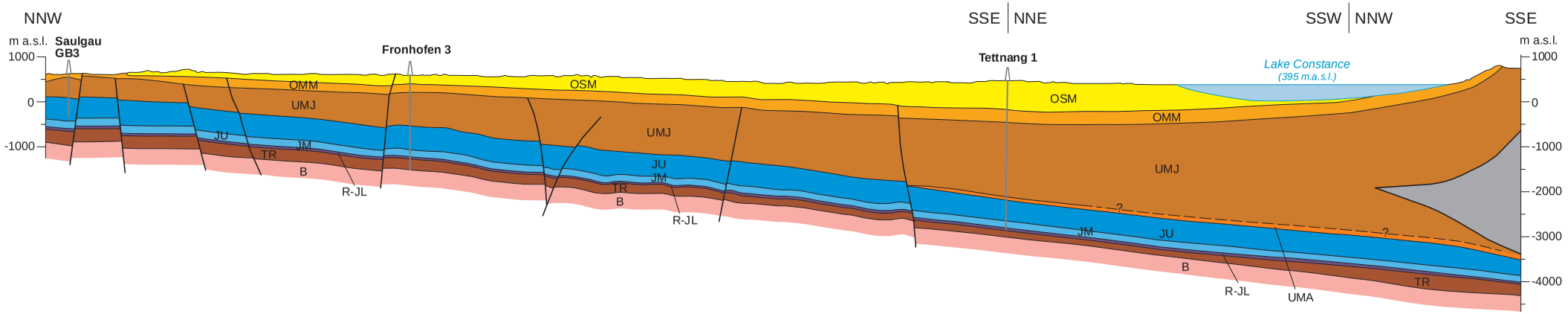

Cross-section 6

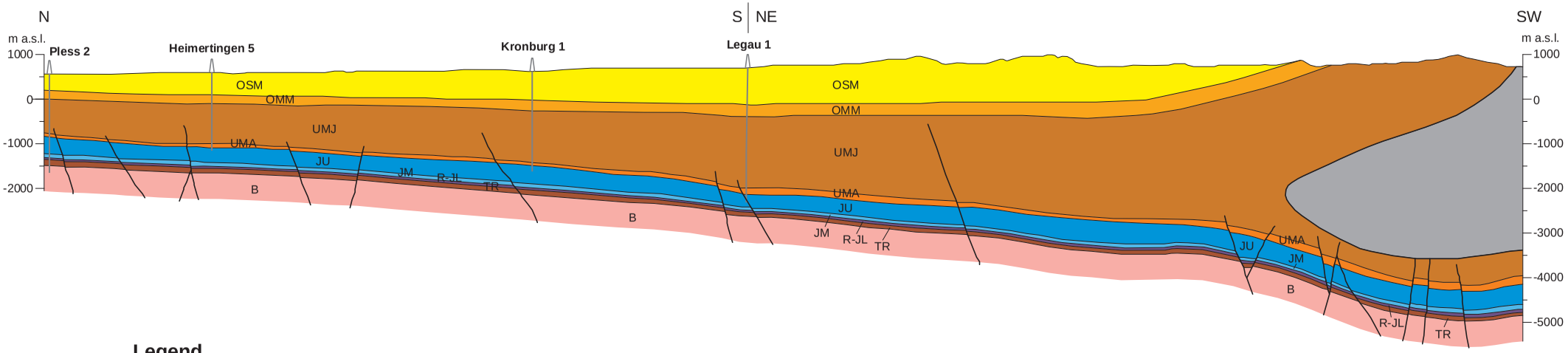

Legend

OSM	Upper Freshwater Molasse	JU	Upper Jurassic	B	Basement
OMM	Upper Marine Molasse	JM	Middle Jurassic		Subalpine Molasse and Alpine units not modelled in GeoMol
UMJ	Younger Lower Molasse	R-JL	Rhaetian – Lower Jurassic		Borehole partly projected
UMA	Older Lower Molasse	TR	Triassic		Fault

0 5 10 km

Vertical scale 2x exaggerated

Table 8.3-1: Amount of input data used for the geological model of LCA (LCA-A: sub-area Austria, LCA-BW: sub-area Baden-Württemberg, LCA-BY: sub-area Bavaria, LCA-CH: sub-area Switzerland).

Sub-area	Number of wells used	Seismic sections used	
		Number of sections	Total length (km)
LCA-A	1	30	318
LCA-BW	107	135	2,373
LCA-BY	169	106	2,033
LCA-CH	20	46	793
Total LCA	**297**	**317**	**5,516**

The general workflow as applied for 3D geological model building in all sub-areas was subdivided into four main working steps: (1) Seismic interpretation (and partly horizon modelling) of visible seismic reflectors and faults in time domain, (2) time-depth conversion of the seismic interpretation, (3) surface modelling of horizons and faults in depth domain and (4) modelling of additional horizon surfaces based on thickness distribution information. A general description of the modelling workflows used in GeoMol is given in Chapter 5, the workflow adjusted to the LCA pilot area will be described in more detail in GeoMol Projektteam LCA (2015).

Table 8.3-2 lists the horizons of the geological model and the construction methods for each sub-area of the LCA, performed with different software and in different coordinate systems (see Table 4.4-1). GIS software and special software for geo-data processing was employed, e.g. for the preparation of input data, exchange of working data and the derivation of 2D data from the 3D model.

Table 8.3-2: Horizons and construction methods for the geological model of the LCA pilot area (LCA sub-areas: -A: Austria (Vorarlberg), -BW: Baden-Württemberg, -BY: Bavaria, -CH: Switzerland; FWM-R = framework model reference, construction basis: S = seismic interpretation, T = thickness distribution, X = not modelled).

Horizon (surface)	FWM-R	Coding	Horizon construction			
			LCA-A	LCA-BW	LCA-BY	LCA-CH
Base Quaternary	Top of OSM	B_Q	X	FM	FM	FM
Base Upper Freshwater Molasse	Top of OMM	B_OSM	T	T	S	S
Base Steinhöfe-Formation	OMM	B_SH	X	T	X	X
Base Baltringen-Formation	OMM	B_BA	T	T	S	X
Base Upper Marine Molasse	Top of UMJ	B_OMM	T	S	S	S
Top Lower Marine Molasse	Base of UMJ	B_UMJ	S	T	S	X
Top Tonmergelschichten	UMA	T_TM	T	T	T	X
Base Tertiary	Base of UMA	B_T	S	S	S	S
Top Impressamergel-Formation	JU	T_TJUI	T	T	T	S
Top Middle Jurassic	Base of JU	T_JM	S	T	S	S
Top Lower Jurassic	Top of R-JL	T_JL	T	S	S	S
Top Triassic	Base of R-JL	T_TR	T	T	T	S
Top Lower Keuper	TR	T_KL	T	T	T	T
Top Muschelkalk	TR	T_M	T	T	T	S
Top Heilbronn-Formation	TR	T_MMH	T	T	T	T
Top Paleozoic	Top of B	T_B	S	S	S	S

8.3.3 Evaluation of geopotentials

The basic prerequisite for the evaluation of geopotentials is the profound knowledge of the geological situation. This knowledge critically depends on the availability of information on the structure of the subsurface (ideally provided by 3D geological models), on the temperature distribution and on physical rock properties (see Chapter 2.3 and 6). This applies to the assessment of the individual geopotential as well as to possible interferences of competing uses.

Due to possible interferences, usages may be mutually exclusive even if at different depths of the subsurface. Other usages can take place contemporaneously or consecutively as well as one above the other or side by side. Due this complexity geopotentials may vary laterally within one geological unit. Likewise the other pilot areas only a qualitative assessment of the theoretical geopotential was implemented as a first step approach for site location assistance (cf. Chapter 6).

The geopotential of the subsurface of the Lake Constance - Allgäu area has been assessed applying the general criteria as described in chapter 6. The following compilation gives only a general overview for the immediate comparison with the other pilot areas. Methods applied and results derived thereof will be discussed in more detail in GeoMol Projektteam LCA (2015).

Geothermal potential

Geothermal is by far the most important geopotential of the Alpine Foreland Basins. Even though foreland basins are considered hypothermal (cooler than normal) with low geothermal gradient and heat flow (Allen & Allen 2005) the Alpine Foreland Basins, particularly the NAFB, feature the highest geothermal potential in Central Europe (e.g. Paschen et al. 2003). Due to highly productive aquifers at great depths an average geothermal gradient of about 3.0 °C/100 m in the NAFB – but varying considerably on a regional scale (cf. Figures 7.4-2 and 8.3-3) – allows for viable geothermal installations.

Thermal water, by definition T ≥ 20 °C, may occur in any aquifer of the Molasse Basin at greater depth. Delimiting factor for its **balneological use** is the potential yield of the aquifer at depth. According to this, principal targets in the LCA are Upper Jurassic carbonates (main potential), the Upper Marine Molasse and the Lower Marine Molasse. Currently deep groundwater for balneological and curative purposes is used in several spas in the Baden-Württemberg part of the LCA (*Bad Saulgau, Bad Aulendorf, Bad Waldsee, Bad Wurzach, Kißlegg, Bad Buchau, Jordanbad, Überlingen, Friedrichshafen* and *Meersburg*) and in the Bavarian part (*Breitenbrunn-Bedernau* and *Bad Wörishofen*) (Figure 2.3-3). At elevated temperatures the deep thermal groundwater in addition is used for direct heating.

Thermal water in the range of 60 °C to 100 °C is viable for **direct heating** using open-loop systems, in which a production well discharges hot water from the deep aquifer. The highest potential for such systems, due to its high potential yield, can be expected in the Upper Jurassic carbonates, suitable also for **geothermal power generation** if temperatures markedly exceed 100 °C. The temperature distribution at the top of the Upper Jurassic, ranging from 18 °C in the north to 195 °C in the southeast, is illustrated in figure 8.3-4. Across the line *Markdorf-Ravensburg-Leutkirch-Kaufbeuren*, the Upper Jurassic carbonates feature a significant facies change from layered and biohermal limestones and marls of the Swabian Facies with generally higher permeability in the north, to increasingly bituminous deep-water limestones of the Helvetic Facies featuring a low permeability in the south. This means, that the highest subsurface temperatures occur in areas where rock permeability is low and explorations must aim at faults and fractures forming zones of higher permeability and thus higher potential yield.

So far, there is no utilisation of deep thermal groundwater for power generation in the LCA area, direct heating is deployed in connection with balneological use only (cf. figure 2.3-3 and the respective maps at http://maps.geomol.eu).

Petrothermal systems use geothermal energy mainly for power generation from rocks with poor natural permeability and temperatures well above 120 °C. These temperatures occur in the northern part of the LCA in depths of 1,300 to 2,000 m below surface and in the south in depths of 2,300 to about 3,000 m (Figure 8.3-3). Subsurface temperatures above 150 °C are reached in the north at depths between 3,000 and 3,300 m and in the far southeast between 4,300 and 4,800 m below surface. The most favourable geologic units for petrothermal energy production are the Permo-Carboniferous and the Crystalline Basement.

Drinking water

Use of near surface groundwater for water supply is widespread. Given the economic viability of the drilling and development measures and a low groundwater vulnerability the principal aquifers occur in Quaternary fluvio-glacial deposits and in shallow Tertiary units. The most important drinking water reservoir of the LCA area, however, due to its high water quality, is Lake Constance providing drinking water for about 4.5 million people in Baden-Württemberg and Switzerland.

Geological storage of CO_2

Recent studies concerning the potential of CO_2 storage (based on the criteria of depth and thickness of reservoir and barrier rocks as described in chapter 6) have identified some geologic units and regions where the geological storage of CO_2 in the Baden-Württemberg and Bavarian parts of the LCA might be possible (Fehn & Wirsing 2011, Diepolder & Schulz 2011). The following units can act as reservoir rocks: Lower Marine Molasse (Bausteinschichten), Middle Jurassic (Eisensandstein-Formation), Middle Triassic (Löwenstein-Formation (Stubensandstein)) and Middle Triassic (Rottweil-Formation (Trigonodus-Dolomit). However, the areas complying with the minimum requirements concerning depth and thickness of appropriate pairs of reservoir and barrier rock units have been identified on a 2D basis and thus disregard the spatial set-up. Now, the 3D geological model of the LCA area allows for an insight into the structural features and thus the first step screening of the nature of the lateral seal and the spill point. Further steps of site location assistance require a sound volumes assessment which, due to insufficient data, cannot be provided by GeoMol. The promising areas have to be investigated in more detail for a final confirmation on the basis of all relevant criteria (see Chapters 2.3 and 6).

Oil and gas production

After decades of investigation resulting in a considerable number of discoveries, the Central Molasse Basin was considered mature in terms of hydrocarbon exploration by the end of the 20th century. Most oil and gas fields were economically depleted, new large discoveries were unlikely. However, technical progress generated new prospects and improved exploration efficiency. The units, of which oil (o) and/or gas (g) was produced in the past, and which have potential for hydrocarbon production using advanced techniques, are the Younger Lower Molasse (o, g), the Older Lower (Marine) Molasse (o), the Middle Jurassic (g), the Lower Jurassic (g) and the Triassic (o, g).

Main targets of oil and gas prospection in the LCA were primarily sandstones of the Upper Freshwater Molasse and the Lower Marine Molasse, Lower and Middle Jurassic sandstones, and Keuper sandstones. In the 1960's to 1980's exploration focussed on deeper Triassic carbonates (the Rottweil-Formation (Trigonodus-Dolomit).

At the moment, there is no hydrocarbon production in the LCA. Resumption of production is currently under investigation at *Bedernau* in the *Arlesried* oilfied.

Storage of natural gas

The volume for underground gas storage is most economically provided by depleted hydrocarbon deposits which proved their suitability by encapsulating oil and gas over millions of years. Suitable geological units are the targets of hydrocarbon exploration as above. Suitable bedrock structures (structural traps) have been investigated by the E&P industry during exploration campaigns and are coarsely outlined in the 3D models: Most oil and gas fields are bound to NE–SW striking, northerly dipping antithetic downthrow faults. The principal oil- and gas-bearing structural traps in the LCA are related to the faults of the *Pfullendorf-Saulgau*-Lineament and the *Meersburg-Arlesried-Schwabmünchen*-Lineament.
Further steps of the site selection procedure require volumetric considerations which, due to lack of data, GeoMol cannot provide.

The only existing underground storage facility for hydrocarbons in the LCA is situated in the former oil field *Fronhofen* where gas is stockpiled in the porous carbonates of the Upper Muschelkalk (Rottweil-Formation).

Table 8.3-3: Compilation of theoretical geopotential in the Lake Constance – Allgäu pilot area.

Unit (Framework model reference)	drinking water	balneology	direct heating	power generation	oil and gas production	coal production	natural gas storage	CO_2 storage
Quarternary								
Upper freshwater molasse (OSM)								
Upper marine molasse (OMM)								
Younger lower freshwater molasse (UMJ)								
Older lower marine molasse (UMA)								
Upper Jurassic (JU)								
Middle Jurassic (JM)								
Lower Jurassic (JL)								
Triassic (TR)								
Basement incl. Permo-Carboninferous troughs (B)								

unit contains layers with geopotential
unit possibly contains layers with geopotential
unit contains no geopotential

8.3.4 Model application – assessment of geothermal potential

Principles of use of geothermal energy are discussed in detail in Chapter 2.3-1.

Among the various geological factors that influence the economic viability of hydrothermal systems, fault zones are of particular importance as they can act as preferential pathways for the thermal water. However, due to insufficient knowledge of their spatial distribution, of their hydraulic properties, but also of facies variations within geological units, hydrological aspects were not considered in the assessment of geothermal potential. These aspects have to be addressed in studies at local scales.

For this study, the assessment was based on a geo-statistical 3D model of underground temperatures (Chapter 7) and on the geometries of geothermal units, which were derived from the 3D geological model (Chapter 5). Combining the two models, the following temperature maps were elaborated and are made available via the GeoMol MapViewer:

- temperatures at depths of 500 m, 1,000 m, 1,500 m, 2 km, 3 km and 4 km below surface
- depths of the 60 °C, 100 °C and 150 °C isotherms
- temperatures at the top of the Upper Marine Molasse, the Upper Jurassic and the Upper Muschelkalk, bearing the most prominent aquifers for potential geothermal use.

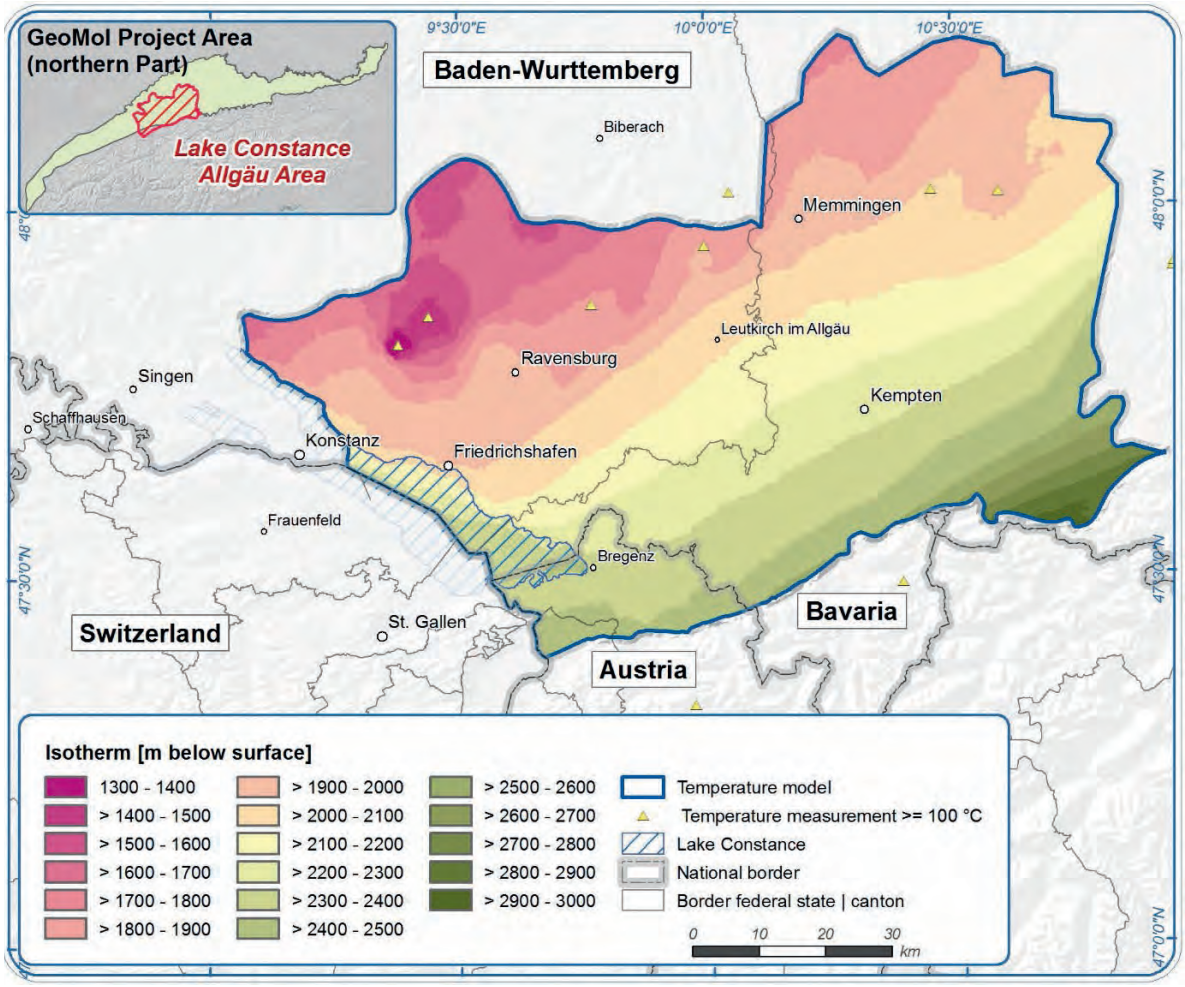

Figure 8.3-3: Depth of the 100 °C isoterm in m below ground indicating a marked decrease of the geothermal gradient from NNW to SSE.

Temperatures of thermal waters in the LCA pilot area range from 20 °C to more than 200 °C. As an example, figure 8.3-3 shows the depth of the 100 °C isotherm. The depth increases from about 1,300 m below surface in the northwest (south of *Pfullendorf*) to about 2,900 m below surface in the far southeast in the *Füssen* area, reflecting the general trend of a SSE dipping isothermal plane. This implies a decrease of the geothermal gradient towards the southeast.

The temperature distribution was also used to produce maps estimating the geothermal potential at the following depth levels and geological settings:

- at 500 m, 1,000 m, 1,500 m, 2 km, 3 km and 4 km below surface
- at the top of the Upper Marine Molasse, the Upper Jurassic and the Upper Muschelkalk.

Figure 8.3-4 provides an overview of the geothermal potential at the top of the Upper Jurassic carbonates, based on the modelled temperature distribution. The karstified carbonates of the Upper Jurassic exhibit the highest hydrothermal potential in the area, whereas the carbonates of the Upper Muschelkalk as well as Tertiary sediments are of minor importance.

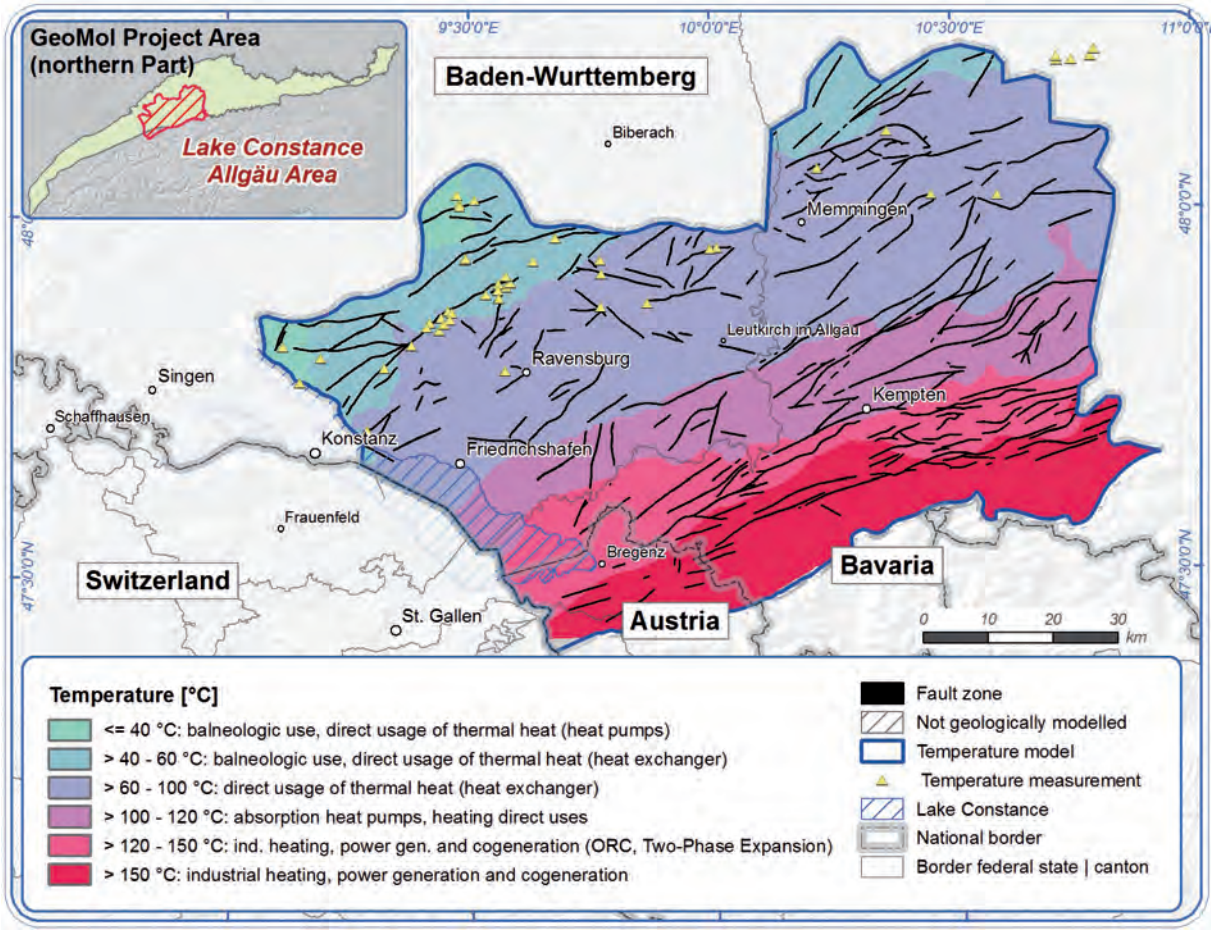

Figure 8.3-4: Geothermal potential at the top of Upper Jurassic carbonates, based on the modelled temperature distribution. The network of major faults intersecting the Upper Jurassic may form zones of higher permeability and thus higher potential yield. However this depends on the small-scale fault characteristics which are not considered in GeoMol.

8.4 Upper Austria – Upper Bavaria area (UA – UB)

Pilot activities in the area of Upper Austria – Upper Bavaria were focussed on the evaluation of hydrothermal potential and the application of the geological 3D model for the study of groundwater flow. The area of interest is defined by a large system of thermal groundwater circulating within the karstic Upper Malm (Upper Jurassic) aquifer beneath the southern Bavarian and Upper Austrian Molasse Basin. According to the Regensburg convention, a group of German and Austrian hydrothermal experts is responsible for the common management and sustainable utilisation of this aquifer (EXPERTENGRUPPE THERMALWASSER 2012). A trans-border hydrogeological model and thermal water flow model was set up in 1999 and until now serves as the basis for decisions on new uses and extraction limits. Even though a trans-boundary structural map for the top of the target horizon – the Malm aquifer – was published, a highly demanded 3D model of the subsurface geology was never realised. The creation of a 3D model was one of the principal targets within the GeoMol project. The model, the results of pilot activities, but also the outcomes of other GeoMol actions in the UA – UB area will be published by the end of 2015 in a separate volume of the Geological Survey of Austria journal (GBA 2015).

8.4.1 Study area and geological setting

The surface extent of the UA – UB pilot area amounts to 4,730 km^2. It stretches roughly 50 km to the east and west of the German-Austrian border and covers the Molasse Basin between *Mühldorf am Inn* and *Schärding* in the north and the *Chiemsee* and *Straßwalchen* in the south (Figure 8.4-1).

The uppermost unit within the pilot area is the Upper Freshwater Molasse (OSM) with fluvial and limnic sediments of Pannonian to Karpatian age (cf. Figure 2.2-6). These sediments were used for coal mining in some areas but build up only a relatively thin layer of 90 m on average and 300 m maximum. The underlying sediments of the Ottnangian Upper Marine Molasse (OMM) reach thicknesses of up to 800 m although the average amounts to 250 m. These mainly clayey, in upper sections sandy sediments originate from a shallow marine environment. Underlying is the formation of the Eggenburgian OMM comprising shallow marine, pelagic and transgressive sediments. Clayey marls predominate and are interbedded with sandstones which are partly gas-bearing. The thickness of this formation reaches up to 800 m with an average of 500 m. The underlying Younger Lower Marine Molasse (younger UMM or UMJ), where thicknesses reach 2,200 m at the Alpine thrust front and average at about 600 m, represents the largest volume body of the model. This formation consists of Aquitanian and Chattian deep marine sediments, mainly clays and clayey marls. These serve as seals for natural gas contained in intercalated sandstones, consequently making this formation the main target for the oil and gas industry within the pilot area. To the west the environment changes to shallow marine conditions in which shelf sediments consisting of sands and subordinate marls were deposited. Underlying is the formation of the Older Lower Marine Molasse (older UMM or UMA) with Rupelian and Lattorfian deep marine deposits. The mainly clayey sandstones, banded marls and claystones reach up to 400 m thickness and are oil- and gas-bearing in some areas. The deepest unit of the Tertiary sedimentary succession is the Oldest Molasse/Perwang Group (UME) of Eocene age which predominantly consists of shallow marine limestones, interfingered by sandstones. The formation is oil and gas bearing and reaches a maximum thickness of about 120 m. Separated by a pronounced foreland unconformity, these sediments rest on the pre-Tertiary basin footwall rocks (Figure 2.2-6).

Starting with the deepest unit, the crystalline rocks of the Bohemian Massive are composed of gneisses from the Moldanubian and Moravian units as well as of granites from Variscan plutonic

bodies. The Landshut-Neuöttinger Hoch (cf. Figure 8.4-2) is a dominant NW-SE striking crystalline subcrop, about 5 to 10 km broad and crossing the entire pilot area. This structure was a major focus of the modelling work because it acts as a hydraulic barrier for thermal groundwater flow. On top of the Bohemian Massive, deposits of middle to upper Jurassic carbonates represent the main thermal water aquifer within the pilot area but they also bear oil in some structures. A thin layer of clastic Dogger (Middle Jurassic) sediments is superposed by up to 600 m of Malm (Upper Jurassic) carbonates which are widely karstified in the upper 240 m and serve as main target for geothermal usage. The overlying sediments of upper Cretaceous age reach up to 1,000 m thickness averaging at about 400 m. Cenomanian sandstones at the base are often connected to the karstic Malm unit and also serve as target for hydrothermal exploration. Additionally, these sandstones are oil-bearing in parts and together with the overlying uppermost Cretaceous succession constitute hydrocarbon reservoirs. Regarding formation age and preferred strike direction, two generations of antithetic and synthetic fault systems can be distinguished. Pre-Tertiary, NNW–SSE striking faults show displacement rates of up to 1,000 m while Oligocene faults run parallel to the long axis of the basin in W–E direction and feature displacement rates of maximum 300 m. Most of the hydrocarbon-bearing structures are bound to W–E striking, antithetic structures (cf. Figure 2.3-4 C).

8.4.2 Geological model

Altogether, the 3D geological model comprises ten geological units representing the Molasse Basin sediments, the Mesozoic sequence and the top of the crystalline basement. These units were chosen with respect to contrasting lithology, hydrogeological importance, for economic reasons like oil, gas or coal occurrences, but also for functional reasons like their visibility within seismic sections or their correspondence to well log units defined by the oil and gas industry (Figure 8.4-2).

For the creation of the model data from different sources were used. In general, input data for both countries were similar but data density varies significantly. Legal aspects in Germany allow access to data gained by the E&P industry with some restrictions regarding publication and dissemination. In contrast, data policy in Austria is rather strict (cf. Chapter 3.3) Except for one pre-existing regional Bavarian 3D model containing Mesozoic horizons and the crystalline basement, the 3D model had to be built up from the start in both countries. A large amount of input data is based on the interpretation of reprocessed 2D seismic lines, several 3D seismic surveys (on the Bavarian side) and paper plots of 2D seismic lines. In Austria seismic data were provided by oil and gas exploring companies (mainly RAG – Rohöl-Aufsuchungs-Aktiengesellschaft, some by OMV – Österreichische Mineralölverwaltung Aktiengesellschaft). Well data containing seismic travel time information such as check shot data were transformed to time domain to serve as reference for the recognition of reflectors in seismic surveys. Picked and interpreted in the time domain, horizons were converted into depth to coincide with well markers by using individual velocity cubes for each country. Well markers represent essential depth constraints and were compiled from various sources. For Bavaria, the extensive “Kohlenwasserstoff-Fachinformationssystem” (hydrocarbon database, www.lbeg.niedersachsen.de) as well as LfU’s own database “Bodeninformationssystem Bayern, BIS” (www.bis.bayern.de) were used. In Austria the main source for well data was a newly created database containing published wells. Additionally, RAG and OMV provided some well data with sets of markers. Published structural and thickness maps were processed and also partly used for the Austrian side of the pilot area.

Two similar software packages were used for modelling. The SKUA system with an automated structural modelling workflow which is more suitable for large amounts of seismic input data was used by the LfU. In Austria the GoCAD system with a more manual workflow was better suited for

the structural data mainly in depth domain. The big advantage of using similar software was a fast and seamless procedure of harmonising and exchanging the modelled horizons since data formats remain the same for GoCAD and SKUA.

As for the modelling workflow, the stratigraphic intervals from borehole data were assigned to the units to be modelled and quality checked. During seismic interpretation, detectable horizons and faults were picked, cross-checked and harmonised with pre-existing models and structural maps in the time domain. Subsequently, a structural model containing faults and horizons was built-up and time-depth converted. To improve model quality, the horizons were fitted to meet well markers and structural maps in the depth domain. Data exchange between the two modelling partners was attained by swapping re-adapted surfaces in GoCAD-format until one connected and harmonised model was achieved. Due to the fact that every partner used a local coordinate system, for every re-adaption of surfaces in GoCAD a transformation was necessary. This step was done within the software GST (cf. Chapter 10). Table 8.4-1 lists the individual model units, their respective names in Austria and Bavaria, as well as age, stratigraphy, thickness and lithology.

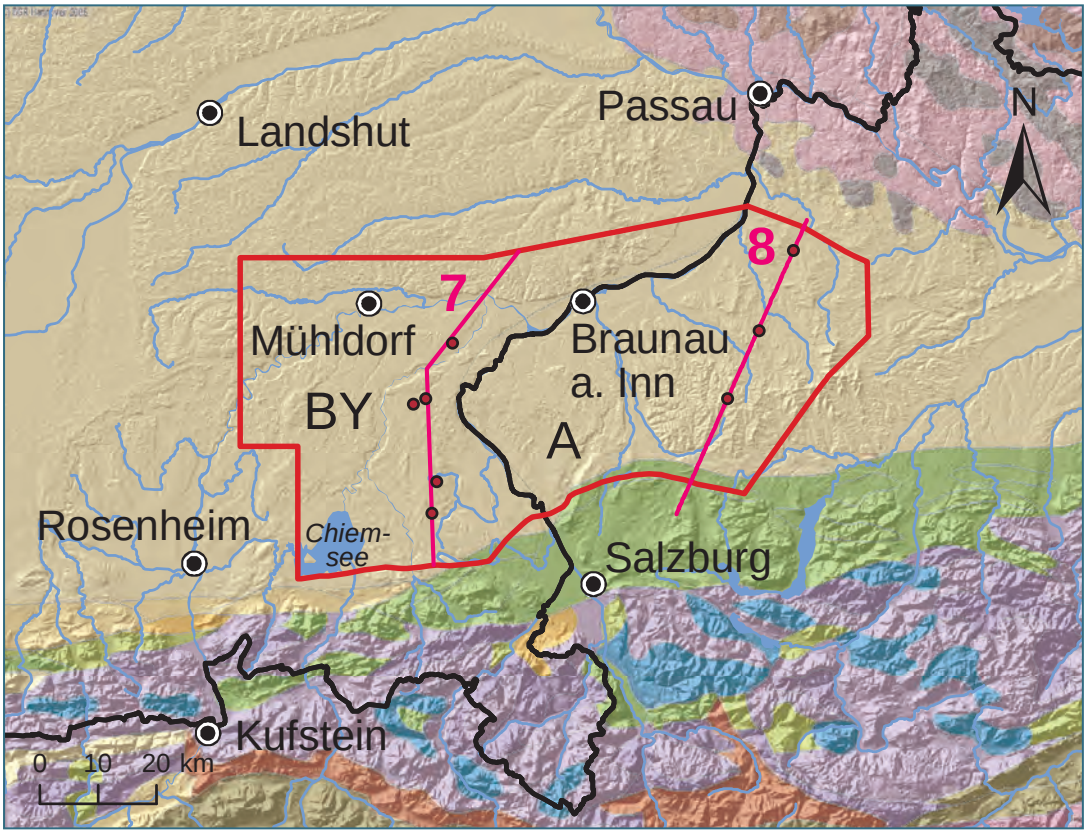

Figure 8.4-1: Extent of Upper Austria - Upper Bavaria pilot area as well as the location of cross-sections and boreholes in figure 8.3-2. Background map: The 1 : 5 Million International Geological Map of Europe and Adjacent Areas (IGME 5000), https://www.bgr.de/karten/IGME5000/igme5000.htm. The outcropping Tertiary units of the Molasse Basin fill are shown in beige colours. The green colours refer to Cretaceous units complexly folded and intensely interlaced with Jurassic (blue) and Triassic (purple) units forming the Alpine nappes. Pink and grey colours in NE represent the crystalline rock suites of the Bohemian massif.

Figure 8.4-2 (following page): Cross-sections through the Upper Austria – Upper Bavaria pilot area as derived from the 3D geological model.

Cross-section 7

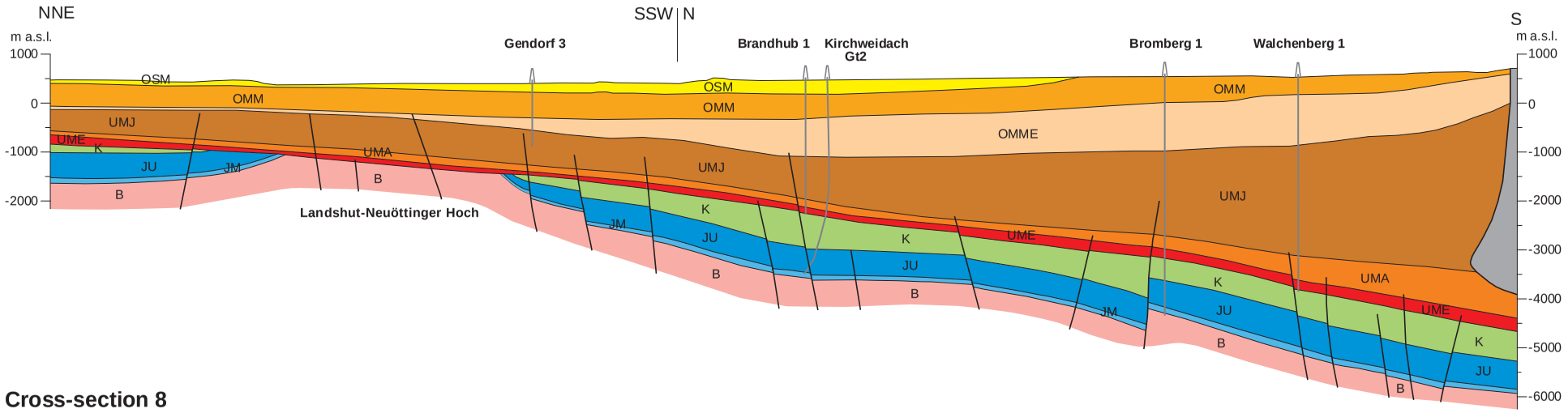

Cross-section 8

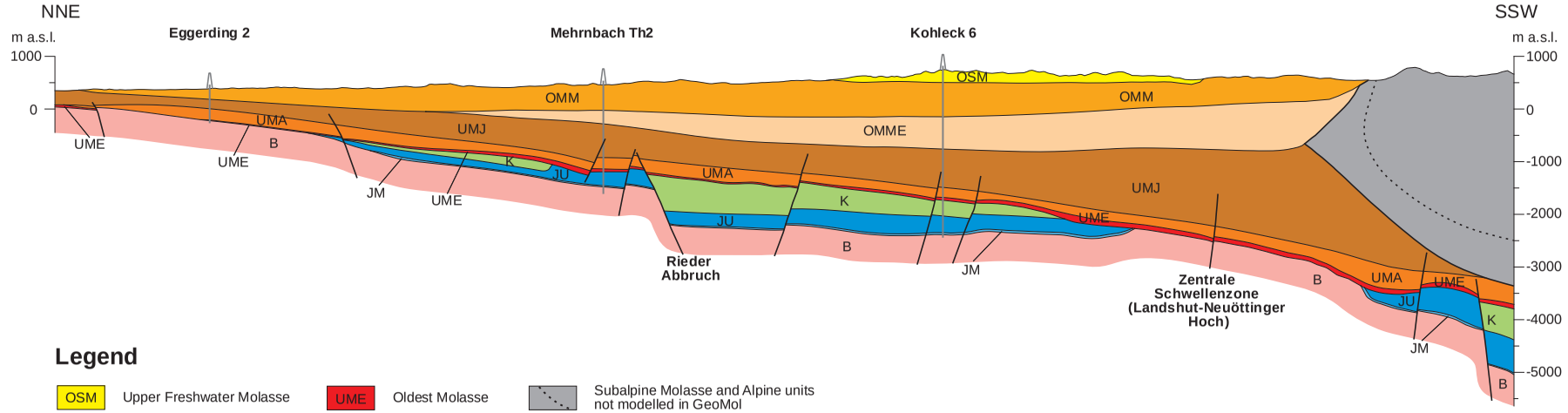

Legend

OSM	Upper Freshwater Molasse	UME	Oldest Molasse		Subalpine Molasse and Alpine units not modelled in GeoMol
OMM	Upper Marine Molasse	K	Cretaceous		Borehole partly projected
OMME	Oldest Upper Marine Molasse	JU	Upper Jurassic		Fault
UMJ	Younger Lower Molasse	JM	Middle Jurassic		
UMA	Older Lower Molasse	B	Basement		

0 5 10 km

Vertical scale 2x exaggerated

Table 8.4-1: Units modelled in the pilot area Upper Austria – Upper Bavaria area (FWM-R: Framework model reference)

Unit	FWM-R	Age/Stratigraphy	Thickness	Lithology
Quaternary and Upper Freshwater Molasse	OSM	Quaternary to Karpatian	< 300 m	sand, silt, gravel
Upper Marine Molasse	UMM	Ottnangian	< 800 m	clay / marl, in upper sections sand(-stones)
Oldest Upper Marine Molasse	OMME	Eggenburgian	< 1,000 m	sandstones, marls (-stones)
Younger Lower marine molasse	UMJ	Aquitanian and Chattian	< 3,000 m	mainly marlstones, to the west increasing sand content
Older Lower Marine Molasse	UMA	Rupelian and Lattorfian	< 500 m	marl(-stones)
Oldest Molasse	UME	Eocene (Priabonian)	< 150 m	sandstones, limestones
Upper Cretaceous including Gault-Sandstone	K	Late Cretaceous and Upper Aptian	< 1,000 m	mainly, marl- and claystones; sandstones, limestones
Upper Jurassic including Purbeck	JU	Upper Jurassic (Malm)	< 600 m	limestones, marlstones
Middle Jurassic	JM	Middle Jurassic (Dogger)	< 100 m	mainly sandstones; marlstones and claystones
Basement including Permo-Carboniferous	B	"(pre-)Variscan", Late Carboniferous to Permian		gneisses / granites, sandstones and conglomerates in troughs

8.4.3 Evaluation of geopotentials

Table 8.4-2 gives an overview of model units with their geopotential broadly classified in layers. In general, groundwater potential for the supply of drinking water can be found in near-surface sediments whereas geothermal groundwater use is restricted to deeper layers (Oligocene and older). The potential for geothermal electricity generation is limited to the Upper Jurassic karst aquifer. Oil and gas potential is present in all units below the Freshwater Molasse, suitable structures of these units can also serve for storage of natural gas or the geological storage of CO_2.

Coal

Coal-bearing layers in the pilot area are related to early Miocene clay deposits of the Upper Freshwater Molasse with thicknesses up to 60 meters (GROISS 1989). Close to the Bavarian – Upper Austrian border the *Trimmelkam* mine was in production from 1952 to 1993 (MAYRHOFER 2007). The most extensive exploration of this formation was in the area of the *Hausruck* in the very east of the pilot area but production ceased in 2007.

Oil or gas production

Oil and gas exploration has started some 100 years ago and still plays an important economical role within the pilot area. The sedimentary record of the Molasse Basin bears hydrocarbon traps in various depths and different formations. Also the underlying autochthonous Mesozoic sequence appears as reservoir rocks. Targets represent stratigraphic traps which can roughly be described as mostly sandstone layers interbedded with clays as seals or structural traps where porous layers are confined by faults (NACHTMANN 1995). Recent exploration efforts in Upper Austria and Salzburg focus on the Imbricated Molasse (Subalpine Molasse) on the Alpine thrust front (HINSCH 2013), where the largest gas field of the Molasse Basin (*Haidach*) was discovered in 1997. In the Bavarian part

of the pilot area only one small gas field (*Assing*) entered production in the past thirty years. Recent activities focus on the redevelopment of the oilfield *Ampfing* which was the first economic oil find in Bavaria (Lemcke 1988).

Storage of natural gas

The depleted hydrocarbon field of *Puchkirchen* was the first converted into a natural gas storage in the Austrian Molasse Basin starting in 1982 and completed in 2009. With a storage capacity of almost 6 billion m³ of natural gas which equals about 70 % of Austria´s annual consumption, the company RAG is Europe´s fourth largest storage operator. All of their six storage facilities are located within the pilot area and contribute to a reliable supply especially in times of political and economic crises. Gas is stored in the autochthonous Molasse (Foreland Molasse) where large gas fields have been transformed to serve as storage (http://www.rag-austria.at/en/business-area/store.html). In the Bavarian part of the pilot area the depleted gas field *Bierwang* was the first to be transformed into a gas storage site in the mid 1970's, followed by the gas field *Breitbrunn-Eggstätt* in the mid 1990's. Both storage fields are located in the Foreland Molasse and bear a capacity of about 2.5 billion m³ of natural gas (LBEG 2014).

Geothermal use

The deep aquifer of the karstic Malm stretches through the pilot area from NW to SE and is used for balneology and geothermal heat/energy purposes. The utilisation of this hydrothermal potential is regulated by the "Regensburger Vertrag" since 1992 to satisfy spa- as well as heat/energy-producing operators from both countries (Expertengruppe Thermalwasser 2012). The thermal water is believed to circulate from the area of Regensburg in the NW heading SE, bounded by the structural high of the Landshut-Neuöttinger Hoch to the south, by the pinching out of the karst to the north and draining into the river Danube in the east (Goldbrunner et al. 2007). The latest geothermal project for high temperature district heating in Austria in the area of *Ried – Mehrnbach* showed the need for an improved hydrological flow model. Pumping here was predicted not to affect neighbouring wells, but during production strong disturbances were observed in the area.

Geological storage of CO_2

The potential of CO_2 storage is limited to the formations also used for hydrocarbon production and natural gas storage. The paper by Scharf & Clemens (2006) mentions two potential storage sites within the pilot area, *Atzbach-Schwanenstadt* and *Voitsdorf* which both constitute hydrocarbon reservoirs. So far the utilisation for natural gas storage was favoured, as the regulatory framework does not allow any storage of CO_2 except for research purposes with less than 100 kt storage capacity (https://www.ris.bka.gv.at/Dokumente/BgblAuth/BGBLA_2011_I_144/BGBLA_2011_I_144.html). Calculations on practical and matched capacities for CO_2 storage in Austria were carried out by Geologische Bundesanstalt (GBA) and the Royal Belgium Institute of Natural Science (RBINS) in 2013.

Drinking water

In the northern part of the pilot area, deep aquifers of drinking water quality are present as confined, mostly artesian groundwater bodies. The aquifers are usually made up of Tertiary sands and sandstones covered by clays and claymarls. The oldest of these units is represented by the Ottnangian sediments but further to the north, closer to the outcrop trace of the Bohemian Massif Egerian sands also represent groundwater reservoirs. These aquifers are in wide parts drained by hundreds of individual wells, often with low productivity and discharge rates of less than 1 l/s (Schubert et al. 2003).

Table 8.4-2: Theoretical geopotentials within the model units of the Upper Austria – Upper Bavaria pilot area. See text for discussion.

Unit (Framework model reference)	drinking water	balneology	direct heating	power generation	oil and gas production	coal production	natural gas storage	CO_2 storage
Quaternary and Upper Freshwater Molasse (OSM)								
Upper Marine Molasse (UMM)								
Oldest Upper Marine Molasse (OMME)								
Younger Lower Marine Molasse (UMJ)								
Older Lower Marine Molasse (UMA)								
Oldest Molasse (UME)								
Upper Cretaceous including Gault (K)								
Upper Jurassic including Purbeck (JU)								
Middle Jurassic (JM)								
Basement including Permo-Carboniferous (B)								

unit contains layers with geopotential

unit possibly contains layers with geopotential

unit contains no geopotential

8.4.4 Model application – temperature model and conceptual model of the hydrothermal system

Temperature model

Based on the 3D geological model of the pilot area, a 3D numerical model was set up in FEFLOW to depict the geothermal potential in the area. The numerical model consists of the 10 main formations within the pilot area boundaries and extends from ground level to a depth of 7,000 m below sea level. The values for heat conductivity were taken from literature data as starting values for the subsequent parameter estimation. Main temperature conditions were applied to the top slice with an altitude dependent temperature distribution as well as to the terrestrial heat flux boundary, represented by a temperature distribution at 7,000 m below sea level (Przybycin et al. 2014). The model only considers heat flow by conduction and was calculated for static conditions. The convective heat flow is quite complex in the pilot area due to the hydrothermal groundwater flow system, and was not implemented in the numerical model. However, the convective part of the heat flow is represented by the residuals between the modelled temperature distribution and the measured data. To portray the geothermal potential in the pilot area, several temperature maps at various depths as well as isotherm maps for 60 °C, 100 °C and 120 °C were derived and made available via the GeoMol web map services. On these maps, the temperature distribution is predicted for

depths of 500 m, 1,000 m, 2,000 m, 3,000 m and 4,000 m below surface. The most important factor influencing the distribution of geothermal energy in the pilot area is the hydrothermal system circulating in the Malm aquifer, which is illustrated by a temperature map for the top of the Malm formation.

The maps predict temperatures up to 35 °C in 500 m depths, which corresponds to an average temperature gradient of 3 °C per 100 m. At a depth of 1,000 m, the temperature ranges from 30 °C to 45 °C with a relatively even distribution. Between 2,000 m and 3,000 m depth, temperatures are influenced by convective heat-flux and their distribution reflects the depth distribution of the Malm aquifer. At 2,000 m depth, temperatures range from 40 °C to 100 °C, at 3,000m depth from 70 °C to 115 °C. Finally, the maps at 4,000 m and 4,500 m show temperatures between 90 °C and 145 °C. The influence of thermal groundwater seems to be less important at these depths, and temperature distribution mostly controlled by conductive heat-flux. However, at these depths there are almost no temperature measurements available and an area-wide quality check is not possible.

Combining the results of the numerical model for conductive heat flow with the residuals of measured temperature data for convective heat flow, figure 8.4-3 shows the map of the 100 °C isotherm in the pilot area. The map clearly illustrates the rise of the 100 °C isotherm towards the northeast, reaching depths of about 1,000 m below sea level in the spa region of Upper Austria. In the area of *Altötting* the 100 °C isotherm descends to about 3,000 m below sea level, rising again in the area of *Mühldorf am Inn* to a level of about 2,300 m below sea level. The isotherm then descends southwards reaching a maximum depth of about 3,800 m below sea level.

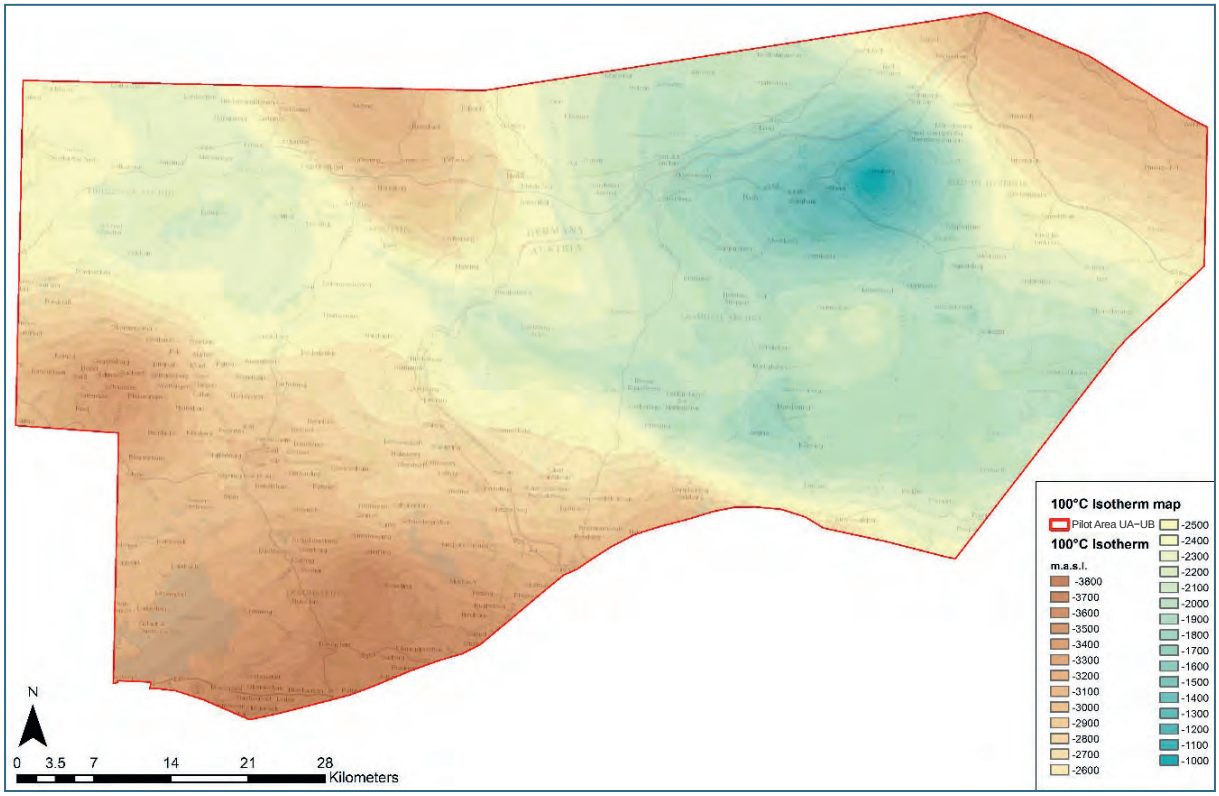

Figure 8.4-3: 100 °C isotherm map for the pilot area Upper Austria – Upper Bavaria

Finally, by reclassification of the temperature maps, geothermal potential maps were generated. These maps link different temperature intervals (i. e. 40 – 60 °C, 60 – 100 °C, 100 – 120 °C, etc.) to potential geothermal utilisations. The geothermal potential maps illustrate where specific types of

geothermal usage are potentially possible and at which depths. In accordance with the temperature intervals described in chapter 6.1, the types of usage which were considered include

- balneological use,
- direct use of thermal heat by heat pumps,
- direct use of thermal heat by heat exchanger,
- direct heating through absorption heat pumps,
- industrial heating, power generation and co-generation.

Figure 8.4-4 shows the geothermal potential at the top of the Upper Jurassic Malm formation. Areas where no Upper Jurassic is present, like the Landshut-Neuöttinger Hoch crossing the UA – UB area NW–ESE, are void. The map shows high geothermal potential in the spa region of Upper Austria due to convection (Figure 7.4-2). In the southern part there is also an increased geothermal potential reflecting the dip of the Upper Jurassic down to depths of about 5,000 m below sea level.

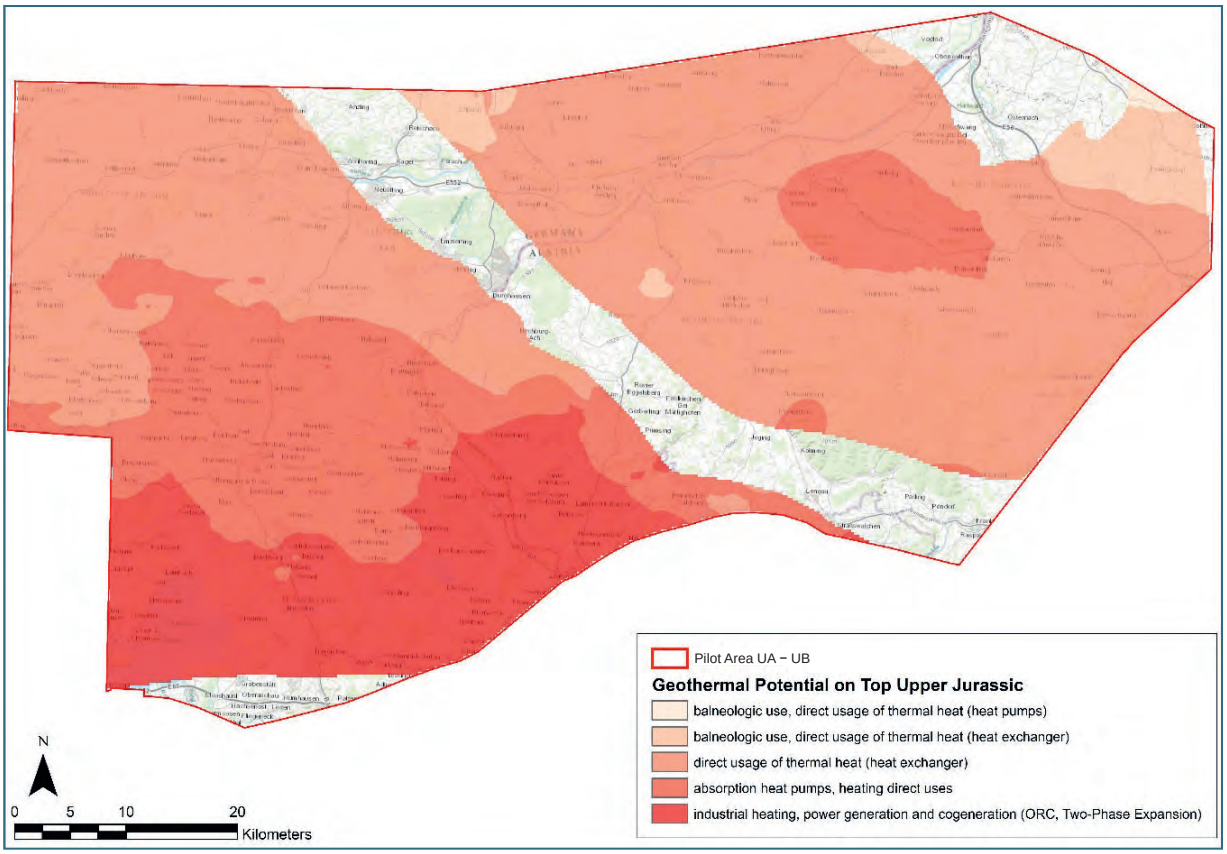

Figure 8.4-4: Geothermal potential map at the top of the Upper Jurassic Malm formation in the Upper Austria – Upper Bavaria pilot area (see text for discussion).

8.4.5 Conceptual model of the hydrothermal system

The existing 2D hydrological flow model of the Upper Jurassic Malm aquifer dates from 1999 and was recently shown to be based on partly implausible assumptions and to yield incorrect forecasts. The new 3D geological model now built in the pilot area offers the possibility to fine-tune the exis-

ting flow model, to extend it further towards the southeast and to newly evaluate the hydrological role of tectonic elements such as the Landshut-Neuöttinger Hoch and the *Ried* fault line.

Using the interpreted seismic lines and the modelled horizons, the inventory of fault zones was updated and the transmissivity of units assessed. In addition, all available borehole data were integrated including geological profiles, geophysical logs, water levels, hydraulic test results, hydrochemical data, isotope analyses and temperature measurements. The latter were used to define temperature gradients for the Malm aquifer. Temperature-corrected, isothermal water levels were calculated and used to construct potentiometric surfaces.

The geological model could verify the occurrence of Upper Jurassic sediments southwest of the Landshut-Neuöttinger Hoch and map their regional extent in 3D. The model reveals that Malm carbonates do not continuously overly the structure. This means that the karst aquifers within the *Wasserburg* trough to the south and the *Braunau* trough to the north are not connected hydraulically and thermal groundwater reservoirs are limited to the south, north and east by the extent of the carbonates. At significant fault lines such as the *Pocking* and *Ried* faults, but also at more local faults, the 3D model was used to pinpoint layers offsets which disconnect parts of the hydraulic system. Shear zones with small slip rates are visible in the seismic sections and interpreted as brittle deformation features with increased hydraulic conductivity.

Isotope and hydrochemical data approve that the thermal waters are of meteoric origin, of the Na-HCO_3-Cl type and contain approximately 1 g/l dissolved solids. Aquifer temperatures show that geothermal gradients are highest in the area of *Inntal* and *Rottal* reaching values of 4.9 – 5.5 °C/100 m. Contouring the gradients reveals that the *Ried* fault zone separates the hanging wall and footwall thermally. Towards the southwest a decreasing trend of geothermal gradients is observed with a local high stretching from *Altheim*, *Geinberg* and *Ried* towards *Haag*.

Potentiometric surfaces were compared to earlier results from the years 1972–1979 and 1999. They confirm the hydraulic barrier of the *Ried* fault and the discharge zones of *Inntal* and *Rottal*. Contrary to previous maps, a flow of thermal waters in the area of *Innviertel* was newly observed to be directed towards the northwest. Overall, hydraulic and geothermal gradients show similar regional trends due to the strong effect of convection on the distributions of groundwater temperatures in the karst aquifer.

8.5 Brescia-Mantova-Mirandola area (BMMA)

Pilot activities in the area of Brescia-Mantova-Mirandola addressed the characterisation of geothermal potential at low (< 90 °C) and medium temperature (> 90 °C and < 150 °C) up to a maximum depth of 4,000–5,000 meters. Given the low temperature gradients in the area, the main use of geothermal resources is heating (small geothermal plants) or district heating (medium/large geothermal plants), another use is for balneology. Only at certain locations within BMMA, and at great depths, there is the potential for the production of electrical energy.

The second principal focus of pilot activities was on the natural and human-induced seismic risks, as debated in public especially after the May–June 2012 seismic sequence. Specific actions were therefore carried out to identify and characterise active faults and seismogenic sources the pilot area (Maesano et al. 2015a, 2015b). Collaborations were set up with the Consiglio Nazionale delle Ricerche (CNR) and the Istituto Nazionale di Geofisica e Vulcanologia (INGV), while Mantova and Cremona Provincial Administrations cooperated to design a new approach to territorial and urban planning. This approach properly considers seismic risk and possible local knock-on effects such as the sand liquefaction phenomena which occurred during the May–June 2012 seismic sequence.

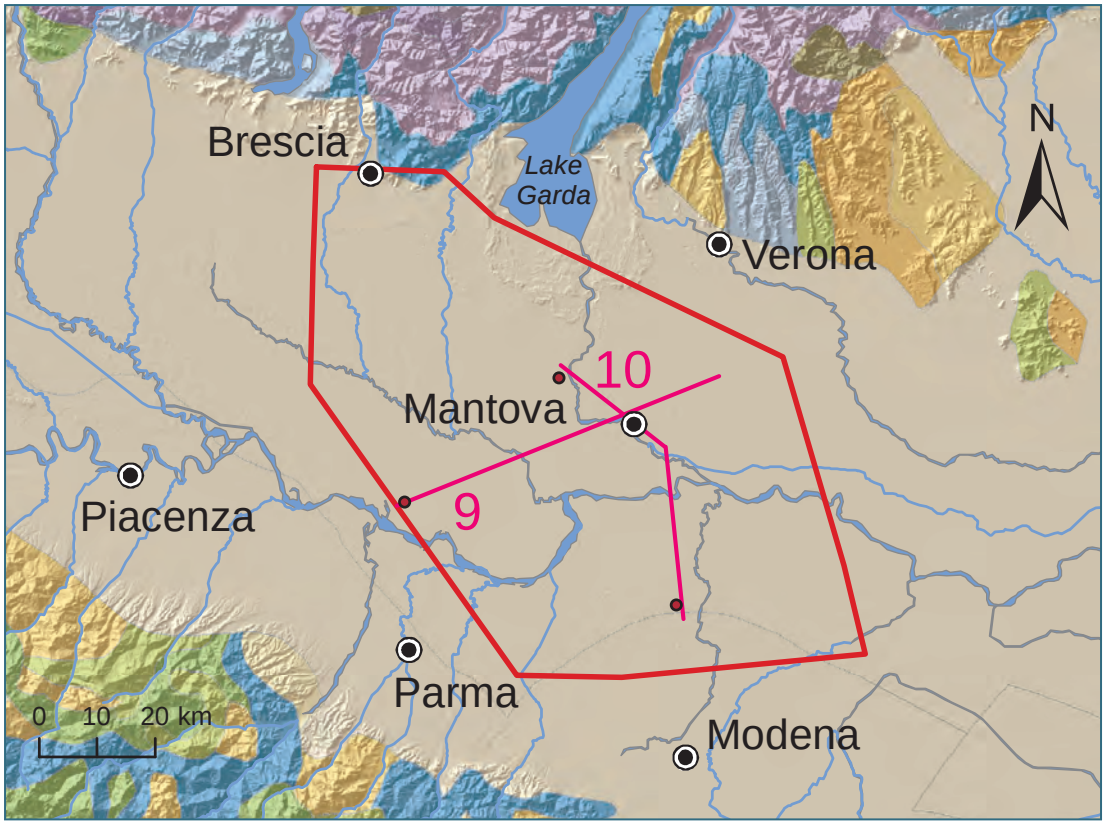

Figure 8.5-1: Extent of the Brescia-Mantova-Mirandola pilot area (BMMA) and location of cross-sections and boreholes as in figure 8.5-2. Background map: The 1 : 5 Million International Geological Map of Europe and Adjacent Areas (IGME 5000), https://www.bgr.de/karten/IGME5000/igme5000.htm. The continental Pleistocene as the uppermost unit of the Po Basin fill is shown in beige colours.

Figure 8.5-2 (following page): Cross-sections through the Brescia-Mantova-Mirandola area pilot area as derived from the 3D geological model. For more detailed description of the modelled units refer to table 8.5-1.

Cross-section 9

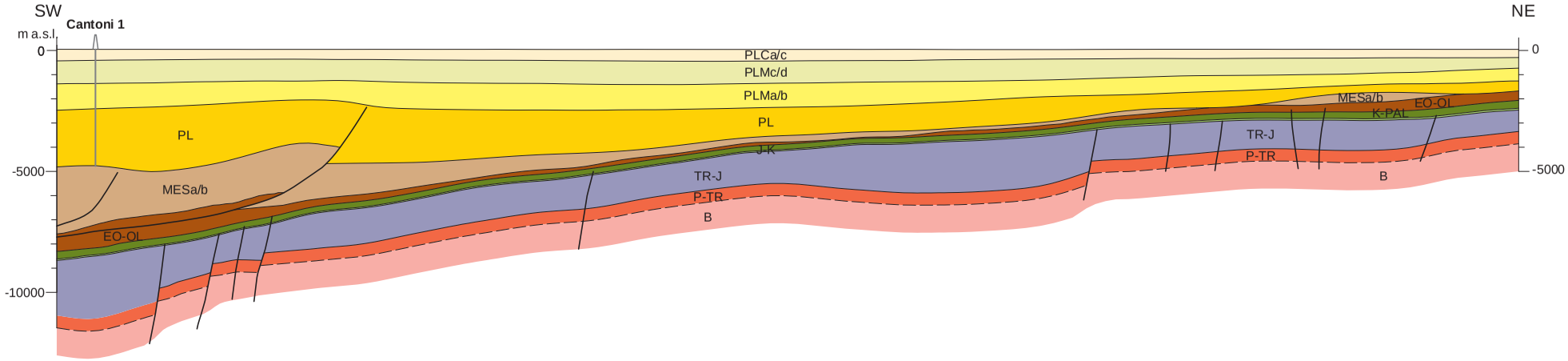

Cross-section 10

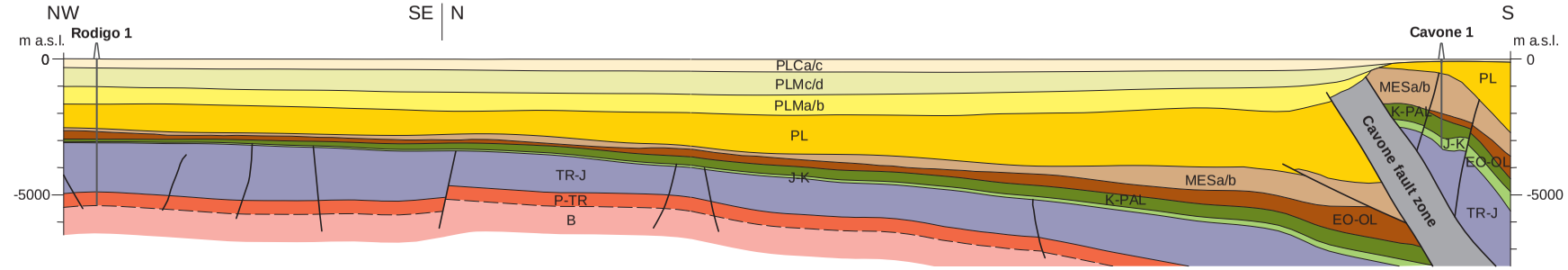

PLCa/c	Pleistocene continental units	MESa/b	Upper Miocene	J-K	Middle Jurassic – Early Cretaceous		Borehole projected
PLMc/d	Pleistocene marine upper units	MIO	Lower – Upper Miocene	TR-J	Late Triassic – Early Jurassic		Fault
PLMa/b	Pleistocene marine lower units	EO-OL	Eocene – Oligocene	P-TR	Permian – Carnian		
PL	Pliocene	K-PAL	Early Cretaceous – Paleocene	B	Basement		

0 5 10 km

Vertical scale 2x exaggerated

While the uppermost geological units have been mapped in 2D at a regional level by the Regions of Emilia-Romagna (DI DIO 1998) and Lombardia (CARCANO & PICCIN 2002) in cooperation with the National Italian Oil Company ENI E&P, and some regional subsurface geological sketches have been published in recent years, a complete and harmonised geological model of the entire Po Plain is still needed. Extent and location of the pilot area permitted to analyse both the Alpine and Apennines sides of the basin, to harmonise their different but interrelated sedimentary and tectonic evolutions and to achieve a common approach to the subsurface study between the two regional partners (Regions of Lombardia and Emilia-Romagna) under supervision of the Servizio Geologico d'Italia (ISPRA).

8.5.1 Study area and geological setting

The Italian pilot area is located in the central-eastern part of the Po Plain between two mountain ranges, the Alps and the Apennines. The area covers 5,690 km², from the city of Brescia at the Alpine fringe, through the Lake Garda glacial amphitheatre and the *Mantova* and *Cremona* plain, across the Po River up to the area of *Mirandola*, a few kilometres north of the Emilia Apenninic fringe.

The morphology is mostly flat except for some gentle hills south of Brescia (*Castenedolo*, *Ciliverghe* and *Monte Netto* hills) due to the emergence of Alpine anticlines, and for the moraine hills south of Lake Garda (Figure 9.1-1). The northern sector is characterised by the coalescent alluvial fans of the *Oglio, Mella, Chiese* and *Mincio* rivers flowing from the Alpine valleys towards the Po River, the plain's main river which originates in the western Alps and flows eastward to the Adriatic Sea. The southern sector is built by the alluvial fans of the *Taro, Parma, Enza, Secchia* and *Panaro* rivers coming from the Apennines and also reaching the Po River (Figure 8.5-1).

From the geological point of view, this area is a complex foreland basin situated between two opposing mountain chains (Alps and Apennines), filled by a thick and articulated "Molasse like" clastic sediment sequence of Oligocene to Pleistocene age, and sustained by a mainly carbonate sequence of Triassic to Eocene age. The architecture of this sediment fill is shaped by the mutual tectonic activity of the two chains, south verging structures of the late phases of Alpine activity and north verging structures of the more recent Apennines. In the *Cremona* area, the two are facing one another at a few kilometers distance in the subsurface (Figure 2.2-9 D).

The geology of the Po Plain is the result of a complex sedimentary and tectonic history (see GHIELMI et al., 2013, and the literature cited therein). In short, the Po Plain formed between the Alps and the Apennines – with some contributions from the Dinarides in the east – on a Mesozoic pattern of condensed sedimentary successions on top of structural highs, and thicker sediments within troughs. Conditioned by N–NW trending extensional faults, the foreland basin developed since the Oligocene in a sequence of multiple, interrelated sedimentary and tectonic phases. After formation of the syntectonic clastic wedge of Gonfolite at the South Alpine margin, which is related to Oligocene-Miocene Neoalpine tectonic phases, the progressive northward migration of the Apennine thrust and fold systems tilted the Mesozoic Alpine plateau to form a gently southward dipping monocline. On top of this monocline, a migrating foredeep developed and was filled by a Plio-Pleistocene clastic sequence, controlled by the growing anticlines of the Apennine thrust systems.

8.5.2 Geological model

Within the pilot area, hydrocarbon exploration during the 1960's and 1970's left a heritage of nearly 12,000 km of 2D seismic sections, some 3D seismic models and 123 well logs. Data vary in age and

quality but are nevertheless very useful for geological and structural interpretation. They are owned by ENI SpA and access is generally restricted even if some of the data, mainly well logs, are published in the Italian Government data catalogues (UNMIG). For the GeoMol project, Italian partners came to an agreement with ENI SpA and gained access to all existing 2D seismic data and well logs in a dedicated data-room, equipped with workstations and the software tools suited to interpret seismic horizons and faults in the time domain. The interpretation results were then exported, processed by GIS, converted into the depth domain using a geology-based velocity model with well data cross-checks, and finally modelled using the 3D modelling software Move.

Table 8.5-1: Description of geological units modelled in the Brescia-Mantova-Mirandola area (MIS: Marine Isotope Stage; Fm.: Formation). For the graphic representation of the stratigraphic scheme refer to Figure 2.2-8.

Horizon name	Horizon description	Unit code: stratigraphic units between horizons	Thickness (m)	Lithology (depositional environment)
QC3	Pleistocene unconformity	PLCc : From 0.45 Ma (MIS12) to present	0–200	Sand and gravel (continental)
QC2	Pleistocene unconformity	PLCb: From 0.63 Ma (MIS16) to 0.45 Ma (MIS12)	0–230	Sand and gravel, locally silt (continental)
QC1	Pleistocene unconformity	PLCa: From 0.87 Ma (MIS22) to 0.63 Ma (MIS16)	0–195	Sand silt and locally gravel (continental and locally transitional)
QM3	Pleistocene unconformity	PLMd: From 1.07 Ma (MIS31) to 0.87 Ma (MIS22)	0–700	Silt, sand and locally gravel (marine, transitional and locally continental)
QM2	Pleistocene unconformity	PLMc: From 1.25 Ma (MIS37) to 1.07 Ma (MIS31)	0–740	Sand and silt (marine and locally transitional)
QM1	Pleistocene unconformity	PLMb: From from 1.5 Ma to 1.25 Ma (MIS37)	0–900	Sand and silt (marine), locally gravel (submarine fans)
GEL	Gelasian unconformity	PLMa: Argille del Santerno Fm. p.p., Porto Garibaldi Fm. p.p.	0–950	Shale and sand (marine, locally fine grained turbidites)
PL	Zanclean unconformity	PL: Argille del Santerno Fm. p.p., Porto Corsini Fm., Porto Garibaldi Fm. p.p.	0–4,600	Shale and sand (marine, locally fine grained turbidites)
ME3	Intra-Messinian unconformity	MESb: Fusignano Fm., Sergnano Fm.	0–1,820	Gravel and sand (marine deltaic fans)
ME1	Latest Tortonian unconformity	MESa: Marne di Gallare, Gonfolite Fm., Gessoso Solfifera Fm.	0–2,500	Marl, sand and locally gravel; silt with evaporites (marine-transitional)
MLW	Miocene unconformity	MIO: Marne di Gallare, Gonfolite Fm.	0–2,900	Marl, sand and locally gravel
		EO-OL: Early Eocene-Oligocene: Scaglia Cinerea Fm. Oligocene – Late Miocene: Marne di Gallare Fm., Gonfolite Fm.	0–1,560	Marl, sand and locally gravel
SCA	Top Scaglia (middle Eocene)	K-PAL: Early Cretaceous – Paleocene: Marne del Cerro, Marne a Fucoidi, Brecce di Cavone and Scaglia Fms.	350	Marl, calcareous marl
MAI	Top Maiolica (Aptian)	J-K: Middle – Late Jurassic: Lumachella, Oolite di San Vigilio, Calcari a Posidonia, Concesio, Rosso Ammonitico and Calcari ad Aptici Fms.; Late Jurassic – Early Cretaceous: Maiolica Fm.	100	Platform carbonates
NOR	Top Calcari Grigi (Lias)	TR-J: Late Triassic and Early Jurassic: Dolomia Principale, Calcari Grigi, Corna and Medolo Fms.	1550	Platform carbonates
TE	Top Permian–Carnian	P-TR: Permian–Carnian units	-	

Starting from recently published geological descriptions of units mainly concerning Miocene and Plio-Pleistocene sequences, and after verification of their traceability throughout the study area, a succession of 16 units, described by 15 main horizons of different origin, was defined. Other minor horizons were locally traced in order to define and map geological bodies representing crucial phases of basin evolution or interesting targets for geopotentials (Table 8.5-1).

The remaining Pleistocene sequence, well developed and articulated in the Po Plain basin, was resolved in more detail and subdivided into 6 units, limited at the base by surfaces defined by their respective age (Ma) and by the corresponding climatic stage (MIS) where applicable (Scardia et al. 2006, 2012). QM1 (1.5 Ma), QM2 (1.25 Ma, MIS37) and QM3 (1.07 Ma, MIS31) represent the bases of three mainly marine sand units (PLMb, PLMc and PLMd respectively). The horizons QC1 (0.87 Ma, MIS22), QC2 (0.63 Ma, MIS16) and QC3 (0.45 Ma, MIS12) form the bases of three sand and gravel units deposited in transitional and continental environments (PLCa, PLCb and PLCc respectively). Most of these surfaces also correspond to minor unconformities, well developed especially at the Apennines margin and therefore very useful to constrain the tectonic evolution of the buried structures both within Alpine and Apennines domains.

Numerous tectonic structures were also mapped and modelled following their classification into four main groups:

- mainly high angle, extensional faults trending N/NW which conditioned the sedimentation of the Mesozoic succession
- E–W trending, south-verging low to medium-angle Alpine thrust fronts (locally associated with backthrusts), turning towards NNE in the Lake Garda sector, due to the influence of the transpressive Giudicarie belt
- north-verging, low to medium-angle Apennines thrust fronts, often influenced by Mesozoic high-angle faults
- NW–SE trending, transtensive high-angle faults, belonging to the Schio-Vicenza system and dissecting the Alpine thrust fronts.

8.5.3 Evaluation of geopotentials

The subsurface of the pilot area has been intensively explored for hydrocarbons since the 1960's, mainly by the National Italian Oil Company ENI SpA and, more recently, by different international companies. The targets, mainly concerning gas reservoirs, are located at few kilometres depth within sandy deposits of Miocene and Early Pliocene, folded by the progression of South Alpine and Apennines structures and sealed by shaly Pliocene units. Other targets, explored and locally exploited in recent years, are located at greater depth (3 to 7 km) in the upper part of the Mesozoic sequence, mainly in carbonates of Triassic up to Cretaceous age. The same units targeted for hydrocarbon production may also serve for storage of natural gas or CO_2.

As for the geothermal potential, three main groups were defined. The shallowest one includes the Pleistocene units PLMa to PLMd which can be primarily used for balneology and direct heating. Below, the group of Miocene and Pliocene units (MIO to PL) mainly carries a potential for direct heating and, as secondary usage, for balneology. The third group includes the carbonate geothermal units (TR-J to K-PAL) which can be used for electricity generation and direct heating. Groundwater potential exists in the continental, possibly also in the marine, upper Pleistocene units (PLC and PLM). Table 8.5-2 gives an overview of the model units and their theoretical geopotential.

Table 8.5-2: Compilation of the theoretical geopotential of the model units in the Brescia-Mantova-Mirandola pilot area

Unit	drinking water	balneology	direct heating	power generation	oil and gas production	natural gas storage	CO_2 storage
Continental Pleistocene, PLCc							
Continental Pleistocene, PLCb							
Continental Pleistocene, PLCa							
Upper Marine Pleistocene, PLMd							
Upper Marine Pleistocene, PLMc							
Lower Marine Pleistocene, PLMb							
Lower Marine Pleistocene, PLMa							
Pliocene, PL							
Upper Miocene, MESb							
Upper Miocene, MESa							
Lower – Upper Miocene, MIO							
Eocene – Oligocene, EO-OL							
Early Cretaceous – Paleocene, K-PAL							
Middle Jurassic – Early Cretaceous, J-K							
Late Triassic – Early Jurassic, TR-J							
Permian – Carnian, P-TR							

unit contains layers with geopotential; unit possibly contains layers with geopotential; unit contains no geopotential; not investigated

8.5.4 Model application – geothermal potential and seismogenic structures

The assessment of geothermal potential was focussed on possible usage at medium depths. Besides using all available data from hydrocarbon wells and literature, all temperature measurements were digitised, analytically validated and statistically analysed. According to the geological and structural model of the pilot area, geothermal gradient models were calculated for three depth sections, K0 (ground level – QM1), K1 (QM1 – SCA) and K2 (SCA – base of 3D model). The three gradient models were obtained for each well, followed by geo-statistical interpolation between wells for

the entire pilot area. Three grids containing the gradients were obtained and used to calculate temperatures at the depth of surfaces derived from the geological model. The geological-structural setting strongly affects the geothermal pattern in certain sectors of the pilot area. Different analytical solutions were adopted for these sectors to produce the final thematic maps. It is planned to conduct a temperature measuring survey in water wells in the northern sector of the pilot area in order to identify possible thermal anomalies where warm water ascends along open faults and mixes with fresh groundwater within alluvial deposits.

Tectonic activity is ongoing in the Po Plain, as evidenced by the May 2012 earthquake which affected the Modena, Reggio Emilia and Mantova Provinces with a long sequence of tremors including six main shocks of $M_w > 5$ magnitude (maximum M_w 6.1). Identification and characterisation of seismogenic sources and active faults in the area is described separately in chapter 9.1. The study permitted to update the Italian Database of Seismogenic Sources (DISS) and will provide an independent source of information to properly evaluate the sustainable development of geopotentials.

As additional result, regional and provincial guidelines for seismic zoning in urban planning will be updated and consider phenomena such as sand liquefaction which caused the most damage during the May 2012 seismic event. Mapping the “seismic basement”, the reference surface beyond which the horizontal speed of seismic waves exceeds 800 m/s, will help engineers to properly calculate ground motion effects and design earthquake-proof buildings.

The methodology applied in localisation and assessment of seismogenic structures and is described in more detail in the subsequent chapter 9.1.

9 Special studies

A principal objective of GeoMol is to provide harmonised information on the NAFB and on the five pilot areas (although each with a specific emphasis) based on the comparable base data preparation and common modelling methods to ensure an overall comparability of the results. However, in some areas there are specific issues – attributed to regional peculiarities in the geological set-up and/or as a special request of stakeholders – which cannot be dealt with on a full scale, thus are subject to particular in-depth studies or use cases in selected areas.

Three special studies have been implemented

- on the localisation and assessment of seismogenic structures and active faults in the Po Basins pilot area, realised by ISPRA in collaboration with INGV (Instituto Nazionale Geofisica e Vulcanologia). The results presented are the deliverables of a convention between ISPRA and INGV (Chapter 9.1).
- on the assessment of the geopotential of medium-deep borehole heat exchangers (MBHE) carried out in Baden-Württemberg's share of the Lake Constance Allgäu area by LGRB and RVBO (Chapter 9.2),
- on the application of GeoMol's methods beyond the Alpine foreland basins and under particularly adverse conditions with respect to data availability, tested in the Mura-Zala Basin by GeoZS (Chapter 9.3).

9.1 Assessment of seismogenic structures and active faults of the central Po Plain

As already experienced in recorded cases of induced and/or triggered[1] seismicity all around the world (e. g. Evans et al. 2012, Zoback & Gorelick 2012, National Research Council 2013, Keranen et al. 2014), after the Emilia seismic sequence of May-June 2012 (M_w max 6.1), following a strong public concern, a scientific and political debate started (ICHESE 2014, Cartlidge 2014) to address and investigate the possible interaction between the impact of human activities in the subsurface (e. g. oil and gas production) and the seismicity.

The induced or triggered seismicity is a well known problem, but a commonly accepted solution has not yet been found, as stated by Dahm et al. (2010): *"Earthquakes occurring in spatial and temporal proximity to such (human) operations are immediately under suspicion to be triggered or induced. The discrimination between natural, triggered, and induced earthquakes is a difficult task, and clear rules and scientific methods are not well established or commonly accepted".*

However as reported in the conclusions of the ICHESE Report 2014: *"New hydrocarbon/geothermal exploration activities must be preceded by preliminary desk study and field-based screening evaluation based on an extensive and detailed 3-D geophysical and geological study, allowing the determination of the main fault systems which can be suspected to be active and their seismogenic characteristics (fault length, occurrence rate, etc.)".*

[1] **Induced:** where external anthropogenic activities produce stress changes, which are sufficiently large to produce a seismic event. **Triggered:** where a small perturbation generated by human activity has been sufficient to move the system from a quasi-critical state to an unstable state; the event would have eventually occurred anyway although **probably** at some unknown, later time.

Therefore the geopotential assessment cannot be separated from the understanding and analysis of the geological structures. The geological knowledge, thus, as much as the engineering and technical solutions, becomes strategic for the sustainable use of natural resources of the subsurface.

Located in a densely populated, highly urbanised plain area featuring important industry, the Italian pilot area of the GeoMol project represents an ideal case study to define and test the contribution of 3D geological modelling for both, geopotential assessment and analysis of geological risks. Unfortunately, despite the common perception that "plain" is equivalent to "stable", this wide strategic plain area is characterised by different natural hazards:

- floods (e. g. 2000, 1994, 1951; with 190 casualties and 220,000 displaced),
- natural and human-induced subsidence up to 70 mm/year (Carminati & Martinelli 2002),
- destructive earthquakes (e. g. May 2012 - Emilia Romagna, M_w 6.1; December 1117 - Veronese, M_w 6.7; June 1891 - Valle d'Illasi, M_w 5.9, the latter was felt in 403 localities from Rome to Innsbruck, DBMI11 - Italian Macroseismic Database, Locati et al. 2011) (Figure 9.1-1).

The Po Plain's underground hosts the Southern Alps and the Apennines (e. g. Emilia-Ferrara) thrust systems (Section 2.2.1.2), containing one of the main hydrocarbon provinces in Italy (e.g. Cortemaggiore, Villafortuna-Trecate, Malossa plays) and natural gas storage sites (Figure 9.1-2). Recently also some geothermal energy concessions have been granted in the Po Plain by the Ministry of Economic Development.

The blind thrusts which generated the May–June 2012 earthquake sequence are located inside the Po Basin pilot area and are associated with anticline structures hosting exploited hydrocarbon plays (e. g. Cavone) or interested by debated research concession for gas storage (Rivara).

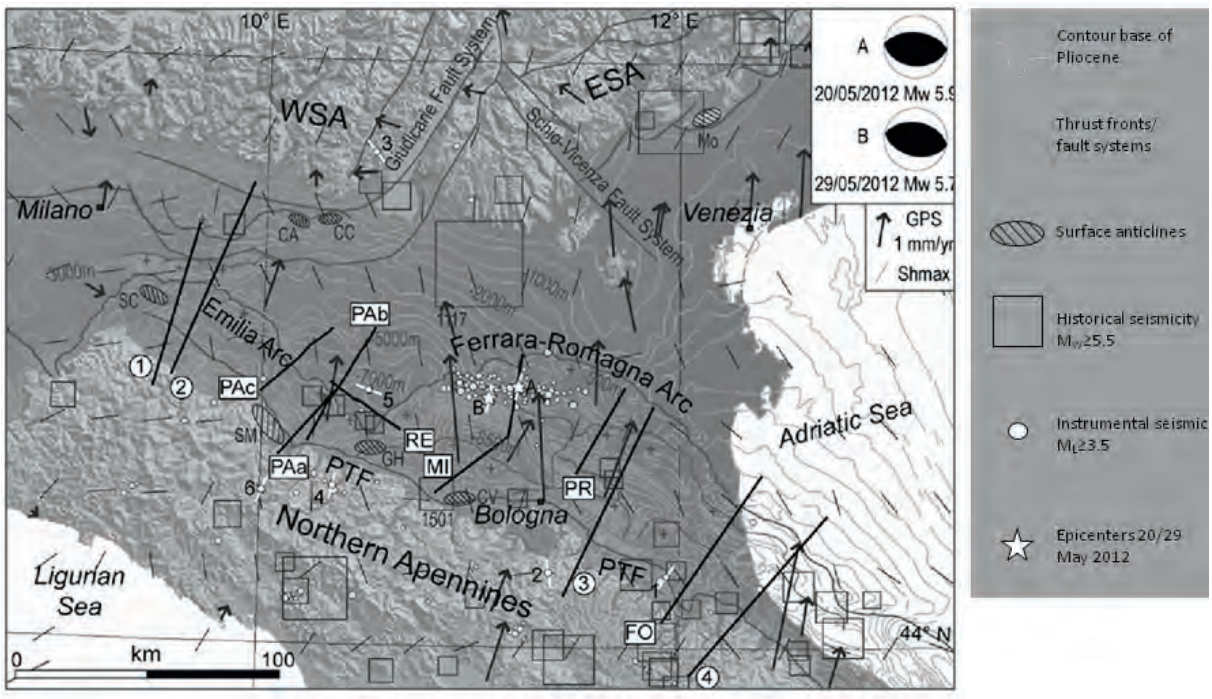

Figure 9.1-1: Schematic structural and seismotectonic map of the Po Basin (modified after Maesano et al. 2015a). CA: Castanedolo, CC: Capriano al Colle, CV: Castelvetrano, GH: Ghiardo, MO: Montello, SC: San Colombano, SM: Salsomaggiore. Instrumental seismicity period 2005–2013 (ISIDe Working Group 2010), historical seismicity from CPTI11-catalogue (Rovida et al. 2011), focal mechanisms from Scognamiglio et al. (2012), Sh_{max} axes from Carafa & Barba (2013), GPS vectors from Caporali et al. (2011).

Although the discrimination between natural, triggered, and induced seismicity is beyond the scope of the GeoMol Project, the 3D model of the the Brescia-Mantova-Mirandola pilot area was built to address both, the geopotential assessment as implemented for all pilot areas (Chapter 8) and, as a special use case, the better knowledge of the seismogenic structures and active faults. These studies were carried out in collaboration with the Istituto Nazionale di Geofisica e Vulcanologia (INGV).

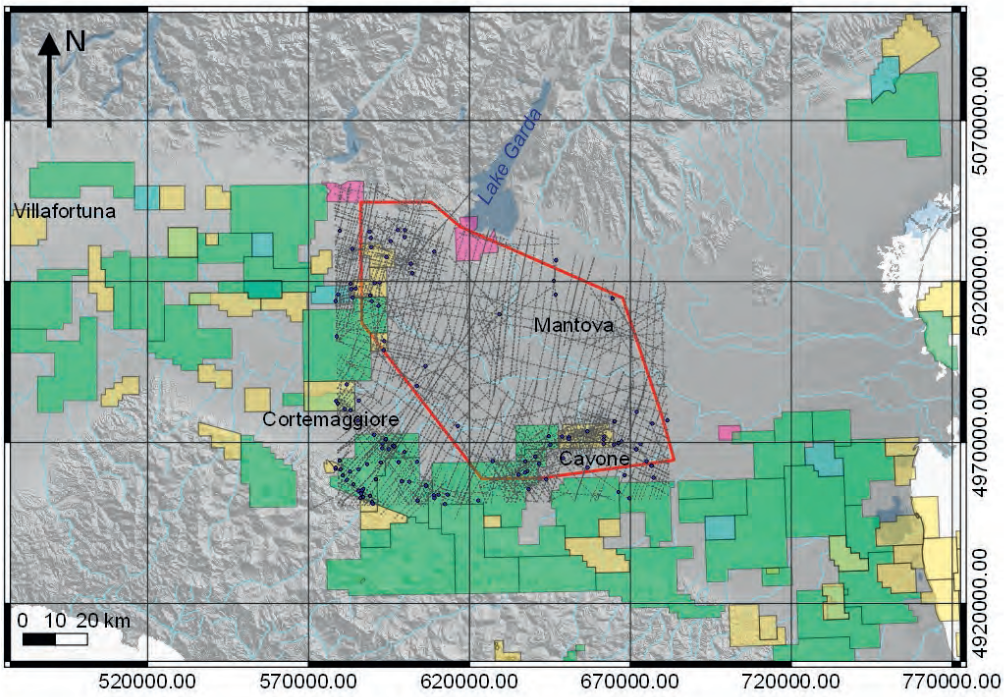

Figure 9.1-2: Distribution of permits (polygons): green – oil and gas exploration, yellow – oil and gas production, light blue – gas storage, pink – geothermal exploration and production (data from Ministry of Economic). The red line marks the outline of the Brescia-Mantova-Mirandola pilot area, blue points are borehole locations, grey lines are seismic sections (ENI SpA dataset).

9.1.1 Characterisation of faults

The structural elements in the 3D model of the Po Basin were reconstructed with particular detail to obtain the best constraint of their geometry, to support their parameterisation, and to allow the identification and analysis of tectonic structures deemed to be active. The identification of these structures is often difficult in plain areas where sedimentary processes generally conceal the tectonic effects.

The fault traces were mapped in section during seismic interpretation, focusing on the position of the fault tip; the evidences of dislocation or folding on horizons younger than 1.6 Ma were highlighted. Moreover, where possible, age constraints have been obtained with new special analyses carried out on wells along the Southern Alps margin (in collaboration with the Istituto di Geologia Ambientale e Geoingegneria – CNR IGAG). These data enabled the identification of the age of inception for each fault.

Subsequently the faults have been differenced on the basis of their kinematics (compressional, extensional and transcurrent) and their position in relation to the stratigraphic succession, e. g. position of the detachment level and mechanical properties of the intersected units (Figure 9.1-3).

Moreover the distribution of the instrumental (ISIDE WORKING GROUP 2010), historical seismicity (ROVIDA et al. 2011) and data on present day stress field (e. g. World Stress Map www.world-stress-map.org, GPS velocities) were collected and analysed.

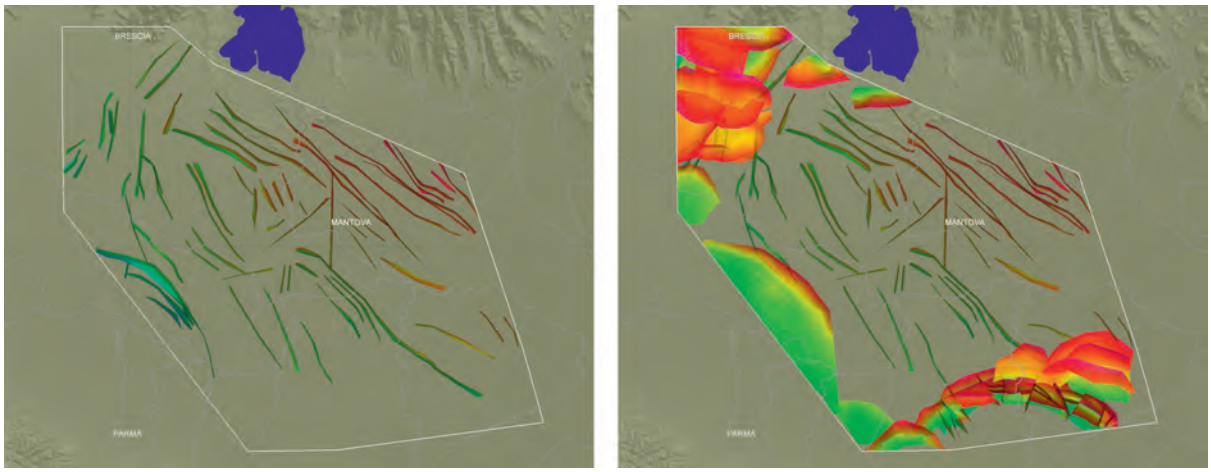

Figure 9.1-3: Left: extensional faults cutting the Mesozoic carbonate succession; right: the entire set of faults of the pilot area. The colours indicate the depth of the fault surfaces.

9.1.2 Active faults and seismogenic sources

The characterisation of the fault activity and of their seismogenic potential have been based on consolidated restoration and analysis workflow (MAESANO et al. 2013, 2015a), and on the characteristics and parameters defined for the seismogenic sources in BASILI et al. (2008) and as used by the DISS WORKING GROUP (2010).

Only faults with a length of more than 8–10 km have been considered for the evaluation of their activity and seismogenic potential and divided into five groups according to the type key in table 9.1-1.

Table 9.1-1: Classification of faults in the Po Basin pilot area

Type	Existing in DISS	Seismogenic potential	Hierarchy	Seismogenic	Active	Inception
SS	Yes	Large earthquakes*	Primary structures	Yes	Yes	Formed in the present tectonic regime
PSS	No	Large earthquakes*	Primary structures	Yes	Yes	Formed in the present tectonic regime
PSS	No	Large earthquakes*	Primary structures	Yes	Yes	Inherited and reactivated
AFa/ AFo	No	Small earthquakes	Secondary faults connected to a primary structural element	No	Yes	Formed in the present tectonic regime
AFa/ AFo	No	Small earthquakes	Secondary faults connected to a primary structural element	No	Yes	Inherited and reactivated
BDF	No	No earthquakes/ small earthquakes/ triggered seismicity	Primary and secondary faults not favorably oriented in the active stress regime, may be reactivated during seismic sequences	No	No	Inherited and not reactivated
UKN	No	Unknown	Primary and secondary faults, lack of detailed information	Unknown	Un-known	Unknown, most probably inherited
Type key: **SS**: Seismogenic Sources, **PSS:** Potential Seismogenic Sources**, AFa/AFo**: Active Faults/Folds **BDF**: Bedrock Faults, **UKN**: Unknown Type *) M 5.5 or larger as the bottom line considered in the DISS database						

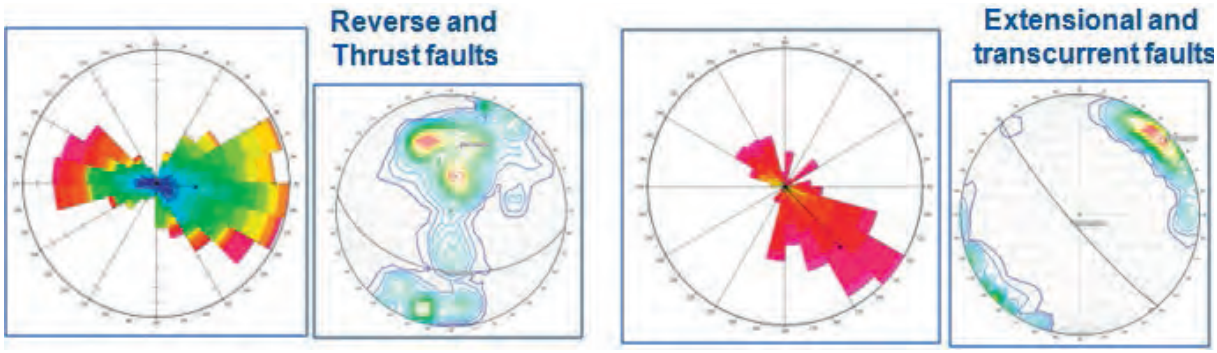

Figure 9.1-4: Plot diagram of faults orientation azimuths (see text for discussion).

The faults with an orientation, according to the azimuth range depicted in figure 9.1-4, which are compatible for a reactivation in the present day stress field, and the faults associated with deformations (dislocation or folding) in horizons younger than 1.6 Ma were defined as active faults. Although there is not a fixed rule about what geological time scale should be used to address the activity of a fault, the use of 1.6 Ma is in agreement with the definition of Quaternary active faults proposed by the Western States Seismic Policy Council (WSSPC 1997) and was defined considering the recent tectonic history of the Po Plain and related stress field. However in different tectonic regimes it should be necessary to define a different age according to the regional tectonic history.

These faults were studied in more detail independent of their position in relation to the geopotential targets (if these structures are also seismogenic, they could be the source of earthquakes greater than M_w 5.5).

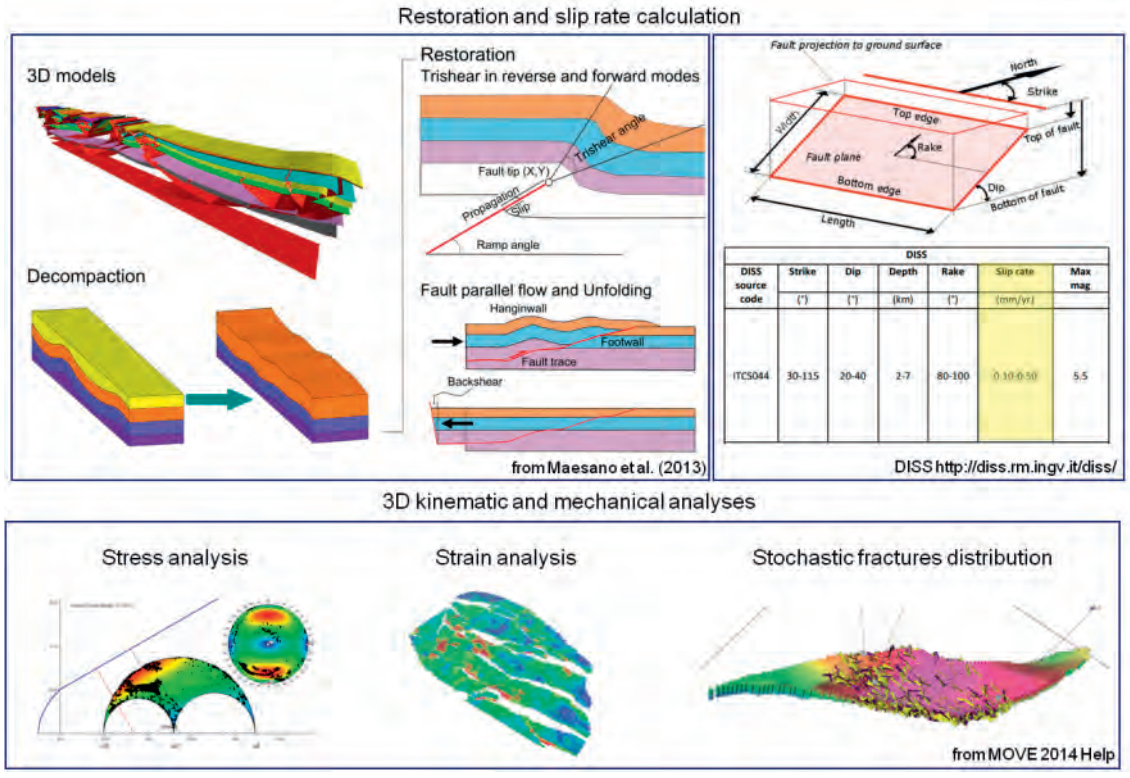

Figure 9.1-5: Workflow for slip rate calculation

Where possible (e.g. horizons with good age constraint and good definition of the fault tip) the workflow proposed by Maesano et al. (2013, 2015a) has been applied. It allows to calculate the slip rate also when the evidences of folding and growth strata are elusive (e.g. mild folding with low amplitude and high wave length). It can be summarised in the following steps (Figure 9.1-5):

- 3D modelling,
- decompaction on the target horizon,
- restoration with appropriate algorithm (trishear, fault parallel flow, simple shear) based on the type of deformation observed,
- slip rate calculation and uncertainties estimation.

The slip rate values obtained supplemented the seismogenic sources parameterisation.

9.1.3 Results

The detailed 3D geological model of the Po Basin pilot area supported the improved characterisation of already known structural elements, especially the thrusts of both, the Southern Alps and the Northern Apennines, but also the analysis of previously poor constrained inherited faults affecting the deeper portion of the sedimentary succession up to the top of Scaglia formation.

Moreover the new subsurface data and interpretation derived from the 3D model enabled a more precise definition of the geometry of the seismogenic sources, of their segmentation along strike and down-dip (only thrust planes cutting through Mesozoic limestone) and finally the identification of new active thrusts potentially seismogenic (Figure 9.1-6).

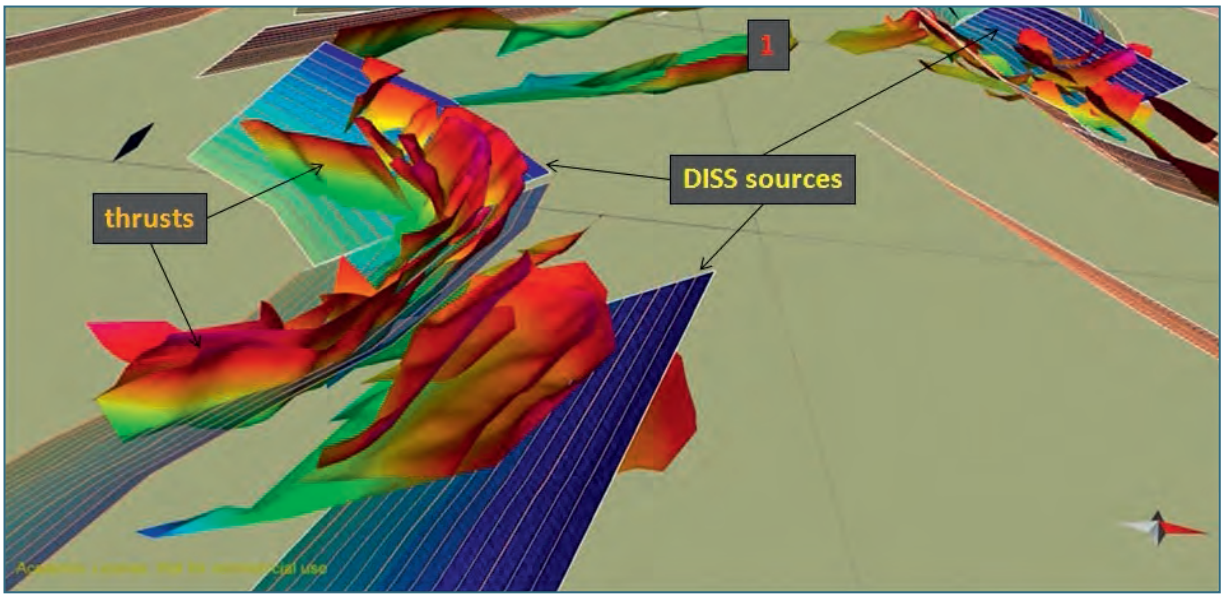

Figure 9.1-6: Comparison of seismogenic sources with thrusts in the 3D model and new active thrusts potentially seismogenic (1 in figure).

The final results are the improvement in the definition of the seismogenic sources already included in DISS database and the creation of new Composite Seismogenic Sources: the Piadena Composite Source (Figure 9.1-7), related to the Northern Apennines thrust front, the Desenzano-Garda and the Peschiera-Valpolicella Composite Sources, related to the Southern Alps thrust front.

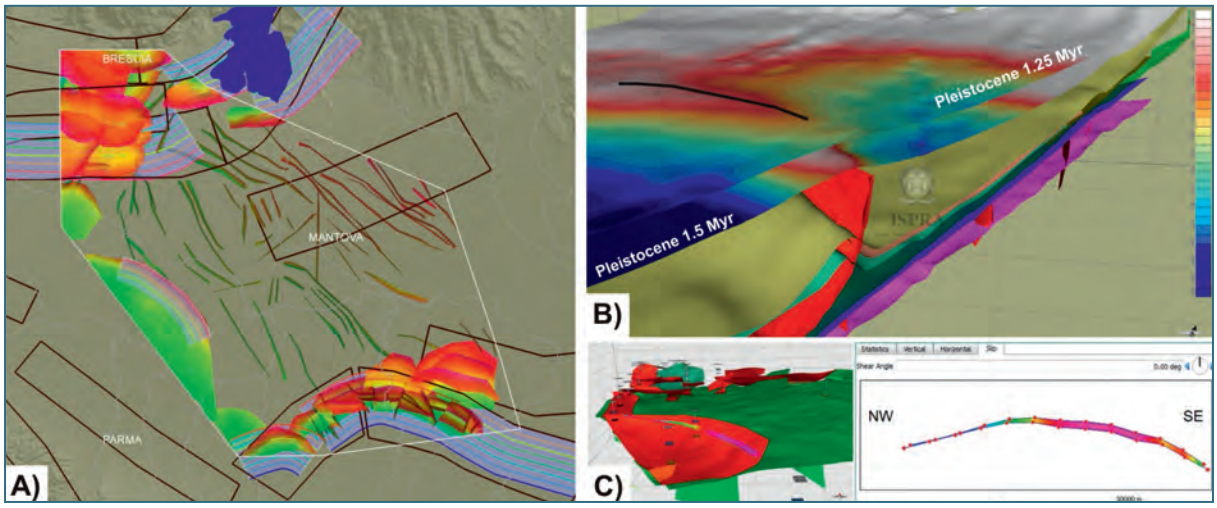

Figure 9.1-7: A) Faults and seismogenic sources in the Po Basin pilot area. The bold lines indicate the seismogenic sources already known in DISS database, the light blue polygons are the new or modified seismogenic sources derived from the 3D geological model of GeoMol. B) Solarolo thrust and deformed Pleistocene horizons used for slip rates calculation. C) Displacement on the base of Pliocene along the Solarolo thrust.

The 3D model supported also the calculation of slip rates on the main thrusts; the results have been partly published by Maesano et al. (2015a, b), and are presented in detail in the report of the Italian pilot area (ISPRA 2015). They are attached as attribute to the related faults trough the web viewer.

The obtained results highlight the basic role of consistent 3D geological models as the best synthesis of complex data; collectively, this information provides the foundation in analysing and monitoring the geological structures both for their possible geopotential usage and for their geodynamic behavior, as the seismic activity.

These results are basic input data for predicting the possible conflicts between subsurface hazards and usage and their likely consequences for human society.

According to an increasing need of consistent geological and seismotectonic knowledge, the Italian public, national and local, authorities with responsibilities on authorisation procedures for subsurface usages (e. g. geothermal, oil and gas, gas storage, CCS) will benefit from the data and information deriving from this study.

All the calculated parameters of faults, active faults and seismogenic sources in the Po Basin Pilot area will be publicly available through the GeoMol 3D-Explorer (Chapter 10); moreover all the seismogenic sources will be described in 3D through the GeoMol MapViewer.

9.2 Assessment of the geothermal potential of medium-deep borehole heat exchangers in the Lake Constance – Allgäu area

9.2.1 Introduction and aim of the case study

In addition to shallow ground source and deep geothermal systems, medium-deep to deep borehole heat exchanger (MBHE) technology can contribute to meet the energy demand by means of renewable energy resources (see Chapter 2.3.1). Therefore, the Regionalverband Bodensee-Oberschwaben (RVBO) as a regional planning authority stimulated a case study in order to assess the geothermal potential of MBHE in the Baden-Württemberg part of the Lake Constance – Allgäu pilot area (LCA) (cf. Chapter 8).

In addition to (open) hydrothermal and deep petro-thermal systems, geothermal energy can also be extracted from greater depths by means of closed loop MBHE systems (see Figure 2.3-2). This technology exploits underground temperatures at depths between 400 m and about 3,000 m. There is no exact limit for deep geothermal systems, which by definition directly utilise geothermal energy without additional enhancement of temperature (PK TIEFE GEOTHERMIE 2007), that means, they provide temperatures of more than 60 °C. Compared to the hydrothermal system, MBHE technology has little exploration risk concerning the choice of location. In principle, closed systems can be established at any site, but are subject to the geological, hydrogeological and drilling-technical suitability and water management restrictions.

In MBHE systems the borehole is completed as a coaxial or double-U probe. Within the probe, a heat transfer medium circulates with a temperature for heat extraction several Kelvin below the subsurface temperature around the borehole wall. As a result, heat is extracted conductively from the subsurface. The heat transfer fluid has no direct contact with groundwater or the country rock. Heat transfer from the subsurface to the circulating fluid in the borehole heat exchanger causes a temperature gradient which leads to the continued flow of heat from the surrounding of the borehole. The heat transfer medium flows from the borehole heat exchanger/probe pipes through pipelines to heat exchangers or heat pumps, where it is cooled (thermal recovery) and fed back into the borehole heat exchanger/probe. In general the same technically well-developed principle is used as in shallow geothermal borehole heat exchangers.

The aim of this study is

- to identify thermally and economically suitable systems of medium-deep borehole heat exchangers (MBHE),
- to assess the geothermal potential by calculating the recoverable amount of heat for standardised MBHE-types and for defined load cases and
- to investigate the dependence of the geothermal potential on site-specific subsurface characteristics.
- Besides the two GeoMol partners LGRB and RVBO, the Hochschule Biberach (Biberach University of Applied Science, Institut für Gebäude- und Energiesysteme, HBC), and two civil engineering companies with a special expertise on shallow ground source heat pumps, tewag GmbH, Starzach and Baugrund Süd, Bad Wurzach were involved in the study as contractors (HBC 2014, TEWAG 2014).

9.2.2 Methods

The following parameters were considered as input data for the assessment of the extractable amount of heat by means of MBHE:

- the load profile, depending on users' needs
- the type of borehole heat exchanger
- the depth of the borehole
- the design of tubing and completion of the borehole
- the longtime average of surface temperature and
- site-specific subsurface parameters as the temperature and the specific thermal conductivity of the rocks encountered.

The study is subdivided into six partly interacting processing steps (cf. Figure 9.2-1):

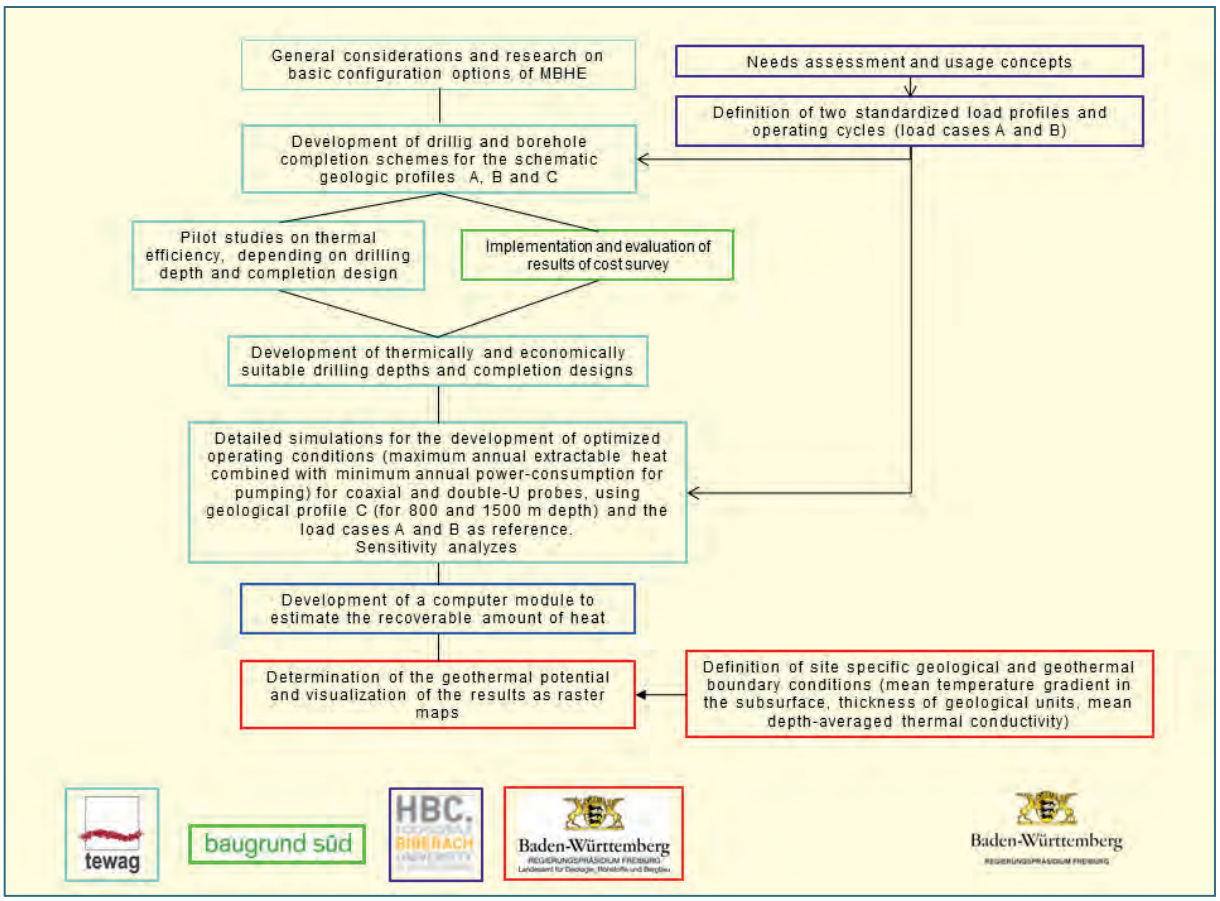

Figure 9.2-1: Flow chart showing the assessment of the geothermal potential of medium-deep borehole heat exchangers in the Lake Constance – Allgäu area (colours of frames refer to the partners and contractors in charge).

- Needs assessment and installation of usage concepts,
- determination of boundary conditions for borehole drilling and completion, cost estimation (e. g. drilling and design of completion, type of borehole heat exchanger, backfilling),

- development of optimised operating conditions,
- development of a calculation module for grid-based, site-related estimation of the quantity of extractable heat for standardised utilisation scenarios,
- determination of site-related geological and geothermal boundary conditions (temperature distribution in the subsurface, geological succession, thermal conductivity), and
- assessment of geothermal potential and visualisation of results as raster maps.

9.2.3 Results

9.2.3.1 Identification of load profiles

Possible users and possible usages of MBHE were identified in the framework of a short study, carried out by the Hochschule Biberach (HBC 2014) on behalf of RVBO. Based on temperatures that can be reached by MBHE in the pilot area in principle all usages up to a temperature level of 50 °C are suitable. The greatest amount of heat can be achieved by MBHE operated as uniform as possible (base load). In addition, an operation system was chosen which is suitable for example for heat supply of residential buildings, representing an important possible user reference. Therefore, two operating scenarios were developed to provide a base load operation (scenario A) and a rather extraction output-oriented operation (scenario B). Due to the low outlet flow temperature level in the considered MBHEs (see Section 9.2.3.2), direct utilisation of the geothermal energy is excluded for both operating scenarios. Therefore, in both cases, rise of temperature level by heat pumps is required.

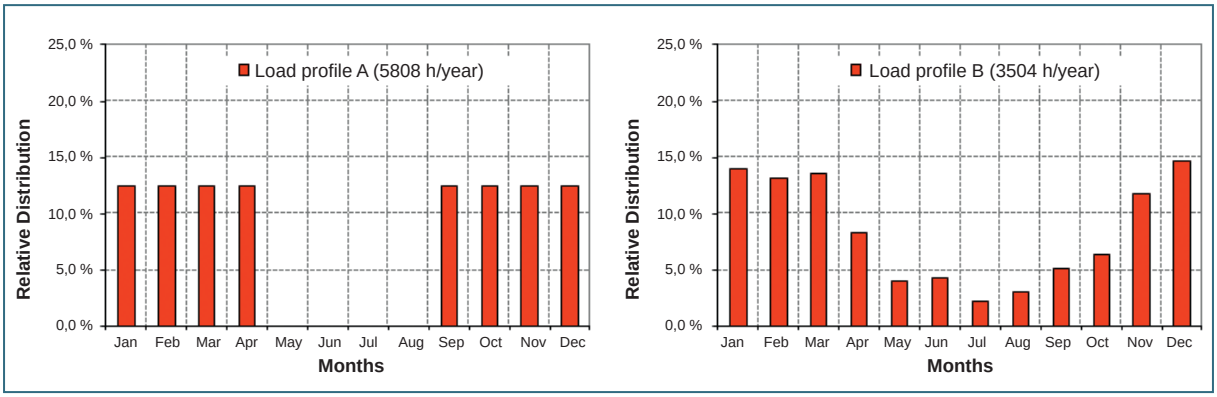

Figure 9.2-2: Load profiles A and B with relative monthly distribution of total operating hours (see text for discussion).

Two load profiles were defined:

- Scenario A describes the continuous operation of the borehole heat exchanger over a period of 8 months (winter and transitional period) and the subsequent regeneration phase of 4 months (summer season) (Figure 9.2-2, left). 5,808 full operation hours per year are equally spread over the annual operation period of 8 months. This scenario represents the coverage of the base load of a local heating network with (residential) buildings or other utilisations at a low temperature level up to an approximate maximum of 50 °C. The objective is to maximise extraction energy.

- Scenario B describes a rather extraction output-oriented operation. In contrast to scenario A, the extraction energy is seasonally distributed. 3504 full utilisation hours per year are spread unequally over the annual operation period (Figure 9.2-2, right). The annual distribution of the extracted

energy is derived from the heating requirement distribution of a detached home which was determined according to VDI (2008) for a newly built house, used by 3–4 people, with a living space of 145 m², an annual heating requirement of 45 kWh/m² and domestic hot water consumption. This scenario represents the multivalent heat supply of residential buildings or a group of it.

The subsequent thermal simulations are based on these two scenarios.

9.2.3.2 Definition of types of borehole heat exchangers and of drilling depths

For further consideration, three schematic geological profiles were derived (schematic geologic profiles A, B and C (HBC 2014). They lie on a geologic cross section, running almost northwest – southeast through the Baden-Württemberg part of the Molasse Basin. Next, casing and completion schematics were developed for these profiles, focusing on the protection of existing groundwater use and deeper, potentially exploitable groundwater resources.

Using the southernmost geologic profile C, preliminary simulations were carried out in order to define thermically and hydraulically efficient variants, depending on basic completion options such as type of the MBHE (pre-assembled double-U or coaxial geothermal heat exchanger or a coaxial probe as a riser pipe, both fully encased and sealed against the subsurface) and depth of the MBHE.

Based on a survey of several qualified drilling companies, the drilling and completion costs for MBHE with construction depths of 500 m to 1,500 m were compiled for the three geological profiles and the three completion variants mentioned above. In combination with thermal efficiency, heat development costs [€/MWh] were derived. This was done by dividing the thermal efficiencies of the defined MBHE types by the drilling and completion costs, depending on depth. On this basis, two basic completion options were finally derived:

- “Coaxial probe”: Installation of a riser pipe made of fibre glass reinforced plastic (GRP) in a fully encased borehole which is sealed against the subsurface (cement foot). Depth of the Coaxialprobe: 800 m and 1,500 m respectively

- “Double-U probe”: Installation of a Double-U probe as geothermal borehole heat exchanger and subsequent cementing of the borehole annular space. Depth of the Double-U probe: 800 m.

9.2.3.3 Definition of optimum operating conditions

Combination of the two load profiles (scenario A and scenario B, see Section 9.2.3.1) with the two types of borehole heat exchangers and the drilling depths (see Chapter 3.2) leads to six reference scenarios. For these, optimised operating conditions, maximum achievable extraction power as well as annual heat extraction were defined by detailed simulations, using the Finite-Difference-Modell SBM (Superposition Borehole Model, Eskilson 1986). This was done by varying the circulating volume flow and the temperature difference at the borehole head (i. e. the thermal extraction power). The simulation aimed at a minimum back flow temperature of +5.0 °C in the probe after 50 years of operation, and at an acceptable energy expenditure for pump operations from the pressure loss (maximum of the net energy recovery as the difference between the annual heat extraction and energy expenditure for pump operations). The optimisation is determined at 1,500 m construction depth at a spread of 5 K at the probe head and at 800 m construction depth at a spread of 3 K at the probe head. Operating conditions and calculated extractable heat are summarised in Table 9.2-1.

At 800 m construction depth, extractable heat by the coaxial probe is higher compared to the double-U probe, both for maximum extraction power in operation (scenario A, 15 %) and for maximum heat extraction output-oriented operation (scenario B, 20 %) (Table 9.2-1). At 1,500 m construction depth, the efficiency of the coaxial probe, operated with scenario A is 200 MWh/a, respectively about 25 % higher compared to scenario B. In contrast, extraction power in operation with the coaxial probe operated with scenario B is 34 kW respectively 20 % higher than with scenario A at the same depth.

Sensitivity studies were carried out to investigate amongst others the influence of different borehole diameters and tubing schemes on the effective thermal borehole resistance. It could be shown, that these parameters do not significantly affect the effective thermal borehole resistance. Therefore, a uniform effective borehole resistance can be used in the calculation module GEO-HAND^{POT} (see Section 9.2.4).

Table 9.2-1: Optimal operating conditions and associated recoverable annual heat extraction heat, using the schematic geologic profile C as reference (“1500 A GFK-COAX”: construction depth 1500 m, operating scenario A, Coaxial probe; “800 B Double-U”: construction depth 800 m, operating scenario B, Double-U probe).

	1.500 A GFK-COAX	1.500 B GFK-COAX	800 A GFK-COAX	800 B GFK-COAX	800 A Double-U	800 B Double-U
Operating hours	5808	3504	5808	3504	5808	3504
Spreading at probe head [K]	5	3	3	3	3	3
Circulation rate [m³/h]	24	30	13	16	11	13
Pressure drop [bar]	4.3	6.4	0.7	1.1	2.1	2.7
Required pump capacity [approx. kW]	4.3	8.0	0.4	0.7	0.9	1.5
Extraction power in operation [kW]	140	174	45	56	38	45
Heat extraction [MWh/a]	811	611	263	196	223	159

9.2.4 Development of the calculation module GEO-HAND^{POT}

The calculation module GEO-HAND^{POT} was developed by HBC for the raster-based assessment of the magnitude of annual heat extraction and the spatial distribution of the annual heat extraction of different completion variants at a specific site (TEWAG 2014). The program is based on the manual calculation method developed at the HBC for shallow geothermal borehole heat exchangers (GEO-HAND^{light}, KOENIGSDORFF 2011).

Maximum extraction power and maximum annual heat extraction can be iteratively calculated for the 6 scenarios, listed in Table , maintaining a minimal fluid inlet temperature of 5 °C in the probes for 50 years. At each calculation point, site-specific, depth-averaged, weighted geological and thermal parameters are considered. For the raster-based computation over large investigation areas, GEO-HAND^{POT} handles given text files in which the values of the necessary geological parameters are summarised for all raster points. The results can be displayed as raster maps for the entire study area.

The validation of the calculation module GEO-HAND^{POT} was carried out on the basis of reference scenarios, calculated with the Finite-Difference-Model SBM (Superposition Borehole Model). A very good match could be achieved with GEO-HAND^{POT} and the SBM simulation results (TEWAG 2014).

GEO-HAND^{POT} can be used only for geothermal potential assessment based on standardised load profiles and types of MBHE which are not influenced by other ground source heat pumps nearby. GEO-HAND^{POT} cannot replace any detailed planning and site-specific design of MBHEs.

9.2.5 Determination of geological and geothermal boundary conditions (geothermal gradient, geologic sequence, thermal conductivity)

As site-specific geological and geothermal parameters, the mean geothermal gradient and the mean thermal conductivity were taken into account. The mean geothermal gradient which is averaged over the respective construction depths of 800 m and 1,500 m is derived from the temperature model built within the framework of GeoMol (Chapter 7). The mean depth-averaged thermal conductivity is based on the 3D geological model (layer sequence and thickness, Chapter 6) and the thermal conductivity of the corresponding model units. The thermal conductivities of the model units were taken from RATH & CLAUSER (2005) and CLAUSER & KOCH (2006). Convective heat transfer by circulating (thermal) groundwater has not been taken into account.

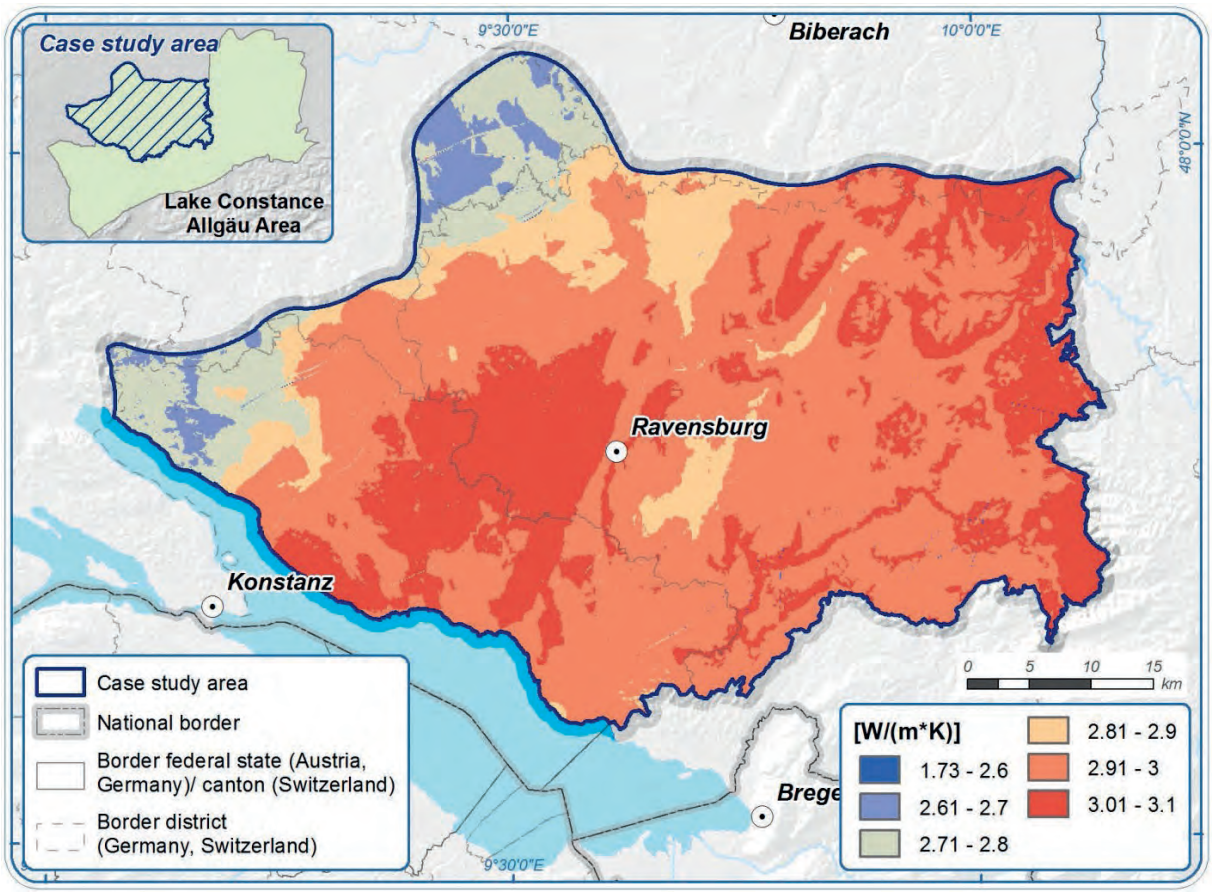

Figure 9.2-3: Spatial distribution of the depth-averaged and weighted thermal conductivity [W / (m * K], construction depth of 1,500 m.

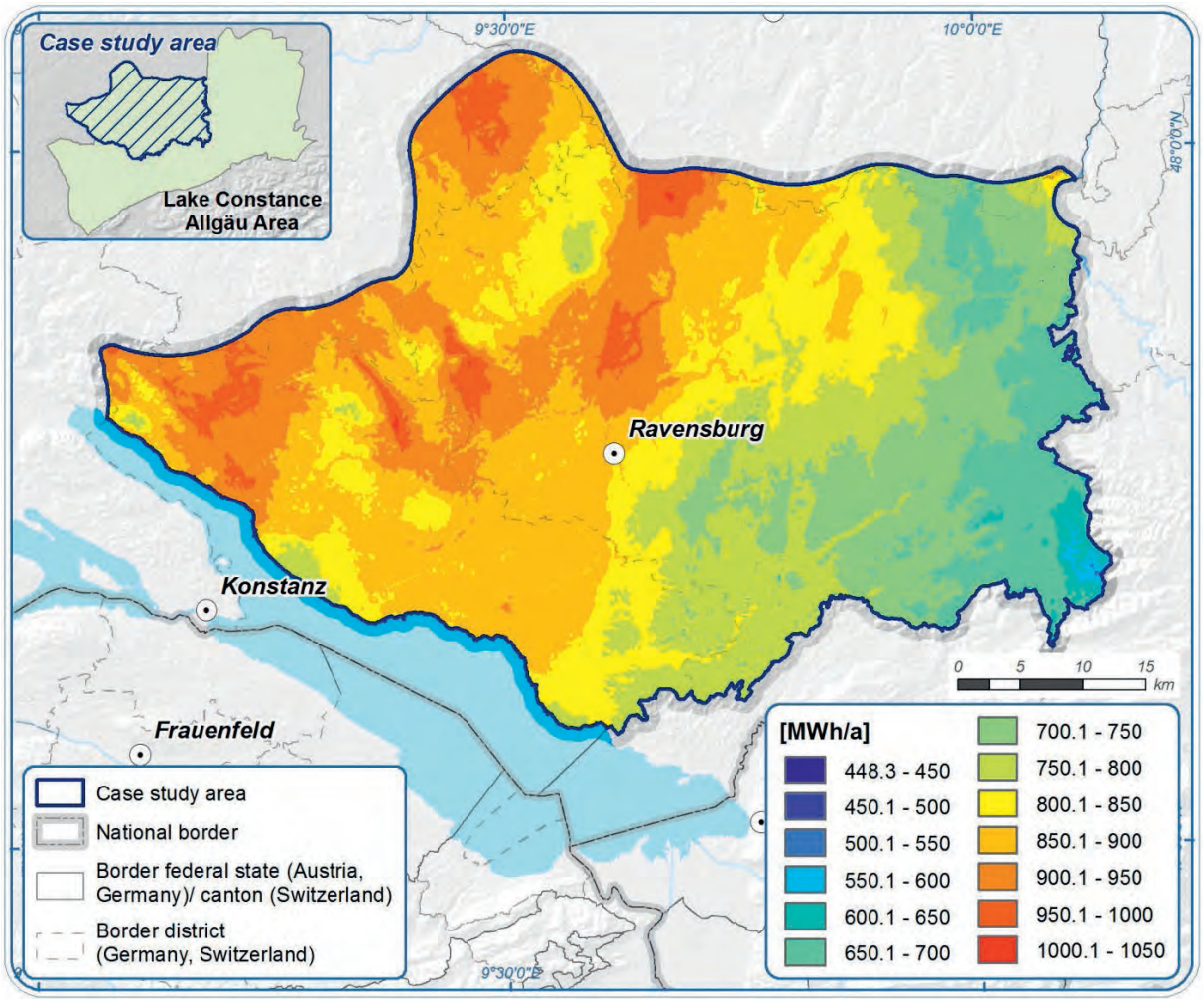

Figure 9.2-4: Raster map of heat extraction [MWh/a], coaxial probe with construction depth of 1,500 m, load profile (scenario) A (note: The results of this study are not suitable for the design of concrete projects, see text).

9.2.6 Assessment of geothermal potential and visualisation of results

Extraction power in operation as well as heat extraction was derived for six standardised scenarios as summarised in Table 9.2-1). The resulting 12 data sets were visualised in raster maps available via the GeoMol Map Viewer (Chapter 10).

As an example, the annual heat extraction [MWh/a] is shown in figure 9.2-4 for the Baden-Württemberg part of the LCA area. The calculation is based on a 1500 m deep coaxial probe and on the load profile A (scenario A, see Section 9.2.3.1). Annual heat extraction is 448 to 1020 MWh/a, with an area average about 825 MWh/a. In Baden-Württemberg, the highest amount of heat can be extracted in the northwestern part of the LCA. Areas with the highest extraction rate coincide with areas in which there are the greatest depth-averaged temperature gradients. Differences in depth-averaged thermal conductivities also become apparent in the amount of heat extraction, however in a smaller extent.

Due to the relatively high drilling costs, MBHEs are not economically viable compared to shallow ground source heat pumps. However, shallow borehole heat exchangers or ground water coupled heat pumps may not be suitable everywhere, for example, they may be inappropriate in densely populated urban areas due to the space required. Ground water coupled heat pumps furthermore may be inapt in areas of insufficient ground water discharge. In such cases MBHE systems could be a worthwhile option.

The assessment of the recoverable amount of heat is based on the conservative assumption of a purely conductive heat transport. In the LCA, (thermal) groundwater had been identified in different stratigraphic horizons: the Upper Marine Molasse, the Upper Jurassic, and the Upper Muschelkalk (Bertleff et al. 1988). If groundwater of these units is encountered by MBHE drillings the efficacy of the probes can be considerably increased by convective heat transfer.

Basically, the method developed in this study can also be applied to other GeoMol areas and beyond if the site-specific geothermal parameters (depth-averaged thermal conductivity, geothermal temperature gradient) are adjusted accordingly. However, the results of this study as well as the developed calculation module are valid only for single MBHEs not impacted by other geothermal installations.

The results of this study are not suitable for the concrete planning of individual projects. For this purpose, project specific user requirements, the demand-driven dimensioning of the MBHE and site specific characteristics of water management and hydrogeological conditions are to be considered.

Drilling techniques as well as design of completion have to be customised project specifically in order to protect the groundwater resources and to minimise risks of drilling.

9.3 The 3D geological model and geopotentials of the Mura-Zala Basin

9.3.1 Introduction and objectives of this case study

The Pannonian Basin is an extensive Tertiary sedimentary basin, which can be considered the retro-Foreland Basin of the Carpathian orogeny – likewise the Po Basin for the Alpine orogeny. The Pannonian Basin is characterised by a major system of Neogene basins resting on a highly deformed and complexly faulted substrate of Mesozoic, Paleozoic, and Precambrian rocks of the Inner Carpathian foldbelt (Dolton 2006).

Shared by many Central and Eastern European countries the basin features a variety of huge and diverse geopotentials – among others, oil and gas deposits, abundant hydrothermal potential, and vast drinking water reservoirs (Dolton 2006, Horváth et al. 2015, Rman et al. 2015). Thus, the sustainable management of the subsurface and the assessment of the Pannonian Basin's diverse geopotentials require a common understanding of the geology and its structures and a clear vision of how to mitigate possible use conflicts, shared by all countries involved. Several transnational assessments for certain issues of sustainable use and resource efficiency have been implemented over the last years within the T-JAM and TRANSENERGY projects (e. g. Fodor et al. 2011, Nador et al. 2013), but these studies, unlike GeoMol, are lacking a tool to visualise the model in 3D and therewith make it more attractive to potential users.

This case study represents an application of GeoMol's methods outside the Alpine foreland basins in a strict sense. It may thus be regarded as a first trial for the transfer of methodology to other deep sedimentary basins. However, the scope of GeoMol – as confined to the Alpine Space Cooperation Area – did not allow addressing these issues in a truly transnational approach also beyond Slovenian territories (cf. Figure 2.1-1). Major work steps of GeoMol such as the harmonisation of the baseline data and the continuous adjustment of intermediate products between adjacent countries could be disregarded. Furthermore, due the legal framework of Slovenia, seismic data have not been available for interpretation and modelling. A major work step of GeoMol's best effort procedure for model building thus could not be applied and tested.

The 3D framework model of the Mura-Zala Basin was developed by the Slovenian WP6 members exploiting the good practice evolved within GeoMol. Model building and geopotential assessment incorporated components of legacy models such as the Bad Radkersburg - Hodoš pilot area of the TRANSENERGY project (cf. Fuks et al. 2013) and of NE Slovenia (Rman 2013).

9.3.2 3D geological framework model

9.3.2.1 Model area and baseline data

The model area covers the north-eastern part of Slovenia, with smaller cross-border areas spreading into Austria, Hungary and Croatia (Figure 9.3-1). The total area of the model sums to about 5,400 km^2, with an E–W extent of 120 km and 90 km in N–S direction. Scale of geological data is 1 : 200,000. Vertically, the model extends to a maximum depth of about 5,000 m, from the surface to the top of the metamorphic rocks which form the basement of sedimentary basin.

As discussed, no seismic data have been accessible for model building. The 3D geological model, thus, is based on log data from deep boreholes and re-interpretations of existing geological models, predominantly in 2D.

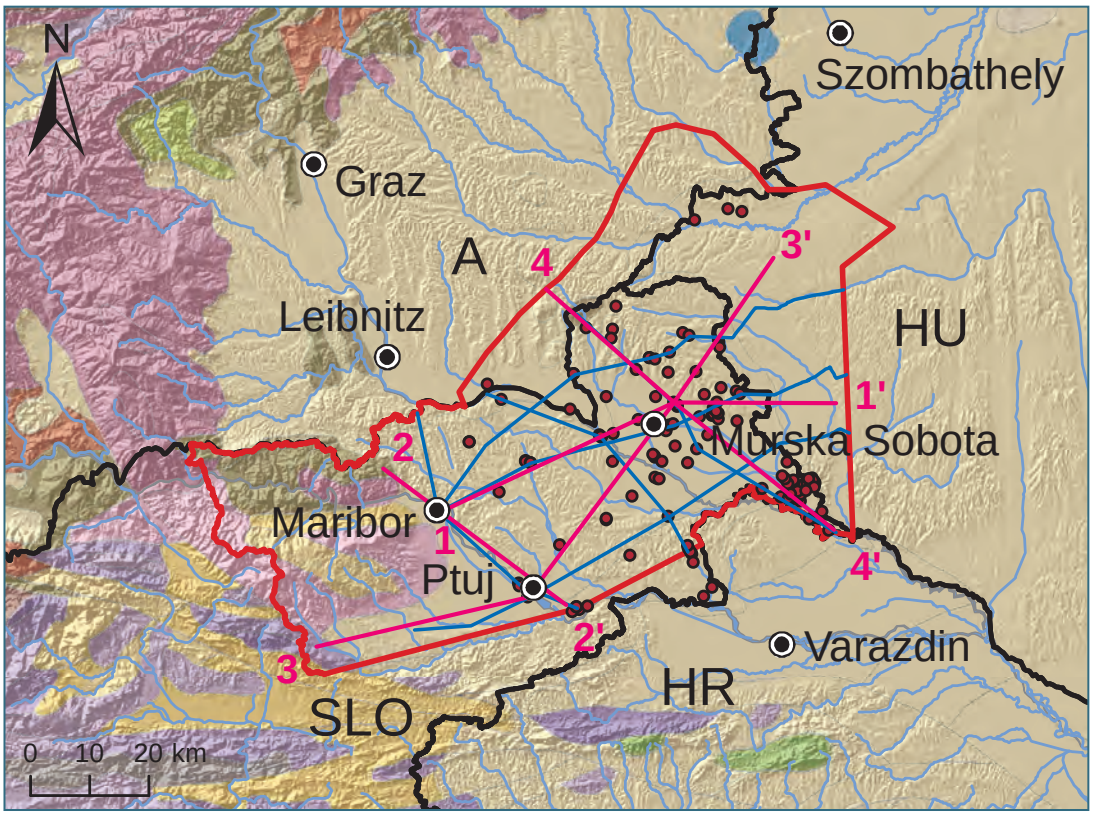

Figure 9.3-1: Outline of the 3D geological model of the Mura-Zala Basin (red line), the location of the borehole evidence used (red dots), the resultant cross-sections representing the model input (blue lines) and the four cross-sections derived from the 3D model (magenta lines) as in figure 9.3-2. Background map: The 1 : 5 Million International Geological Map of Europe and Adjacent Areas (IGME 5000), https://www.bgr.de/karten/IGME5000/igme5000.htm.

Data of overall 150 deep wells have been available, summing up to 325 interpolation points (see Table 9.3-1). The borehole evidence is very unevenly distributed over the model area, clustered in and around urban realms and in areas of higher oil and gas, and geopotential probability. Since high investments are required to drill new deep boreholes, it is rather unlikely that the whole area could ever be sufficiently investigated with a point-to-point approach. Consequently, any assessment of geopotentials is rather difficult to be performed without looking at “the big picture”, e. g. a reliable regional geological model of the subsurface.

Geometries of the geological structure have been re-interpreted using various legacy geological models: the pre-Neogene basement depth model (Lapanje et al. 2007), the 1 : 100 000 scale Basic Geological Map of Yugoslavia and Slovenia (see http://kalcedon.geo-zs.si/website/OGK100/viewer.htm), the litostratigraphic and tectonic structural map of the T-JAM project area at 1 : 100 000 scale (Jelen & Rifelj 2011), geological models of T-JAM (Fodor et al. 2011) and TRANSENERGY (Maros 2012) projects and the model of NE Slovenia (Rman 2013).

9.3.2.2 Model preparation

In the 3D framework model of the Mura-Zala Basin nine lithological units have been distinguished, from pre-Quaternary deposits to the Mesozoic carbonate and Paleozoic metamorphic basement rocks (Table 9.3-1). The interpreted boreholes, 2D spatial information as summarised in figure 9.3-1, and the conceptual model of the basin evolution were used to construct three SW–NW and three NW–SE cross-sections (see Figure 9.3-1), which were the main input for model building.

Based on surface geological maps and borehole data, outcrop lines for each unit have been constructed and sub-crops have been interpolated.

Table 9.3-1: Classification and colour coding of the geological units as distiguished in the 3D geological model of the Mura-Zala Basin. BH*: number of boreholes intersecting the formation.

Formation	Period	BH*	Depositional environment (sediments)
Ptuj-Grad Formation	youngest Upper Pannonian to Pliocene	58	Alluvial plain (predominantly silt)
Mura Formation	top Lower Pannonian to Upper Pontian	91	Delta plain (predominantly silt)
			Delta front (predominantly sand)
Lendava Formation	Upper Pontian	77	Slope (predominantly marl)
	Lower Pannonian		Turbidites (predominantly sand)
Špilje Formation	Middle Badenian to Lower Pannonian	73	Shallow and deep marine (marlstone and sandstone)
	Lower Badenian to Sarmatian		Shallow and deep marine (marlstone and sandstone)
Haloze Formation	Karpatian to Lower Badenian	26	Shallow and deep marine, terrestrial (predominantly marlstone)
Pre-Neogene basement rocks	Paleozoic to Oligocene		Metamorphic and carbonate rocks

For 3D modelling the JewelSuite™ 2014 software was used. Model building was divided in several consecutive stages aimed at the interconnection of (parts of) the legacy models, incorporating available information to close the gaps in between and to update it for a conjunct new model:

- collection and comparison of regional models (or cut-outs) from previous studies,
- harmonisation of the stratigraphic borders for a seamless new model,
- harmonisation of joint lithostratigraphical horizons of the new model,
- update of the model using new well log interpretations,
- construction of cross sections based on data from boreholes,
- digitisation of cross sections,
- preparation of outcrop lines for all formations,
- interconnection of digitised cross-sections and outcrop lines,
- creation of TriMesh from lines,
- update of TriMesh based on borehole data,
- alignment and update of all information according to surface geological maps.

The resulting model is a flying-carpet model depicting the elevation and superordinate structures of the base of each lithostratigraphical unit. Due to lack of seismic sections and other data on the structural inventory, the fault network could not be considered. Some of the flexures or stairs-like structures identifiable in the model could also be assigned to displacements along fold plains. With respect to the assessment of geopotentials, many of them bound to structural traps, this is certainly the principal limitation of the model. The 3D model can be visualised in the GeoMol 3D-Explorer.

9.3.2.3 Results of the model

Even though 3D geological situations are difficult to be visualised in 2D, results of the Mura-Zala Basin geological model are portrayed as four cross-sections in various directions (Figure 9.3-2). Figure 9.3-3 provides a 2.5D insight into the Mura-Zala Basin by unveiling the deformed top of the pre-Neogene basement and displaying the structure of the basin-fill by means of a fence diagram.

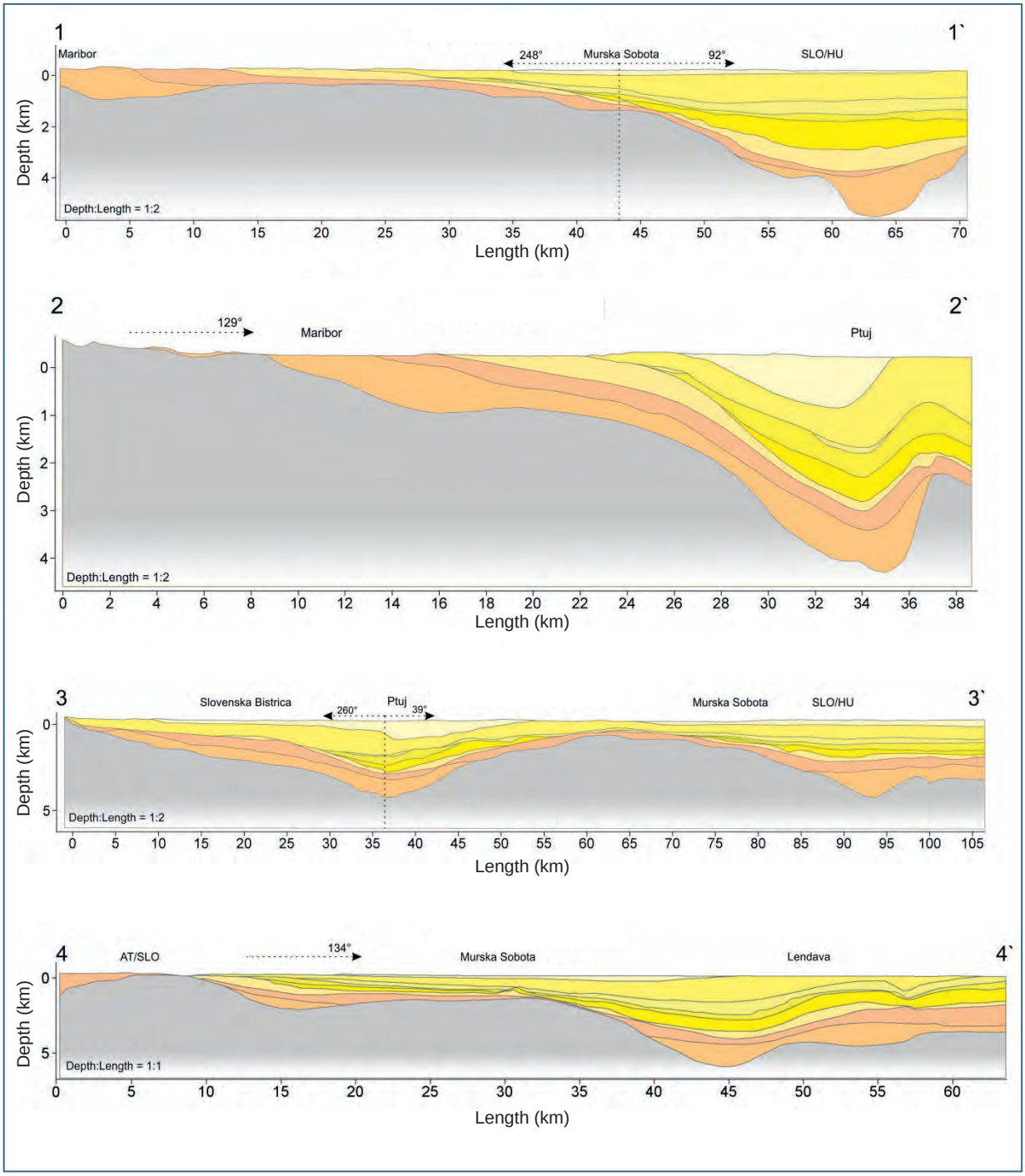

Figure 9.3-2: Cross-sections through the Mura-Zala basin (for the direction of the sections see Figure 9.3-1, for colour coding refer to Table 9.3-1). Note the different scales – cross-sections 1, 2, and 3 are 2x vertically exaggerated. Arrows indicate the azimuth.

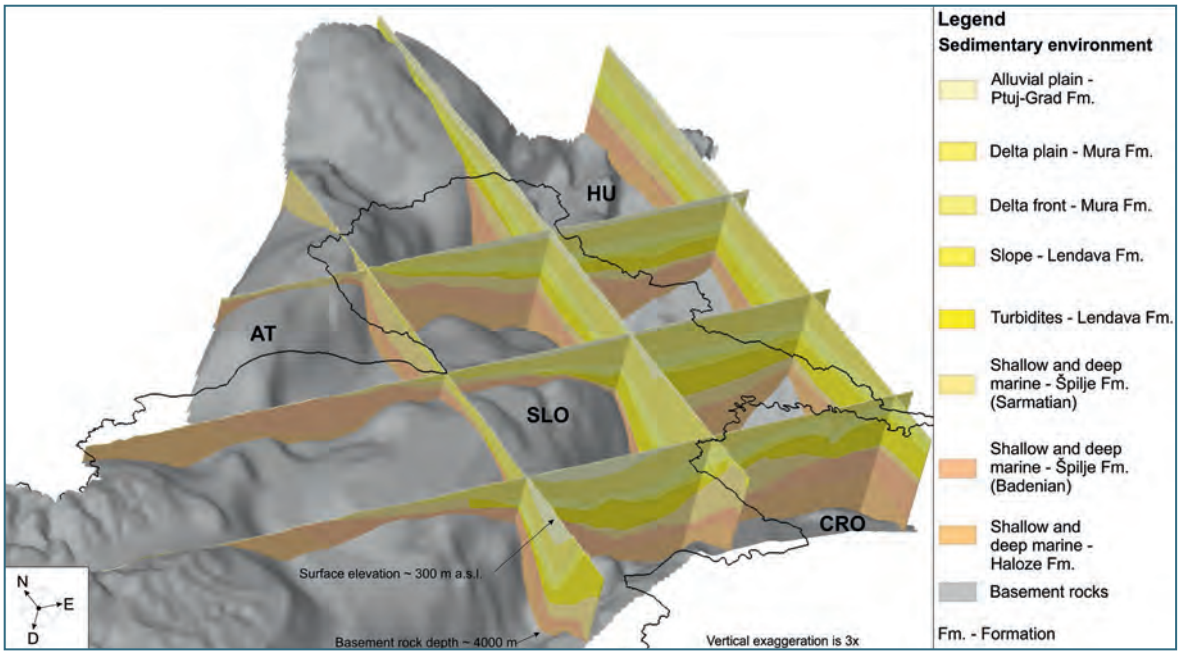

Figure 9.3-3: Perpendicular fence diagram of the basin fill superposed on the deformed sub-crop of the pre-Neogenic basement beneath the Mura-Zala Basin, perspective view from southwest.

9.3.3 Geopotential assessment

9.3.3.1 Oil and gas

The Slovenian part of the Pannonian Basin is considered mature in terms of conventional hydrocarbon exploitation, but with one concession for oil production (Dolina) and one for gas production (Petišovci, cf. Figure 9.3-4) left (Štih et al. 2014). New conventional discoveries are unlikely thus shifting the focus of exploration towards unconventional targets. However, any new prospects weather on conventional or on unconventional targets must be based on geological models considering the structural inventory in detail. The unavailability of seismic data to the national GSO is a fundamental impediment to the evaluation of the hydrocarbon potential as well as other geopotentials dependent on subsurface structures.

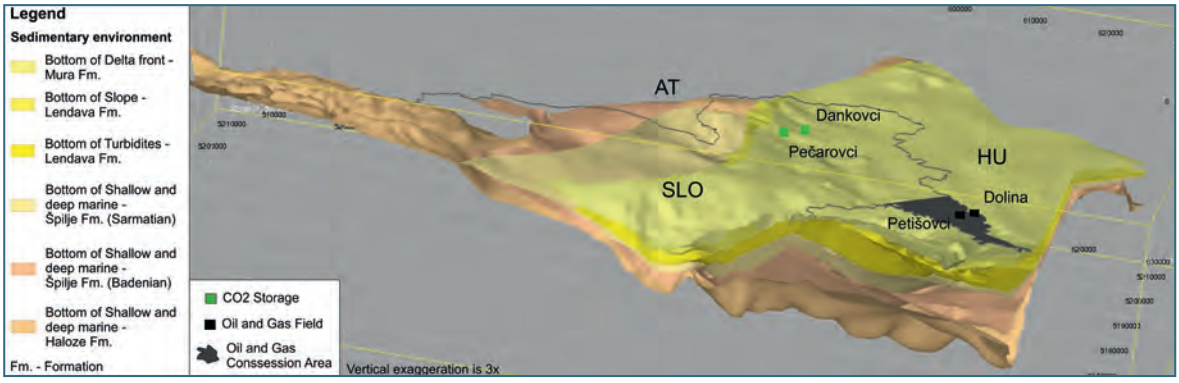

Figure 9.3-4: Perspective view of the Mura-Zala Basin from southeast showing the extent of the Lendava and Špilje formations turbidites, potential horizons for hydrocarbon production and CO_2 storage (CCS).

9.3.3.2 Gas storage and CO_2 sequestration

A very similar approach as implemented in Switzerland (Diamond et al. 2010) and Germany (Müller & Reinhold 2011) has been applied in Slovenia within the scope of the project "Possibilities for geological storage of CO_2 in Slovenia and abroad" in 2011 (Archives GeoZS). Principal findings are that three possibilities of CO_2 storage exist in Slovenia: saline aquifers, depleted oil and gas deposits and coal seams, but all are very limited. CO_2 storage in coal seams was found to be not feasible, due to adverse compositional alteration of the coal beds. Saline aquifers, basically, show a high potential for CO_2 storage due to their regional extension, totalling 92 Mt of CO_2 storage capacity (Eu Geocapacity Consortium 2009). However, a use for CCS is ruled out because of the aquifers' extensive exploitation for thermal water production. Depleted or partially depleted oil and gas deposits represent the most prospective structures for CO_2 storage. Two such fields, Doline and Petrišovci, are located in the north-eastern most part of Slovenia (green squares in Figure 9.3-4). CO_2 injection could be used for enhanced oil recovery which considerably decreases the costs of the system – but both fields have quite limited capacity.

9.3.3.3 Temperature potential

The Pannonian basin as a retro-foreland basin has not been affected by crustal thickening driven by the orogenic processes as in pro-foreland basins (Naylor & Sinclair 2008). Due to the thinner Earth's crust the heat flux of the Pannonian Basin is considerably higher than e. g. in the North Alpine Foreland Basin. The average geothermal gradient in the Pannonian Basin is about 3.6 °C/100 m, and in places well exceeds 5.8 °C/100 m (Dolton 2006).

The entire Slovenian part of the Pannonian Basin represents the regional geothermal anomaly, featuring geothermal gradients up to 8.5 °C/100 m. Formation temperature distribution maps were prepared on the basis of in-depth temperature measurements in boreholes and clearly show the highest temperature at depth towards the east, at the Slovene-Hungarian border (Figure 9.3-5).

Elevated geothermal gradients occur due to the shallow depth of the metamorphic rocks and convection zones in these fissured rocks. At 500 m depth temperatures up to 52 °C have been measured while at 1,000 m depth they reach more than 65 °C at maximum, both due to free convection. Temperatures at 1,500 m are mostly between 60 and 75 °C but may reach up to 95 °C. The highest temperatures at 2,000 m depth are 115 °C, and up to 125–135 °C at 2,500 m depth. At 3,000 m depth the highest temperatures, up to 160 °C, are expected again close to Hungarian territory.

Depth contour charts for formation temperatures of 60 °C and 100 °C – commonly referred to as thresholds for direct use in district heating resp. electric power generation – as well for 150 °C, show the most promising thermal anomalies. The minimum depth to reach temperatures of 60 °C, at less than 0.8 km, is located around Benedikt, between Maribor and Murska Sobota (cf. Figure 9.3-6, top). Minimum depths to reach 100 °C, at less than 2 km, are found north and south of Murska Sobota and around Lendava along the border with Hungary. The later applies also for 150 °C with less than 3.5 km, and even less than 3 km in a smaller area (Figure 9.3-6, bottom).

Possibilities for implementation of EGS systems for binary or direct electricity production (Rajver et al. 2012) have been identified in areas with higher temperatures at reasonable depths of 4 to 5 km (Figure 9.3-7). Because rather low permeable rocks are expected there, hydrofracturing would be needed to develop a successful geothermal loop.

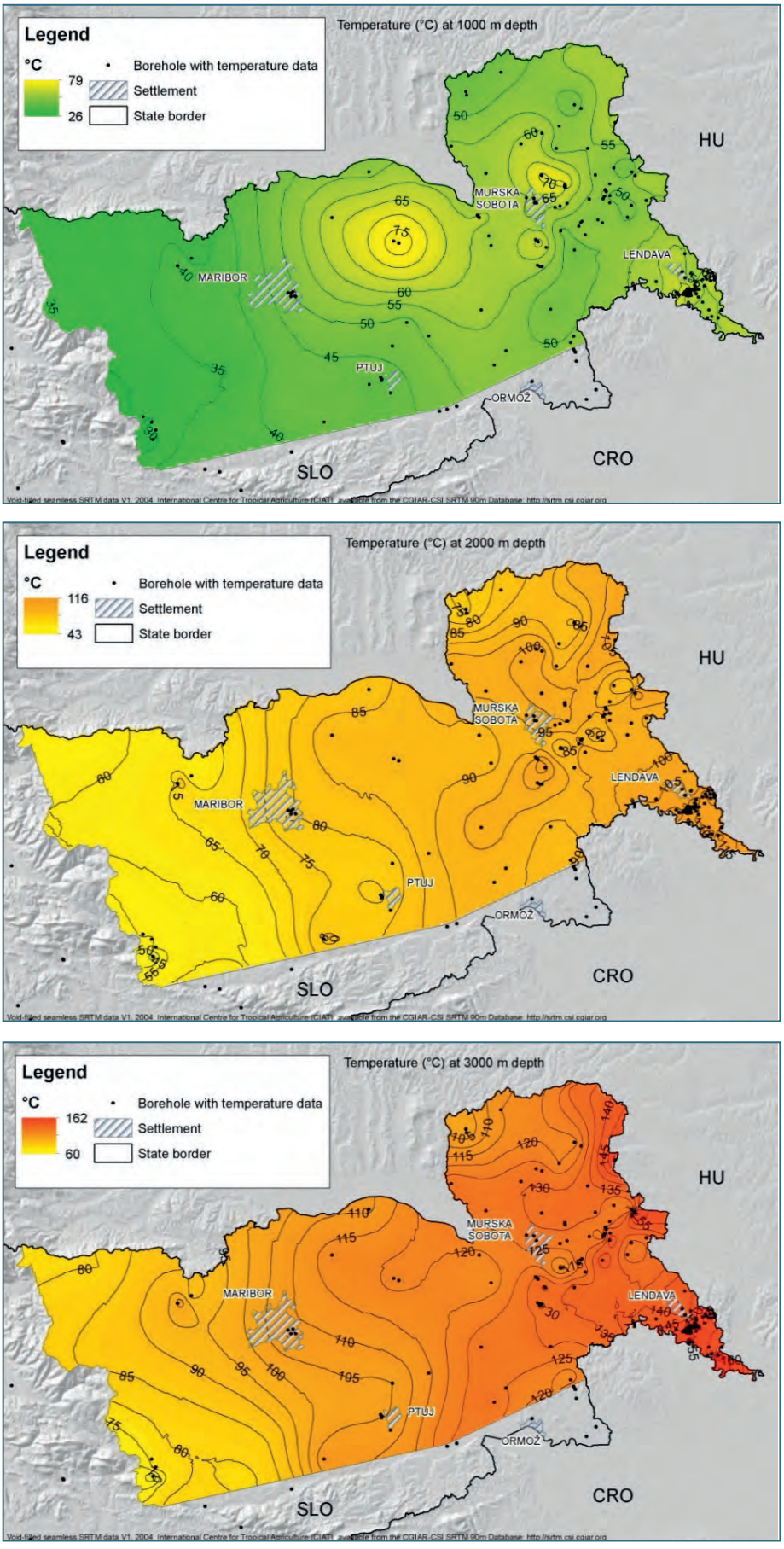

Figure 9.3-5: Temperature distribution in the Mura-Zala Basin at 1,000 m (top), 2,000 m (centre) and 3,000 m (bottom) depth.

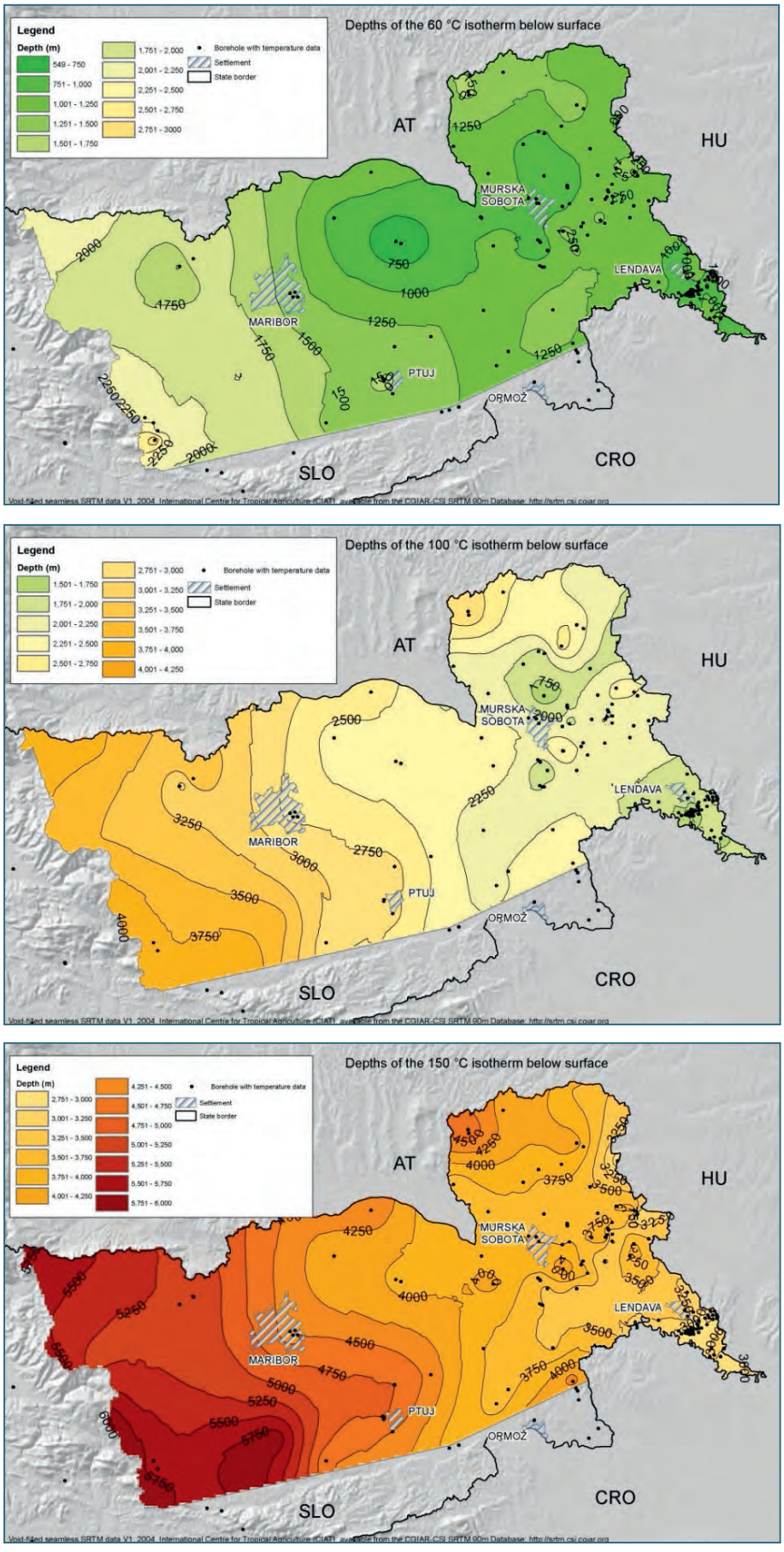

Figure 9.3-6:
Depth below surface of the 60 °C (top), 100 °C (centre) and 150 °C (bottom) isotherms in the Mura-Zala Basin.

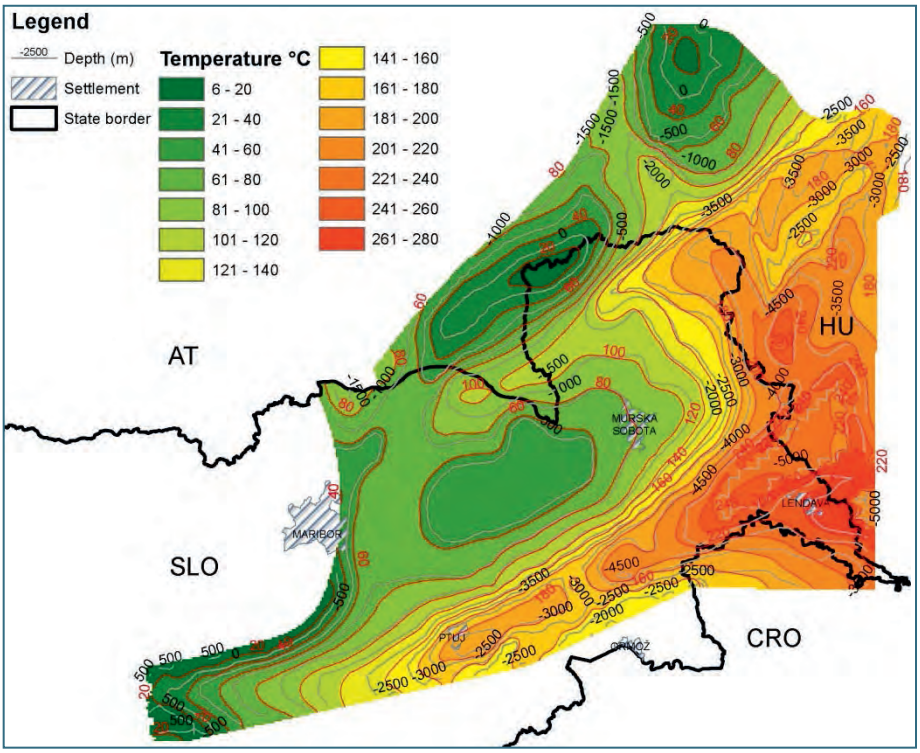

Figure 9.3-7: Simulated temperature at top of the Pre-Neogene sedimentary sequence with depths of basement rocks (FEFLOW 6.2 heat and flow model)

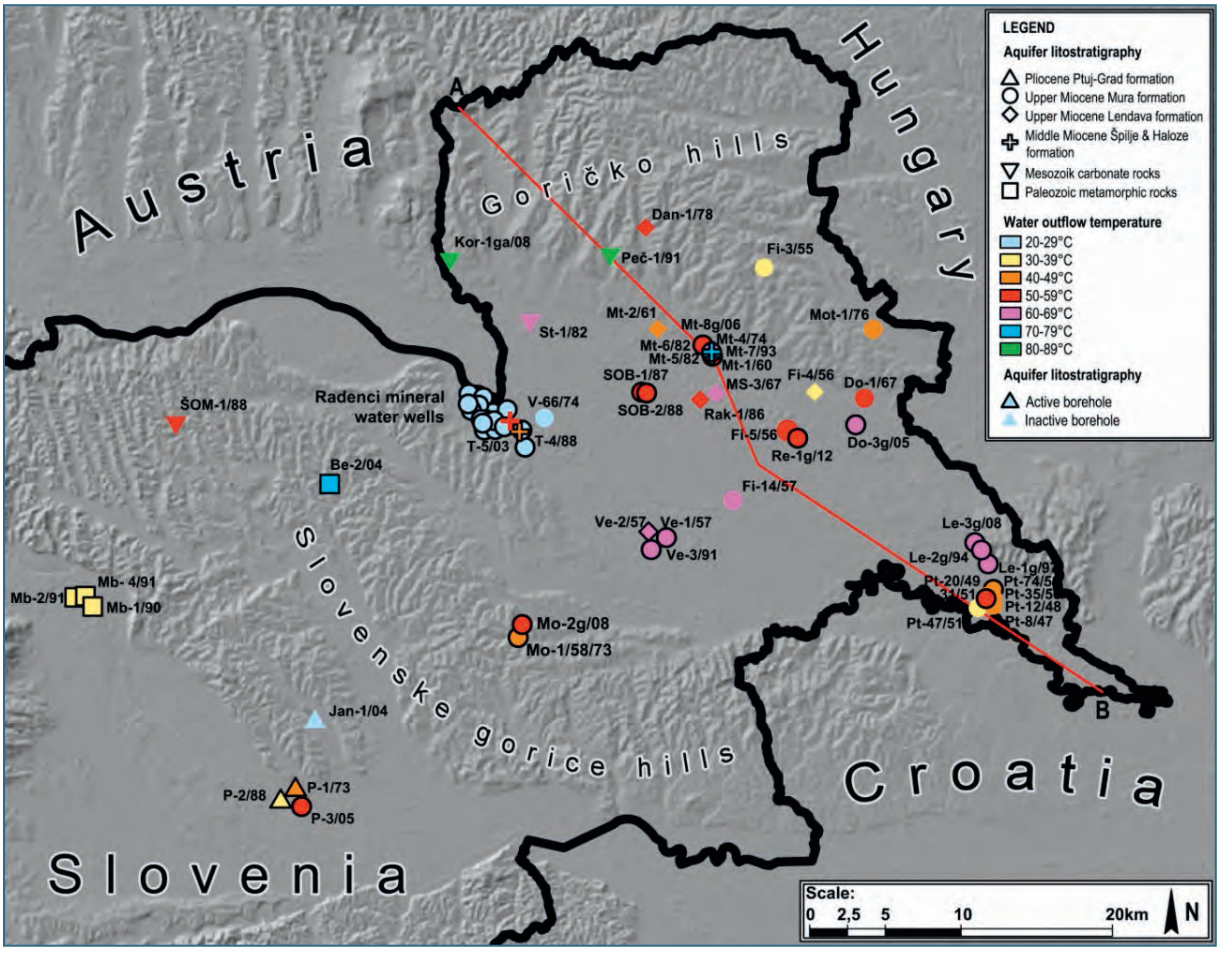

Figure 9.3-8: Active and inactive geothermal wells in north-eastern Slovenia (from RMAN 2014)

9.3.3.4 Hydrogeothermal potential

In 2014, there were 20 geothermal wells taping the Neogene geothermal aquifers producing thermal water (T > 20 °C) and one for reinjection (Figure 9.3-8). The highest annual production comes from the Mura formation, 2.4 Mm^3, followed by slightly colder water from the Ptuj-Grad formation, 0.26 Mm^3, and 0.17 Mm^3 of thermomineral water from the Špilje formation (Figure 9.3-9). Annual abstraction from basement rocks in Zreče, Maribor and Benedikt sums to approximately 0.18 Mm^3. Produced quantity does not vary much over the years since poor development has occurred recently, however, trends show that space heating of greenhouses and district heating systems are getting more attractive. According to the concession applications, a two to three-fold increase is foreseen in the produced quantity for different aquifers, and total legislative potential sums to approximately 5.5 Mm^3. Technical potential of existent active and inactive wells is evaluated to be approximately 7 Mm^3. Hydrogeological potential has been calculated only for the Mura formation aquifer where it sums to approximately 1.3 Mm^3 per year. Additional abstraction rates would have to be reinjected back in the aquifer to enable its sustainable exploitation. More information is given in articles of RMAN et al. (2011, 2012, 2015), RMAN (2014), NADOR et al. (2012) and reports of T-JAM (http://en.t-jam.eu/domov/) and TRANSENERGY (http://transenergy-eu.geologie.ac.at/) projects.

Temperature distribution in geothermal aquifers is favourable for direct use: geothermal heating systems and balneological use. Temperature at top of the regional and trans-boundary Mura Formation delta front sands is expected to be between 45 °C at 500 m depth and 90 °C at 1500 m depth (Figure 9.3-9). Due to thickness of the sediments it increases from 70 °C at 1000 m to 136 °C in the deepest parts at about 2500 m depth.

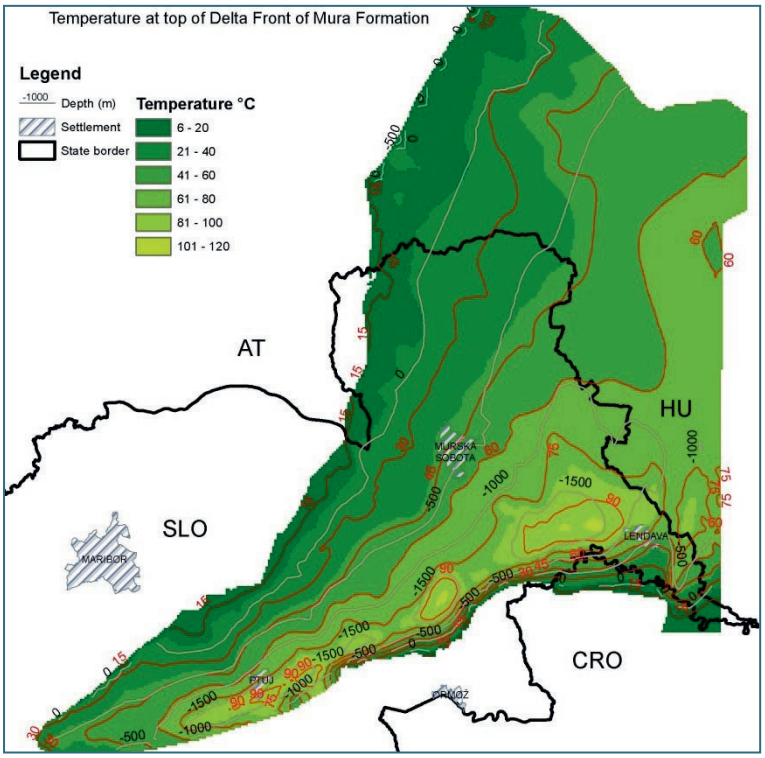

Figure 9.3-9: Simulated temperature at top of the Mura Formation delta front sands with depths (FEFLOW 6.2 heat and flow model)

9.3.4 Summary of the geopotential assessment and the 3D model building

Geopotentials available in the formations of the Mura-Zala basin as considered in this study are summarised in Table 9.3-2. This synopsis, however, is based on the overall rock composition and the formation temperatures at suitable depths only and does not take in account the structural features that are essential for the appraisal of volumes and capacities of the reservoirs as well as for seal integrity. The factual suitability and appropriateness thus has to be proved by detailed structural models on a local scale.

Table 9.3-2: Compilation of the theoretical geopotentials in the formations of the Mura-Zala Basin

Unit	drinking water	balneology	direct heating	power generation	oil and gas production	coal production	natural gas storage	CO_2 storage
Quaternary *(not included in 3D model)*								
Pliocene Ptuj-Grad Formation								
Upper Pannonian Mura-Formation delta plain silt								
Upper Pannonian Mura Formation delta front sand								
Lower Pannonian Lendava Formation sandstone and siltstone								
Middle Miocene Špilje Formation sandstone and siltstone								
Lower Miocene Haloze Formation siltstone								
Mesozoic carbonate basement rocks								
Paleozoic metamorphic basement rocks								

unit contains layers with geopotential

unit possibly contains layers with geopotential

unit contains no geopotential

The three-dimensional framework geological model of the Slovenian part of the Mura-Zala sub-basin represents a starting point for future evaluations and decision making of developers, users and managers of the subsurface. New utilisations of geopotentials (e. g. CO_2 storage, gas storage) that are competing with existent uses such as drinking and thermal water or oil and gas production can now be delineated and evaluated in their true spatial setting. By visualising the spatial distribution of the main lithostratigraphic units which host the different potentials, the focused yet harmonised subsurface management eventually becomes an achievable goal.

10 Distribution of results

All information provided by GeoMol, textual as well as spatial, is available on the Internet. Central access point for this information is the website www.geomol.eu. In line with the funding programs regulations for appropriate and immediate information and publicity it was launched at the very beginning of the project implementation in November 2012. Continually developed and enhanced since then, it now holds available all channels of information for the different product lines designed for different stakeholder groups and for raising the awareness of the general public. Implemented incrementally since June 2014, the GeoMol website now features the access to the 3D-Explorer as a browser-analyst for visualisation, for query of open source 3D geological models and the web map service (WMS) for dissemination of the project's "of-the-shelf" spatial 2D products, either derived from the 3D models of the expert live system. To ensure that GeoMol's outputs are immediately usable by the cross-domain community addressed, the live system's information has been converted into ready-to-use products customised to the users' needs as defined in the stakeholder survey (Chapter 3.1).

For the dissemination of GeoMol's products several web-based channels are provided:

- the **GeoMol Website** as the online library for all textual information such as PDF documents of reports, guidelines and scientific publications and the hub for all web applications (Chapter 10.1),
- the web application **3D-Explorer** for web based visualisation and interactive analysis of 3D geological information (Chapter 10.2),
- the web application **MapViewer** for web based visualisation and interactive analysis of ready-to-use 2D thematic maps (Chapter 10.3),
- the **SearchCatalogue** as a web application for providing information on the availability of spatial data, access to services and restrictions of use (Chapter 10.4),
- **GeoMol's web map services** for the integration of 2D thematic map information into Desktop GIS and in external web applications (Chapter 10.5).

In addition to the web-based dissemination of products, this Project Report and the reports on the pilot areas in the respective national languages will be provided as printed media in publication series and via dissemination channels of the respective GeoMol partner states (Capar et al. 2015, GBA 2015, GeoMol Projektteam LCA 2015, ISPRA 2015, Šram et al. 2015).

10.1 The GeoMol Website

Released in November 2012 on occasion of the Kick-off Conference and incrementally adapted and extended with new features developed within the project, GeoMol's website www.geomol.eu serves as the public hub for information on the project's objective, scope and reach as well as its progress and events. General information on the topics covered by the project, like the explanation of principal geopotentials, is provided in all national languages of the partner states. Technical issues are addressed in English, including the project papers as published in scientific publication series and congress proceedings (http://www.geomol.eu/home/technique/). The website also holds available the presentations of all major GeoMol information events, the Kick-off Conference, the Brussels Information Day, and the Mid-term Conference (http://www.geomol.eu/events/).

Furthermore, the website provides access to GeoMol's web applications. The responsive web design ensures easy browsing on PCs as well as on mobile devices.

Figure 10.1-1: The GeoMol Homepage (www.geomol.eu) as the initial address for all web-based information channels of GeoMol.

All documents related to project results and designed for download and print as PDF documents are made available in the section “Products”, comprising the Project Report with maps, stratigraphic charts, explanations as well as guidelines. Web applications for the interactive use of GeoMol’s spatial data can be accessed via the sections “3D-Explorer” for 3D data and “MapViewer” for 2D data including the sub-section “SearchCatalogue” which enables users to search and browse for spatial data and web services and to retrieve information on possible restrictions for the use of data.

10.2 The GeoMol 3D-Explorer

The use of classified data for 3D model building and the legal constraints with respect to data policy in the project’s member states (Chapter 3.3) imposed particular requirements on the distribution of the 3D geological information prepared. Access restrictions due to data protection regulations require that all 3D models of the expert system have to be stored and maintained at the legally mandated regional or national GSO and may be made available for authorised users only. Only 3D models cleared for open access can be visualised via the public login of the 3D-Explorer. This clea-

rance is subject to the national data policy and has to be implemented at GSO in charge. Thus, a distributed organised system is necessary for both, the seamless visualisation of public domain models as well as the fusion of the "national" parts of the expert system. However, at the outset of GeoMol no adequate tool was available to gather, merge, and distribute multi-dimensional geo-information of different sources constrained by diverse database systems and software solutions. The geological community then lacked the ability to exchange 3D geological data efficiently across the diverse systems (see DIEPOLDER 2011) and to present them in an overall picture merged from different national repositories. A key objective of GeoMol was thus, to build up a software-independent infrastructure for multi-dimensional geological data ensuring full interoperability among the partners in order to provide cross-border harmonised information.

10.2.1 The requisite behind the scenes – the GST 3D data base

Core of GeoMol's IT developments – invisible for the user – is a hub which allows for linking the proprietary data stores of the GSOs. Via this hub the 3D models (or spatially restricted portions thereof) can be merged, and visualised and queried exploiting the functionalities of the web portal (see GIETZEL et al. 2014). GeoMol's hub for the share and exchange of multi-dimensional geo-information is based on a software development called GST, **G**eo Sciences in **S**pace and **T**ime (GABRIEL et al. 2011). Developed initially for the ProMine project (http://promine.gtk.fi/) at the TU Bergakademie Freiberg it was extended, refined and customised to the project's requirements and the partner's proprietary IT environments.

Major technical characteristics and principal features of GST have been described previously (DIEPOLDER 2011, GABRIEL et al. 2011). The fundamental object-relational data model has lately been published in detail (LE et al. 2013). In summary, GST's objective is to give access to, visualise and organise geo-objects using open standards, aimed at the generation of geo-models which use thematic geo-information gathered at various scales to store and visualise the key spatial, geological, geophysical and geochemical parameters. A major issue is the management of large models, e. g. GeoMol's framework model, and the ability of 3D tiling into spatially restricted models with refined resolution, e. g. models of GeoMol's pilot areas. The object-relational data model allows an easy integration of existing metadata models into the newly developed 3D environment.

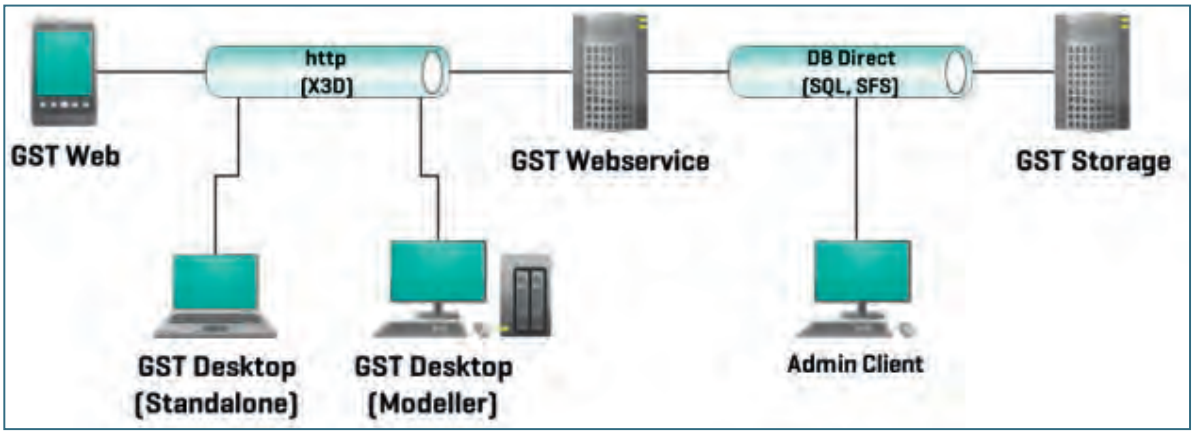

Figure 10.2-1: General three tier architecture of GST. Separating the data tier (right) from the presentation tier (left), the internal and external communication is based on existing standards like SQL, SFS, HTTP and X3D, thus enabling the use of other system and replace components.

GST is based on simplex structures, allowing to store pointsets, linesets, facesets (where a face is a single triangle), and tetrahedron sets, thus enabling to store geo-objects that originate from geo-modelling software like GoCAD, Petrel, Move or AutoCAD. Additionally, properties can be attached to the objects, stored either on a vertex level or a cell level, which means e.g. that a triangle network has a property stored for each triangle. The stored geometries are conveyed via the OGC standard Simple Feature SQL (SFS) (OGC 2011) ensuring that not only the developed client software can be used to retrieve the data, but any client understanding SFS can be used for access to the database. The basic principle of GST is to model classes, e.g. surfaces or faults. These classes are made up of one single basic type, e. g. triangle network. Each class has its own properties which could be of any data type supported by the involved database system. The properties can be discrete, e. g. rock type, or continuous like porosity. GST enables the user to query just the geometry as SFS or to query the properties without any geometry or, of course, to retrieve both, geometry and property. Thus, GST comprises some basic GIS functions like the query of specific objects with a particular property.

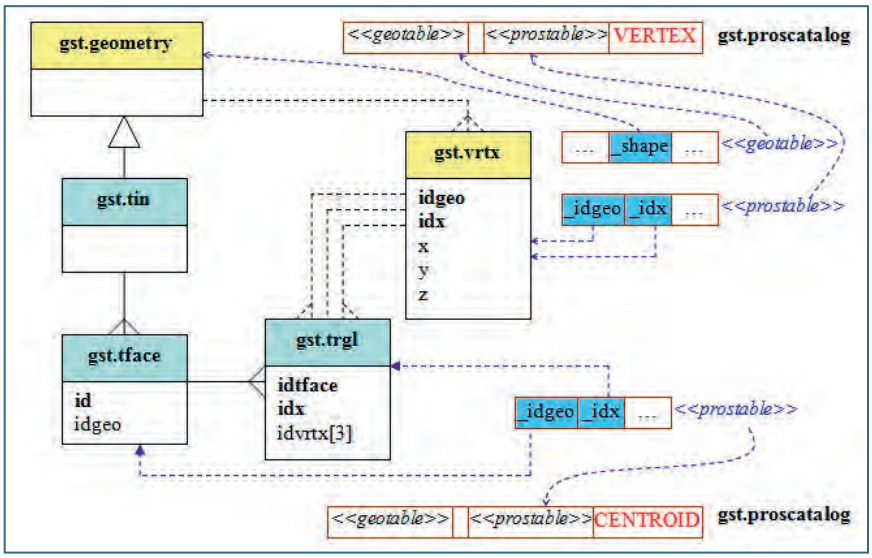

Figure 10.2-2: The internal structure of a triangulated irregular network (TIN) object in GST v.0.1 (from GABRIEL et al. 2011).

As discussed in chapter 3.3, the legal constraints of national data policies imposed special requirements on the share of the information provided. As a stringent necessity a role based login system has been developed for the restricted access data including a group management tool for the case-controlled share of data among defined user groups. Thus it is possible for each GeoMol partner to maintain a pool of private data but also to share cleared sets with the project partners and entitled third parties or to provide open access data for the general public. Based on this approach GST enables each data provider to define the visibility and retrieval of their data in line with the applicable regulation.

A further concern in multinational projects is the coexistence of different coordinate reference systems used by the partners. In order to facilitate the handling of datasets originating from different coordinate reference systems GST has introduced a coordinate transformation which allows the distortion-free transformation of almost any coordinate reference system compliant with the seven parameter definition using the so called *Helmert* or seven-parameter transformation. This allows e. g. models from the different pilot areas of GeoMol, stored in different coordinate reference systems, to be portrayed within one viewer component.

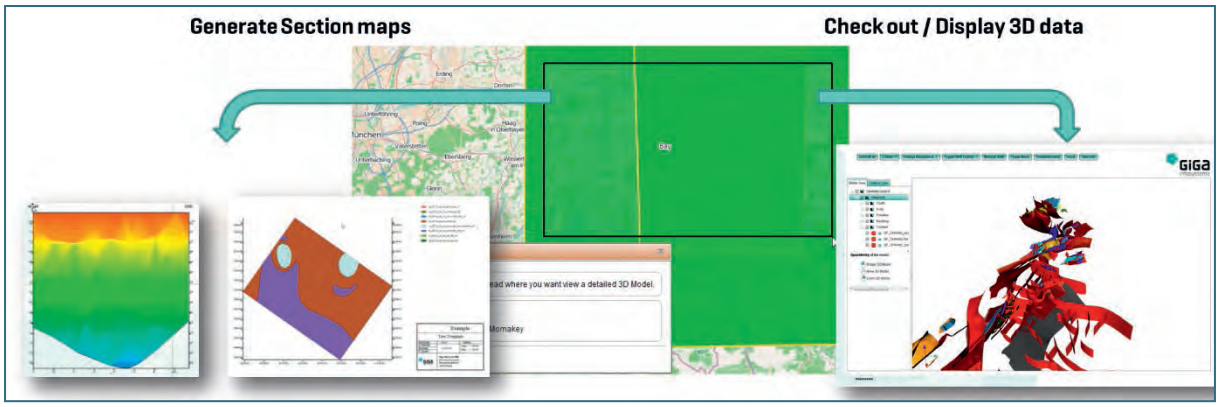

Figure 10.2-3: Subareas of complex models can be selected using the 2D web mapping application (centre), for appropriate and efficient visualisation. A modelled property like temperature can be displayed in vertical cross-sections as well as in generating 2D maps at a given depth (left). The selected portion of the 3D geo model within the box can be visualised as an interactive WebGL scene (right) without any additional visualisation software.

10.2.2 The visualisation and query tool

In May 2014 GeoMol's 3D-Explorer has been officially introduced through release of the beta-version on occasion of the Mid-term Conference. This innovative development allows exploring 3D geological models in ordinary web browsers without the need for installing plug-ins. However, this web application is using the WebGL (Web Graphics Library, https://www.khronos.org/webgl/) technology and requires a web browser that is capable of handling WebGL contents (e. g. Firefox, Chrome, Opera or Safari). The data that can be visualised via the 3D-Explorer may be a set of base and top horizons ("flying-carpet" models), faults, point data, and volumes.

Depending on the classification of the data two different modes of access to the 3D-Explorer are provided: the public login for all open source information and data rendered anonymous, and the password-protected login for classified information according to the legal requirements in the country of origin and the providing GSO.

The public account holds available all information that has been earmarked as public domain by the data provider. Authenticated users such as the GeoMol partners can retrieve all data and are entitled to change the data of their domain according to the authorisation defined by unique credentials.

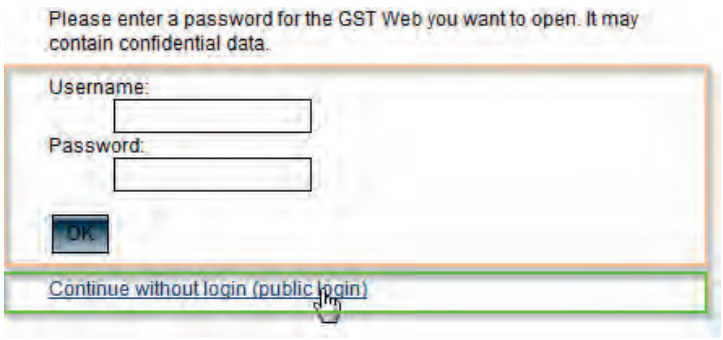

Figure 10.2-4: The two different modes of access to the 3D-Explorer. The public login (link in the green box) provides access to all public domain information and does not require any username or password. The access to classified information requires the user group intrinsic authentication using unique credentials (beige box). Country specific licensing systems for geo-data (e. g. www.geolizenz.org) may be integrated into this restricted access login.

These user groups may also upload data to the GeoMol 3D-Explorer and may set up the access rules for these datasets.

The data sets being displayed in the viewer are delivered directly from the GeoMol 3D-Explorer based on the GST 3D data base (see Section 10.2.1). It allows the user to select the data dynamically and to edit the data in the preferred spatial reference system by coordinate transformation on the fly. The web viewing component enables selecting any available 3D data individually or grouped into models comprising several objects according to geographical or thematic criteria.

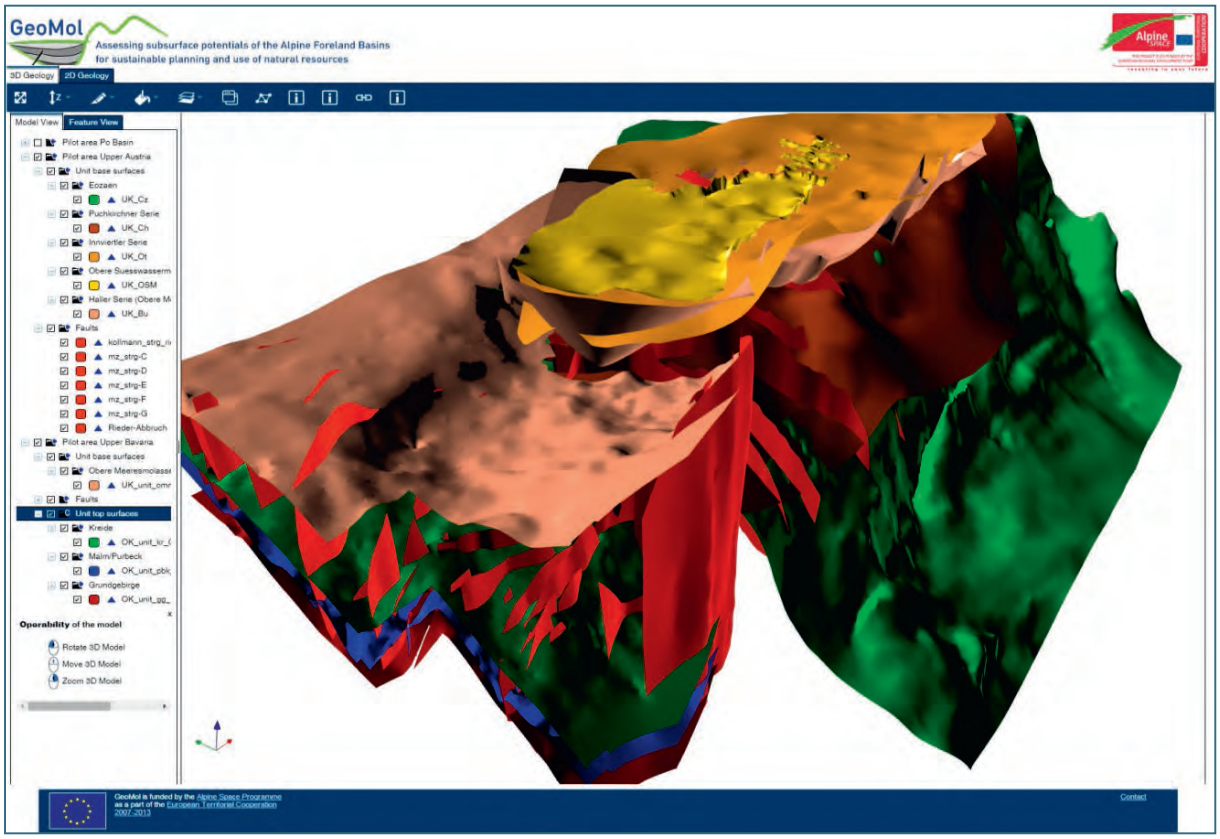

Figure 10.2-5: Screenshot of the GeoMol 3D-Explorer (beta version as of March 2015) showing the user interface of the Upper Austria – Upper Bavaria pilot area. In the main window the surfaces and faults of the model are displayed as an interactive real time 3D view. On the left panel the interactive legend can be used to toggle individual 3D objects. The top bar provides tools to browse and modify the 3D scene (e. g. exaggerating the z-scale) and allows for switch to the 2D mode (Tab “2D Geology”).

To facilitate the users’ orientation within a 3D model the viewer provides the option to display topographic maps (Figure 10.2-6) exploiting the web map services (WMS) of external sources. A choice of predefined WMS is hold available, but basically all WMS can be integrated and used accordingly. The coordinates of the cursor position and the current spatial reference system are displayed beneath the legend (Figure 10.2-7).

By exaggeration of the z-scale the 3D-Explorer enables exploded views of the model thus facilitating the insight into the models’ internal structures and the textures of the layer surfaces. The viewer also offers the feature to slice though the model for revealing the geological set-up in a series of arbitrary cross-sections.

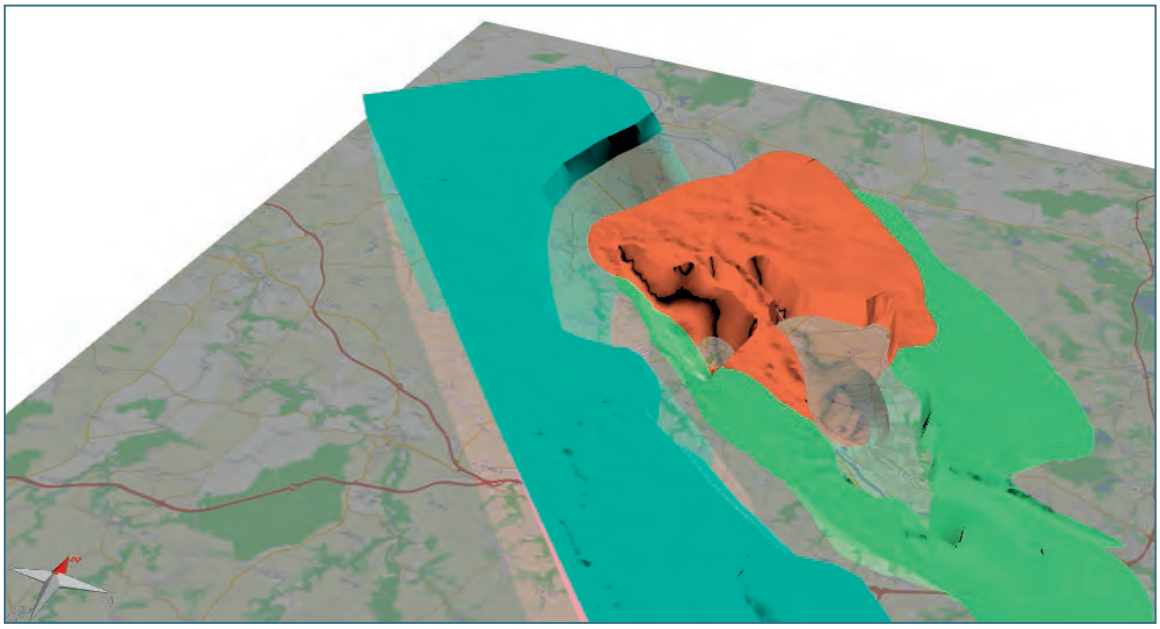

Figure 10.2-6: Topographic maps of a predefined selection catalogue and other textures from any WMS can be overlain at arbitrary depth (z-axis) levels to facilitate the orientation in space.

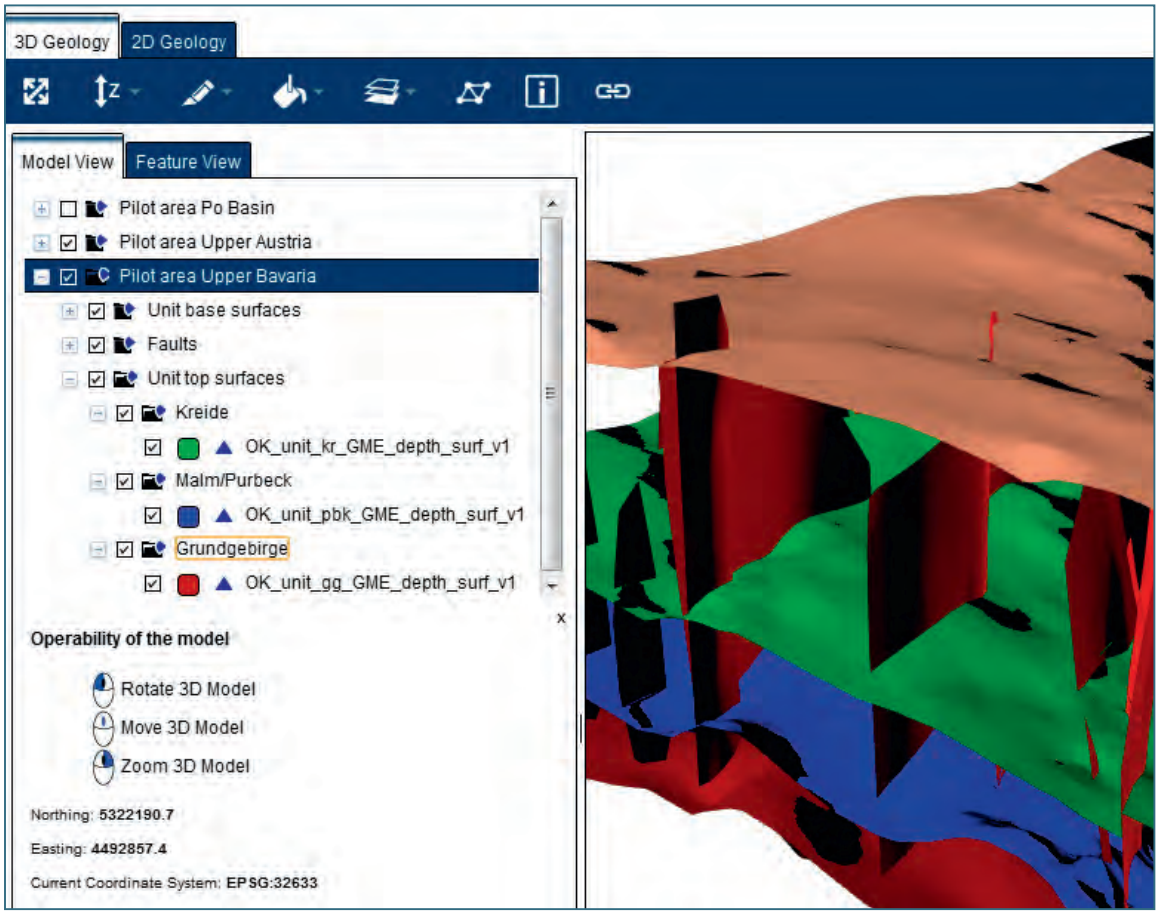

Figure 10.2-7: The interactive legend allows toggling data to be visualised in the 3D scene. On the top tabs the user can switch the application from 3D mode (“3D Geology”) to 2D mode (“2D Geology”). On bottom left, below the legend and the instructions for the mouse operability, the coordinates of the current cursor position are displayed.(Screenshot of the GeoMol 3D-Explorer, beta version as of March 2015).

Beyond the mere visualisation features for 3D models GeoMol's 3D-Explorer comprises a 2D map view providing tools for querying the models and the selection of model cut-outs for the enhanced insight and measurement (Figure 10.2-8). The functionalities of the query tools include the generation of virtual bore holes, vertical cross-sections, and horizontal sections. The position of the boreholes respectively the start and end points of the sections can be entered either mouse-controlled on the map or manually. The results returned can be queried via a single URL which allows their integration into semi automatic reports generated in external systems like GIS.

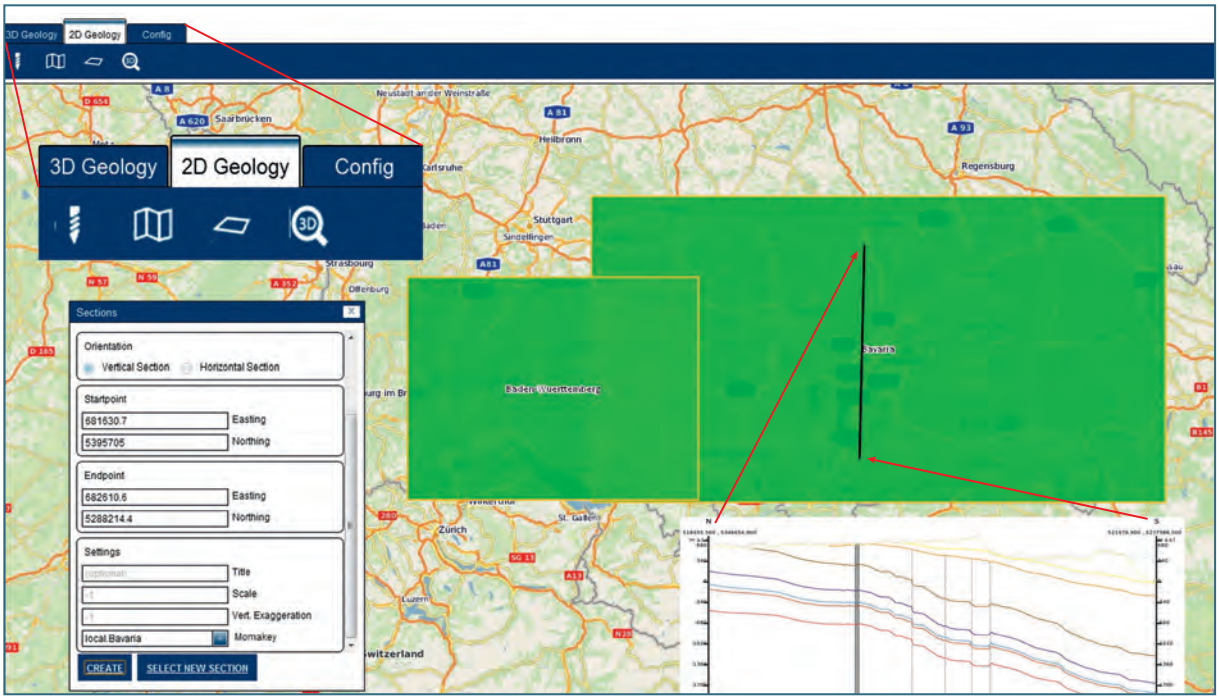

Figure 10.2-8: The 2D mode ("2D Geology") of GeoMol's 3D-Explorer features an overview of the available 3D models (green areas as an example) and provides tools for the generation of virtual boreholes, vertical sections (see clip of a print-out in the inset at the bottom) and horizontal sections as well as a browser for rectangular model cut-outs by dragging a box with the mouse.

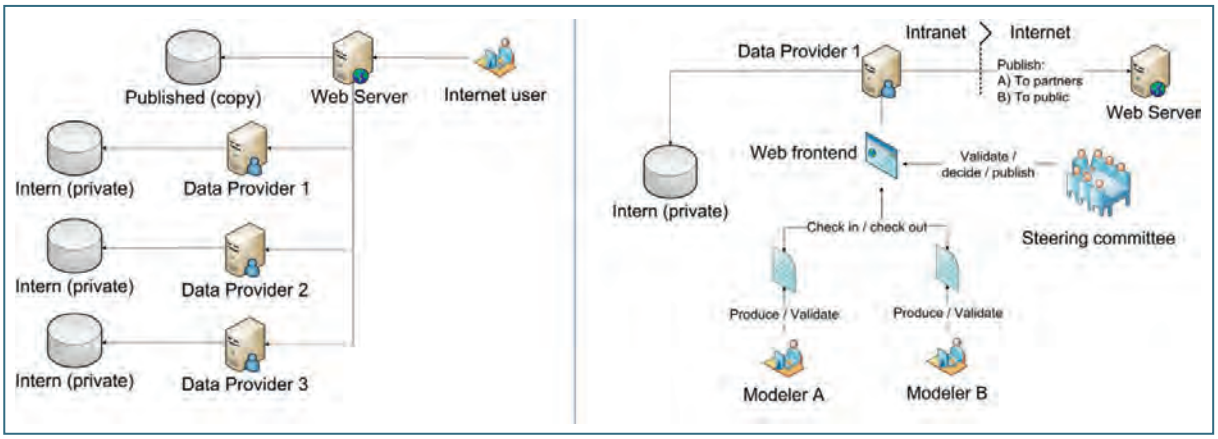

Figure 10.2-9: Central GeoMol server accessing each partners GST instance in order to present a complete model to the internet user (left). For each of the data providers a web frontend allows to publish data to partners or for the public access.

In order to allow the full integration of further data providers also beyond the GeoMol partnership, GST has been extended to a service interface, enabling several GST instances running and to retrieve data from these instances (Figure 10.2-9). Since this also introduces a physical data separation it allows for an enhanced partitioning of the data in addition to the distinction between providers. Above and beyond the role-based access levels which have been implemented to meet the partners' distinct data policies, this facilitates to set up a complex data infrastructure with one central access point and a sophisticated data access and share module for the cross-domain stakeholder communities.

10.3 The GeoMol MapViewer

The MapViewer web application enables users to select, query, analyse, save and print 2D thematic maps of the GeoMol project areas on the Internet. The MapViewer is accessible through GeoMol's Website or directly via the URL: http://maps.geomol.eu. By selecting an area from a clickable map on the viewer's home page, the user is routed to 2D thematic maps available for the particular area of interest (Figure 10.3-1).

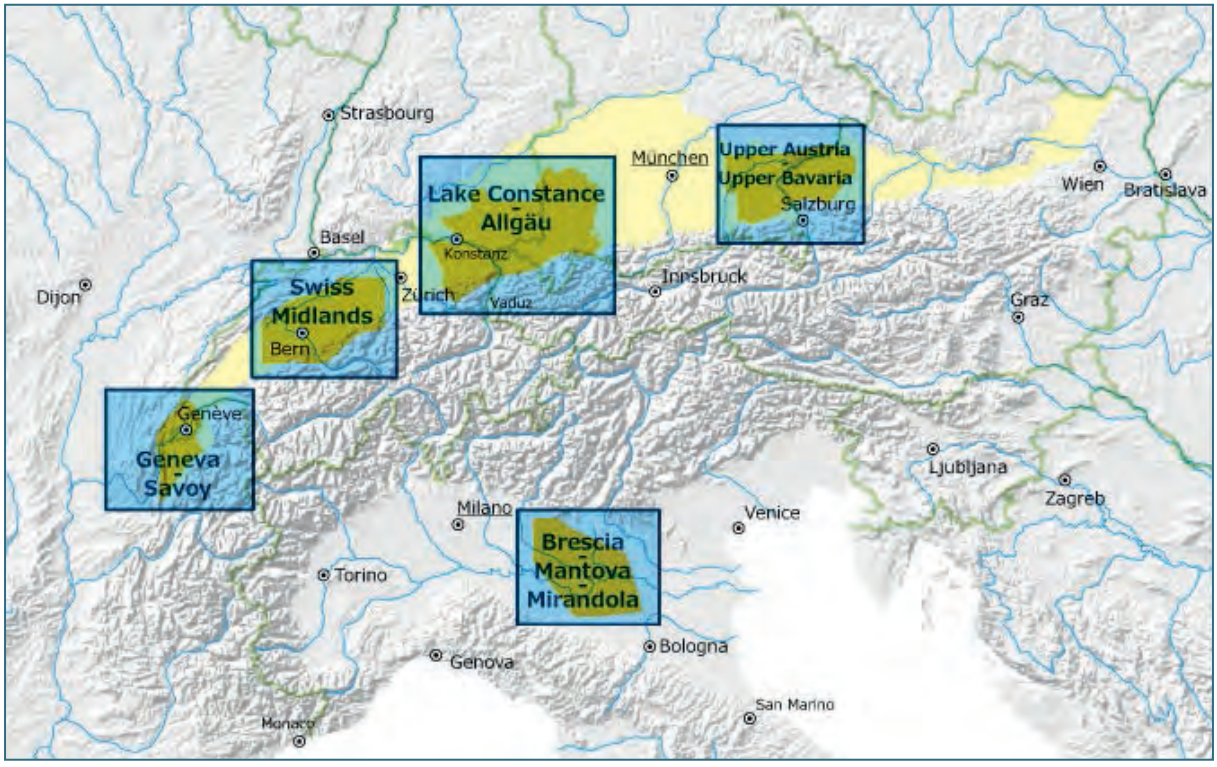

Figure 10.3-1: Homepage of GeoMol's MapViewer providing a clickable map for selecting the area of interest, e.g. one of the project's pilot areas (clip of a screenshot from http://maps.geomol.eu)

The application is designed for browsing on PCs as well as on mobile devices. The graphical user interface is available in English, German, French and Italian. Map titles, legends and attribute information are kept in English for the framework model and in the national language of the GSOs providing the web services for respective pilot areas.

The maps have been assigned to the following thematic blocks and map categories in the table of content of the MapViewer:

- Basic data with maps showing:
  - the extent of the modelling areas
  - locations of seismic sections and bore holes
  - the surface geology
  - traces of faults projected onto the surface

- Distribution of geological units with maps showing the depth position and occurrences of stratigraphic layers derived from 3D modelling

- Geothermal / hydrothermal potential with maps showing:
  - temperature distribution at certain depths or stratigraphic layers surfaces
  - depths below surface contours for certain temperatures
  - classification of geothermal potential based on the temperature distribution
  - the occurrences of structural traps as targets for competing use (e. g. oil and gas)
  - the bulk storage potential for geological repositories of CO_2

- Gas storage with maps showing:
  - the fault network highlighting structural traps
  - gas storage concessions or sites in operation

- Potential active faults with:
  - general structural maps (faults and folds) and active stress vectors
  - maps of potentially active faults and their relation to the geopotential settings
  - maps of lateral variations of slip rates along main structures.

The maximum scale for visualisation of all 2D thematic maps is 1:80,000. This scale commonly is deemed appropriate in terms of data protection regulations stipulating to render anonymous sensitive data. Regarding topographic base maps, users can choose between raster and vector display with the option to add relief data. Map coordinates of the cursor position can be displayed as geographic coordinates (WGS84), in the European system ETRS89 UTM and in all country-specific coordinate reference systems used in the selected area (see Table 10.5-1).

The navigation toolbar of the MapViewer features functions for easy orientation and location in the map window like zoom in / zoom out, zoom to an arbitrary rectangle dragged in the map window, panning and resizing to the previous or full extents. The toolbar's info button returns information on queryable object attributes. Data and information of external web map services can be added to the map window.

The "Search places" tool enables to query and switch to locations in the map window. The table of content allows activation, continuous transparency adjustment and the display of the legend for each layer. While the table of content is fixed, the arrangement of active maps can be organised by using the "My selection" tab. Using the "Print" function of the MapViewer map views can be saved and printed as PDF documents at pre-defined scales not exceeding 1 : 80,000 (see above). In addition to the map information the PDF document also provides the legend of all activated map features as well as the source of information and a disclaimer.

A comprehensive video tutorial on the MapViewer application is available on the GeoMol Website.

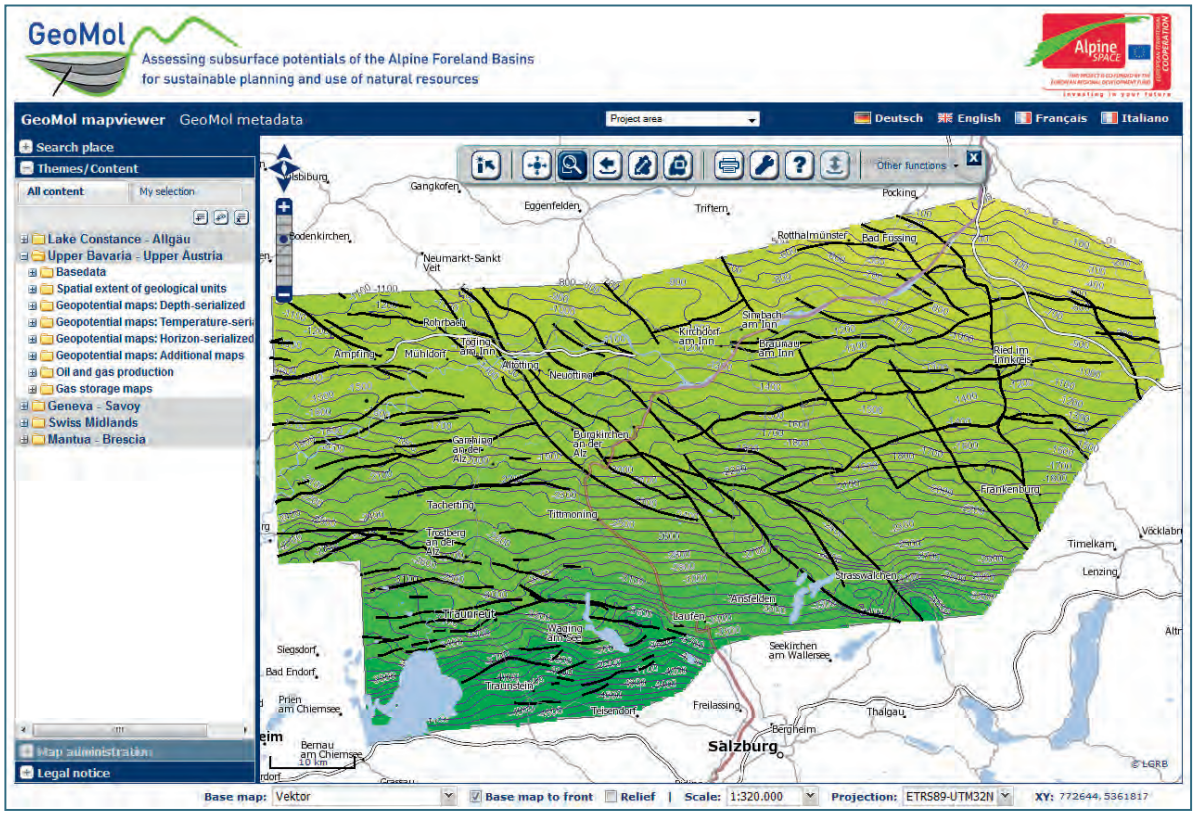

Figure 10.3-2: Screenshot of the GeoMol MapViewer (http://maps.geomol.eu) for the illustration of the user interface, taking the contour map of the base of Tertiary in the Upper Austria – Upper Bavaria pilot area as an example.

10.4 The GeoMol SearchCatalogue

The web application SearchCatalogue enables users to search for 2D thematic maps and web services of GeoMol on the basis of a structured metadata description. The SearchCatalogue is accessible through GeoMol's Website or directly via the URL http://meta.geomol.eu. The graphical user interface of the application is available in English, German, French and Italian.

Simple searches can either be performed on the basis of keywords, map titles or abstracts or can be restricted to individual theme blocks or web map services. The advanced search function allows target-oriented queries within specific fields of the metadata description.

Search results of the SearchCatalogue can be expanded to show the full metadata descriptions of 2D thematic maps and web map services. In addition to information on the thematic content and spatial extent the metadata also contain contact information for obtaining data and information on restrictions of use. In addition, the metadata includes links referring to relevant PDF products of GeoMol (e. g. reports or chapters thereof, guidelines).

The metadata descriptions are based on the EN ISO standards 19115 and 19119 and are compliant with the requirements of the EU INSPIRE directive (INSPIRE 2007) and with the national and regional spatial data infrastructures GDI-DE (http://www.geoportal.de/DE/GDI-DE/) and E-GEO.CH (http://www.e-geo.ch/). The technical implementation of the SearchCatalogue is based on the Open

Geospatial Consortium standard CSW 2.0.2 (OGC 2007). The web service has been adjusted to the requirements of the INSPIRE directive for Discovery Services (INSPIRE 2011).

Users can easily toggle between the web applications MapViewer and SearchCatalogue. From the SearchCatalogue, 2D thematic maps can be loaded directly into the MapViewer using the "Map Preview" tool. Vice versa, extracted tags of the metadata information can be displayed in the MapViewer selecting “Show metadata” in the table of contents. From the opening pop-up window, users can again switch to the full metadata description.

To facilitate the full utilisation of the SearchCatalogue application a comprehensive video tutorial in English is provided on the GeoMol Website.

10.5 GeoMol’s web map services (WMS)

The spatial data derived from the 3D models of GeoMol are used to generate 2D thematic maps provided by web map services (WMS). As web map services are defined as standard protocols for serving georeferenced map raster images via the Internet, other web mapping applications and most common geographic information systems (GIS) are capable of integrating WMS as layer information. Thus, GeoMol’s WMS can easily be linked and combined with spatial data from external sources allowing for an integrated and comprehensive cross-domain spatial analysis.

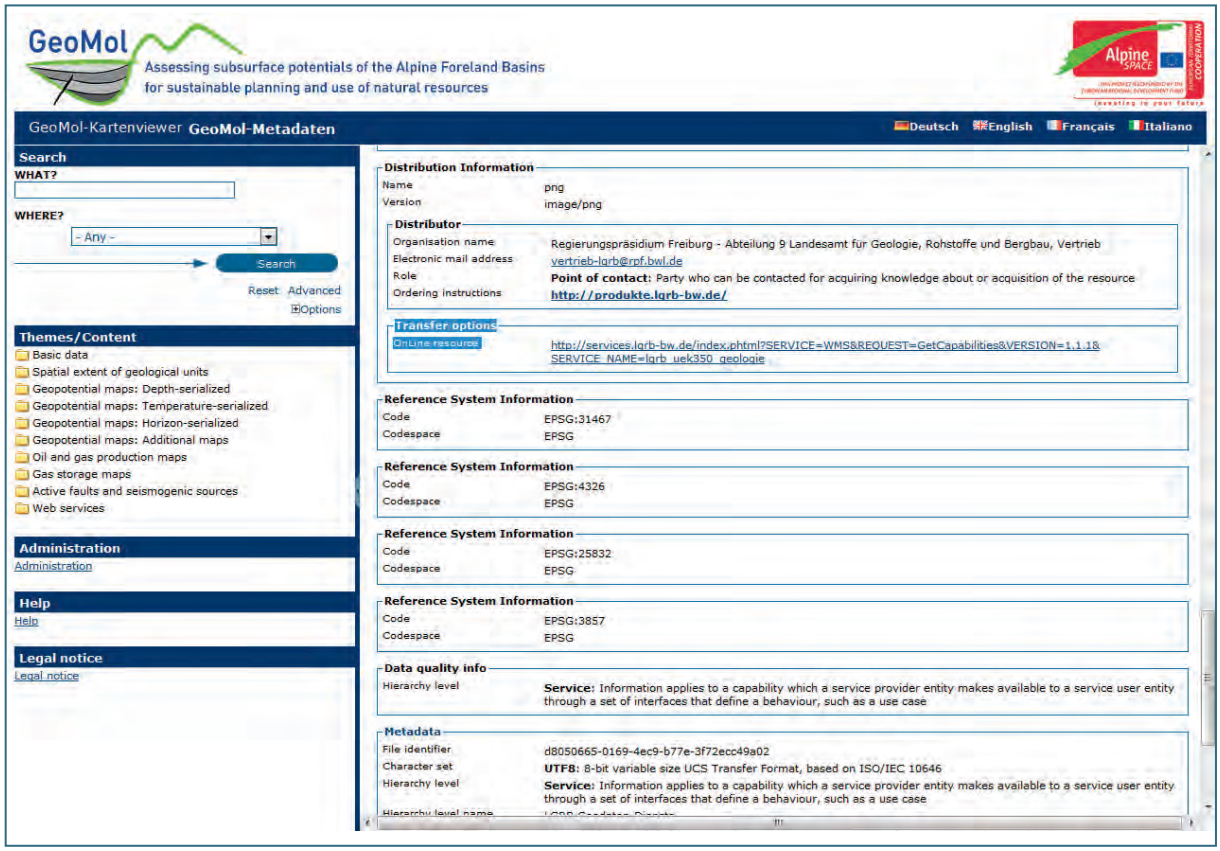

Figure 10.4-1: Screenshot of GeoMol’s SearchCatalogue (http://meta.geomol.eu as of April 2015) showing search options by keywords, region and themes/content (left panel). In the example metadata description (right panel), information about access to the map is given by the GetCapabilites of its web map service.

In order to add a WMS service to an external web application or GIS, users necessarily need to know about its specific GetCapabilities request. For all of GeoMol's WMS, the GetCapabilities request is given in the full metadata description of the service in the section "Distribution Information | Transfer options" (Figure 10.4-1). Any GetCapabilities request returns detailed parameters about the WMS, e.g. the provider, supported map image formats, version compatibility, available layers, spatial extent, supported coordinate reference systems and the URI (Unique Resource Identifier) of the data. Apart from the GetCapabilities and GetMap requests mandatory for any web map service, GeoMol's WMS also support the GetFeatureInfo request in order to retrieve information about the object attributes that can be queried.

The technical implementation of GeoMol's WMS is based on the Open Geospatial Consortium (OGC) standard WMS version 1.1.1 (OGC 2002) and WMS version 1.3 (OGC 2004), respectively. To allow an efficient update of the spatial information and the WMS with relevant new evidence and to ensure that all data are maintained at the institution in charge of a specific area, a system of distributed resources was set up featuring different WMS providers. Table 10.5-1 summarises the data and WMS service providers, languages of the WMS, theme blocks available and supported coordinate reference systems for model areas of GeoMol as described in chapter 2.1.

Table 10.5-1: Details of GeoMol's web map services

GeoMol Area	Data Provider	Web Service Provider	Language	Theme Blocks	Coordinate Systems (EPSG Codes)
NAFB Framework Model	BRGM GBA LFU LGRB swisstopo	LGRB	English	Basic data	WGS 84 (4326) Web Mercator (3857) ETRS89 UTM 31N (25831) ETRS89 UTM 32N (25832) ETRS89 UTM 33N (25833)
Geneva-Savoy	BRGM swisstopo	Etat de Genève	French	Basic data, Spatial extent of geological units, Geothermal/hydrothermal potential	WGS 84 (4326) Web Mercator (3857) ETRS89 UTM 31N (25831) ETRS89 UTM 32N (25832) CH 1903+ / LV95 (2056) Lambert 93 (2154)
Lake Constance – Allgäu	GBA LfU LGRB swisstopo	LGRB	German	Basic data, Spatial extent of geological units, Geothermal/hydrothermal potential	WGS 84 (4326) Web Mercator (3857) ETRS89 UTM 32N (25832) DHDN GK 3 (31467) DHDN GK 4 (31468) CH 1903+ / LV95 (2056) MGI Austria GK M28 (31257)
Brescia-Mantova-Mirandola	ISPRA	ISPRA	Italian	Basic data, Spatial extent of geological units Geothermal/hydrothermal potential, Potential active faults	WGS 84 (4326) Web Mercator (3857) ETRS89 UTM 32N (25832) WGS 84 UTM Zone 32 (32632)
Swiss Midlands	swisstopo	swisstopo	German	CO_2 sequestration	WGS 84 (4326) Web Mercator (3857) ETRS89 UTM 32N (25832) CH 1903+ / LV95 (2056)
Upper Austria – Upper Bavaria	GBA LfU	LfU	German	Basic data, Spatial extent of geological units, Geothermal/hydrothermal potential, Gas storage	WGS 84 (4326) Web Mercator (3857) ETRS89 UTM 32N (25832) ETRS89 UTM 33N (25833) DHDN GK 4 (31468) MGI Austria GK M31 (31258)

11 Summary and outlook

The Alpine Foreland Basins, shared by six countries, are striking geological structures that feature a variety of subsurface potentials in terms of energy security and the reduction of greenhouse gases. Thanks to the EU cohesion policy and European Territorial Cooperation / Alpine Space funding scheme it was possible for the first time to bring together all Geological Survey Organisations in charge, having a territorial rather than an overarching mandate, for the joint transnational revision of the geological knowledge and the provision of harmonised three-dimensional geological information allowing a seamless insight into the deep subsurface of the Alpine forelands and the holistic assessment of the geopotentials.

Huge efforts have been made by the GSOs to acquire and compile the baseline data from multiple sources and to prepare state-of-the-art quality controlled data pools as a basis for interpretation, evaluation and 3D model building. As data access restrictions demanded a distributed implementation, the successful resolution of cross-border issues required the comprehensive harmonisation of the concepts, interpretations and methods. The best practice had to cope with disparate data densities and historical settings, with regional geological peculiarities and with the diverse legal frameworks concerning data policy.

Apart from technical solutions GeoMol's partnership developed several strategies to mitigate these obstacles in harmonisation. Still, disparities in terms of data availability and dissemination, varied data quality and density, and the complex geological setting in space and time, giving rise to various regional approaches applied for decades, required some oversimplifications in order to agree on the least common denominator applicable for the seamless overall view. These generalisations in conjunction with the data situation have markedly constrained the rigour and resolution of the geological synopsis and the scope of geopotential assessment. Specifically the paucity of rock property data did not allow for a potential assessment of more than the theoretical geopotential. Nevertheless, with the preparation of the outputs GeoMol's partnership succeeded in the harmonisation of methods and techniques to interpret, evaluate and represent complex geological situations for cross-domain coordination in subsurface planning and the interaction with a larger stakeholder community. The spatial information GeoMol makes available is immediately applicable as a basic input in numerical modelling of physical processes. Thus, it assists further advancements in applied geosciences and subsurface planning.

Exploiting modern 3D modelling techniques, the transnational collaboration of GeoMol made it possible for the first time to address the geological set-up and tectonic evolution of the entire Northern Molasse Basin and to localise and assess seismogenic structures in the Po Basin in the three-dimensional spatial context. These approaches allowed for new scientific insights but also posed new questions and revealed deficiencies in places – they clearly disclosed areas where further investigations are needed to address issues sufficiently.

The use of 3D geological models for the validation of cross-border harmonisation and as the resource of geopotential derivation imposed particular requirements on the collaboration platform and on the contents and modes of product dissemination:
Recent technological advancements have supplied tools for the three-dimensional visualisation which allow a straightforward insight into the subsurface. However, no infrastructure was available for cross-linked work processes and to share, merge, and distribute 3D geological models from different national repositories. Thus, a key development of the project was the software-independent transnational collaborative environment for multi-dimensional geo-information. Implemented incrementally, GeoMol now makes available a web-based geo data infrastructure providing overall inter-

operability among entitled institutions and facilitating the communication with the stakeholder community. Although the full exploitation of its functionalities is constrained by data protection regulations, GeoMol's geo data infrastructure features principal components of interoperability suitable to interconnect the cross-domain user community and to serve administrative bodies in terms of e-governance.

Disparities of data policy have been evident for a long time past, and to abolish them is far beyond the reach of GeoMol. However, utilising the technical interoperability for the peer-to-peer juxtaposition of "national best efforts" manifestly exposes gaps and discrepancies resulting from the disparate and substantial restriction enjoined by data privacy provisions. This lack of overarching regulations and a matching data policy clearly foils the EU's call for trans-nationally harmonised information.

Many GeoMol partners identified the alignment of the national statutory provisions with respect to subsurface data – in terms of giving full access to all baseline data and the open disclosure of the interpretations and metadata – a key issue to fulfil their role as the legal custodians of the subsurface, within their area of responsibility as well as for cross-territorial issues. In order to make geoscientific surveying more rigorous and sustainable it has been regarded a crucial topic to be addressed by the EU harmonisation policy.

The implementation of GeoMol and the concomitant information measures strongly raised the awareness for the issues related to the subsurface, not only of the academia and professionals but also in politics and administration, albeit to different extends. Basically, the political perception of the project in the GeoMol partner states seems to reflect the present trend of the public opinion and the people's concerns regarding underground utilisations and their possible environmental impact.

Owing to the activities and results of GeoMol, 3D geological modelling has become an acknowledged priority task at the GSOs e.g. in Austria and Switzerland. Other project partners expect a systematic expansion of their 3D modelling applications for a multitude of issues demanded by the administrative and planning authorities.

The cross-fertilising collaboration among the project partners – contributing knowledge, experience and skills thereby bringing the partners to a common, higher level – has been invaluable and mutual benefit, continuing after the end of the project. The established expert network, including stakeholders from other domains and beyond the territorial reach of GeoMol, safeguards the sustained dialogue over the upcoming challenges of subsurface planning and its utilisation. It facilitates an effective knowledge transfer in order to assess the geopotentials of other foreland basins, also by sharing the tools and concepts developed for technical interoperability, thus fulfilling the objectives and the spirit of the European Territorial Cooperation.

12 Abbreviations, acronyms, trade names and units

Abbreviations, acronyms

The abbreviations and acronyms of the partners of the GeoMol Consortium are listed on page 3. Abbreviations of geological units, unless mentioned in the text, are explained in the legends or captions of the respective figures.

ATES	Aquifer Thermal Energy Storage
BHT	Bottom Hole Temperature (T_{max} measures during well drill logging)
BMMA	Brescia-Mantova-Mirandola (Pilot) Area
CAES	Compressed Air Energy Storage
CCS	Carbon Capture and Storage (carbon dioxide (CO_2) sequestration)
DST	Drill Stem Test (hydraulic test in oil and gas wells)
E&P	Exploration and Production
GIS	Geographical Information System
GPS	Global Positioning System
GSA	Geneva-Savoy (Pilot) Area
GSC	GeoMol Steering Committee
GSO	Geological Survey Organisation
ISO	International Organisation for Standardisation
LCA	Lake Constance – Allgäu (Pilot) Area
LSQ	Least Square Fit
MBHE	Medium Deep Borehole Heat Exchanger
MIS	Marine Isotope Stage
MZB	Mura-Zala Basin
NAFB	North Alpine Foreland Basin
OBM	Obere Brackwasser Molasse / Upper Brackish Molasse
OGC	Open Geospatial Consortium
OMM	Obere Meerwasser Molasse / Upper Marine Molasse
ORC	Organic Rankine Cycle
OSM	Obere Süßwasser Molasse / Upper Freshwater Molasse
SDI	Spatial Data Infrastructure
SEG-Y	Society of Exploration Geophysicists' standard file format for storing geophysical data
SFS	Single Feature Structured Query Language
SMA	Swiss Midlands (Pilot) Area
SQL	Structured Query Language
TIN	Triangulated Irregular Network
TVD	True Vertical Depth (of a drilling)
TWT	Two Way Travel Time (of the acoustic pulse in seismic surveys)
UA – UB	Upper Austria – Upper Bavaria (Pilot) Area
UBM	Untere Brackwasser Molasse / Lower Brackish Molasse
UMM	Untere Meerwasser Molasse / Lower Marine Molasse
URL / URI	Uniform Resource Locator / Identifier (reference to web sites)
USM	Untere Süßwasser Molasse / Lower Freshwater Molasse
UTES	Underground Thermal Energy Storage
UTM	Universal Transverse Mercator (coordinate system)
VSP	Vertical Seismic Profile
WebGL	Web Graphics Library
WGS	World Geodetic System (coordinate system)
WMS	Web Map Service(s)
X3D	ISO standard to represent 3D computer graphics

Trade names

The use of trade names (®/™) in this report is for descriptive purposes only and does not imply endorsement. Common trade names (e.g. of web browsers) are not listed.

ArcGIS	Geographic information system by ESRI
AutoCAD	Software for 2D and 3D computer-aided design (CAD) by Autodesk Inc.
ESRI	Geographic information system company
FEFLOW	Finite Element subsurface flow system simulation by DHI-WASY
Kingdom Suite	Geophysical and geological interpretation software by IHS Kingdom
GeoModeller	3D modelling software by Interpid
GiGa	GiGa Infosystems - Software Company
GST	Geosciences in Space and Time (data base system by GiGa)
GoCAD	3D modelling software by the Gocad Research Group and Paradigm
JewelSuite	3D modelling software suite by Baker Hughes Inc
Move	3D modelling software package by Midland valley
Petrel	E&P reservoir software by Schlumberger
SeisSpace ProMax	Seismic procession software by Halliburton
SeisVision	Seismic interpretation software by GeoGraphix (GGX)
SeisWorks	Seismic interpretation software by Landmark
SKUA	3D modelling software suite by Paradigm
Surfer	3D modelling software suite by Golden Software

Symbols and units of measure

a	year(s)
°C	degree Celsius scale
g/l	gram(s) per liter (unit of mass concentration, e.g. of dissolved solids)
K	Kelvin (°C −273.15)
kt	kiloton (10^3 tons)
kW	kilowatt (10^3 watts)
kWh	kilowatt-hour
kWh/m^2	kilowatt-hour per square meter
m^3/h	cubic meter(s) per hour (unit of flow rate)
Ma	Million years
m a.s.l.	meters above sea level
m b.s.l.	meters below sea level
mD	millidarcy (unit of permeability)
M_L	Local Magnitude scale (magnitude number of an earthquake)
Mm^3	Million cubic meters
Mt	megaton (10^6 tons)
M_w	Moment magnitude scale (measure of earthquakes in terms of the energy released)
MW	megawatt (10^6 watts)
MWh	megawatt-hour
MWh/a	megawatt-hour per year
MWt	Megawatt thermal (thermal power produced)
T	Temperature (unless stated otherwise: °C)
T_{max}	maximum Temperature
v	Velocity (unless stated otherwise: m/s)
W/(m*K)	watts per Kelvin meters (unit for thermal conductivity)

13 References

Agemar, T., Brunken, J., Jodocy, M., Schellschmidt, R., Schulz, R. & Stober, I. (2013): Untergrundtemperaturen in Baden-Württemberg. Z. Dt. Ges. Geowiss. **164/1**: 49–62, DOI 10.1127/1860-1804/2013/0010

Allen, P. A. & Allen, J. R. (2005): Basin Analysis: Principles and Applications, 2nd ed., 549 pp, ISBN 0-632-05207-4

Allen, P. A., Crampton, S. L. & Sinclair H. D. (1991): The interception and early evolution of the North Alpine foreland basin. Basin Res. **3**: 143–163, DOI 10.1111/j.1365-2117.1991.tb00124.x

Amorosi, A., Pavesi, M., Ricci Lucchi, M., Sarti, G. & Piccin, A. (2008): Climatic signature of cyclic fluvial architecture from the Quaternary of the central Po Plain, Italy. Sediment. Geol. **209**: 58–68, ISSN 0037-0738

Anelli, L., Mattavelli, L. & Pieri, M. (1996): Structural-stratigraphic evolution of Italy and its petroleum systems. – In: Ziegler, P. A. & Horváth, F. (eds.): Peri-Tethys Memoir 2: Structure and Prospects of Alpine Basins and Forelands. Mémoirs du Muséum National d'Histoire Naturelle **170**: 455–483 (Paris)

Bachmann, G. H. & Müller, M. (1991): The Molasse basin, Germany: evolution of a classic petroliferous foreland basin. In: Spencer, A. M. (ed.): Generation, accumulation, and production of Europe's hydrocarbons. Spec. Publ. European Assoc. of Petroleum Geoscientists **1**: 263–276, (Oxford, University Press)

Bachmann, G. H. & Müller, M. (1992): Sedimentary and structural evolution of the German Molasse Basin. Eclogae geol. Helv. **85/3**: 519–530, ISSN 0012-9402

Bachmann, G. H., Müller, M. & Weggen, K. (1987): Evolution of the Molasse Basin (Germany, Switzerland). Tectonophysics **137**: 77–92, ISSN 0040-1951

Bachu, S. (2003): Screening and ranking of sedimentary basins for sequestration of CO_2 in geological media in response to climate change. Environmental Geology **44**: 277–289, DOI 10.1007/s00254-003-0762-9

Basili, R., Valensise, G., Vannoli, P., Burrato, P., Fracassi, U., Mariano, S., Tiberti, M. M. & Boschi, E. (2008): The Database of Individual Seismogenic Sources (DISS), version 3: summarizing 20 years of research on Italy's earthquake geology. Tectonophysics **453**: 20–43, DOI 10.1016/j.tecto.2007.04.014

Baujard, C., Signorelli, S. & Kohl, T. (2007): Atlas des ressources géothermiques de la Suisse Occidentale. Schweizerische Geophysikalische Kommission. Beiträge zur Geologie der Schweiz – Geophysik **40**

BayGLA [Bayerisches Geologisches Landesamt] (Hrsg.) (1996): Erläuterungen zur Geologischen Karte von Bayern 1 : 500.000, 4. Aufl., 329 S. (München, Bay. GLA)

BayGLA [Bayerisches Geologisches Landesamt] (Hrsg.) (2004): GeoBavaria – 600 Millionen Jahre Bayern. 92 S. (München, Bay. GLA)

BayLfU [Bayerisches Landesamt für Umwelt] (2014): Klimaprogramm Bayern 2020 (KLIP): Tiefe Geothermie im bayerischen Molassebecken – 3D-Untergrundmodell zur Minderung der Erschließungs- und Nutzungsrisiken (Augsburg, LfU – unpubl.)

BayLfU [Bayerisches Landesamt für Umwelt] (2012): Geothermische Charakterisierung von Karst-Kluft-Aquiferen im Großraum München – Geothermie Großraum München, Endbericht. Umwelt Spezial, 40 S., (Augsburg, LfU), http://www.bestellen.bayern.de/shoplink/lfu_bod_00090.htm

BayStMIVT [Bayerisches Staatsministerium für Wirtschaft, Infrastruktur, Verkehr und Technologie] (Hrsg.) (2010): Bayerischer Geothermieatlas, 2. Aufl., 104 S., Karten-CD, (München)

Bertleff, B., Joachim, H., Koziorowski, G., Leiber, J., Ohmert, W., Prestel, R., Stober, I., Strayle, G., Villinger, E. & Werner, J. (1988): Ergebnisse der Hydrogeothermiebohrungen in Baden-Württemberg. Jh. Geol. LA Baden-Württemberg **30**: 27–116 + Beilagen (Freiburg i. Br., LGRB)

Bigi G., Cosentino D., Parotto M., Sartori R. & Scandone P. (1990): Structural Model of Italy and Gravity Map 1 : 500,000. Quad. Ric. Scientifica **114/3**, (Florence, S.EL.CA)

Brink, H. J., Burri, P., Lunde, A. & Winhard, H. (1992): Hydrocarbon Habitat and Potential of Swiss and German Molasse Basin – a Comparison. Eclogae geol. Helv. **85/3**: 715–732

Champagnaca, J.-D., Schlunegger, F., Norton, K., von Blanckenburg, F., Abbühl, L. M. & Schwab, M. (2009): Erosion-driven uplift of the modern Central Alps. Tectonophysics **474/1**: 236–249, DOI 10.1016/j.tecto.2009.02.024

Capar, L., Couëffé, R., Brenot, A., Courrioux, G., Dezayes, C., Gabalda, S., Lopez, S., Marc, S., Rambourg, D., Siméon, Y., Andenmatten, N., Clerc, N., Meyer, M. & Rusillon, E. (2015): GeoMol – Évaluation des ressources naturelles dans les bassins d'avant-chaîne alpins pour une utilisation et une gestion durable du sous-sol – Zone Pilote Genève-Savoie. Rapport BRGM **64744-FR** (Orléans, BRGM), http://infoterre.brgm.fr/rapports/RP-64744-FR.pdf

Capar, L. & the GeoMol Team (2013): Contribution of seismic processing to put up the scaffolding for the 3-dimensional study of deep sedimentary basins: the fundaments of trans-national 3D modelling in the project GeoMol. Geophysical Research Abstracts **15**: EGU2013-5349-1

Caporali, A., Barba, S., Carafa, M. M. C., Devoti, R., Pietrantonio, G. & Riguzzi, F. (2011): Static stress drop as determined from geodetic strain rates and statistical seismicity. J. Geophys. Res. **116**: B2410, DOI 10.1029/2010JB007671

Carafa, M.M.C. & Barba, S. (2013): The stress field in Europe: optimal orientations with confidence limits. Geophys. J. Int. **193**: 531–548, DOI 10.1093/gji/ggt024

Carcano, C. & Piccin, A. (eds.) (2002): Geologia degli Acquiferi Padani della Regione Lombardia. 130 p. (Firenze, S. EL. CA.)

Carminati, E. & Martinelli, G. (2002): Subsidence rates in the Po Plain (Northern Italy): the relative impact of natural and anthropic causation. Engineering Geology **66**: 241–55, DOI 10.1016/S0013-7952(02)00031-5

Cartlidge, E. (2014): Human activity may have triggered fatal Italian earthquakes, panel says. Science **344**: 141, DOI 10.1126/science.344.6180.141

Casper, S. & Zosseder, K. (2015): Vergleich der verschiedenen Temperaturprognosen im Molassebecken im Rahmen des GeoMol-Projektes aus dem „Alpine Space"-Förderprogramm. Abschlussbericht zum Forschungsvorhaben AccordTemp@GeoMol. 17 S. (München, TU – unpubl., *available at LfU*)

Čermak, V. & Hurtig, E. (1979): Heat Flow Map of Europe 1 : 5,000,000. In: Čermak V. & Rybach L. (eds.): Terrestrial Heat Flow in Europe, Enclosure (Berlin / Heidelberg / New York, Springer)

Chadwick, A., Arts, R., Bernstone, C., May, F., Thibeau, S. & Zweigel, P. (eds.) (2008): Best practice for the storage of CO_2 in saline aquifers. British Geological Survey Occasional Publ. **14**, 267 pp., ISBN 978-0-85272-610-5

Clauser, C. & Koch, A. (2006): Erstellung statistisch abgesicherter thermischer und hydraulischer Gesteinseigenschaften für den flachen und tiefen Untergrund in Deutschland, Phase 1 – Westliche Molasse und nördlich angrenzendes Süddeutsches Schichtstufenland. Bericht zum BMU-Projekt FKZ 0329985, 220 S., http://www.gge.eonerc.rwth-aachen.de/go/id/dnir/file/49675

Clauser, C., Deetjen, H., Hartmann, A., Höhne, F., Rath, V., Rühaak, W., Schellschmidt, R., & Zschocke, A. (2002): Erkennen und Quantifizieren von Strömung: Eine geothermische Rasteranalyse zur Klassifizierung des tiefen Untergrundes in Deutschland hinsichtlich seiner Eignung zur Endlagerung radioaktiver Stoffe. Endbericht zum Auftrag 9X0009-8390-0 des Bundesamtes für Strahlenschutz (BfS), (Aachen, RWTH)

Crotogino, F., Donadei, S. & Dietrich, L. (2009): Nutzungskonkurrenz bei Speichern im geologischen Untergrund. Solarzeit **4/2009**: 23–30, ISSN 0937-3802

Dahm, T., Hainzl, S., Becker, D., Bisschoff, M., Cesca, S., Dost, B., Fritschen, R., Kuhn, D., Lasocki, S., Klose, C. D., Meier, T., Ohrnberger, M., Rivalta, E., Shapiro, S., Wegler, U. (2010). How to discriminate induced, triggered and natural seismicity. In: Proceedings of the Workshop induced seismicity, November 15–17, 2010. Cahiers du Centre Européen Géodynamique Séismologie **30**: 69–76 (Luxembourg, Centre Européen de Géodynamique et de Séismologie)

d'Ambrogi, C. & Congi, M. P. (2010): 3D geological modeling and visualization supporting seismic hazard assessment. Geophysical Research Abstracts **12**, EGU2010-2766

Diamond, L. W., Leu, W., Chevalier, G., Burlini, L., Deichmann, N., Naef, H., Pini, R. & Wyss, R. (2010): Studie zur Abschätzung des Potenzials für CO_2-Sequestrierung in der Schweiz / Potential for geological sequestration of CO_2 in Switzerland. BfE-Schlussbericht, 31.08.2010, 23 S. (Bern, Bundesamt für Energie BfE)

di Dio, G. (ed.) (1998): Riserve idriche sotterranee nella Regione Emilia-Romagna. Regione Emilia-Romagna & ENI-AGIP, 119 pp., 9 sheets (Firenze, S. EL. CA.)

DIEPOLDER, G.W. (2011): 3D modelling at the Bavarian State Geological Survey – examples for cooperation towards 3D standards. – In: Three-Dimensional Geological Mapping, Workshop Extended Abstracts, Minneapolis, Minnesota – October 8, 2011, Geol. Survey Canada, Open File **6998**: 17–21, http://isgs.illinois.edu/sites/isgs/files/files/3Dworkshop/2011/diepolder.pdf

DIEPOLDER, G.W. (2015): Das internationale Projekt GeoMol als Beispiel für die Erkundung von Geopotenzialen – Hintergründe, Implementierung und Rechtshemmnisse. In: KMENT, M. (Hrsg.): Unterirdische Nutzungen – Systematisierung und planerische Steuerung, Gewinnpartizipation und Haftung. Schriften zum Infrastrukturrecht **3**: 1–19 (Tübingen, Mohr Siebeck), ISBN 978-3-16-153469-0

DIEPOLDER, G.W. & KINDERMANN, T. (2013): Den alpinen Geopotentialen auf der Spur – über Ländergrenzen hinweg. bbr – Leitungsbau Brunnenbau Geothermie **12-2013:** 72–77 (Bonn, Wirtschafts- und Verlagsgesellschaft Gas und Wasser) ISSN 1611-1478

DIEPOLDER, G.W., PAMER, R. & THE GEOMOL TEAM (2014): Transnational 3D modeling, geopotential evaluation and active fault assessment in the Alpine Foreland Basins – the project GeoMol. Rend. Online Soc. Geol. It. **30**: 19–23, DOI 10.3301/ROL.2014.05

DIEPOLDER, G.W. & SCHULZ, U. (2011): Tiefliegende Speicher- und Barrieregesteinskomplexe in Bayern – ein Überblick. Schriftenr. Dt. Ges. Geowiss. **74**: 118–136, ISSN 1860-1782

DIEPOLDER, G.W. & THE GEOMOL TEAM (2015): Transnational Geo-potential Assessment Serving the Sustainable Management of Geothermal Energy and Resources Efficiency – the Project GeoMol. Proceedings World Geothermal Congress 2015, Melbourne, Australia 19–25 April 2015, **16013**: 1–7, ISBN 978-1-8777040-02-3

DISS WORKING GROUP (2010): Database of Individual Seismogenic Sources (DISS) http://diss.rm.ingv.it/diss/ Version 3.1.1: A compilation of potential sources for earthquakes larger than M 5.5 in Italy and surrounding areas. Istituto Nazionale di Geofisica e Vulcanologia, DOI 10.6092/INGV.IT-DISS3.1.1

DIX, C.H. (1955): Seismic velocities from surface measurements. Geophysics **20**: 68–86

DOLTON, G.L. (2006): Pannonian Basin Province, Central Europe (Province 4808) – Petroleum geology, total petroleum systems, and petroleum resource assessment. U.S. Geological Survey Bulletin **2204–B**: 47 pp. (Reston VA, U.S. Geological Survey), http://pubs.usgs.gov/bul/2204/b/pdf/b2204-b_508.pdf

DOPPLER, G., HEISSIG, K. & REICHENBACHER, B. (2005): Die Gliederung des Tertiärs im süddeutschen Molassebecken. Newsl. Stratigr. **41**: 359–375, DOI 10.1127/0078-0421/2005/0041-0359

ESKILSON, P. (1986): Superposition Borehole Model, Manual for Computer Code. Department of Mathematical Physics, University of Lund, Sweden, 144 pp.

EU [COUNCIL OF THE EUROPEAN COMMUNITIES] (1990): Council Directive 90/313/EEC on freedom of access to information on the environment. Official Journal **L158**: 56-58, http://eur-lex.europa.eu/LexUriServ/LexUriServ.do?uri=CELEX:31990L0313:EN:HTML

EU [Report from the Commission to the Council and the European Parliament] (2000): On the experience gained in the application of Council Directive 90/313/EEC of 7 June 1990, on freedom of access to information on the environment. COM/2000/400: 46 pp., http://eur-lex.europa.eu/LexUriServ/LexUriServ.do?uri=COM:2000:0400:FIN:EN:PDF

EU [Report from the Commission to the European Parliament, the Council, the European Economic and Social Committee and the Committee of the Regions] (2013): On the implementation of the Raw Materials Initiative. COM/**2013/0442**:19 pp., www.ipex.eu/IPEXL-WEB/dossier/document/COM20130442.do

EU GeoCapacity Consortium (2009): Assessing European Capacity for Geological Storage of Carbon Dioxide, final report for project EU GeoCapacity, 63 pp., http://www.geology.cz/geocapacity/publications/D42%20GeoCapacity%20Final%20Report-red.pdf

Evans, K.F., Zappone, A., Kraft, T., Deichmann, N. & Moia, F. (2012): A survey of the induced seismic responses to fluid injection in geothermal and CO_2 reservoirs in Europe. Geothermics **41**: 30–54, DOI 10.1016/j.geothermics.2011.08.002

Expertengruppe Thermalwasser (2012): Grundsatzpapiere zur Thermalwassernutzung im niederbayerisch-oberösterreichischen Molassebecken. (Augsburg, LfU / München, BayStUG / Linz, Land Oberösterreich / Wien, Lebensministerium – unpubl.)

Fantoni, R. & Franciosi, R. (2010): Tectono-sedimentary setting of the Po Plain and Adriatic foreland. Rend. Fis. Acc. Lincei **21**–**1**: 197–209, DOI 10.1007/s12210-010-0102-4

Fehn, C. & Wirsing, G. (2011): Speicherpotenziale im tiefen Untergrund Baden-Württembergs. Schriftenr. Dt. Ges. Geowiss. **74**: 164–175, ISSN 1860-1782

Fodor, L., Uhrin, A., Palotás, K., Selmeczi, I., Nádor, A., Tóth-Makk, A., Scharek, P., Rižnar, I., Trajanova, M., Rifelj, H., Jelen, B., Lapanje, A., Mozetič, S., Muráti, J., Budai, T. & Tullner, T. (2011): Geological conceptual model in the framework of the project T-JAM. (Budapest, MAFI / Ljubljana, GeoZS), http://en.t-jam.eu/projectresults

Fuks, T., Janža, M. & Lapanje, A. (2013): Utilization potentials of the low-enthalpy geothermal aquifer of the Bad Radkersburg – Hodoš pilot area – based on 3D modelling results of the Transenergy project, Proc. of the European Geothermal Congress 2013, Pisa, Italy, 1–10. Proc. European Geothermal Congress 2013, Pisa, Italy, June 3–7, 2013, 10 pp.

Gable, R. (1978): Acquisition et rassemblement de données géothermiques disponibles en France. Rapport BRGM **78SGN284GTH** (Orléans, BRGM)

Gabriel, P., Gietzel, J., Le, H.H. & Schaeben, H. (2011): A network based datastore for geoscience data and its implementation. Proceedings of the 31st Gocad Meeting, Nancy, http://tu-freiberg.de/fakult3/IS4GEO/gOcad2011.pdf

GBA [Geologische Bundesanstalt] (ed.) (2015): GeoMol – Geologische 3D Modellierung des oberösterreichischen - oberbayerischen Molassebeckens und Anwendungen in der Hydrogeologie und Geothermie im Grenzgebiet Oberösterreich / Oberbayern. Jahrbuch der Geologischen Bundesanstalt (Wien, GBA), in preparation

GeoMol Projektteam LCA (2015): GeoMol – Geopotenziale für die nachhaltige Nutzung des tieferen Untergrunds in den alpinen Vorlandbecken. Abschlussbericht für das Pilotgebiet Bodensee – Allgäu. LGRB-Informationen **30** (Freiburg, LRGB), in preparation

GeORG Projektteam (2013): Geopotenziale des tieferen Untergrunds im Oberrheingraben. Fachlich-technischer Abschlussbericht des INTEREG-Projekts GeORG, Teil 1. LGRB-Informationen **28**: 104 S., ISSN 1619-5329

Ghielmi, M., Minervi, M., Nini, C., Rogledi, S., Rossi, M. & Vignolo, A. (2010): Sedi-mentary and tectonic evolution in the eastern Po-Plain and northern Adriatic Sea area from Messinian to Middle Pleistocene (Italy). Rend. Lincei **21**: 131–166, DOI 10.1007/s12210-010-0101-5

Ghielmi, M., Minervi M., Nini, C., Rogledi, S. & Rossi, M. (2013): Late Miocene-Middle Pleistocene sequences in the Po Plain - Northern Adriatic Sea (Italy): The stratigraphic record of modification phases affecting a complex foreland basin, J. Mar. Petrol. Geol. **42**: 50-81, DOI 10.1016/j.marpetgeo.2012.11.007

Gietzel, J., Schaeben, H. & Gabriel, P. (2014): Managing and delivering 3D geo data across institutions has a web bases solution – intermediate results of the project GeoMol, Geophysical Research Abstracts **16**: EGU2014-10167

Goldbrunner, J., Gold, M., Heiss, H.P., Shribaz, A., Kohl, T. & Baujard, C. (2007): TAT - Thermische Auswirkungen von Thermalwassernutzungen im oberösterreichisch-niederbayerischen Innviertel. Endbericht Projekt TAT im Auftrag des Freistaats Bayern, der Republik Österreich und des Amts der Oberösterreichischen Landesregierung vom 25.06.2015, 291 S. (unpubl.)

Groiss, R. (1989): Geologie und Kohlebergbau im Hausruck (Oberösterreichische Molasse). Archiv für Lagerstättenforschung der Geologischen Bundesanstalt **11**: 167–178

Grünthal, G. & Wahlström, R. (2012): The European-Mediterranean Earthquake Catalogue (EMEC) for the last millennium. J. Seismol. **16/3**: 535–570, DOI 10.1007/s10950-012-9302-y

Guellec, S., Mugnier, J.-L., Tardy, M. & Roure, F. (1990): Neogene evolution of the western Alpine foreland in the light of ECORS data and balance cross-section. – In: Roure, F., Heizman, P. & Polino, R. (eds.): Deep structures of the Alps. Mem. Soc. Geol. France **156**: 165–184

HBC [Hochschule Biberach] (2014): Kurzstudie zur Bedarfsanalyse und zu Nutzungskonzepten für die Mitteltiefe Erdwärmesondengeothermie im Pilotgebiet Lake Constance Allgäu–Area – Endbericht, 28 S. (Biberach, HBC – unpubl., *available at LGRB*)

Hinsch, R. (2013): Laterally varying structure and kinematics of the Molasse fold and thrust belt of the Central Eastern Alps: Implications for exploration. AAPG Bulletin **97/10**: 1805-1831, DOI 10.1306/04081312129

Hirschberg, S., Wiemer, S. & Burgherr, P. (eds.) (2015): Energy from the Earth – Deep Geothermal as a Resource for the Future? Zentrum für Technologiefolgen-Abschätzung TA-SWISS **62/2015**: 526 S., DOI 10.3218/3655-8

Homuth, S., Götz, A.E. & Sass, I. (2014): Lithofacies and depth dependency of thermo- and petrophysical rock parameters in the Upper Jurassic geothermal carbonate reservoirs of the Molasse Basin. Z. Dt. Ges. Geowiss. **165 (3)**: 469–486, DOI 10.1127/1860-1804/2014/0074

Horner, D.R. (1951): Pressure Build-Up in Wells. Third World Petroleum Congress, The Hague, Proceedings Sect. **2**: 503-521 (Leiden, Brill)

Horváth, F., Musitz, B., Balázs, A., Végh, A., Uhrine, A., Nádor, A., Koroknaia, B., Papd, N., Tóth, T. & Wóruma, G. (2015): Evolution of the Pannonian basin and its geothermal resources. Geothermics **53**: 328–352, DOI 10.1016/j.geothermics.2014.07.009

ICHESE [International Commission on Hydrocarbon Exploration and Seismicity in the Emilia region] (2014): Report on the Hydrocarbon Exploration and Seismicity in Emilia Region. 213 pp. (Rome, Department of Civil Protection of the President of Council of Ministers)

IEA [International Energy Agency] (2011): Technology Roadmap – Geothermal Heat and Power. 45 pp, (Paris, IEA)

INSPIRE [Infrastructure for Spatial Information in Europe] (2007): INSPIRE Metadata Implementing Rules: Technical Guidelines based on EN ISO 19115 and EN ISO 19119. http://inspire.jrc.ec.europa.eu/documents/Metadata/MD_IR_and_ISO_20131029.pdf

INSPIRE [Infrastructure for Spatial Information in Europe] (2011): Technical Guidance for the implementation of INSPIRE Discovery Services. http://inspire.jrc.ec.europa.eu/documents/Network_Services/TechnicalGuidance_DiscoveryServices_v3.1.pdf

IPCC [Intergovernmental Panel on Climate Change] (2005): Chapter 5 – Underground geological storage. – In: Metz, B., Davidson, O., de Coninck, H.C., Loos, M. & Meyer, L.A. (eds.): IPCC Special Report on Carbon Dioxide Capture and Storage, 195–277, ISBN 13 978-0-521-86643-9

ISIDe Working Group (2010): Italian Seismological Instrumental and parametric database. http://iside.rm.ingv.it/iside/standard/index.jsp

ISPRA [Istituto Superiore per la Protezione e la Ricerca Ambientale] (2015): Modello geologico 3D e geopotenziali della Pianura Padana centrale (Progetto GeoMol). Rapporti ISPRA: http://www.isprambiente.gov.it/it/pubblicazioni/rapporti, in preparation

Jelen, B. & Rifelj, H. (2011): Surface litostratigraphic and tectonic structural map of T-JAM project area, northeastern Slovenia 1:100,000. (Ljubljana, GeoZS), http://www.geo-zs.si/podrocje.aspx?id=489

Keranen, K.M., Weingarten, M., Abers, G.A., Bekins, B.A. & Ge, S. (2014): Sharp increase in central Oklahoma seismicity since 2008 induced by massive waste water injection. Science **345 (6195)**: 448-451, DOI 10.1126/science.1255802

Karich, F. (2010): Erstellung eines Standalone Programms zur Koordinatentransformation von GoCAD Objekten im Projekt GeORG. BSc Arbeit, Inst. Geophysik und Geoinformatik, TU Bergakademie Freiberg, 30 S. (Freiberg, TU-BAF – unpubl.)

KEMPF, O. & PROSS, J. (2005): The lower marine to lower freshwater Molasse transition in the northern Alpine foreland basin (Oligocene; central Switzerland - south Germany): age and geodynamic implications. Int. J. Earth Sci. **94**: 160–171, DOI 10.1007/s00531-004-0437-0

KESSLER, H., CAMPBELL, D., FORD, J., GILES, J., HUGHES, A., JACKSON, I., PEACH, D., PRICE, S., SOBISCH, H.-G., TERRINGTON, R. & WOOD, B. (2009): Building on geological models – the vision of an environmental modelling platform. In: Three-Dimensional Geological Mapping, Workshop Extended Abstracts, Geological Society of America 2009 Annual Meeting, Portland, Oregon – October 17, 2009, http://isgs.illinois.edu/sites/isgs/files/files/3Dworkshop/2009/kessler.pdf

KOENIGSDORFF, R. (2011): Oberflächennahe Geothermie für Gebäude – Grundlagen und Anwendungen zukunftsfähiger Heizung und Kühlung. 323 S. (Stuttgart, Fraunhofer IRB), ISBN 3-8167-8271-1

KRÖLL, A., WAGNER, L., WESSELY, G. & ZYCH, D. (2001): Geologische Themenkarte Molassezone Niederösterreich und angrenzender Gebiete 1:200.000. (Wien, GBA)

KRÖLL, A., WESSELY, G. & ZYCH, D. (2006): Geologische Themenkarte Molassezone Salzburg – Oberösterreich 1 : 200.000. (Wien, GBA)

KÜHNE, K. (2006): Das Fachinformationssystem Geophysik und seine Nutzung über das Internet. – In: MERKEL, B., SCHAEBEN, H., WOLKERSDORFER, C. & HASCHE-BERGER, A. (Hrsg.): GIS – Geowissenschaftliche Anwendungen und Entwicklungen, 57. Berg- und Hüttenmännischer Tag 2006, Wiss. Mitt. Institut f. Geologie 31: 227–231, ISSN 1433-1284

KUHLEMANN, J. & KEMPF, O. (2002): Post-Eocene evolution of the North Alpine Foreland Basin and its response to Alpine Tectonics. Sediment. Geol. **152**: 45–78, ISSN 0037-0738

LACHENBRUCH, A. H. & BREWER M. C. (1959): Dissipation of the temperature effect of drilling a well in Arctic Alaska. Geological Survey Bulletin **1083 C**: 73–109

LAPANJE, A., BÄK, R., BUDKOVIČ, T., DOMBERGER, G., GÖTZL, G., HRIBERNIK, K., KUMELJ, Š., LAPANJE, A., LETOUZÉ, G., LIPARSKI, P., POLTNIG, W., RAJVER, D., JANŽA, M., MEGLIČ, P., MOZETIČ, S. & WEIXLER, S. (2007): Geotermalni viri severne in severovzhodne Slovenije (Geothermal resources of northern and north-eastern Slovenia). 124 pp., (Ljubljana, GeoZS / Dravograd, RRA Koroška) ISBN 978-961-6498-10-4

LBEG [LANDESAMT FÜR BERGBAU, ENERGIE UND GEOLOGIE] (2007): Bei der Erforschung der Kohlenwasserstoff-Potentiale Süddeutschlands gewonnenen Erkenntnisse über den tieferen Untergrund. Eine erdölgeologische Spurensicherung. Teil 1: Alpen und Alpenvorland („Alpenvorlandstudie“). 690 S., 2 CDs, (Hannover, LBEG)

LBEG [LANDESAMT FÜR BERGBAU, ENERGIE UND GEOLOGIE] (2014): Erdöl und Erdgas in der Bundesrepublik Deutschland 2013. 63 S., (Hannover, LBEG)

LE, H. H., GABRIEL, P., GIETZEL, J. & SCHAEBEN, H. (2013): An object-relational spatio-temporal geo-science data model. Computer & Geosciences **57**: 104–117, DOI 10.1016/j.cageo.2013.04.014

Leblanc, Y., Pascoe, L.J. & Jones, F.W. (1981): The temperature stabilization of a borehole. Geophysics **46**: 1301–1303.

Lemcke, K. (1988): Das bayerische Alpenvorland vor der Eiszeit, Geologie von Bayern **1**: 179 S. (Stuttgart, Schweizerbart), ISBN 978-3-510-65135-1

Lindquist, S.J. (1999): Petroleum Systems of the Po Basin Province of Northern Italy and the Northern Adriatic Sea: Porto Garibaldi (Biogenic), Meride/Riva di Solto (Thermal), and Marnoso Arenacea (Thermal). USGS Open-File Report **99-50-M**: 35 pp, http://pubs.usgs.gov/of/1999/ofr-99-0050/OF99-50M/

Livio, F.A., Berlusconi, A., Michetti, A.M., Sileo, G., Zerboni, A., Trombino, L., Cremaschi, M., Mueller, K., Vittori, E., Carcano, C. & Rogledi, S. (2009): Active fault-related folding in the epicentral area of the December 25, 1222 (Io=IX MCS) Brescia earthquake (Northern Italy): Seismotectonic implications. Tectonophysics **476**: 320–335, DOI 10.1016/j.tecto.2009.03.019

Locati, M. Camassi, R. & Stucchi, M. (eds.) (2011): DBMI11, la versione 2011 del Database Macrosismico Italiano. DOI 10.6092/INGV.IT-DBMI11, http://emidius.mi.ingv.it/DBMI11

Maesano, F.E., d'Ambrogi, C., Burrato, P. & Toscani G. (2015a): Slip-rates of blind thrusts in slow deforming areas: examples from the Po Plain (Italy). Tectonophysics **643**: 8–25, DOI 10.1016/j.tecto.2014.12.007

Maesano, F.E., d'Ambrogi, C., Ferri, F. & The Italian GeoMol Team (2015b): 3D geological model of the central Po Plain (Italy): subsurface potentials vs. geological hazards. 8th European Congress on Regional Geoscientific Cartography and Information Systems (EUREGEO), Proceedings: 40–41 (Barcelona, Institut Cartogràfic i Geològic de Catalunya ICGC) ISBN 978-84-393-9292-7

Maesano, F.E. & the Italian GeoMol Team (2014): Integrating data sources for 3D modeling: the Italian activities in the GeoMol Project. Rend. Online Soc. Geol. It., **30**: 28–32, DOI 10.3301/ROL.2014.07

Maesano, F.E., Toscani, G., Burrato, P., Mirabella, F., d'Ambrogi, C. & Basili, R. (2013): Deriving thrust fault slip rates from geological modeling: Examples from the Marche coastal and offshore contraction belt, Northern Apennines, Italy. J. Mar. Petrol. Geol. **42**: 122–134, DOI 10.1016/j.marpetgeo.2012.10.008

Malzer, O., Rögl, F., Seifert, P., Wagner, L., Wesseley, G. & Brix, F. (1993): Die Molassezone und deren Untergrund. – In: Brix, F. & Schultz, O. (eds.): Erdöl und Erdgas in Österreich, S. 281–322 (Wien, Naturhist. Museum)

Manhenke, V. (1999): Überblick über das Geopotential des Landes Brandenburg. Brandenburgische Geowiss. Beiträge **6**: 5–20, (Kleinmachnow/Cottbus, LBGR), http://www.geobasis-bb.de/GeoPortal1/produkte/fachkarten/lbgr/pdf/1_99_Manhenke_5-20.pdf

Maros, G. (ed.) (2012): Summary report of the geological models, TRANSENERGY project. (Budapest, MFGI / Ljubljana, GeoZS / Vienna, GBA / Bratislava, ŠGÚDŠ), http://transenergy-eu.geologie.ac.at/

Mayrhofer, W. (2007): SAKOG [Salzach-Kohlen-Bergbau-Ges.m.b.H.]. Oberösterreichisches Landesarchiv, 53 S., http://www.landesarchiv-ooe.at/xbcr/SID-1B93A1F8-155581DB/Sakog.pdf

Mazzotti, M., Burdet, A., Conrad, C., Diamond, L., Häring, M., Leu, W., Liniger, H.U., Shell, J. & Zappone, A. (2013): Roadmap for a Carbon Dioxide Capture and Storage pilot project in Switzerland. Report for the Swiss Federal Office of Energy. 29 S. (Bern, Bundesamt für Energie BfE)

Midttømme, K., Banks, D., Ramstad, R.K., Sæther, O.M. & Skarphagen, H. (2008): Ground-source heat pumps and Underground Thermal Energy Storage – energy for the future. – In: Slagstad, H. (ed.): Geology for Society. Geol. Soc. Norway Special Publications **11**: 93–98, ISSN 2387-3159

Molinari, F.C., Torri, G., Martini, A. & The Italian GeoMol Team (2015): 3D temperature model of the central Po Plain (Italy). 8th European Congress on Regional Geoscientific Cartography and Information Systems (EUREGEO), Proceedings: 109–110 (Barcelona, Institut Cartogràfic i Geològic de Catalunya ICGC) ISBN 978-84-393-9292-7

Müller C. & Reinhold, K. (Hrsg.) (2011): Speicher-Kataster Deutschland – Geologische Charakterisierung tiefliegender Speicher und Barrierehorizonte in Deutschland. Schriftenr. Dt. Ges. Geowiss. **74**: 277 S., ISSN 1860–1782

Mugnier, J.-L. & Menard, G. (1986): Le développement du bassin molassique suisse et l'évolution des Alpes externes: un modèle cinématique. Bulletin du Centre Recherches Exploration-production Elf-Aquitaine 10: 167–180, ISSN 0181-0901

Muttoni, G., Carcano, C., Garzanti, E., Ghielmi, M., Piccin, A., Pini, R., Rogledi, S., & Sciunnach, D. (2003): Onset of major Pleistocene glaciations in the Alps. Geology **31**: 989–992, DOI 10.1130/G19445.1

Nachtmann, W. (1995): Bruchstrukturen und ihre Bedeutung für die Bildung von Kohlenwasserstoff-Fallen in der OÖ Molasse. Geol. Pal. Mitt. Innsbruck **20**: 221–230

Nádor, A., Lapanje, A., Tóth, G, Rman, N., Szőcs, T., Prestor, J., Uhrin, A., Rajver, D., Fondor, L., Murati, J. & Székely, E. (2012): Transboundary geothermal resources of the Mura-Zala basin: a need for joint thermal aquifer management. Geologija **55/2**: 209–224, DOI 10.5474/geologija.2012.013

Nádor, A., Rotár-Szalkai, Á., Prestor, J., Tóth, G., Goetzl, G., Lapanje, A., Rman, N., Szőcs, T., Cernak, R., Schubert, G. & Svasta, J. (2013): Transboundary geothermal energy resources of Slovenia, Austria, Hungary and Slovakia (TRANSENERGY) – contributions to integrated resource management policies and regional development. Proc. European Geothermal Congress 2013, Pisa, Italy, June 3–7, 2013, 10 pp., DOI 10.13140/2.1.2608.4809

Nathan, H. (1949): Geologische Erkenntnisse der Erdölböhrungen im Bayerischen Innviertel. Geologica Bavarica **1**: 68 S. (München, Bay. GLA)

National Research Council (2013): Induced Seismicity Potential in Energy Technologies. 248 pp. (Washington DC, National Academies Press)

Naylor, M. & Sinclair H.D. (2008): Pro- vs. retro-foreland basins. Basin Research **20**: 285-303, DOI 10.1111/j.1365-2117.2008.00366.x

Nelson, S.A. (2012): Physical Geology – Energy Resources. Tulane University EENS 1110, http://www.tulane.edu/~sanelson/eens1110/energy.htm

OGC [Open Geospatial Consortium Inc.] (2002): Web Map Service Implementation Specification. OGC 01-068r3, v. 1.1.1, http://portal.opengeospatial.org/files/?artifact_id=1081

OGC [Open Geospatial Consortium Inc.] (2004): Web Map Service Implementation Specification. OGC 06-042, v. 1.3.0, http://portal.opengeospatial.org/files/?artifact_id=14416

OGC [Open Geospatial Consortium Inc.] (2007): OpenGIS® Catalogue Services Specification. OGC 07-006r1, v. 2.0.2, http://portal.opengeospatial.org/files/?artifact_id=20555

OGC [Open Geospatial Consortium Inc.] (2011): OpenGIS® Implementation Standard for Geographic information – Simple feature access – Part 1: Common architecture. OGC 06-103r4, v.1.2.1, http://portal.opengeospatial.org/files/?artifact_id=25355

Odello, C. & Marillier, F. (2004): Etude sismique du bassin molassique du Plateau suisse. Rapport pour la Commission Géophysique Suisse Année 2003 http://sgpk.ethz.ch/static/jahresbericht/2003/Marillier.htm

Pamer, R. & Diepolder, G.W. (2010): 3D geological modelling in Bavaria – state-of-the-art at a State Geological Survey. Z. Dt. Ges. Geowiss.**161/2**: 189–203, ISSN 1860-1804

Pamer, R. & The GeoMol Team (2015): The limits of interoperability – model fusion needs more than technical solutions. 8th European Congress on Regional Geoscientific Cartography and Information Systems (EUREGEO), Proceedings: 46–47 (Barcelona, Institut Cartogràfic i Geològic de Catalunya ICGC) ISBN 978-84-393-9292-7

Paschen, H., Oertel, D., Grünwald, R. (2003): Möglichkeiten geothermischer Stromerzeugung in Deutschland – Sachstandsbericht. Büro für Technikfolgen-Abschätzung beim Deutschen Bundestag (Hrsg.) TAB-Arbeitsbericht **84**: 124 S. (Berlin, TAB).

Pasquale, V., Chiozzi, P., Gola, G. & Verdoya, M., (2008): Depth-time correction of petroleum bottom-hole temperatures in the Po Plain, Italy, Geophysics, 73, 187–196.

Pfiffner, O.A. (2009): Geologie der Alpen. 359 S. (Bern / Stuttgart / Wien, Haupt Verlag) ISBN 978-3-8252-8416-9.

Pfiffner, O.A., Erard, P.F. & Stäuble, M. (1997): Two cross sections through the Swiss Molasse Basin (Lines E4-E6, W1, W7-W10). – In: Pfiffner, O.A., Lehner, P. Heitzmann, P. Mueller, S. & Steck, A. (eds.): Deep Structure of the Swiss Alps: Results from NRP 20, pp. 64–72 (Basel, Birkhäuser)

Pieri, M. & Groppi, G. (1981): Subsurface geological structure of the Po Plain, Italy. Progetto Finalizzato Geodinamica – Agip **414**: 1–13

PK Tiefe Geothermie (2007): Nutzungen der geothermischen Energie aus dem tiefen Untergrund (Tiefe Geothermie) – Arbeitshilfe für Geologische Dienste. 25 S. http://www.infogeo.de/infogeo/dokumente/download_pool/tiefe_geothermie_arbeitshilfe_08022007.pdf

PK NtU [Personenkreis Nutzung tieferer Untergrund der Ad-hoc-Arbeitsgruppe Geologie] (2014): Charakterisierung der Nutzungspotenziale des geologischen Untergrundes in Deutschland als Bewertungsgrundlage für unterirdische Raumnutzungen – Abschlussbericht. 31 S. + Anlagen, http://www.infogeo.de/aktuelles/ntu_bericht

Pondrelli, S., Salimbeni, S., Morelli, A., Ekström, G., Postpischl, L., Vannucci, G. & Boschi, E. (2011): European-Mediterranean Regional Centroid Moment Tensor Catalog: solutions for 2005–2008. Phys. Earth Planet. Int. **185**: 74–81

Przybycin, A., Scheck-Wenderoth, M. & Schneider, M. (2014): The 3D conductive thermal field of the Northern Alpine Foreland Basin – Influence of the deep structure of the adjacent European Alps. Geophysical Research Abstracts **16**, EGU2014-2942-2

Rajver, D. (2012): Možnosti proizvodnje elektrike iz geotermalne energije v Sloveniji v naslednjem desetletju (Possibilities for electricity production from geothermal energy in Slovenia in the next decade). Geologija **55/1**: 117–140, DOI 10.5474/geologija.2012.009

Rath, V. & Clauser, C. (2005): Erkennen und Quantifizieren von Strömungen: Eine geothermische Rasteranalyse zur Klassifizierung des tiefen Untergrundes in Deutschland hinsichtlich seiner Eignung zur Endlagerung radioaktiver Stoffe, Fortsetzung. Endbericht zum Auftrag 9X0009-8497-2 des Bundesamtes für Strahlenschutz (BfS), 209 S. (Stolberg, Geophysica Beratungsgesellschaft)

Raviglia, A., Seno, S., Toscani, G. & Fantori, R. (2006): Mesozoic extension controlling the Southern Alps thrust geometry under the Po Plain, Italy: insights from sandbox models. J. Struc. Geol. **28**: 2084–2096, DOI 10.1016/j.jsg.2006.07.011

Regione Emilia-Romagna & ENI-AGIP (1998): Riserve idriche sotterranee della Regione Emilia-Romagna. (Firenze, S. EL. CA.)

Rman, N. (2013): Analysis of the extraction of thermal water from low enthalpy geothermal resources in sedimentary basins: a case study of the Mura-Zala sedimentary basin: PhD thesis, 182 pp. (Ljubljana, Faculty of Natural Sciences and Engineering University of Ljubljana)

Rman, N. (2014): Analysis of long-term thermal water abstraction and its impact on low-temperature intergranular geothermal aquifers in the Mura-Zala basin, NE Slovenia. Geothermics **51**: 214–227, DOI 10.1016/j.geothermics.2014.01.011

Rman, N., Gál, N., Marcin, D., Weilbold, J., Schubert, G., Lapanje, A., Rajver, D., Benová, K. & Nádor, A. (2015): Potentials of transboundary thermal water resources in the western part of the Pannonian basin. Geothermics **66**: 88–98, DOI 10.1016/j.geothermics.2015.01.013

Rman, N., Lapanje, A. & Prestor, J. (2011): Water concession principles for geothermal aquifers in the Mura-Zala Basin, NE Slovenia. Water Resources Management **25/13**: 3277–3299, DOI 10.1007/s11269-011-9855-5

Rman, N., Lapanje, A. & Rajver, D. (2012): Analiza uporabe termalne vode v severovzhodni Sloveniji (Analysis of thermal water utilization in the northeastern Slovenia). Geologija **55/2**: 225–242, DOI 10.5474/geologija.2012.014

Rovida, A., Camassi, R., Gasperini, P. & Stucchi, M. (eds.) (2011): CPTI11, la versione 2011 del Catalogo Parametrico dei Terremoti Italiani. http://emidius.mi.ingv.it/CPTI/

Rupf, I. & Armbruster, V. (2008): Das geologische Modell des Informationssystems Oberflächennahe Geothermie für Baden-Württemberg. – In: Merkel, B., Schaeben, H., Wolkersdorfer, C. & Hasche-Berger, A. (Hrsg.): GIS - Geowissenschaftliche Anwendungen und Entwicklungen, 59. Berg- und Hüttenmännischer Tag 2008, Wiss. Mitt. Institut f. Geologie **37**: 179–182, ISSN 1433-1284

Rupf, I. & Nitsch, E. (2008): Das Geologische Landesmodell von Baden-Württemberg: Datengrundlagen, technische Umsetzung und erste geologische Ergebnisse, LGRB-Informationen **21**: 82 S., ISSN 1619-5329

Rupf, I. & the GeoMol Team (2013): 3D-modelling work-flows for trans-nationally shared geological models – first approaches from the project GeoMol. Geophysical Research Abstracts **15**, EGU2013-8924-1

Rybach, L. (1992): Geothermal Potential of the Swiss Molasse Basin. Eclogae geol. Helv. **85/3**: 733–744, ISSN 0012-9402

Sattler, S. & Pamer, R. (2009): A 3D structural model of the Bavarian basement. 6th European Congress on Regional Geoscientific Cartography and Information Systems (EUREGEO), Proceedings **I**: 202–203 (München, LfU)

Scardia, G., Muttoni, G., & Sciunnach, D. (2006): Subsurface magnetostratigraphy of Pleistocene sediments from the Po Plain (Italy): Constraints on rates of sedimentation and rock uplift: Geol. Soc. Am. Bull. **118**: 1299–1312, DOI 10.1130/B25869.1

Scardia, G., de Franco, R., Muttoni, G., Rogledi, S., Caielli, G., Carcano, C., Sciunnach, D., & Piccin, A. (2012): Stratigraphic evidence of a Middle Pleistocene climate driven flexural uplift in the Alps. Tectonics **31**: TC6004, 18 pp., DOI 10.1029/2012TC003108

Scardia, G., Festa, A., Monegato, G., Pini, R., Rogledi, S., Tremolada, F., Galadini F. (2014): Evidence for late Alpine tectonics in the Lake Garda area (northern Italy) and seismogenic implications. Geol. Soc. Am. Bull. B30990.1, DOI 10.1130/B30990.1

Scharf, C. & Clemens, T. (2006): CO_2-Sequestration Potential in Austrian Oil and Gas Fields. EAGE Annual Conference and Exhibition, 12–15 June, Vienna, Austria, **SPE-100176**: 10 pp., DOI 10.2118/100176-MS

Schellschmidt, R. & Stober, I. (2008): Untergrundtemperaturen in Baden-Württemberg. LGRB-Fachbericht **2**: 28 S. (Freiburg, LGRB)

Schubert, G., Lampl, H., Pavlik, W., Pestal, G., Rupp, C., Shadlau, S. & Wurm, M. (2003): Hydrogeologie. In: BMLFUW [Bundesministerium für Land- und Forstwirtschaft, Umwelt und Wasserwirtschaft] (ed.): Hydrologischer Atlas Österreichs, 1. Lieferung, Kartentafel 6.2., (Wien, BMLFUW), ISBN 3-85437-250-7

Scognamiglio, L., Margheriti, L., Mele, F.M., Tinti, E., Bono, A., De Gori, P., Lauciani, V., Lucente, F.P., Mandiello, A.G., Marcocc,i C., Mazza, S., Pintore, S. & Quintiliani, M. (2012): The 2012 Pianura Padana Emiliana seimic sequence: locations, moment tensors and magnitudes. Ann. Geophys. **55(4)**: 549–559, DOI 10.4401/ag-6159

Signorelli, S., Andenmatten Berthoud, N. & Kohl, T. (2004): Geothermischer Ressourcenatlas der Schweiz. Erarbeitung und Bewertung des geothermischen Potentials der Schweiz. BfE-Schlussbericht, 12.2004, 55 S. (Bern, Bundesamt für Energie BfE)

Signorelli, S. & Kohl, T. (2006): Geothermischer Ressourcenatlas der Nordschweiz. Schweizerische Geophysikalische Kommission, Beiträge zur Geologie der Schweiz – Geophysik: **39**

Sommaruga, A., Eichenberger, U. & Marrilier, F. (2012): Seismic Atlas of the Swiss Molasse Basin, edited by the Swiss Geophysical Commission. Matériaux Géol. Suisse – Géophysique **44**, 88 pp., 24 maps, ISSN 0253-1186

Šram, D., Rman, N., Lapanje, A., Rižnar, I., Rajver, D. & Koren, K. (2015): Razvoj trodimenzionalnega geološkega modela Mursko Zalskega bazena / Development of 3D geological model of the Mura-Zala basin. Geologija **58/2** (Ljubliana, Geološki zavod Slovenije)**,** in preparation

Steward, R., Welsh, C. & Purucker, T. (2009): An introduction to Spatial Analysis and Decision Assistance (SADA). 612 S., http://www.sadaproject.net/SADAVersion5UserGuide.pdf

Štih, J., Senegačnik, A. & Šolar, S.V. (2014): Pregled podatkov proizvodnje ter zalog in virov nekovinskih mineralnih surovino (Overview of data on production and reserves of non-metal mineral resources). In: Senegačnik, A. (ed.): Mineralne surovine v letu 2013, 14–45 (Ljubljana, Geološki zavod Slovenije), ISSN 1854-293X, http://www.geo-zs.si/UserFiles/677/File/Publikacije/Bilten_MS_PDF/Bilten%202013%20web%20S.pdf

Strunck, P. & Matter, A. (2002): Depositional evolution of the western Swiss Molasse. Eclogae geol. Helv. **95**: 197–222, ISSN 0012-9402/02/020197-26

Suchi, E., Dittmann, J., Knopf, S., Müller, C. & Schulz, R. (2014): Geothermie-Atlas zur Darstellung möglicher Nutzungskonkurrenzen in Deutschland. Z. Dt. Ges. Geowiss. **165/3**: 439–453, DOI 10.1127/1860-1804/2014/0070

Swisstopo (ed.) (2005): Geological Map of Switzerland 1:500,000, http://www.swisstopo.admin.ch/internet/swisstopo/en/home/products/maps/geology/geomaps/gm500.html

Swisstopo (ed.) (2012): GeoCover - Geological vector datasets, http://www.swisstopo.admin.ch/internet/swisstopo/en/home/products/maps/geology/geocover.html

Tardy, M., Deville, E., Fudral, S., Guellec, S., Ménard, G., Thouvenot, F. & Vialon, P. (1990): Interprétation structural des données du profil de sismique réflexion profonde ECORS-CROP Alpes entre le fronr Pennique et la ligne du Canavese (Alpes occidentales). – In: Roure, F., Heizman, P. & Polino, R. (eds.): Deep structures of the Alps. Mem. Soc. Geol. France **156**: 217–226

Tewag (2014): GeoMol - Entwicklung standardisierter Bohr- und Ausbaudesigns sowie von zwei Rechenmodulen zur Potenzialabschätzung der Mitteltiefen Erdwärmesondengeothermie im Pilotgebiet Lake Constance – Allgäu Area. Abschlussbericht der Fa. tewag, BauGrund Süd und der Hochschule Biberach vom 01.12.2014, 54 S. + Anhang (Starzach, tewag – unpubl., *available at LGRB*).

Trümpy, R. (1980): Geology of Switzerland, a guide book. Part A: An outline of the geology of Switzerland. 104 p. (Basel, Wepf & Co) ISBN 978-3859770621

Turner, K. & d'Agnese, F. A. (2009): The Role of Geological Modeling in a Web-based Collaborative Environment. Three-Dimensional Geological Mapping, Workshop Extended Abstracts, Portland, Oregon – October 17, 2009, http://isgs.illinois.edu/sites/isgs/files/files/3Dworkshop/2009/turner.pdf

van der Krogt, R., Pedersen, M., Tulstrup, J., Robida, F., Serrano, J.-J., Grellet, A., Lee, K., Harrison, M., Demicheli, L., Delfini, C., Hugelier, S. & van Daalen, T. (2014): Design and Implementation Aspects of the Geological Data Infrastructure for European Society. Geophysical Research Abstracts **16**, EGU2014-13414-2

VDI (2008): Referenzlastprofile von Ein- und Mehrfamilienhäusern für den Einsatz von KWK-Anlagen. VDI-Richtlinie **4655** (Berlin, Beuth Verlag)

VDI (2010): Thermische Nutzung des Untergrunds - Grundlagen, Genehmigung, Umweltaspekte. VDI-Richtlinie **4640**: 30 S. (Berlin, Beuth Verlag)

Wagner, L. R. (1998): Tectono-stratigraphy and hydrocarbons in the Molasse Foredeep of Salzburg, Upper and Lower Austria. – In: Mascle, A., Puigdefàbregas, C., Lutherbacher, H. P. & Fernàndez, M. (eds.): Cenozoic Foreland Basins of Western Europe. Geol. Soc. Spec. Publ. **134**: 339–369, (London)

WSSPC [Western States Seismic Policy Council] (1997): Active fault definition for the Basin and Range Province. WSSPC Policy Recommendation **97-1**: 3 (San Francisco, WSSPC White Paper)

Zekiri F. (2011): Erstellung von Temperaturkarten in verschiedenen Tiefen im südlichen Wiener Becken. Diplomarbeit Universität Wien, http://othes.univie.ac.at/14913/1/2011-06-07_0209940.pdf

Zoback, M. D. & Gorelick S. M. (2012): Earthquake triggering and large-scale geologic storage of carbon dioxide. PNAS [Proceedings Natl. Academy of Sciences United States of America] **109 (26)**: 10125-10126, DOI 10.1073/pnas.1202473109

Zschocke, A. (2005): Correction of non-equilibrated temperature logs and implications for geothermal investigations, J. geophys. Eng., **2**: 364–371